

Alma Mater Studiorum – Università di Bologna

DOTTORATO DI RICERCA IN

**SCIENZE DELLA TERRA, DELLA VITA E DELL'
AMBIENTE**

Ciclo 29°

**Settore Concorsuale di
afferenza**

05/A1 BOTANICA

**Settore Scientifico
disciplinare**

BIO/01 BOTANICA GENERALE

**FACTORS INVOLVED IN POLLEN
GERMINATION PLAYING A CRITICAL ROLE
ALSO IN
ALLERGIC SENSITIZATION**

Dott.ssa IRIS ALOISI

Coordinatore Dottorato

**Prof.ssa Barbara
Mantovani**

Relatore

Prof. Stefano Del Duca

Esame finale anno 2017

Index

	Pg
Preface	1
Introduction	3
Microsporogenesis	3
Pollen adhesion to the stigma	
Pollen rehydration	4
Pollen germination and tube elongation	6
PART I: Pollen as a model of study and polyamines as a tool	
Chapter I	21
Polyamines in pollen: from microsporogenesis to fertilization	
Chapter II	35
Natural polyamines and synthetic analogues modify the growth and the morphology of <i>Pyrus communis</i> pollen tubes affecting ROS levels and causing cell death	
Chapter III	69
Spermine affects pollen tube growth by perturbing calcium concentration, actin organization and cell wall structure	
PART II: Pollen as a source of allergens: air monitoring and <i>in vitro</i> studies	
Chapter IV	113
Behaviour of profilins in atmosphere and <i>in vitro</i> , and their relationship with the performance of airborne pollen	
Chapter V	138
Differences in atmospheric concentration of airborne <i>Poaceae</i> pollen and allergens	
Chapter VI	152
Purification and characterization of Amb a 1 and Art v 6, two pectate lyase enzymes from weed pollen	
Final Remarks	169
List of publications	171

Preface

Understanding the processes involved in pollen maturation and pollen tube growth is of great importance as these processes are involved in fertilization thus crop production.

However, besides the great agricultural interest behind pollen study, the ease of *in vitro* growth of pollen, combined with the ease with which live imaging is performed with pollen tube; make it one of the most exciting systems for the studies of polarity, tip growth and also cell wall deposition. Pollen has provided, over the last decades, important cues about the global rearrangements and the shaping of plant cells. For this reason, it was chosen in this study as a promising model for studying how external stimuli are integrated within the cell and how several signalling molecules and processes are interconnected. In particular, understanding how the overall shaping of the pollen tube tip and how several well-known factors are interconnected were the main goals of this study. In fact, while molecules and factors involved in the apical growth of the pollen tube are well-known individually, details on the reciprocal interactions between these factors are missing. The first part of the theses ("Pollen as a model of study and polyamines as a tool") exactly deals with these doubts and goals and puts the basis for an integration of several factors of pollen tube growth. As the proper growth of the pollen tube depends on an elaborate mechanism that integrates several molecular and cytological sub-processes its growth mechanism is controlled by several signaling molecules such as polyamines (PAs), which control different aspects of pollen tube germination, e.g. by structuring pollen cell wall and by modulating protein assembly (a deepening of PAs involvement during the whole life span of pollen development can be found in Chapter 1). In pollen, the homeostasis of PAs is finely regulated and the perturbation of this balance has provided, over the years, interesting evidences about how PAs carry out some of their functions in the cell. For these reasons, PAs were taken into consideration to be used as perturbing molecules, used to spread light in understanding not only the reciprocal interactions among factors, but also the timing of the events (Chapter 2 and 3).

Besides the great interest about pollen as a model of study, pollen is a relevant topic also because it is the main trigger of seasonal allergies, which are sometimes referred to as hay fever or allergic rhinitis. Seasonal allergies develop because the body's immune system has become sensitized and overreacts to proteins present in the environment that are normally not harmful to other people, the so-called "allergens". Thanks to a tight collaboration with Consiglio Nazionale delle Ricerche, CNR (Bologna) and Professor Delia Fernández-González (University of León, Spain) and a training period spent in the research group of Professor Fatima Ferreira (University of Salzburg) also the topic pollen as a source of allergens was investigated and the main findings can be found in the second part of the thesis ("Pollen as a source of allergens: air monitoring and *in vitro* studies"). It is well-known that many factors can influence the severity of allergy symptoms but also the abundance of airborne allergens. However, it often happens that the only "pollen count" do not completely mirror the potential allergenicity of the air. Here from, the necessity to integrate the forecasting of allergenic pollen in the atmosphere with the monitoring of airborne allergenic proteins, both if pan-allergens (Chapter 4) and specific allergens (Chapter 5). In these studies, the amount of airborne allergens were put in correlation not only with pollen counts but also with meteorological factors in order to obtain a broad panel of evidences about factors that may affect pollen and allergen dispersion. Finally, *in vitro* studies also focused on the characterization of two allergenic enzymes, deeply involved in pollen cell wall organization and hugely secreted during pollen rehydration, i.e. pectate-lyases from *Ambrosia artemisiifolia* and *Artemisia vulgaris*. The physico-chemical characterization of these allergens is reported in Chapter 6.

Before starting, a brief introduction about what is pollen, how it develops and how pollen tube grows to achieve fertilization will be outlined.

Introduction

Microsporogenesis

Pollen, the mature male gametophyte (microgametophyte), is a highly specialized cell type that develops within the anthers of the flower through a complex series of processes.

During anther development, the reproductive or sporogenous cells, located centrally within the anther, give rise to the pollen mother cells; i.e. the microsporocytes, while the surrounding non-reproductive cells form sporophytic epidermal, cortical and tapetal cell layers. Pollen development from microsporocytes can be divided into microsporogenesis and microgametogenesis. During microsporogenesis, microsporocytes undergo a meiotic division, with the four haploid spores, initially staying together in the form of a tetrad. These tetrads are embedded in a thick wall, mainly consisting of callose, and surrounded by the locular fluid inside the anther locules. The innermost cell layer of the locule form the so-called tapetum, an essential tissue for microsporogenesis as it secretes nutrients, carbohydrates, cell wall components and enzymes needed for the proper maturation of the pollen grains and takes part also in the deposition of the pollen cell wall (Müller and Rieu, 2016).

Pollen grain cell wall is extremely unique and at maturity, the pollen surface can be divided into three principal layers, with the relative amount of each varying between species: an outer exine wall, itself multilayered, composed of the chemically resistant polymer sporopollenin and interrupted by openings called apertures; an inner intine, also sometimes multilayered, made primarily of cellulose; and a pollen coat, composed of lipids, proteins, pigments, and aromatic compounds, that fills the sculptured cavities of the pollen exine (Edlund et al., 2004).

Once pollen grains are completely formed, thanks to callases that digest the callose walls of the tetrads, they are released within the locules. During subsequent microgametogenesis, the microspores undergo vacuolization, expansion and a

mitotic, asymmetric division, resulting in the formation of binuclear pollen grains, harbouring a larger vegetative and smaller generative cell. At this stage, the tapetum undergoes programmed cell death. Pollen will then mature and desiccate. In the case of tri-nucleate pollen, a second mitotic division of the generative cell into two sperm cells occurs before desiccation, while in binucleate pollen grains this happens after pollen germination (Müller and Rieu, 2016). In order to keep viable and metabolically quiescent, the extent of pollen desiccation is extremely high, ranging from 15 to 35% water content, when released from the anthers (Heslop-Harrison, 1979; Buitink et al., 2000; Edlund et al., 2004).

Pollen adhesion to the stigma

To capture pollen grains, stigmas engage biotic and abiotic pollinators (such as insects and wind) and use rapid and strong adhesive interactions to retain pollen grains. The pollen–stigma interface can differ from species to species as a result of the wide variability in the morphology and content of stigma exudates, exine layers, and pollen coats. After exine-mediated adhesion, mobilization of the pollen coat occurs, leading to mixing of lipids and proteins to form a first contact on the stigma surface. There is now extensive evidence that the proteins and lipids in the pollen coat, and proteins on the stigma surface, also contribute to adhesion, albeit most likely at a later stage than at the time of initial contact (Edlund et al., 2004).

Pollen re-hydration

As pollen lands on a stigma, water, nutrients, and other small molecules are transported rapidly into the grain from the stigma exudate or stigma papillae by mechanisms that remain unclear. The discovery of aquaporin expression in the stigma has prompted the exciting model that water channels are involved in the rapid and regulated water release from the stigma to the pollen (Dixit et al., 2001). Regardless of the mechanism of transfer, pollen hydration often is regulated, both temporally and spatially. Inappropriate hydration can have disastrous consequences, leading to premature germination within the anther (Johnson and McCormick, 2001) or germination on the wrong surface.

The genetic and molecular dissection of the lipid-rich matrices found in the pollen coat has progressed considerably in recent years. In *Arabidopsis*, the pollen coat contains long- and short-chain lipids along with a small set of proteins, including six lipases and eight Gly-rich oleosin proteins that contain a lipid binding domain. Disrupting pollen coat lipids or pollen coat proteins in Brassicaceae species can delay or block pollen hydration. Mutations that affect pollen coat proteins are less extreme, perhaps because of partial functional redundancy (Mayfield et al., 2001;Edlund et al., 2004;Fiebig et al., 2004).

The lipid-rich stigma exudate of plants with wet stigmas is thought to be functionally analogous, in part, to the pollen coat. Based on these findings, it is possible to propose a model in which the presence of lipids, whether provided by the male or the female surface, modulates water transfer to desiccated pollen, while highly diverse proteins and peptides mediate self and foreign pollen recognition(Dickinson, 1995;Edlund et al., 2004).

Independently of where and how the water required for pollen rehydration comes from, what is well known is that a huge amount of proteins is released in the hydration medium during this process. This phenomenon may, in part, be due to the bursting of some pollen grains, thus resulting in the release of proteins into the medium. However, it was demonstrated that several protein are over expressed and released into the rehydration medium (Sheoran et al., 2009). During in vitro germination of canola pollen in fact a huge number of proteins is released into the germination medium, including cruciferin, oleosin, cysteine-rich repeat secretory protein 26 precursor, enolase, pyrophosphatase, polygalacturonase and pectinesterase inhibitor (Sheoran et al., 2009), thus proteins involved in carbohydrate and energy metabolism, transport and wall remodeling. Besides proteins involved in those functions, also cell-wall remodeling protein, e.g. pectate lyases and expansins, and proteins involved in signalling are extruded from the pollen tube. What is worth of notice is that many proteins extruded actively or passively during pollen rehydration, is that they are often allergenic proteins (or allergen-related proteins), representing a threat to human health as pollen is an important source of seasonal allergens (Grote et al., 2000;Grote et al., 2003;Radauer and Breiteneder, 2006;Vega-Maray et al., 2006).

Pollen germination and tube elongation

Hydration transforms a pollen grain into a highly polarized cell as the grain organizes its cytoplasm and cytoskeleton to support the extension of the pollen tube. These changes occur within minutes after hydration and include the formation of a filamentous actin cytoskeleton highly polarized toward the site of tube emergence (Gossot and Geitmann, 2007; Cheung and Wu, 2008; Fu, 2015), reorientation of the vegetative nucleus so that it enters the extending tube before the generative cells (Åström et al., 1995; Laitinen et al., 2002; Edlund et al., 2004), movement of mitochondria and polysaccharides at the site of tube emergence (Cresti et al., 1977), and delivering of secretory vesicle containing newly synthesized cell wall material at the site of tube emergence (Wang et al., 2005; Hepler et al., 2013).

It is not yet clear how the polarization signal is perceived and subsequently transduced to select a single point for tube emergence. Several candidate signals have been suggested, including water, lipids, and ions. Polarization signals ultimately trigger the recruitment of several signalling factors and the establishment of calcium gradients at tube tips (Edlund et al., 2004).

Once the cell has established its internal polarity relative to an external signal, the pollen tube must breach the exine wall to emerge from the grain and can enter the style, seeking to reach the ovary, after transiting the stigma barrier.

To efficiently reach the ovary, pollen tubes elongate at an astonishing rate (up to 1 cm/hr) to an extraordinary length by polarized tip growth, which is strictly dependent on polar exocytosis that delivers cell membrane and wall materials to the growing tip (Hepler et al., 2001; Qin and Yang, 2011). Pollen tube growth requires a highly polarized cytoplasmic organization and finely-tuned molecular machineries. The tip region displays an apical zone essentially packed with exocytic vesicles accumulated as a typical “V shape” to facilitate massive tip-targeted exocytosis. This zone is called “clear-zone” so named because the amyloplasts and vacuoles are prevented from moving into this apical part. In the subapical and shank regions there are organelles, nuclei, and vacuoles that may extend toward the grain (Cheung and Wu, 2008; Qin and Yang, 2011; Hepler et al., 2013). Cytoplasmic streaming drives organelles moving rapidly back and forth

along the main axis of the pollen tube in a reverse fountain pattern, which maintains the distribution of membranous structures and releases exocytic vesicles to the apical zone (Cai and Cresti, 2009). Several signaling networks control tip growth in pollen tubes via inter-connection with the cytoskeletal elements and the polarized exocytosis (Qin and Yang, 2011)

In the next part of the introduction, the main factors and processes involved in pollen tube growth will be discussed more in detail. As this process is extremely complicated and regulated and as the more that research investigates pollen tube growth, the more factors appear to be involved, a large number of molecules, although no less important, will not be discussed in detail.

The structural system

The cytoskeleton

Pollen tubes contain both microtubules and actin microfilaments, which are highly organized and dynamic through their interaction with various actin-binding proteins (ABP) and microtubule-associated proteins (Staiger and Blanchoin, 2006;Fu, 2010;Staiger et al., 2010). While microtubules are thought to be mostly involved in organelle movement (Qin and Yang, 2011), recent discoveries show how microtubules are involved in exocytosis and endocytosis, besides the movement of organelles, suggesting a potential role for microtubules in the regulation of pollen tube tip growth (Idilli et al., 2013;Cai et al., 2015;Fu, 2015). Most assuredly is that actin microfilaments are essential for tip growth. They form long cables axially aligned in the shank, providing the main tracks for the movement of organelles and vesicles, regulating the cytoplasmic streaming (Vidali and Hepler, 2001;Bove et al., 2008;Cai et al., 2015). This cables-dependent cytoplasmic streaming rapidly brings exocytic vesicles to the subapical zone, where, a collection of shorter and thinner actin cables constitutes a ring-like actin structure. It was proposed that the subapical F-actin participates in vesicular

trafficking in the apical region (Gu et al., 2003). The dynamic microfilaments are regulated by Rho-related GTPase of plants (ROP) and many ABP. Pharmacological and genetic studies combined with live cell imaging have revealed multiple distinct populations of microfilaments that carry out specific functions in pollen tubes, respectively. Low concentrations of latrunculin B, which did not affect the longitudinal actin cables, inhibited pollen tube growth, suggesting an essential role for a dynamic form of microfilaments (Vidali et al., 2001).

Genetic studies of various ABPs more clearly define the role for each microfilament form. A series of ABPs that regulate the construction of longitudinal microfilament bundles have been characterized including actin-nucleating factor, actin-bundling proteins, fimbrin, villin, profilin and actin depolymerizing factor (ADF) that are important for the turnover of microfilaments in the shank region. The regulation of these ABP reflects the regulation of actin turnover and microfilaments organization, creating fine-tuned machinery, often difficult to be studied. For example, monomer-binding proteins, profilin and ADF, are thought to function synergistically to enhance turnover and the exchange of subunits between monomer and polymer pools. How individual actin filaments behave in living cells, however, remains largely unexplored (Staiger et al., 2010). Most assuredly is that the actin cables provide the tracks for the movement of large organelles and the cytoplasmic streaming during pollen tube tip growth. The subapical actin fringe is proposed to participate in vesicle trafficking in the apex as well as in control the apical clear-zone formation and maintenance (Qin and Yang, 2011;Fu, 2015). It maintains its length and apical location to keep in step with growth. How the subapical fringe modulates the directionality of pollen tube growth remains to be determined (Fu, 2015).

Cell wall composition and mechanics

The rapid and continuous tip growth has to rely on efficient and ample supply of membrane materials, enzymes, signaling molecules, and, mostly, of new cell wall components. Because of high turgor pressure in pollen tubes as in other plant cells, biosynthesis-based growth via exocytic delivery of cell wall materials has to be coordinated with the mechanics of the cell wall that facilitate localized cell expansion only at the tip. In fact, the pollen tube cell wall is not comparable to that

of other plant cells. The most striking difference is that deposition of new cell wall components occurs along the growth axis in an accurate temporal sequence. Methyl-esterified pectins are first secreted at the apex of pollen tubes (O' Neill et al., 1990). After deposition, they are chemically converted into acid pectins at the apex/subapex edge (Rockel et al., 2008), where they bind calcium, thereby contributing to strengthen the cell wall (Palin and Geitmann, 2012; Wolf and Greiner, 2012). This prevents additional deformation of the cell wall and contributes to maintain the cylindrical shape of pollen tubes. The balance between pectin secretion and activity of pectin methyl-esterase (PME) thus yields a gradient at the pollen tube apex with highly methyl-esterified pectins at the extreme apex and a less esterified mix of polymers progressively away from the apex. As a consequence, the extreme apical wall is 'softer' than the cell wall in the pollen tube shank and, during oscillatory growth, episodes of rapid growth are preceded by local softening of the apical cell wall (Wolf and Greiner, 2012). In addition to pectins, the pollen tube cell wall contains other components such as callose, cellulose and arabinogalactan proteins. Callose is usually absent from the apex while both arabinogalactan proteins and cellulose could also be detected in the hemispherical apical dome (Mollet et al., 2013). In support of this, the cellulose synthase complex has been found close to the pollen tube apex in *Nicotiana tabacum* (Cai et al., 2011) and *Arabidopsis thaliana* (Chebli et al., 2012). A temporal analysis of secretion has been made using different methods and indicates that, as the pollen tube growth rate oscillates, so too does the exocytosis of pectin with the same period, but with a clearly different phase. An analysis of the phase relationship using cross-correlation reveals that pectin is deposited in advance of the increase in growth rate (McKenna et al., 2009; Hepler et al., 2013). While emphasis is usually focused on exocytosis, it is important to note that endocytosis is also a major contributor to pollen tube growth (Hepler et al., 2013). Based on the amount of material needed to support the ever-expanding cell wall, it becomes evident that a considerable excess of plasma membrane is delivered during the secretory process. This excess membrane is retrieved through endocytosis (Onelli and Moscatelli, 2013).

The regulatory system

Pollen grains generate pollen tubes *in vitro* in the absence of external signals, suggesting that their tip growth is controlled by a self-organizing system. Studies over the last decade have demonstrated the existence of a self-organizing signaling network, which is centered on a tip-localized Rho GTPase (ROP1) and tip-focused Ca^{2+} gradients and their interactions with the actin cytoskeleton and vesicular trafficking (Qin and Yang, 2011). Also reactive oxygen species (ROS) are involved in keeping the polarity of the process, creating a cross-talk with the Ca^{2+} gradient (Potocky et al., 2007;Lassig et al., 2014;Pottosin et al., 2014).

ROPs

ROP GTPases (also called RACs) belong to a subfamily of conserved Rho GTPases and have been established as one of the central regulators of tip growth in pollen tubes by virtue of their apical localization, their essential role for tip growth, and the spatiotemporal dynamics of their activities (Gu et al., 2003;Yan et al., 2009). These GTPases act as molecular switches by cycling between the biologically inactive GDP-bound and the active GTP-bound forms. In Arabidopsis pollen tubes, several ROPs are expressed, with the pollen-specific ROP1 playing a predominant role in determining polarity of the pollen tube at the apical plasma membrane (Li et al., 1998). Disrupting ROP1 signaling inhibits pollen tube tip growth, whereas expressing a constitutively active form of ROP1 induces a dramatically enlarged active ROP1 cap, leading to tip depolarization and balloon-like pollen tubes (Zheng and Yang, 2000;Guan et al., 2013).

ROP1 is activated at the apical region, where it activates multiple downstream pathways to determine the site and dynamics of exocytosis, which in turn leads to polarized growth. RIC3 and RIC4 interact with the active GTP-bound form of ROP1 at the apex of pollen tubes and regulate tip growth by regulating F-actin dynamics (Gu et al., 2003). The RIC4 pathway promotes F-actin assembly and induces the transport and accumulation of vesicles to the tip region. ROP1 also activates the RIC3 pathway, which promotes tip F-actin disassembly by regulating Ca^{2+} dynamics, thus facilitating the fusion of exocytic vesicles to the plasma membrane of the tip of pollen tubes (Gu et al., 2005). As a key regulator of the self-organizing pollen tube system, the activity and distribution of ROP1 are fine-tuned by both

positive and negative feedback mechanisms (Hwang et al., 2010). The positive and negative ROP1 feedbacks might be coupled through F-actin-mediated exocytosis, continuously generating the oscillation of apical ROP1 activity to sustain tip growth. Apically localized active ROP1 promotes polarized exocytosis through RIC3- and RIC4-dependent F-actin dynamics, and exocytosis. F-actin-mediated exocytosis might facilitate the recruitment factors involved in ROP1 inactivation. As a result, localized ROP1 could be further activated and the distribution of active ROP1 would expand through the apex, leading to enhanced exocytosis and promoted pollen tube growth rate. The current understanding of RopGTPase signaling leaves many unanswered questions. The mechanisms underpinning the regulation of Ca^{2+} gradients through RIC3 are still unknown, and how Ca^{2+} mediates F-actin depolymerization remains to be elucidated (Guan et al., 2013).

Calcium gradients

Cytosolic free Ca^{2+} is an important secondary messenger in the signaling networks regulating pollen tube elongation. *In vivo* pollen tube growth usually relies on external calcium stores in the pistil, and external Ca^{2+} enhances the elongation of pollen tube *in vitro* (Franklin-Tong, 1999;Iwano et al., 2009). Application of either Ca^{2+} channel blockers or Ca^{2+} ionophores inhibits pollen tube growth, indicating the requirement for fine-tuning of cytosolic Ca^{2+} concentration in the elongation of pollen tubes (Guan et al., 2013). Growing pollen tubes display a tip-focused Ca^{2+} gradient, which oscillates in a correlated but lagged phase of growing pollen tube (Malho and Trewavas, 1996;Iwano et al., 2009;Hepler et al., 2012). The interplay between active ROP GTPases and a Ca^{2+} gradient is essential for the oscillating patterns of both factors. Apical ROP1 activity oscillates ahead of both pollen tube growth and tip Ca^{2+} gradients. ROP1 activates its downstream effector RIC3 to mediate the influx of Ca^{2+} across the plasma membrane. The increase of Ca^{2+} in the tip causes F-actin disassembly, thus promoting exocytosis and regulating ROP1 activity. Elevated Ca^{2+} accumulation can then suppress ROP1 activity and balance the F-actin-dependent apical ROP1 activation (Gu et al., 2005;Hwang et al., 2010;Guan et al., 2013).

In addition to the essential regulatory function in F-actin dynamics, Ca^{2+} signals appear to be involved in most signaling processes. The Ca^{2+} binding EF-hands

motif is found in several signaling components of pollen tubes (Guan et al., 2013). Ca^{2+} is perceived by the Ca^{2+} sensor proteins that mediate downstream signaling responses or feedback regulation of Ca^{2+} gradient. Ca^{2+} sensor proteins include calmodulin, calmodulin-like, calcium-dependent protein kinase, and calcineurin B-like protein. The requirement for calmodulin and calcium-dependent protein kinase in pollen tube growth has been elucidated in several studies. However, the detailed regulatory mechanisms of Ca^{2+} sensors and their potential targets in pollen tube growth remain to be revealed (Guan et al., 2013).

The mechanisms that directly regulate tip-focused Ca^{2+} gradients are complex, and involve multiple transport systems that increase or decrease the cytosolic Ca^{2+} concentration (Iwano et al., 2009). Plasma membrane-localized Ca^{2+} channels are key regulators as they enable external Ca^{2+} to enter the cytosol. To date, the characterized Ca^{2+} influx pollen tube plasma membrane channels include the cyclic nucleotide-gated channel (CNGC) and glutamate receptor-like (GLR) channels (Frietsch et al., 2007; Michard et al., 2011). CNGCs are ion channels that function in response to the binding of cyclic nucleotides (cGMP and cAMP) and can be suppressed by elevated calcium levels together with calmodulin.

The negative regulation of tip Ca^{2+} gradient involves the efflux of Ca^{2+} on the plasma membrane and sequestering Ca^{2+} within endomembrane system, both of which may require

Ca^{2+} pumps. The plasma membrane-localized auto-inhibited Ca^{2+} ATPases (ACA) is required for the efflux of Ca^{2+} , whilst ER-localized Ca^{2+} -ATPases may play an important role in moving Ca^{2+} against its concentration gradient into the ER (Steinhorst and Kudla, 2013). Calmodulins are activated by Ca^{2+} and are involved in the regulation of Ca^{2+} gradient. Active calmodulins can negatively regulate CNGCs and positively regulate ACAs, resulting in the negative feedback regulation of cytosol Ca^{2+} gradient (Guan et al., 2013; Steinhorst and Kudla, 2013).

Reactive oxygen species

Reactive oxygen species (ROS) have long been known to play critical roles in processes involved in protecting the plant from biotic and abiotic stresses. However, ROS have also emerged as important regulators of plant development

where they play roles signal transduction and the modulation of cell wall polymer structure (Swanson and Gilroy, 2010).

ROS also play a key role during pollen tube emergence and elongation as they act as wall loosening or stiffening agents (Swanson and Gilroy, 2010; Speranza et al., 2012). In fact, hydroxyl radicals (OH^\bullet) produced in the cell wall induce cell-wall loosening both *in vitro* and *in vivo*, modulating thus the elongation of pollen tube (Schopfer, 2001). Cytoplasmic ROS are mostly produced by mitochondria, chloroplasts and peroxisomes while plasma membrane NADPH-oxidases (NOX) are instead an important source for both cell wall and cytoplasmic ROS. In fact, they produce superoxide anions, $\text{O}_2^{\bullet-}$, the precursor of both OH^\bullet and hydrogen peroxide (H_2O_2), an important signalling molecule (Potocky et al., 2007). The involvement of ROS during pollen tube growth was first speculated by evidences that showed how they localize in the apex of the tube and how the inhibition of NOX by Diphenylene Iodonium chloride (DPI) suddenly arrests tip growth and alters the morphology of the pollen tube (Potocky et al., 2007; Speranza et al., 2012). Moreover, there is a correlation between ROS and Ca^{2+} signaling, that is also essential for plant development and tip-growth, since ROS induce Ca^{2+} influx across cell membranes (Foreman et al., 2003), and cytosolic Ca^{2+} can activate NOX; establishing a positive feedback between NOX activity and ROS-induced Ca^{2+} influx, that supports polarized growth (Kaya et al., 2014; Lassig et al., 2014; Pottosin and Shabala, 2014). Moreover, to avoid an excess of ROS that could lead to oxidative damage, pollen has a powerful antioxidant machinery based on superoxide dismutase (SOD) that catalyzes the dismutation of $\text{O}_2^{\bullet-}$ into H_2O_2 ; the latter is decomposed to water and oxygen by catalase (CAT).

References

- Åström, H., Sorri, O., and Raudaskoski, M. (1995). Role of microtubules in the movement of the vegetative nucleus and generative cell in tobacco pollen tubes. *Sex Plant Reprod* 8, 61–69.
- Bove, J., Vaillancourt, B., Kroeger, J., Hepler, P.K., Wiseman, P.W., and Geitmann, A. (2008). Magnitude and direction of vesicle dynamics in growing pollen tubes using spatiotemporal image correlation spectroscopy and fluorescence recovery after photobleaching. *Plant Physiol* 147, 1646-1658.

- Buitink, J., Leprince, O., Hemminga, M.A., and Hoekstra, F.A. (2000). The effects of moisture and temperature on the ageing kinetics of pollen: Interpretation based on cytoplasmic mobility. *Plant Cell Environ* 23, 967–974.
- Cai, G., and Cresti, M. (2009). Organelle motility in the pollen tube: a tale of 20 years. *J Exp Bot* 60, 495-508.
- Cai, G., Faleri, C., Del Casino, C., Emons, A.M., and Cresti, M. (2011). Distribution of callose synthase, cellulose synthase, and sucrose synthase in tobacco pollen tube is controlled in dissimilar ways by actin filaments and microtubules. *Plant Physiol* 155, 1169-1190.
- Cai, G., Parrotta, L., and Cresti, M. (2015). Organelle trafficking, the cytoskeleton, and pollen tube growth. *J Integr Plant Biol* 57, 63-78.
- Chebli, Y., Kaneda, M., Zerzour, R., and Geitmann, A. (2012). The cell wall of the Arabidopsis pollen tube-spatial distribution, recycling, and network formation of polysaccharides. *Plant Physiol* 160, 1940-1955.
- Cheung, A.Y., and Wu, H.M. (2008). Structural and signaling networks for the polar cell growth machinery in pollen tubes. *Annu Rev Plant Biol* 59, 547-572.
- Cresti, M., Pacini, E., Ciampolini, F., and Sarfatti, G. (1977). Germination and early tube development in vitro of *Lycopersicon peruvianum* pollen: Ultrastructural features. *Planta* 136, 239-247.
- Dickinson, H. (1995). Dry stigmas, water and self-incompatibility in Brassica. *Sex. Plant Reprod.* 8, 1–10.
- Dixit, R., Rizzo, C., Nasrallah, M., and Nasrallah, J. (2001). The brassica MIP-MOD gene encodes a functional water channel that is expressed in the stigma epidermis. *Plant Mol Biol* 45, 51-62.
- Edlund, A.F., Swanson, R., and Preuss, D. (2004). Pollen and stigma structure and function: the role of diversity in pollination. *Plant Cell* 16 Suppl, S84-97.
- Fiebig, A., Kimport, R., and Preuss, D. (2004). Comparisons of pollen coat genes across Brassicaceae species reveal rapid evolution by repeat expansion and diversification. *Proc Natl Acad Sci U S A* 101, 3286-3291.
- Foreman, J., Demidchik, V., Bothwell, J.H., Mylona, P., Miedema, H., Torres, M.A., Linstead, P., Costa, S., Brownlee, C., Jones, J.D., Davies, J.M., and Dolan, L. (2003). Reactive oxygen species produced by NADPH oxidase regulate plant cell growth. *Nature* 422, 442-446.
- Franklin-Tong, V.E. (1999). Signaling and the modulation of pollen tube growth. *Plant Cell* 11, 727-738.
- Frietsch, S., Wang, Y.F., Sladek, C., Poulsen, L.R., Romanowsky, S.M., Schroeder, J.I., and Harper, J.F. (2007). A cyclic nucleotide-gated channel is essential for polarized tip growth of pollen. *Proc Natl Acad Sci U S A* 104, 14531-14536.
- Fu, Y. (2010). The actin cytoskeleton and signaling network during pollen tube tip growth. *J Integr Plant Biol* 52, 131-137.
- Fu, Y. (2015). The cytoskeleton in the pollen tube. *Curr Opin Plant Biol* 28, 111-119.
- Gossot, O., and Geitmann, A. (2007). Pollen tube growth: coping with mechanical obstacles involves the cytoskeleton. *Planta* 226, 405–416.
- Grote, M., Valenta, R., and Reichelt, R. (2003). Abortive pollen germination: a mechanism of allergen release in birch, alder, and hazel revealed by immunogold electron microscopy. *J Allergy Clin Immunol* 111, 1017-1023.

- Grote, M., Vrtala, S., Niederberger, V., Valenta, R., and Reichelt, R. (2000). Expulsion of allergen-containing materials from hydrated rye grass (*Lolium perenne*) pollen revealed by using immunogold field emission scanning and transmission electron microscopy. *J Allergy Clin Immunol* 105, 1140-1145.
- Gu, Y., Fu, Y., Dowd, P., Li, S., Vernoud, V., Gilroy, S., and Yang, Z. (2005). A Rho family GTPase controls actin dynamics and tip growth via two counteracting downstream pathways in pollen tubes. *J Cell Biol* 169, 127-138.
- Gu, Y., Vernoud, V., Fu, Y., and Yang, Z. (2003). ROP GTPase regulation of pollen tube growth through the dynamics of tip-localized F-actin. *J Exp Bot* 54, 93-101.
- Guan, Y., Guo, J., Li, H., and Yang, Z. (2013). Signaling in pollen tube growth: crosstalk, feedback, and missing links. *Mol Plant* 6, 1053-1064.
- Hepler, P.K., Kunkel, J.G., Rounds, C.M., and Winship, L.J. (2012). Calcium entry into pollen tubes. *Trends Plant Sci* 17, 32-38.
- Hepler, P.K., Rounds, C.M., and Winship, L.J. (2013). Control of cell wall extensibility during pollen tube growth. *Mol Plant* 6, 998-1017.
- Hepler, P.K., Vidali, L., and Cheung, A.Y. (2001). Polarized cell growth in higher plants. *Annu Rev Cell Dev Biol* 17, 159-187.
- Heslop-Harrison, J. (1979). An interpretation of the hydrodynamics of pollen. *Am. J. Bot.* 66, 737-743.
- Hwang, J.U., Wu, G., Yan, A., Lee, Y.J., Grierson, C.S., and Yang, Z. (2010). Pollen-tube tip growth requires a balance of lateral propagation and global inhibition of Rho-family GTPase activity. *J Cell Sci* 123, 340-350.
- Idilli, A.I., Morandini, P., Onelli, E., Rodighiero, S., Caccianiga, M., and Moscatelli, A. (2013). Microtubule depolymerization affects endocytosis and exocytosis in the tip and influences endosome movement in tobacco pollen tubes. *Mol Plant* 6, 1109-1130.
- Iwano, M., Entani, T., Shiba, H., Kakita, M., Nagai, T., Mizuno, H., Miyawaki, A., Shoji, T., Kubo, K., Isogai, A., and Takayama, S. (2009). Fine-tuning of the cytoplasmic Ca²⁺ concentration is essential for pollen tube growth. *Plant Physiol* 150, 1322-1334.
- Johnson, S.A., and McCormick, S. (2001). Pollen germinates precociously in the anthers of raring-to-go, an Arabidopsis gametophytic mutant. *Plant Physiol* 126, 685-695.
- Kaya, H., Nakajima, R., Iwano, M., Kanaoka, M.M., Kimura, S., Takeda, S., Kawarazaki, T., Senzaki, E., Hamamura, Y., Higashiyama, T., Takayama, S., Abe, M., and Kuchitsu, K. (2014). Ca²⁺-activated reactive oxygen species production by Arabidopsis RbohH and RbohJ is essential for proper pollen tube tip growth. *Plant Cell* 26, 1069-1080.
- Laitinen, E., Nieminen, K.M., Vihinen, H., and Raudaskoski, M. (2002). Movement of generative cell and vegetative nucleus in tobacco pollen tubes is dependent on microtubule cytoskeleton but independent of the synthesis of callose plugs. *Sex Plant Reprod* 15, 195-204.
- Lassig, R., Gutermuth, T., Bey, T.D., Konrad, K.R., and Romeis, T. (2014). Pollen tube NAD(P)H oxidases act as a speed control to dampen growth rate oscillations during polarized cell growth. *Plant J* 78, 94-106.
- Li, H., Wu, G., Ware, D., Davis, K.R., and Yang, Z. (1998). Arabidopsis Rho-related GTPases: differential gene expression in pollen and polar localization in fission yeast. *Plant Physiol* 118, 407-417.

- Malho, R., and Trewavas, A.J. (1996). Localized Apical Increases of Cytosolic Free Calcium Control Pollen Tube Orientation. *Plant Cell* 8, 1935-1949.
- Mayfield, J.A., Fiebig, A., Johnstone, S.E., and Preuss, D. (2001). Gene families from the *Arabidopsis thaliana* pollen coat proteome. *Science* 292, 2482-2485.
- Mckenna, S.T., Kunkel, J.G., Bosch, M., Rounds, C.M., Vidali, L., Winship, L.J., and Hepler, P.K. (2009). Exocytosis precedes and predicts the increase in growth in oscillating pollen tubes. *Plant Cell* 21, 3026-3040.
- Michard, E., Lima, P.T., Borges, F., Silva, A.C., Portes, M.T., Carvalho, J.E., Gilliam, M., Liu, L.H., Obermeyer, G., and Feijo, J.A. (2011). Glutamate receptor-like genes form Ca^{2+} channels in pollen tubes and are regulated by pistil D-serine. *Science* 332, 434-437.
- Mollet, J.C., Leroux, C., Dardelle, F., and Lehner, A. (2013). Cell Wall Composition, Biosynthesis and Remodeling during Pollen Tube Growth. *Plants (Basel)* 2, 107-147.
- Müller, F., and Rieu, I. (2016). Acclimation to high temperature during pollen development. *Plant Reprod* 29, 107-118.
- O' Neill, M.A., Albersheim, P., and Darvill, A. (1990). The pectic polysaccharides of primary cell walls. . *Methods in Plant Biochemistry, Carbohydrates, Dey P.M., Harborne J.B, editors. , eds (London: Academic Press;) , pp. 415–441.*
- Onelli, E., and Moscatelli, A. (2013). Endocytic Pathways and Recycling in Growing Pollen Tubes. *Plants (Basel)* 2, 211-229.
- Palin, R., and Geitmann, A. (2012). The role of pectin in plant morphogenesis. *Biosystems* 109, 397-402.
- Potocky, M., Jones, M.A., Bezdova, R., Smirnov, N., and Zarsky, V. (2007). Reactive oxygen species produced by NADPH oxidase are involved in pollen tube growth. *New Phytol* 174, 742-751.
- Pottosin, I., and Shabala, S. (2014). Polyamines control of cation transport across plant membranes: implications for ion homeostasis and abiotic stress signaling. *Front Plant Sci* 5, 154.
- Pottosin, I., Velarde-Buendia, A.M., Bose, J., Zepeda-Jazo, I., Shabala, S., and Dobrovinskaya, O. (2014). Cross-talk between reactive oxygen species and polyamines in regulation of ion transport across the plasma membrane: implications for plant adaptive responses. *J Exp Bot* 65, 1271-1283.
- Qin, Y., and Yang, Z. (2011). Rapid tip growth: insights from pollen tubes. *Semin Cell Dev Biol* 22, 816-824.
- Radauer, C., and Breiteneder, H. (2006). Pollen allergens are restricted to few protein families and show distinct patterns of species distribution. *J Allergy Clin Immunol* 117, 141-147.
- Rockel, N., Wolf, S., Kost, B., Rausch, T., and Greiner, S. (2008). Elaborate spatial patterning of cell-wall PME and PME1 at the pollen tube tip involves PME1 endocytosis, and reflects the distribution of esterified and de-esterified pectins. *Plant J* 53, 133-143.
- Schopfer, P. (2001). Hydroxyl radical-induced cell-wall loosening in vitro and in vivo: implications for the control of elongation growth. . *The Plant Journal* 28, 679–688.
- Sheoran, I.S., Pedersen, E.J., Ross, A.R., and Sawhney, V.K. (2009). Dynamics of protein expression during pollen germination in canola (*Brassica napus*). *Planta* 230, 779-793.
- Speranza, A., Crinelli, R., Scoccianti, V., and Geitmann, A. (2012). Reactive oxygen species are involved in pollen tube initiation in kiwifruit. *Plant Biol (Stuttg)* 14, 64-76.

- Staiger, C.J., and Blanchoin, L. (2006). Actin dynamics: old friends with new stories. *Curr Opin Plant Biol* 9, 554-562.
- Staiger, C.J., Poulter, N.S., Henty, J.L., Franklin-Tong, V.E., and Blanchoin, L. (2010). Regulation of actin dynamics by actin-binding proteins in pollen. *J Exp Bot* 61, 1969-1986.
- Steinhorst, L., and Kudla, J. (2013). Calcium - a central regulator of pollen germination and tube growth. *Biochim Biophys Acta* 1833, 1573-1581.
- Swanson, S., and Gilroy, S. (2010). ROS in plant development. *Physiol Plant* 138, 384-392.
- Vega-Maray, A.M., Fernandez-Gonzalez, D., Valencia-Barrera, R., and Suarez-Cervera, M. (2006). Detection and release of allergenic proteins in *Parietaria judaica* pollen grains. *Protoplasma* 228, 115-120.
- Vidali, L., and Hepler, P.K. (2001). Actin and pollen tube growth. *Protoplasma* 215, 64-76.
- Vidali, L., Mckenna, S.T., and Hepler, P.K. (2001). Actin polymerization is essential for pollen tube growth. *Mol Biol Cell* 12, 2534-2545.
- Wang, Q., Kong, L., Hao, H., Wang, X., Lin, J., Samaj, J., and Baluska, F. (2005). Effects of brefeldin A on pollen germination and tube growth. Antagonistic effects on endocytosis and secretion. *Plant Physiol* 139, 1692-1703.
- Wolf, S., and Greiner, S. (2012). Growth control by cell wall pectins. *Protoplasma* 249 Suppl 2, S169-175.
- Yan, A., Xu, G., and Yang, Z.B. (2009). Calcium participates in feedback regulation of the oscillating ROP1 Rho GTPase in pollen tubes. *Proc Natl Acad Sci U S A* 106, 22002-22007.
- Zheng, Z.L., and Yang, Z. (2000). The Rop GTPase: an emerging signaling switch in plants. *Plant Mol Biol* 44, 1-9.

PART I

Pollen as a model of study and polyamines as a tool

Chapter 1

Polyamines in pollen: from microsporogenesis to fertilization

This chapter is based on:

I. Aloisi , G. Cai, D. Serafini-Fracassini and S. Del Duca, *Front. Plant Sci.* **7**:155 (2016)

Abstract

The entire pollen life span is driven by polyamine (PA) homeostasis, achieved through fine regulation of their biosynthesis, oxidation, conjugation, compartmentalization, uptake, and release. The critical role of PAs, from microsporogenesis to pollen–pistil interaction during fertilization, is suggested by high and dynamic transcript levels of PA biosynthetic genes, as well as by the activities of the corresponding enzymes. Moreover, exogenous supply of PAs strongly affects pollen maturation and pollen tube elongation. A reduction of endogenous free PAs impacts pollen viability both in the early stages of pollen development and during fertilization. A number of studies have demonstrated that PAs largely function by modulating transcription, by structuring pollen cell wall, by modulating protein (mainly cytoskeletal) assembly as well as by modulating the level of reactive oxygen species. Both free low-molecular weight aliphatic PAs, and PAs conjugated to proteins and hydroxyl-cinnamic acids take part in these complex processes. Here, we review both historical and recent evidence regarding molecular events underlying the role of PAs during pollen development. In the concluding remarks, the outstanding issues and directions for future research that will further clarify our understanding of PA involvement during pollen life are outlined.

Forms, molecular partners, and tasks of polyamines

In plant cells, metabolism of aliphatic PAs occurs in the cytosol and organelles (Figure 1A); Put has an aliphatic tetra methylene backbone deriving directly from ornithine or indirectly from arginine or citrulline via N-carbamoylputrescine. The biosynthesis of higher PAs occurs by the addition of one or two amino propyl groups to Put to form Spd and Spm, respectively. Whereas Put has positive charges on the primary amino groups, Spd and Spm also bear protonated internal iminic groups, at physiological pH. PAs are present in cells in both free and bound forms and their molecular mechanism of action is often associated with their polycationic groups able to establish hydrogen and ionic interactions with anionic groups of several biological molecules, among which proteins, nucleic acids, and membrane phospholipids. Moreover, they strongly bind *in vitro* to cell wall polysaccharides with a different binding capacity depending mainly upon the number of their positive charges. In addition, the covalent binding to some glutamyl residues of specific proteins, catalyzed by TGase, gives rise either to PA binding to proteins (mono- γ glutamyl-PAs) or to cross-links between proteins (bis- γ glutamyl-PAs) (Figure1B). These conjugates are components of the PCA-insoluble PA fraction (Del Duca *et al.*, 2014). Covalent binding of PAs to phenylpropanoids, such as HCA, abundant in many plant families, give rise to hydroxyl-cinnamicacids amides (HCAAs) (Figure1C), components of the PCA-soluble fractions. These are involved in the organization of the cell wall and are associated to fertility (Martin-Tanguy, 2001; Grienberger *et al.*, 2009). In plant cells, PAs are mostly stored in the vacuole and in the cell wall, but Spm is present also in the nucleus (Belda-Palazon *et al.*, 2012). PAs play a molecular stabilizing role by crossing the DNA double helix and covalently binding to histones, thus controlling transcription. Moreover, PAs are believed to act as radical scavengers thereby protecting DNA from ROS (Das and Misra, 2004). During catabolism, PAs and in particular Spm, are suggested as a source of free radicals (Takahashi and Kakehi, 2010). The role of PAs in plant cell life, therefore, appears multifaceted; in some instances, they act as pro-survival molecules, whereas in others they accelerate PCD (Cai *et al.*, 2015a). Indeed, it is

not astonishing that the perturbation of PA homeostasis influences many fundamental cell processes (Tiburcio *et al.*, 2014), such as organogenesis, cell proliferation, differentiation, senescence/PCD, and stress- and external stimuli-induced homeostatic adjustments. Special issues on PAs have been reported (<http://www.sciencedirect.com/science/journal/09819428/48/7>). Polyamines also control many aspects of pollen development, both under normal and stress conditions. Here, we summarize the involvement of PAs during the entire developmental program and functioning of pollen.

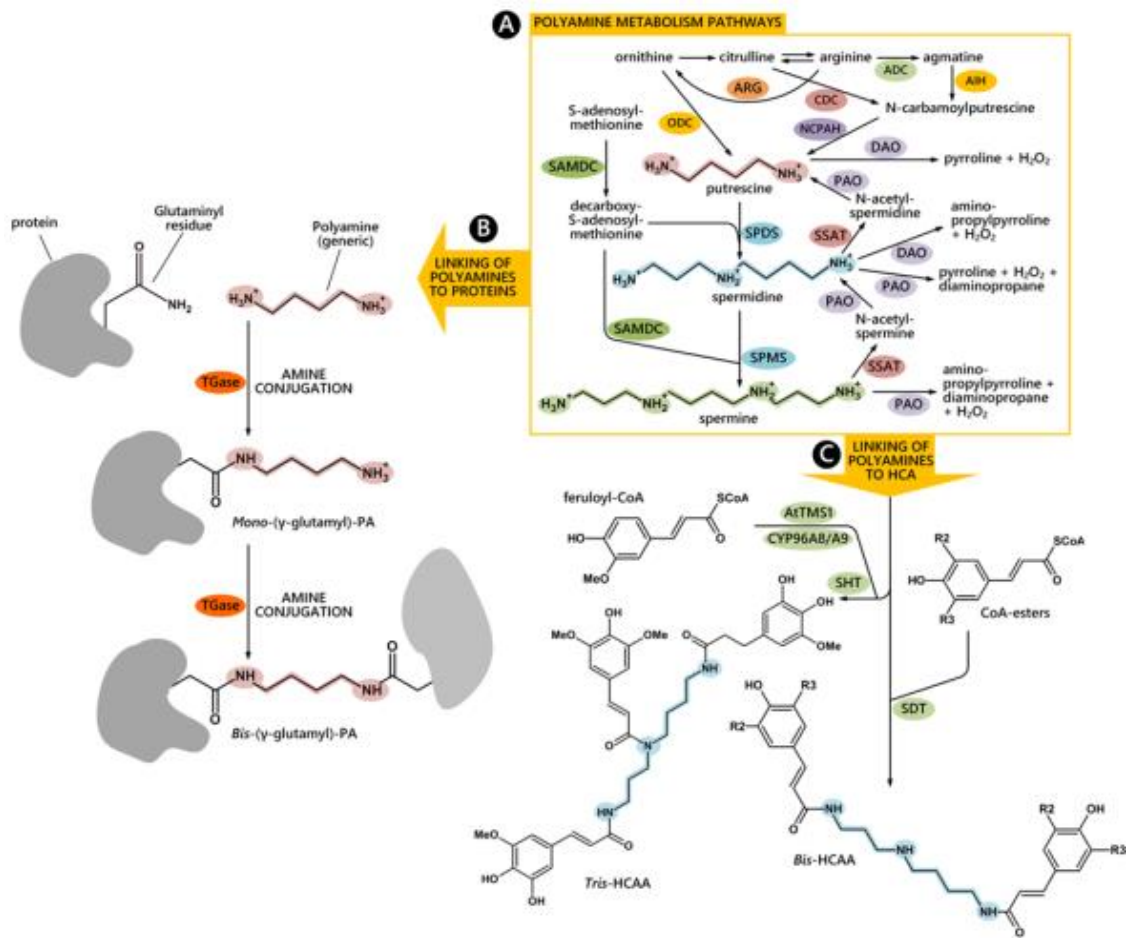


FIGURE 1. PAs metabolism and their conjugating pathways to proteins and to hydroxyl-cinnamic acids (HCA). Free PA biosynthetic and catabolic pathways are highlighted in the yellow rectangle (A). The covalent binding to glutamyl residues of proteins gives rise to mono- γ glutamyl-PAs or to cross-links between proteins (bis- γ glutamyl-PAs) (B). The biosynthetic pathway of hydroxyl-cinnamic acids amides (HCAAs) in *Arabidopsis thaliana* stamens is reported according to Fellenberg *et al.* (2012) (C). ADC, arginine decarboxylase; ARG, arginase; AIH, agmatine imino-hydrolase; CDC, citrulline decarboxylase; NCPAH, N-carbamoylputrescine amidohydrolase; ODC, ornithine decarboxylase; SAMDC, S-adenosylmethionine decarboxylase; SPDS, spermidine synthase; SPMS, spermine synthase; PAO, polyamine oxidase; SSAT, spermidine/spermine N¹-acetyltransferase; DAO, diamine oxidase; TGase, transglutaminase; SHT, Spd hydroxycinnamoyl transferase; CYP98A8/CYP98A9, P450 cytochromes; AtTMS1, *Arabidopsis thaliana* tapetum-specific methyl transferase, SDT, spermidine disinapoyl transferase.

Polyamines in pollen

Microsporogenesis

Transcripts for enzymes involved in PA biosynthetic and oxidative metabolisms are present starting from the early pollen stages as observed during *Nicotiana tabacum* pollen formation inside the anthers (Figure2A). At the stage of uninucleate microspore, transcripts for enzymes involved in the biosynthesis of PAs, mostly Put, have been found, namely transcripts for ADC and ODC (Bokvaj *et al.*, 2015) (Figure2B). At the bicellular pollen stages, other transcripts are present for the oxidative metabolism of Put (e.g., DAO) (Figures1A and 2C); additional transcripts for enzymes that participate in the urea cycle and metabolism of amino groups (e.g., *N*-carbamoylputrescine amidase) are also present (Figure1A). Both the sporophytic tapetal layer of the anther and the gametophyte contribute to the formation of the pollen grain cell wall, consisting of the inner intine and the outer exine layers. This process is not only strictly related to the deposition of cell wall components necessary for fertilization and protection against biotic and abiotic stresses, but is also essential for enzymatic reactions. When present, tryphine, the soluble part of the pollen exine, is the preferential accumulation site of soluble HCAAs. Recent studies in *Arabidopsis thaliana* demonstrated that HCAAs are exported from the tapetum prior to dehiscence of the anthers, which occurs by PCD (Quilichini *et al.*, 2014). HCAAs form a highly variable mixture, made of at least 30 different (HCA)-Spd conjugates (Handrick *et al.*, 2010) (Figure1C). These compounds were shown to crosslink different cell wall polymers via ester and ether linkages, suggesting a role in modulating the rigidity of the cell wall (Moschou *et al.*, 2012). The enzyme SHT (Figure1C), catalyzing the conjugation of hydroxycinnamoyl CoA to Spd in anthers, was recently shown to take part in the organization of the cell wall. The sht mutant displayed irregularities, depressions and decreased auto-fluorescence of the pollen grain (Grienenberger *et al.*, 2009). It also displayed disappearance of tris-HCAAs from Spd conjugates, whereas the qualitative and quantitative pattern of bis-HCAAs was much less affected (Handrick *et al.*, 2010). These conjugates have been found sporadically in other species but their role remains to be established (Fellenberg and Vogt, 2015). Elejalde-Palmett *et al.* (2015) showed that an acyltransferase of *Malus domestica*

was able to complement the *sht* mutant of *Arabidopsis thaliana*. Based on bioinformatic analyses of putative *SHT* orthologs, authors showed a genetic linkage among *SHT* sequences and argued for a common ancestral origin of the *SHT* gene in a common core Eudicotyledon ancestor (Elejalde-Palmett *et al.*, 2015). Recently, a second transferase, Spd disinapoyl transferase (SDT), was shown to be considerably expressed in stamens and involved in the formation of HCAAs (Fellenberg *et al.*, 2012). In addition to the reaction catalyzed by SHT/SDT, at least two subsequent reactions that add phenolic rings were shown to be catalyzed by tapetum-specific CYP98A8/CYP98A9 (Matsuno *et al.*, 2009) and an AtTMS1 (Fellenberg *et al.*, 2008) (Figure 1C). Recently, the biosynthetic pathway of (HCA)-Spd based on the analysis of several *Arabidopsis* knock-out mutants was proposed (Fellenberg *et al.*, 2009). PAs were thus shown to contribute directly to wall architecture. It was, however, proposed that they also control wall stiffening indirectly by regulating PME (Figure 2G) (Charnay *et al.*, 1992). When oxidized by PAO, PAs may play an additional role during pollen development in so far as the reaction product H₂O₂ is involved in cell wall stiffening. Pollen PAOs (Wu *et al.*, 2010; Fincato *et al.*, 2012), but also apoplastic PAOs secreted from the anther, appear to be involved (Figure 2C). In *Oryza sativa* seven PAO isoforms have been identified, and one of these, OsPAO7, is specifically expressed in anthers, with an expression peak at the bicellular pollen stage (Figure 2C); OsPAO7 produces H₂O₂ about 100 times more efficiently than other PAO isoforms (Cona *et al.*, 2006; Liu *et al.*, 2014). In the dioecious kiwifruit, Put and Spd represent biochemical markers for male sterility in female plants by being involved in female pollen degeneration. During microgametogenesis, ADC, ODC, and SAMDC, the latter involved in Spd/Spm biosynthesis (Figure 1A) are active. The aborted pollen grains showed high SAMDC activity in wall residues, while functional pollen (from the male-fertile anthers) showed low SAMDC activity, suggesting a possible regulatory role of Spd in the functionality of kiwifruit pollen (Falasca *et al.*, 2010). The involvement of tapetal SAMDC in pollen development and male fertility was also demonstrated in tomato by RNAi techniques. Down-regulation of several tapetal SAMDC homologs not only led to reduction in cellular PA levels, particularly in the bound and conjugated forms, but also caused partial or complete male sterility in transgenic plants. RNAi-mediated down-regulated SAMDC lines showed morphological

abnormalities only in the pollen grains, which were shrunken and distorted (Sinha and Rajam, 2013).

Quiescence and viability

Pollen can be stored for extended periods without loss of viability under dry and low-temperature conditions leading to reduced metabolism. PAs may contribute to maintaining viability during natural quiescence and/or storage (Figure2D), when the main PA biosynthetic enzymes (i.e., ADC, ODC and SAMDC) were present and active *in vitro* (Falasca *et al.*, 2010). Two different SAMDC gene transcripts were highly expressed together with weak ADC transcription. The combined application in planta of competitive inhibitors of SAMD (methylglyoxal-bis guanylhydrazone) and Spd synthase (SPDS) (cyclohexylamine), or D-arginine (inhibitor of Put synthesis) led to abnormal pollen grains in male-fertile plants with reduced viability and germination (Falasca *et al.*, 2010). Reduced pollen viability was associated to a lower activity of the PA biosynthetic enzymes upon rehydration; in fact, exogenous PAs applied to germination medium were able to restore germination and fertilization of aged pollen grains (Song and Tachibana, 2007) (Figure2D).

Pollen rehydration and pollen tube emergence

Different RNAs and proteins are synthesized at the onset of pollen germination (Linskens *et al.*, 1968; Bagni *et al.*, 1981). Spd was shown to play a role in male gametophyte development of *Marsilea vestita*, a heterosporous fern, by unmasking the translationally inhibited stored mRNAs (Deeb *et al.*, 2010; Boothby *et al.*, 2013). Spd was hypothesized, but not demonstrated, to play a similar role in pollen of flowering plants. It is noteworthy that inhibition of pollen germination by the transcriptional inhibitor actinomycin D (Speranza *et al.*, 1986) or by the protein synthesis inhibitor cycloheximide could be overcome by treatment with exogenous Spd and Spm (Song and Tachibana, 2007). High activities of PA biosynthetic enzymes, in particular during the very early stages of germination, were detected in different pollens (Bagni *et al.*, 1981; Falasca *et al.*, 2010) (Figure2E). Moreover, the inhibition of PA biosynthetic enzymes by bis (guanylhydrazone) strongly affected pollen germination (Antognoni and Bagni, 2008). Despite high

biosynthetic enzyme activities, the amount of both free and bound Spd was shown to decrease concomitantly. The PA was released into the germination medium together with RNAs, neo-synthesized proteins (Bagni *et al.*, 1986), and TGase, suggesting their possible involvement in pollen tube/style adhesion (Di Sandro *et al.*, 2010). In general, profiles of PAs, RNAs, and proteins during germination seem to be finely co-regulated. As PA homeostasis must be finely tuned, exogenous application of PAs has dramatic effects on pollen germination. Low concentrations of exogenous PAs were often shown to stimulate pollen tube emergence while high concentrations drastically altered tube growth and morphology (Antognoni and Bagni, 2008; Wu *et al.*, 2010; Rodriguez-Enriquez *et al.*, 2013; Aloisi *et al.*, 2015). It was suggested that Spd could increase *in vitro* pollen germination by reducing local effects of pollen density, which negatively affects this process (Rodriguez-Enriquez *et al.*, 2013). Interestingly, both RNA and protein biosynthesis (Bagni *et al.*, 1981) were shown to be stimulated by addition of Spd, but were inhibited by an excess of Spm, as first observed in *Petunia* (Linskens *et al.*, 1968). Because PAs (which can also be RNA bound) promote both transcription and translation, a positive feedback could be hypothesized (Bagni *et al.*, 1973, 1986). It has been proposed that Spd and Put may play a role in the developmental change from monosomes to polysomes, the process needed for active protein synthesis during pollen tube germination (Falasca *et al.*, 2010).

Pollen tube growth

A strict regulation of the influx/efflux of inorganic ions (mostly Ca^{2+} and K^{+}) across the plasma membranes, the apical pool of ROS (Potocky *et al.*, 2007) and a highly dynamic and polarized cytoskeleton ensure polarized growth at the pollen tube apex. In Rosaceae, the effect of exogenous PAs during pollen tube growth seems multifactorial and was shown to involve the organization and assembly of the cytoskeleton (Del Duca *et al.*, 2009) and cell wall deposition (Di Sandro *et al.*, 2010). The action of PAs is at least in part mediated by TGase that is present in distinct cell sites, including cytosol, organelles, membranes and cell walls, all involved in PA metabolism. TGase was reported to mediate pollen germination and pollen–style interactions (Del Duca *et al.*, 2013) (Figures 2F, G). In fact, during

pollen tube growth, the activity of cytoplasmic TGase was mainly detected in the tube apex and in the region closest to the grain. PA conjugation to actin and tubulin, catalyzed by TGase, affected their ability to assemble and their interaction with motor proteins both *in vivo* and *in vitro* (Del Duca *et al.*, 2009). TGase, co-localizing with pectins and arabinogalactan-proteins in the cell wall, was released during tube elongation (Del Duca *et al.*, 2013). This extra-cellular TGase and its products localized as aggregates at the surface of *Malus domestica* pollen tubes. As specific TGase inhibitors blocked tube growth, a role for TGase in tip growth and in the reinforcement of the cell wall, supporting the migration of pollen tubes through the style, was proposed (Del Duca *et al.*, 2013) (Figures 2F,G). Moreover, pollen TGase secreted into the medium catalyzed the covalent linkage of PAs to released proteins and their cross-linking *in vitro*. This feature may contribute to regulating the pollen tube-style interaction (Di Sandro *et al.*, 2010). In addition, PAs might also control the assembly and properties of cell wall polysaccharides, such as pectins, which bind to PAs by ionic linkages (D'Orazi and Bagni, 1987). In cell walls of soybean, positively charged PAs competed with acidic pectins in binding calcium ions; moreover, PAs were reported to regulate the activity of PME, thereby leading to decreased levels of acidic pectins and, therefore, to softer cell walls (Charnay *et al.*, 1992) (Figure 2G). In *Arabidopsis thaliana* pollen tubes, exogenously supplied Spd increased the concentration of cytosolic Ca²⁺; Spd oxidation by PAO generated H₂O₂, which activated Ca²⁺ channels, thus inducing Ca²⁺ influx beyond optimal levels and causing the inhibition of tube growth. Activation of Ca²⁺ currents by Spd was significantly disrupted in *pao* knock-out mutants, but Ca²⁺ channels could still be activated following application of H₂O₂ (Wu *et al.*, 2010). Spm was the most effective PA in inhibiting pear pollen tube elongation (Aloisi *et al.*, 2015). Spm rapidly entered the pollen tube tip and caused swelling of the apex, suggesting cell wall relaxation. Spm rapidly induced ROS formation (Pottosin *et al.*, 2014; Aloisi *et al.*, 2015), causing the reduction of pollen viability, followed by activation of the antioxidant machinery. The final event after Spm supply was the degradation of nuclear DNA leading to cell death; this process was proposed to be induced either by Ca²⁺-activated signaling or by the altered redox state (Aloisi *et al.*, 2015).

Pollen–pistil interaction during fertilization and self-Incompatibility

When pollens land on an incompatible stigma they may undergo the Self Incompatibility (SI) response. This is the most important evolutionary system of the Angiosperms to prevent inbreeding and requires a species-specific cell–cell recognition system. The female determinants can be either a cell membrane receptor as in *Papaver rhoeas* or a released molecule, such as stigma/style ribonucleases (termed S-RNases) in Solanaceae, Rosaceae and Plantaginaceae; they enter the pollen and are degraded in compatible pollen while they are active in incompatible ones causing the degradation of pollen RNA (Dresselhaus and Franklin-Tong, 2013). The involvement of PAs in the SI response has been reported both in *Pyrus communis* and in *Citrus grandis*. In *Pyrus communis* the content of free PAs (Put and Spm) was lower during incompatible as compared to compatible pollination (Figures 2F, G). This could be related to the inhibitory effect of PAs on RNases; in fact, Put and Spd, and, even more, Spm, have been shown to halve the activity of RNase in *Malus domestica* pollen (Speranza *et al.*, 1984), as also observed in *Solanum tuberosum* (Altman, 1982). The accumulation of PCA-soluble PAs in reproductive organs, and particularly in pollen, has been associated with fertility. Triferuloyl-Spd, a HCAA of tryphine, is involved in pollination and in pollen–stigma interaction. Moreover, the amount of PCA-soluble PAs was lower in SI-pollinated styles compared to compatible pollinated ones. In the SI-pollination styles, an increase of PCA-insoluble PAs and a higher TGase activity were also observed, concomitantly with the arrest of tube growth and the appearance of a TGase plug at the tip (Del Duca *et al.*, 2010). In contrast to compatible pollination, SI pollination in *Citrus grandis* was characterized by higher amounts of PCA-insoluble PAs, enhanced TGase activity, and increased production of glutamyl-PAs, together with arrested pollen tube growth (Gentile *et al.*, 2012). The direct involvement of the cytoskeleton in SI was so far solely reported in incompatible *Papaver* tubes, where a high Ca^{2+} influx took place after pollen–stigma interaction. Subsequently, F-actin foci were formed by a still uncharacterized cross-linking mechanism, leading to the arrest of tube elongation and to pollen PCD (McClure and Franklin-Tong, 2006). Since enhanced Ca^{2+} influx is a general feature of the SI response, this could account for the fact that activity of TGase (which is a Ca^{2+} -

dependent enzyme) was stimulated in *Pyrus communis* and *Citrus grandis*. This could have led to cross-links among cytoskeleton proteins, generating high-mass aggregates, similar to the actin foci observed in *Papaver*, and forming the tube tip plug (Del Duca *et al.*, 2014; Cai *et al.*, 2015b).

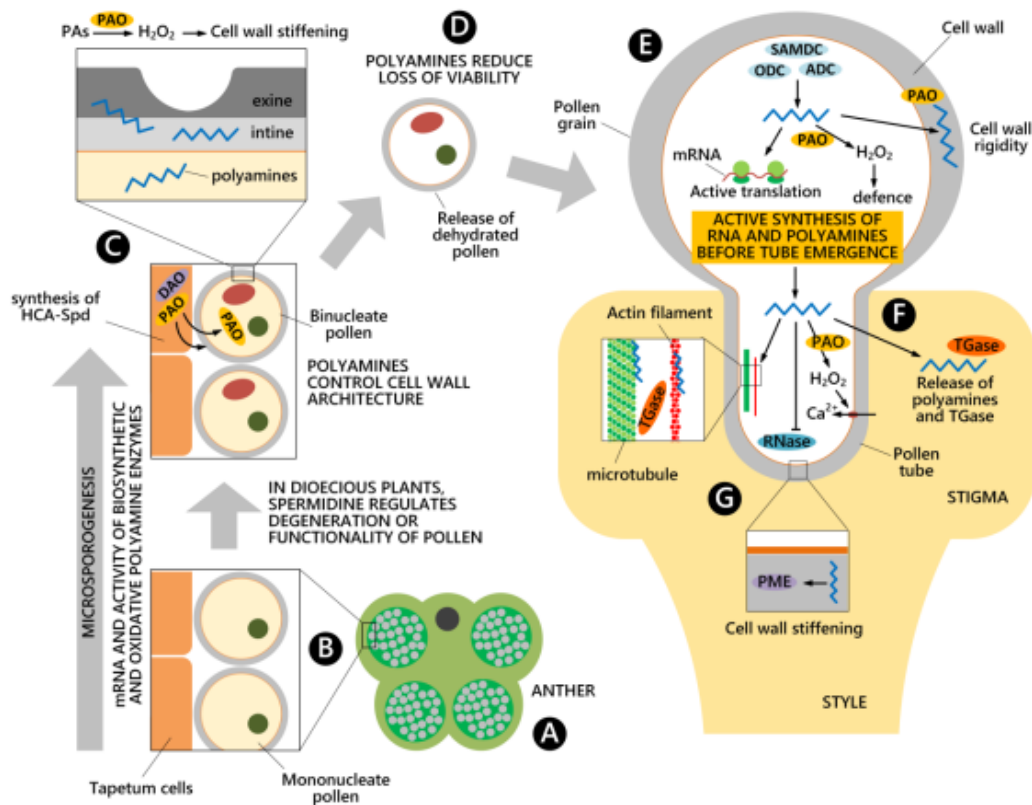


FIGURE 2. Polyamine involvement during pollen development. PA biosynthetic and oxidative metabolisms occur from the early stage of pollen formation inside the anthers (A), when both microspores and the tapetal cell layer of the anther contribute to microspore cell wall architecture (B). Pollen accumulates high levels of free PAs and HCAAs, mainly localized in the cell wall. PA catabolism by PAO and DAO modulates the rigidity of the cell wall (C). Once dehydrated, pollen grains are released and PAs contribute to maintain pollen viability (D). During germination on a stigma (E), PAs promote the translation of transcripts and they are also released in the extracellular space, together with TGase (F). During pollen tube growth in a compatible style, PAs take part in the cytoskeleton organization, in cell wall deposition and remodeling by the PME enzyme as well as in the regulation of ion transport through the plasma membrane. PAs also exert an inhibitory effect on RNase enzymes (G).

Conclusion

Pollen development is a complex and well-coordinated process governed by genetic and enzymatic processes, some of which are modulated by PAs. Hence, these aliphatic polycations drive pollen development throughout its lifespan, as summarized in Figure 2. Progress in past decades has significantly advanced our understanding of how PAs exert multiple roles by different molecular mechanisms. However, further investigations on the physiological function of PAs and their molecular partners are still needed. In particular, knowledge would strongly benefit from a deeper understanding of PA transporters, which have been poorly studied. This could provide new insights on the interactions between the tapetal layer and the pollen grain during its development in the anther. It could likewise explain how HCAAs, PA biosynthetic and oxidative enzymes and other cell wall components are deposited during microsporogenesis. Moreover, despite recent findings on the composition and biosynthetic pathway of pollen HCAAs, clear evidence regarding their functions is still lacking. While some of the roles of PAs are rather evident, e.g., modulation of the cytoskeleton by TGase, others remain elusive, e.g., PA interactions with nucleic acids. Such information could explain their possible role in epigenetic control, the interconnection between PAs and ROS, and the role of free and conjugated PAs in the apoplast during the pollen–pistil interaction.

References

- Aloisi, I., Cai, G., Tumiatti, V., Minarini, A., and Del Duca, S. (2015). Natural polyamines and synthetic analogs modify the growth and the morphology of *Pyrus communis* pollen tubes affecting ROS levels and causing cell death. *Plant Sci.* 239, 92–105. doi:10.1016/j.plantsci.2015.07.008
- Altman, A. (1982). Polyamines and wounded storage tissues—inhibition of RNase activity and solute leakage. *Physiol. Plant.* 54, 194–198. doi:10.1111/j.1399-3054.1982.tb06325.x
- Antognoni, F., and Bagni, N. (2008). Bis (guanylhydrazones) negatively affect *in vitro* germination of kiwifruit pollen and alter the endogenous polyamine pool. *Plant Biol. (Stuttg.)* 10, 334–341. doi:10.1111/j.1438-8677.2007.00016.x
- Bagni, N., Adamo, P., and Serafini-Fracassini, D. (1981). RNA, proteins and polyamines during tube growth in germinating apple pollen. *Plant Physiol.* 68, 727–730. doi:10.1104/pp.68.3.727

- Bagni, N., Serafini-Fracassini, D., Torrigiani, P., and Villanueva, V.R. (1986). "Polyamine biosynthesis in germinating apple pollen" in *Biotechnology and Biology of Pollen*, Eds D. Mulcahy, G. Bergamini, G. Mulcahy, and E. Ottaviano (New York, NY: Springer Verlag), 363–368.
- Bagni, N., Stabellini, G., and Serafini-Fracassini, D. (1973). Polyamines bound to tRNA and rRNA of eukaryotic plant organisms. *Physiol.Plant.* 29, 218–222.
- Belda-Palazon, B., Ruiz, L., Marti, E., Tarraga, S., Tiburcio, A.F., Culianez, F., et al. (2012). Amino propyl transferases involved in polyamine biosynthesis localize preferentially in the nucleus of plant cells. *PLoS ONE* 7:e46907. doi: 10.1371/journal.pone.0046907
- Bokvaj, P., Hafidh, S., and Honys, D. (2015). Transcriptome profiling of male gametophyte development in *Nicotiana tabacum*. *Genom. Data* 3, 106–111. doi: 10.1016/j.gdata.2014.12.002
- Boothby, T.C., Zipper, R.S., Van Der Weele, C.M., and Wolniak, S.M. (2013). Removal of retained introns regulates translation in the rapidly developing gametophyte of *Marsilea vestita*. *Dev. Cell* 24, 517–529. doi: 10.1016/j.devcel.2013.01.015
- Cai, G., Della Mea, M., Faleri, C., Fattorini, L., Aloisi, I., Serafini-Fracassini, D., et al. (2015a). Spermine either delays or promotes cell death in *Nicotiana tabacum* L. corolla depending on the floral developmental stage and affects the distribution of transglutaminase. *Plant Sci.* 241, 11–22. doi:10.1016/j.plantsci.2015.09.023
- Cai, G., Sobieszczuk-Nowicka, E., Aloisi, I., Fattorini, L., Serafini-Fracassini, D., and Del Duca, S. (2015b). Polyamines are common players in different facets of plant programmed cell death. *Amino Acids* 47, 27–44. doi:10.1007/s00726-014-1865-1
- Charnay, D., Nari, J., and Noat, G. (1992). Regulation of plant cell wall pectin methylesterase by polyamines-interactions with the effects of metal ions. *Eur. J. Biochem.* 205, 711–714. doi:10.1111/j.1432-1033.1992.tb16833.x
- Cona, A., Rea, G., Botta, M., Corelli, F., Federico, R., and Angelini, R. (2006). Flavin-containing polyamine oxidase is a hydrogen peroxide source in the oxidative response to the protein phosphatase inhibitor cantharidin in *Zea mays* L. *J. Exp.Bot.* 57, 2277–2289. doi:10.1093/jxb/erj195
- Das, K.C., and Misra, H.P. (2004). Hydroxyl radical scavenging and singlet oxygen quenching properties of polyamines. *Mol. Cell.Biochem.* 262, 127–133. doi: 10.1023/B:MCBI.0000038227.91813.79
- Deeb, F., Van Der Weele, C.M., and Wolniak, S.M. (2010). Spermidine is a morphogenetic determinant for cell fate specification in the male gametophyte of the water fern *Marsilea vestita*. *Plant Cell* 22, 3678–3691. doi: 10.1105/tpc.109.073254
- Del Duca, S., Cai, G., DiSandro, A., and Serafini-Fracassini, D. (2010). Compatible and self-incompatible pollination in *Pyrus communis* displays different polyamine levels and transglutaminase activity. *Amino Acids* 38, 659–667. doi:10.1007/s00726-009-0426-5
- Del Duca, S., Faleri, C., Iorio, R.A., Cresti, M., Serafini-Fracassini, D., and Cai, G. (2013). Distribution of transglutaminase in pear pollen tubes in relation to cytoskeleton and membrane dynamics. *Plant Physiol.* 161, 1706–1721. doi: 10.1104/pp.112.212225
- Del Duca, S., Serafini-Fracassini, D., Bonner, P., Cresti, M., and Cai, G. (2009). Effects of post-translational modifications catalysed by pollen transglutaminase on the functional properties of microtubules and actin filaments. *Biochem.J.* 418, 651–664. doi:10.1042/BJ20081781
- Del Duca, S., Serafini-Fracassini, D., and Cai, G. (2014). Senescence and programmed cell death in plants: polyamine action mediated by transglutaminase. *Front. PlantSci.* 5:120. doi:10.3389/fpls.2014.00120
- Di Sandro, A., Del Duca, S., Verderio, E., Hargreaves, A.J., Scarpellini, A., Cai, G., et al. (2010). An extracellular transglutaminase is required for apple pollen tube growth. *Biochem. J.* 429, 261–271. doi:10.1042/BJ20100291

- D'Orazi, D., and Bagni, N. (1987). *In vitro* interactions between polyamines and pectic substances. *Biochem. Biophys. Res. Commun.* 148, 1259–1263. doi: 10.1016/S0006-291X (87)80268-1
- Dresselhaus, T., and Franklin-Tong, N. (2013). Male-female crosstalk during pollen germination, tube growth and guidance, and double fertilization. *Mol. Plant* 6, 1018–1036. doi:10.1093/mp/sst061
- Elejalde-Palmett, C., De Bernonville, T.D., Glevarec, G., Pichon, O., Papon, N., Courdavault, V., et al. (2015). Characterization of a spermidine hydroxycinnamoyl transferase in *Malus domestica* highlights the evolutionary conservation of trihydroxycinnamoyl spermidines in pollen coat of core Eudicotyledons. *J. Exp. Bot.* 66, 7271–7285.
- Falasca, G., Franceschetti, M., Bagni, N., Altamura, M.M., and Biasi, R. (2010). Polyamine biosynthesis and control of the development of functional pollen in kiwifruit. *Plant Physiol. Biochem.* 48, 565–573. doi: 10.1016/j.plaphy.2010.02.013
- Fellenberg, C., Bottcher, C., and Vogt, T. (2009). Phenylpropanoid polyamine conjugate biosynthesis in *Arabidopsis thaliana* flower buds. *Phytochemistry* 70, 1392–1400. doi:10.1016/j.phytochem.2009.08.010
- Fellenberg, C., Milkowski, C., Hause, B., Lange, P.R., Bottcher, C., Schmidt, J., et al. (2008). Tapetum-specific location of a cation-dependent O-methyltransferase in *Arabidopsis thaliana*. *Plant J.* 56, 132–145. doi: 10.1111/j.1365-313X.2008.03576.x
- Fellenberg, C., and Vogt, T. (2015) Evolutionarily conserved phenylpropanoid pattern on angiosperm pollen. *Trends Plant Sci.* 20, 212–218. doi: 10.1016/j.tplants.2015.01.011
- Fellenberg, C., Ziegler, J., Handrick, V., and Vogt, T. (2012). Polyamine homeostasis in wild type and phenolamide deficient *Arabidopsis thaliana* stamens. *Front. Plant Sci.* 3:180. doi:10.3389/fpls.2012.00180
- Fincato, P., Moschou, P.N., Ahou, A., Angelini, R., Roubelakis-Angelakis, K.A., Federico, R., et al. (2012). The members of *Arabidopsis thaliana* PAO gene family exhibit distinct tissue- and organ-specific expression pattern during seedling growth and flower development. *Amino Acids* 42, 831–841. doi: 10.1007/s00726-011-0999-7
- Gentile, A., Antognoni, F., Iorio, R.A., Distefano, G., Las Casas, G., La Malfa, S., et al. (2012). Polyamines and transglutaminase activity are involved in compatible and self-incompatible pollination of *Citrus grandis*. *Amino Acids* 42, 1025–1035. doi:10.1007/s00726-011-1017-9
- Grienenberger, E., Besseau, S., Geoffroy, P., Debayle, D., Heintz, D., Lapierre, C., et al. (2009). A BAHD acyltransferase is expressed in the tapetum of *Arabidopsis* anthers and is involved in the synthesis of hydroxycinnamoyl spermidines. *Plant J.* 58, 246–259. doi:10.1111/j.1365-313X.2008.03773.x
- Handrick, V., Vogt, T., and Frolov, A. (2010). Profiling of hydroxycinnamic acid amides in *Arabidopsis thaliana* pollen by tandem mass spectrometry. *Anal. Bioanal. Chem.* 398, 2789–2801. doi:10.1007/s00216-010-4129-2
- Linskens, H.F., Kochuyt, A.S.L., and So, A. (1968). Regulation der nukleinsäuren synthesis durch polyamine in keimenden pollen von *Petunia*. *Planta* 82, 111–122. doi:10.1007/BF01305715
- Liu, T., Kim, D.W., Niitsu, M., Maeda, S., Watanabe, M., Kamio, Y., et al. (2014). Polyamine oxidase 7 is a terminal catabolism-type enzyme in *Oryza sativa* and is specifically expressed in anthers. *Plant Cell Physiol.* 55, 1110–1122. doi: 10.1093/pcp/pcu047
- Martin-Tanguy, J. (2001). Metabolism and function of polyamines in plants: recent development (new approaches). *Plant Growth Regul.* 34, 135–148. doi: 10.1023/A:1013343106574
- Matsuno, M., Compagnon, V., Schoch, G.A., Schmitt, M., Debayle, D., Bassard, J. E., et al. (2009). Evolution of a novel phenolic pathway for pollen development. *Science* 325, 1688–1692. doi:10.1126/science.1174095
- McClure, B.A., and Franklin-Tong, V. (2006). Gametophytic self-incompatibility: understanding the cellular mechanisms involved in “self” pollen tube inhibition. *Planta* 224, 233–245. doi:10.1007/s00425-006-0284-2

- Moschou, P.N., Wu, J., Cona, A., Tavladoraki, P., Angelini, R., and Roubelakis-Angelakis, K.A. (2012). The polyamines and their catabolic products are significant players in the turnover of nitrogenous molecules in plants. *J. Exp. Bot.* 63, 5003–5015.doi:10.1093/jxb/ers202
- Potocky, M., Jones, M.A., Bezdova, R., Smirnoff, N., and Zarsky, V. (2007). Reactive oxygen species produced by NADPH oxidase are involved in pollen tube growth. *New Phytol.* 174, 742–751.doi:10.1111/j.1469-8137.2007.02042.x
- Pottosin, I., Velarde-Buendia, A.M., Bose, J., Zepeda-Jazo, I., Shabala, S., and Dobrovinskaya, O. (2014). Cross-talk between reactive oxygen species and polyamines in regulation of ion transport across the plasma membrane: implications for plant adaptive responses. *J. Exp.Bot.* 65, 1271–1283.doi: 10.1093/jxb/ert423
- Quilichini, T.D., Samuels, A.L., and Douglas, C.J. (2014). ABCG26- mediated polyketide trafficking and hydroxycinnamoyl spermidines contribute to pollen wall exine formation in *Arabidopsis*. *Plant Cell* 26, 4483–4498.doi: 10.1105/tpc.114.130484
- Rodriguez-Enriquez, M.J., Mehdi, S., Dickinson, H.G., and Grant-Downton, R.T. (2013). A novel method for efficient *in vitro* germination and tube growth of *Arabidopsis thaliana* pollen. *New Phytol.* 197, 668–679.doi:10.1111/nph.12037
- Sinha, R., and Rajam, M.V. (2013). RNAi silencing of three homologues of S-adenosylmethionine decarboxylase gene in tapetal tissue of tomato results in male sterility. *Plant Mol.Biol.* 82, 169–180.doi:10.1007/s11103-013-0051-2
- Song, J., and Tachibana, S. (2007). Loss of viability of tomato pollen during long- term dry storage is associated with reduced capacity for translating polyamine biosynthetic enzyme genes after rehydration. *J. Exp.Bot.* 58, 4235–4244.doi: 10.1093/jxb/erm280
- Speranza, A., Calzoni, G.L., and Bagni, N. (1984). Evidence for a polyamine- mediated control of ribonucleases activity in germinating pollen. *Physiol. Veg.* 22, 323–331.
- Speranza, A., Calzoni, G.L., and Bagni, N.(1986). "Protein pattern of apple pollen in culture: effect of actinomycin D" in *Biotechnology and Ecology of Pollen*, Eds D. Mulcahy, G. Bergamini, G. Mulcahy, and E. Ottaviano (New York, NY: Springer Verlag),345–350.
- Takahashi, T., and Kakehi, J. (2010). Polyamines: ubiquitous polycations with unique roles in growth and stress responses. *Ann. Bot.* 105, 1–6.doi: 10.1093/aob/mcp259
- Tiburcio, A.F., Altabella, T., Bitrian, M., and Alcazar, R.(2014). The roles of polyamines during the life span of plants: from development to stress. *Planta* 240, 1–18.doi:10.1007/s00425-014-2055-9
- Wu, J., Shang, Z., Jiang, X., Moschou, P.N., Sun, W., Roubelakis-Angelakis, K. A., *et al.*(2010).Spermidineoxidase-derivedH₂O₂ regulates pollen plasma membrane hyper polarization-activated Ca²⁺ -permeable channels and pollen tube growth. *Plant J.* 63, 1042–1053.doi:10.1111/j.1365- 313X.2010.04301.x

Chapter 2

Natural polyamines and synthetic analogues modify the growth and the morphology of *Pyrus communis* pollen tubes affecting ROS levels and causing cell death

This chapter is based on:

I. Aloisi , G. Cai, V. Tumiatti, A. Minarini, and S. Del Duca, *Plant Sci.* 239: 92–105 (2015)

Abstract

Polyamines (PAs) are small molecules necessary for pollen maturation and tube growth. Their role is often controversial, since they may act as pro-survival factors as well as factors promoting Programmed Cell Death (PCD). The aim of the present work was to evaluate the effect of exogenous PAs on the apical growth of pear (*Pyrus communis*) pollen tube and to understand if PAs and reactive oxygen species (ROS) are interconnected in the process of tip-growth. In the present study besides natural PAs, also aryl-substituted spermine (Spm) and methoctramine (Met 6-8-6) analogues were tested. Among the natural PAs, Spm showed strongest effects on tube growth. Spm entered through the pollen tube tip, then diffused in the sub-apical region that underwent drastic morphological changes, showing enlarged tip. Analogues were mostly less efficient than natural PAs but BD23, an asymmetric synthetic PAs bearing a pyridine ring, showed similar effects. These effects were related to PA ability to cause the decrease of ROS level in the apical zone, leading to cell death, counteracted by the caspase-3 inhibitor Ac-DEVD-CHO (DEVD). In conclusions, ROS are essential for pollen germination and a strict correlation between ROS regulation and PA concentration is reported. Moreover, an imbalance between ROS and PAs can be detrimental thereby driving pollen toward cell death.

Introduction

Natural polyamines (PAs) are small widespread polycations known to be necessary for cell growth of all organisms, both prokaryotic and eukaryotic (Tiburcio *et al.*, 2014). Putrescine (Put), spermidine (Spd) and spermine (Spm) are the most common PAs, but recently, evidences also showed plants possessing the isomer thermospermine (tSpm) (Takano *et al.*, 2012). Most of the biological functions of PAs are associated with their polycationic backbone able to establish electrostatic interactions with anion groups of biological molecules, among which proteins and nucleic acids; also the covalent binding to proteins, catalyzed by transglutaminase (TGase) occurs (Walden *et al.*, 1997; Del Duca *et al.*, 2014; Tiburcio *et al.*, 2014). PAs act as regulatory factors in fundamental cellular processes, including cell division, differentiation, gene expression, DNA and protein synthesis, and programmed cell death (PCD), the latter recently reviewed (Moschou and Roubelakis-Angelakis, 2014;Cai *et al.*, 2015). The role of PAs in plant cell death appears to be multifaceted, acting in some instances as pro-survival molecules, whereas in other cases they seem involved in accelerating PCD (Moschou and Roubelakis-Angelakis, 2014;Cai *et al.*, 2015). It thus not astonishing that the perturbation of PAs homeostasis influences the cellular growth and morphology (Dutra *et al.*, 2013). In plant cells, PAs are mostly stocked in the vacuole and in the cell wall, but Spm is present also in the nucleus (Belda-Palazon *et al.*, 2012), where it is supposed, in addition to a molecular stabilizing role, to act as “radical-scavenger” protecting DNA from reactive oxygen species (ROS) (Ha *et al.*, 1998;Das and Misra, 2004).

A multifaceted interaction of PAs with ROS and antioxidants is perhaps among the most complex and apparently contradictory physiological and biochemical process in plants (Andronis *et al.*, 2014; Minocha *et al.*, 2014). Pollen is an useful model to study effect of different factors, as it can be considered like a single cell in culture, it is very sensible, its growth is fast and easy to measure; moreover it is a relevant subject for fertilization and self-incompatibility studies (Cai and Cresti, 2009). As a tip-growing cell in which both the cytoskeleton and the tip-localized Ca²⁺ gradient are critical factors driving pollen tube elongation, PAs as well as other factors involved in the regulation of pollen tube dynamics, are likely to take part in the

process of pollen tube growth (Del Duca *et al.*, 2009; Wudick and Feijo, 2014). The presence and the active biosynthesis of PAs during germination of Rosaceae pollen, as well as their release from the pollen tube in the external medium, has previously been established (Speranza and Calzoni, 1980; Bagni *et al.*, 1981). In pollen, the homeostasis of PAs is finely regulated and the perturbation of this balance has provided, over the years, interesting evidences about how PAs carry out some of their functions in the cell. For example, the inhibition of PA biosynthesis was seen to cause a severe inhibition of pollen tube growth and was correlated with reduced binding to cell wall polysaccharides, indicating the essential role of PAs in pollen tube emergence and elongation (Antognoni and Bagni, 2008). Moreover, also an excess of PAs was shown to affect pollen tube causing its arrest, probably because intracellular PAs, that were reported to be also conjugated to cytoskeletal proteins, can regulate cytoskeletal functional properties (Del Duca *et al.*, 2009; Di Sandro *et al.*, 2010). ROS also play a key role during pollen tube emergence and elongation as they act as wall loosening or stiffening agents (Swanson and Gilroy, 2010; Speranza *et al.*, 2012). In this context, the role of PAs is still largely unknown and in some cases ambiguous, as demonstrated by the double action of PAs in regulation of ROS. In fact, PAs are deaminated by polyamine oxidases (PAOs) in enzymatic reactions that produce hydrogen peroxide (H₂O₂) in the apoplast (Pottosin *et al.*, 2012); on the other hand, different studies have shown the efficient action of PAs in ROS scavenging (Ha *et al.*, 1998; Das and Misra, 2004). It has been suggested that NADPH oxidase (NOX)-derived superoxide (O₂⁻) controls, at physiological concentration, cell expansion during the apical growth of pollen tubes and that it localizes in the apical region of these cells (Potocky *et al.*, 2007). Moreover, there is a correlation between ROS and Ca²⁺ signaling, that is also essential for plant development and tip-growth, since ROS induce Ca²⁺ influx across cell membranes (Foreman *et al.*, 2003), and cytosolic Ca²⁺ can activate NOX; establishing a positive feedback between NOX activity and ROS-induced Ca²⁺ influx, that supports polarized growth (Pottosin and Shabala, 2014). Moreover, to avoid an excess of ROS that could lead to oxidative damage, pollen has a powerful antioxidant machinery based on superoxide dismutase (SOD) that catalyzes the dismutation of O₂⁻ into H₂O₂; the latter is decomposed to water and oxygen by catalase (CAT).

However, details on the reciprocal interactions between these factors are missing. In fact, although many cellular targets of PAs have been described, the precise molecular mechanisms of these interactions are largely unknown and the readily inter-conversion; oxidation and conjugation of PA complicate studies on the functions of the individual PA.

Since natural PAs are rapidly metabolized in cells, substituting the natural PA with analogues offers means to study either the function of an individual PA or the effect of modified PA metabolism on cell physiology. For example, the insertion of one or two aromatic rings on the terminal primary amino groups of natural PAs could modify the hydrophilicity of the molecule, the rate of protonation of amine groups and their interaction with anionic counterpart of biological molecules or the affinity toward enzymes. For this reason, the search for new PA analogues with physiological activity results to be a promising research field. In particular, our research has been focused on the assessment of the effect of natural and synthetic PAs on the apical growth of pollen tubes. Further, the present study aimed to understand if and how PAs and ROS concentration are interconnected in the process of tip-growth. Preliminarily, the effect on germinating pollen tubes caused by the natural PAs Cad, Put, Spd and Spm was assessed. Finding Spm as the most effective, besides natural PAs, symmetrically or asymmetrically substituted Spm, bearing different aromatic groups on one or both terminal amines were examined. The aromatic rings were chosen for their different electronic and/or lipophilic properties in order to evaluate any favorable effect on Spm activity. To this aim, we selected three synthetic Spm analogues, BD6, BD26, and BD23, substituted on one of the terminal primary amino group of Spm with a different aromatic or heteroaromatic moiety such as benzyl, naphthalene, and pyridine, respectively. Spm analogues DL5 and DL6 were also selected due to the presence in their structure of the aromatic ring of vanillin, which is a natural compound endowed with antioxidant properties. Finally, three synthetic tetramines (Met 6-5-6, Met 6-10-6 and Met 5-10-5) related to methoctramine (Met 6-8-6), a M2-muscarinic receptor competitive antagonist (Melchiorre *et al.*, 1987), were also included in this study. These synthetic PAs, characterized by longer polymethylene chains than Spm and a 2-methoxybenzyl group on each terminal nitrogen atom, are able to bind a variety of receptor sites (Minarini *et al.*, 2010) and in here were chosen

due to their NMDA channel blocking activity (Saiki *et al.*, 2013). In fact, NMDA receptor is involved in the Ca²⁺ ions trafficking in mammals (Saiki *et al.*, 2013) and presents homologues in plants, where these glutamate-gated cationic channels, selective for Na⁺, K⁺, and Ca²⁺ ions, are involved in the plant immune response (Forde and Roberts, 2014).

Our results show how important ROS are during pollen germination and that a link between PAs and ROS exists. Moreover, a slight imbalance in the two molecules was demonstrated to be detrimental and drive the pollen toward a cell death.

Materials and methods

Chemicals

All chemicals (unless otherwise indicated) were obtained from Sigma-Aldrich (Milan, Italy).

Synthesis of substituted spermine analogues and methoctramine analogues

The synthetic PA analogues assayed in this study (Fig. 1), all in form of tetrahydrochloride salts, namely N1-(3-aminopropyl)-N4-(3-(benzylamino)propyl)butane-1,4-diamine or N1-benzyl-spermine (BD6) (Bonaiuto *et al.*, 2012), N1-(3-aminopropyl)-N4-(3-((pyridin-3-ylmethyl)amino)propyl)butane-1,4-diamine (BD23), N1-(3-aminopropyl)-N4-(3-((naphthalen-2-ylmethyl)amino)propyl)butane-1,4-diamine (BD26) (Bonaiuto *et al.*, 2013); 4-(((3-((4-((3-aminopropyl)amino)butyl)amino)propyl)amino)methyl)-2-methoxyphenol (DL5), 4,4'-(2,6,11,15-tetraazahexadecane-1,16-diyl)bis(2-methoxyphenol) (DL6) (Minarini *et al.*, 2013), N1,N1'-(pentane-1,5-diyl)bis(N6-(2-methoxybenzyl)hexane-1,6-diamine) (Met 6-5-6), N1,N1'-(decane-1,10-diyl)bis(N6-(2-methoxybenzyl)hexane-1,6-diamine) (Met 6-10-6) (Melchiorre *et al.*, 1987) and N1,N1'-(decane-1,10-diyl)bis(N5-(2-methoxybenzyl)pentane-1,5-diamine) tetrahydrochloride (Met 5-10-5) (Minarini *et al.*, 1991), were synthesized as previously reported.

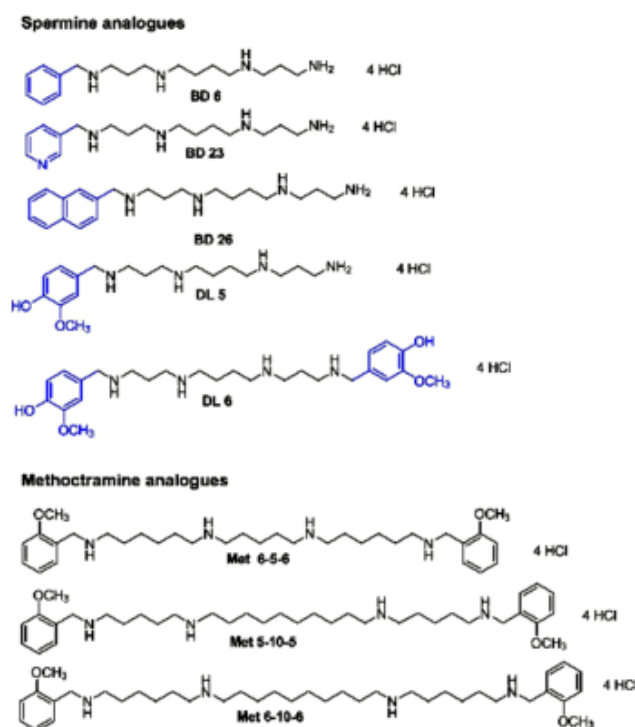


FIGURE 1. PA analogues. In blue the structural components of the molecules different from those of spermine

In particular, the mono-substituted Spm analogues BD6, BD23, BD26 and DL5 were synthesized by reacting tri-Boc-spermine with the appropriate aldehydes (Figure 2, 1 eq.) to afford the corresponding Schiff bases that were reduced in situ with NaBH₄. Acidic deprotection of the tri-Boc protected intermediates led to the corresponding tetraamines as tetrahydrochloride salts. The disubstituted Spm analogue DL6 was obtained by reaction of Spm with 2-methoxybenzaldehyde (Figure 2, 2 eq.) followed by reduction of the Schiff base with NaBH₄.

The methoctramine analogues Met 6-5-6, Met 6-10-6 and Met 5-10-5 have been synthesized following the procedure developed by our research group. As example, the synthesis of compound Met 6-5-6 is reported in Figure 2. Briefly, N-[(benzyloxy)carbonyl]-6-aminocaproic acid was reacted with 1,5-diaminopentane to give the intermediate 1; removal of the N-(benzyloxy)carbonyl group by acidic hydrolysis gave the corresponding diamine diamide 2, which was reacted with 2-methoxybenzaldehyde and then reduced with NaBH₄, to furnish derivative 3; reduction of 3 with BACH-EI (borane N-ethyl-N-isopropyl-aniline complex) in dry diglyme led to the desired tetramine Met 6-5-6.

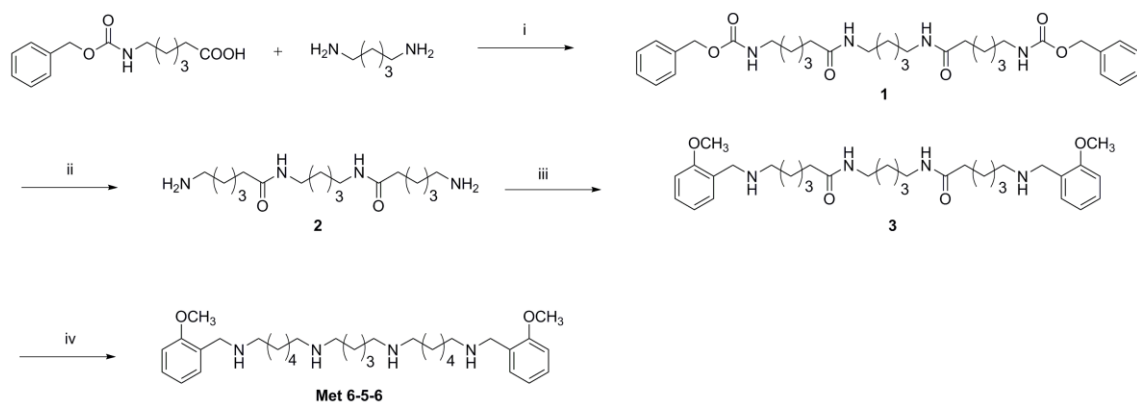


FIGURE 2. Synthesis of compound Met 6-5-6. (i) EtOCOCl, NEt₃, dioxane, room temp., 18h, 84%; (ii) a) HBr 33% in CH₃COOH, room temp., 4h, quantitative yield; b) 2N NaOH, CHCl₃, 14h; (iii) a) 2-methoxybenzaldehyde, MeOH; b) NaBH₄, EtOH, room temp., overnight, 90%; (iv) BACH-EI, diglyme, reflux, 12h, 36%.

Plant material

Mature pollen of pear (*Pyrus communis* cv. Williams) was collected from plants grown in experimental plots at the University of Bologna (Dipartimento di Scienze Agrarie, Università di Bologna). Handling, storage, pollen hydration and germination were performed as previously reported (Bagni *et al.*, 1981; Del Duca *et al.*, 1997). After 1 hour of growth, the medium was supplemented with different concentrations of PAs (Cad, Put, Spd or Spm), PAs analogues (BD6, BD26, BD23, DL5, DL6, Met 6-10-6, Met 5-10-5, and Met 6-5-6) or diphenyleneiodonium chloride (DPI) up to 2 hours unless otherwise indicated. Pollen was visualized under a light microscope (Nikon Eclipse E600) equipped with a digital camera (Nikon DXM1200). For growth recovery experiment, pollen was treated at different times with Spm and BD23 (100 and 500 μM) and then repeatedly washed with germination medium and allowed to germinate again. Recovery was calculated as mean pollen tube length after 2 hour in comparison to the mean pollen tube length after the first hour of germination.

NAD(P)H-Oxidase, Catalase and Superoxide dismutase in gel activity assay

Aliquots of germinating pollen were taken at different times during germination and PAs treatment then centrifuged for 3 min at 5000 g, 4°C. Pelleted pollen was

resuspended in 1 ml PBS 150 mM, pH 7.5, sonicated twice on ice for 15 seconds and centrifuged for 25 min at 5000 g, 4°C. Protein concentration in the supernatant was analyzed by the bicinchoninic acid (BCA) assay kit. Freshly prepared extracts were separated in 12% to check SOD activity or 8% to check the NADP(H)-Ox and CAT activity (w/v) native-PAGE gels and visualized according to (Sagi and Fluhr, 2001; Weydert and Cullen, 2010) with minor modifications. All protein in-gel activity assays were performed at least three times in order to ensure the consistency of results.

Calcium distribution

Ca²⁺ fluorescence was measured after chlortetracycline (CTC) addition and incubation for 2 min. The optimal concentration of CTC, that did not affect pollen growth but still provided good fluorescence signal, was determined to be about 100 µM. Samples were observed under a fluorescence microscope [Nikon Eclipse E600] using a proper filter.

ROS localization and spectrophotometric NBT assay

ROS detection using the fluorescent ROS indicator dye 2',7'-dichlorodihydrofluorescein diacetate (DCFH₂-DA; Molecular Probes) was performed according to literature (Pasqualini *et al.*, 2011). For nitroblue tetrazolium (NBT) staining, after 1 hour of pollen germination, NBT was mixed with germination medium (final concentration 1.2 mM) and incubated for 10 min at room temperature. The staining due to formazan deposits was immediately visualized under a light microscope. The 3,3'-Diaminobenzidine (DAB) staining was performed as described by (Daudi *et al.*, 2012), with few modification. ROS quantification by absorbance of NBT colour by spectrophotometric assay was performed as described by (Wang *et al.*, 2009) with few modifications. Briefly, germinated pollen grains (1 mg/assay) were mixed with 2 mM nitroblue tetrazolium (NBT) and 1 mM nicotinamide adenine dinucleotide phosphate (reduced) (NADH). Negative controls were performed adding diphenyleneiodonium chloride (DPI) at final concentration of 100 and 200 µM. The reaction was conducted at 37 °C for 30 min, and then the suspensions were centrifuged for 3 min at 10620 g. Residual non-reduced NBT was removed by

washing with 1 ml of pure water twice. The formazan sediment was dissolved in 400 μ l of methanol by shaking for 20 min at room temperature. After extraction, the suspensions were centrifuged for 3 min at 10620 g and the absorbance of supernatants was measured at 530 nm.

Conjugation of spermine with fluorescein isothiocyanate (FITC) and Spm-FITC localization

The conjugation of Spm with fluorescein isothiocyanate (FITC) was performed using the FluoroTag FITC Conjugation Kit, according to the manufacturer instructions. A volume of 300 μ l of the pollen suspension was supplemented with FITC-conjugated Spm in the dark. After 10 and 30 min, the suspension was centrifuged for 1 min at 180 g and the germination medium was replaced by an equal volume of BSA 3% (w/v) in PBS, pH 7.4. After 1-hour incubation at 37°C, residual FITC-conjugated Spm was removed by washing with 200 μ l of PBS, pH 7.4. Pollen was thus fixed with 200 μ l methanol for 10 min at -20°C. After fixation, pollen was washed, resuspended in 100 μ l PBS, pH 7.4 and immediately visualized under a fluorescence microscope [Nikon Eclipse E600] adjusted at 488 nm for fluorescein excitation.

Pollen viability assay

To determine pollen viability MTT (2,5-diphenyl tetrazolium bromide) test was used. MTT produces a yellowish solution that is converted to dark blue, water-insoluble MTT formazan by mitochondrial dehydrogenases of living cells. The test solution contained a 1% concentration of the MTT substrate in 5% sucrose. After 15 min incubation at 30°C the pollen samples were visualized under a light microscope. Only germinated pollen was taken into consideration as PAs were supplemented after the first hour germination. Germinated pollen was considered viable if it turned deep purple. At least 60 pollen tubes were observed per treatment, and each treatment was repeated three times in order to ensure the consistency of results. The percentage of viability was normalized on the control samples.

Preparation of pollen DNA and 4',6-diamidino-2-phenylindole (DAPI) staining

100 mg of germinated pollen was pulverized with liquid nitrogen to a fine powder and DNA was extracted following CTAB-based protocol as described by (Lade *et al.*, 2014) with minor modifications. The purity and concentration of the extracted DNA were evaluated by measuring the absorbance at 260 and 280 nm using a NanoDrop Spectrophotometer ND-1000 (EuroClone S.p.A., Italy). Five μg of extracted DNA was checked by electrophoresis on a 1.2% agarose gel and stained with gel red (Biotium). For DAPI staining, germinated pollen was fixed in 1.5% formaldehyde for 20 min, and then collected by centrifugation, 30 seconds at 1500 g at room temperature. The pollen was resuspended in pollen isolation buffer [100 mM NaPO₄, pH 7.5; 1 mM EDTA; 0.1% (v/v) Triton X-100] and DAPI was added at final concentration 1 $\mu\text{g}/\text{ml}$. Samples were observed under a fluorescence microscope [Nikon Eclipse E600] using a DAPI filter.

Data and Statistics

Pollen tube length, in gel-activity bands intensity, ROS and fluorescence distribution analysis, nuclear condensation and distance between vegetative and generative nuclei have been performed using ImageJ software. Differences between sample sets were determined by analysis of variance (two-way and one-way ANOVA, with a threshold *P*-value of 0.05) using GraphPad Prism.

Results

Exogenous PA supply effects on pollen tube elongation

To check the effect of natural PAs on germinating pollen tubes, the length of *Pyrus communis* pollen tubes was measured after addition of different concentrations of Cad, Put, Spd and Spm, after the first hour of germination; treatment of pollen continued for an additional hour then the pollen tube length was measured. The length of control pollen tubes was on average 317 μm after the first hour of germination, but this average value rose to 1,021 μm after the second one (Fig. 3). All the natural PAs, except Cad, were effective on pollen tube elongation in a dose-dependent manner. The most effective was Spm that drastically reduced by

46.32% pollen tube elongation at 10 μM and completely abolished it at 100 μM . In addition, Spd was quite effective, with an inhibition by 35.91% and 43.27% at 100 μM and 250 μM respectively, whereas Put showed a drop of pollen tube elongation by 51.36% and 58.32% only at final concentration of 750 μM and 1 mM respectively; the last value determined the arrest of pollen tube growth (Fig. 3).

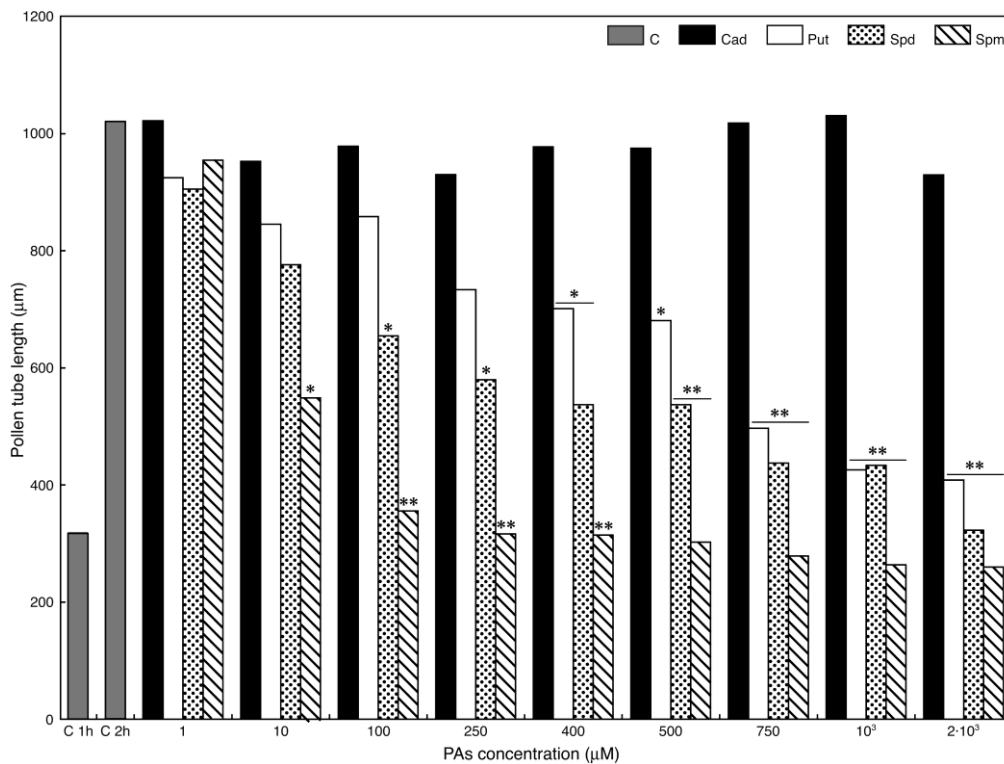


FIGURE 3. Effect of Spm, Spd, Put and Cad on the elongation of pollen tube of *Pyrus communis*. Means derive from at least 40 measurements and the experiment was repeated three times. Means of treated samples were compared with control sample after 2 h germination by Dunnett's Multiple Comparison Test *= $p \leq 0.05$; **= $p \leq 0.01$. SD < 0.15.

Given that ROS are essential for pollen tube elongation and that exogenous PA supplementation blocked this process, the next goal was to understand if ROS and PAs localize in the same region of the pollen tube. Pollen cultures were incubated with the cell-permeable probe DCFH2-DA and the fluorescence due to ROS presence was monitored over time after PAs supplementation. Staining with DCFH2-DA revealed a tip-localized pattern of fluorescence in control tubes after 60 min germination (Fig. 4A a-c).

To monitor ROS formation over time, the incubation with PAs was split in time spans. After the first hour incubation PAs were supplied (100 μM) and within the

first 10 min after PAs supplementation (70 min germination), the scenario was different from the control as the fluorescence intensity was less localized at the tip (Fig. 4A d-f). After 10-15 min from PAs supplementation swollen tips became evident and variability in the localization of the signal occurred as it was diffused and very faint or localized in spots (Fig. 4A g-h). After 20 min treatment (70 min germination), the pollen tips assumed a lollipop-shape and the same heterogeneity observed before was again evident (Fig 4A i-l), with in addition some tips having newly tip-localized ROS (Fig. 4A m).

Localization of Spm-FITC and ROS in the pollen tube

Once established that the concentration of ROS is higher in the apical region of pollen tubes and that the supply of exogenous PAs affected ROS gradient, the entry site of PAs and their distribution in pollen tubes were checked to determine if PAs co-localize with ROS. For this purpose, labelling of Spm by conjugation with fluorescein isothiocyanate (FITC) was performed (Fig. 4B). Grain showed strong auto-fluorescence but fluorescence due to the labelled Spm was clearly detectable and showed that it entered and localized at the pollen tube tip region within 10 min after PA supply (Fig 4B a-b), then diffused and localized in the apical and sub-apical regions, according to a gradient profile with maximum concentration at the tip (Fig. 4B c-d).

Fluorescence-intensity distribution analysis has been performed to understand if PAs and ROS localize in the same region of the pollen tube. ROS in non-treated pollen (Fig. 4C, grey line) are distributed within the first 200 μm of pollen tubes with its maximum at 30 μm . The same ROS concentration profile is present if pollen is treated with 1 μM Spm (Fig. 4C, blue line). After treatment with 100 μM Spm (Fig. 4C black line) pollen tubes were drastically inhibited and the ROS gradient was undetectable. The distribution of the ROS gradient reflected the distribution of FITC-conjugated Spm (Fig. 4C, green line), that also blocked pollen tube elongation and showed a distribution with higher concentration within the first 100 μm , exactly in the same zone of ROS localization (Fig. 4C).

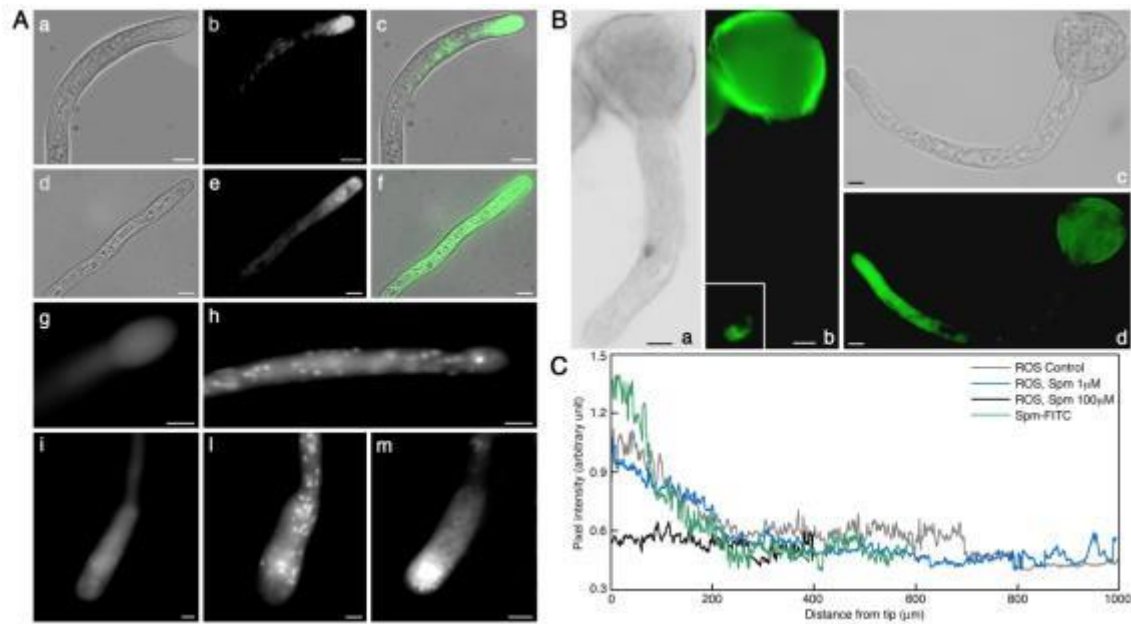


FIGURE 4. Spm co-localizes with ROS in germinating pollen and affects ROS distribution. (A) Tip-localized fluorescence due to the ROS probe DCFH2-DA (a-c) is slightly decreased within 10 min after PAs supplementation (d-f). Variability in the localization of the signal after 11-16 min treatment are shown in g and h, where fluorescence is diffused and faint or localized in spots (g and h respectively). After 20 min treatment the heterogeneity in ROS localization is still evident (i and l), with in addition some tips having newly tip-localized ROS (m). **(B)** FITC-labelled Spm localization in the pollen tube after 10 min supplementation (a-b) and 30 min supplementation (c-d). Bars = 10 μm . **(C)** Line graph with the distribution of ROS in control pollen (grey line) and in pollen treated with Spm 1 and 100 μM (blue and black lines respectively) in comparison to the distribution of FITC-Spm after 30 min incubation.

Effects of synthetic PAs on pollen tube elongation

Since Spm was found to be the most effective among the aliphatic PAs, different Spm analogues have been tested. Four of them, BD26, BD6, DL5, and BD23 are Spm analogues asymmetrically substituted on one of the terminal amine functions with different aromatic groups, while DL6 bears a 2-methoxybenzyl group on each terminal nitrogen atoms of Spm. DL5 and DL6 were selected for the presence in their structure of the aromatic ring of vanillin, which is a natural compound endowed with antioxidant properties. In addition, three synthetic tetramines (Met 6-5-6, Met 6-10-6 and Met 5-10-5) related to methoctramine and characterized by a longer polymethylene chain (when compared to Spm) and a 2-methoxybenzyl group on each terminal nitrogen atoms, were included in the study (Fig. 1). Likewise to the experiment performed with natural aliphatic PAs, we supplemented the pollen germination medium with the different Spm and Met 6-8-6 analogues. All the synthetic PAs were effective on pollen tube elongation in a

dose-dependent manner. Among the PAs mono-substituted on one-terminal primary amino group, the most effective was BD23, which drastically reduced by 69.27% pollen tube elongation at 100 μM , namely less efficiently than Spm.

A similar pattern was observed for DL5, characterized by a different aromatic moiety (a vanillyl group in DL5 vs. a 3-pyridyl moiety in BD23). BD26 was also quite effective, with an inhibition by 54.77% and 71.38% at 100 μM and 250 μM respectively, whereas BD6 caused the arrest of pollen tube growth only at higher concentrations, with a drop of pollen tube elongation by 59.41% at 750 μM (Fig.5A).

All the di-substituted PAs (DL6, Met 6-5-6, Met 6-10-6 and Met 5-10-5) were effective only at a final concentration of 100 μM (or higher than 100 μM) and the most effective was Met 6-5-6, that reduced by 65.72% pollen tube elongation at the concentration of 100 μM . Met 6-5-6, Met 5-10-5 and Met 6-10-6 decreased pollen tube elongation on average by 74% at concentration of 250 μM while DL6, characterized by two vanillyl moieties, displayed the same effect only at 500 μM (Fig. 5B).

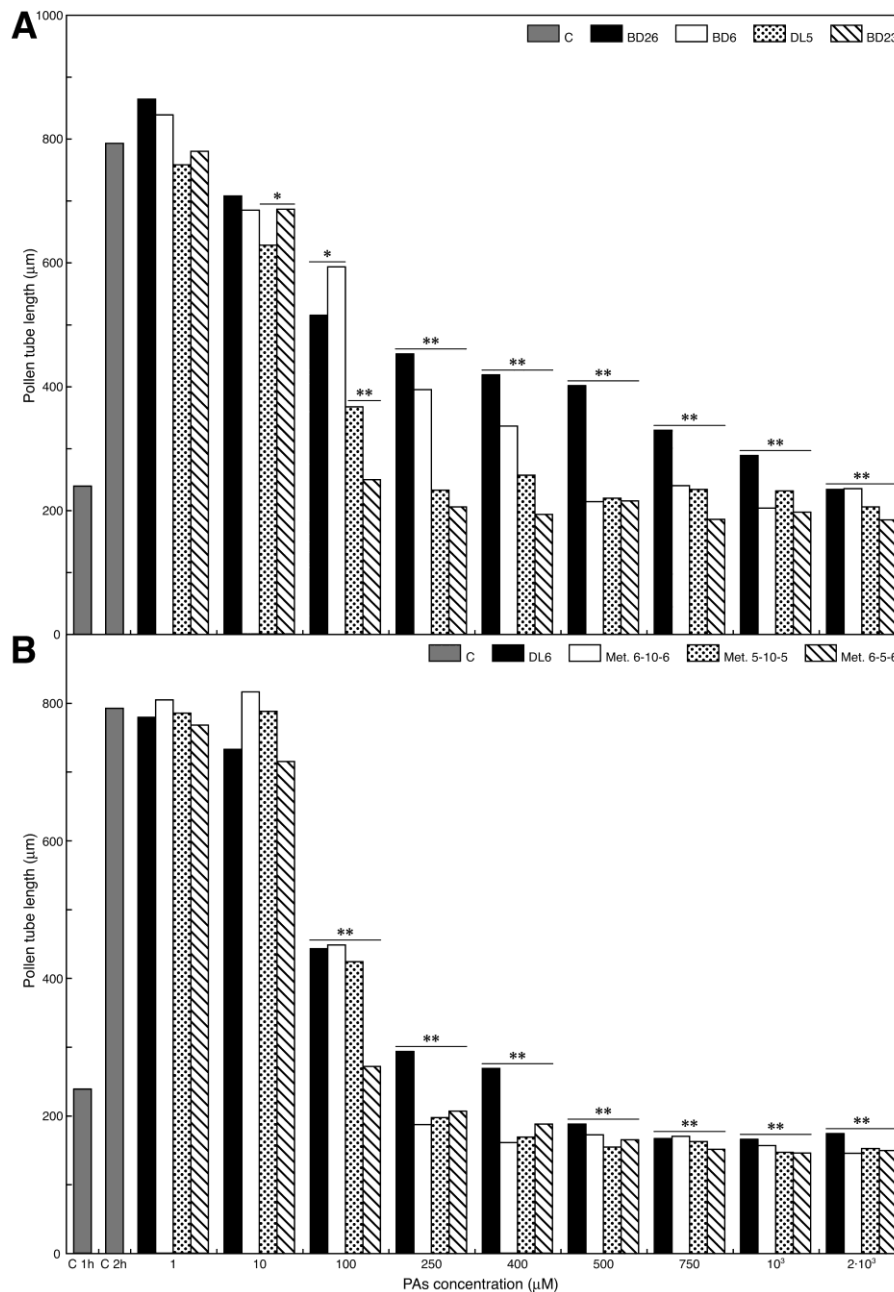


FIGURE 5. Pollen tube length after treatment with different concentration of Spm- analogues. (A) Effect of synthetic PAs with a primary terminal amino group on pollen tube elongation; **(B)** Effect of the synthetic PAs with no primary terminal amino group. Means derive from at least 40 measurements and the experiment was repeated three times. Means of treated samples were compared with control sample after 2 h germination by Dunnett's Multiple Comparison Test. *= $p \leq 0.05$; **= $p \leq 0.01$. SD < 0.15.

Effects on tube morphology and growth recovery of pollen tube after Spm or BD23 treatments

Since Spm and its 3-pyridyl derivative BD23 were the two most effective PAs among the natural and synthetic PAs, respectively, they were used to perform the following experiments. Moreover, one hour-incubation with 100 µM of Spm and

BD23 not only abolished pollen tube elongation, but also caused the swelling of the apex. This morphological change increased when concentrations higher than 100 μM of both PAs were supplied; higher concentrations induced a “lollipop-shape” of the apical region (Fig. 6A). As demonstrated by a time-course experiment, supplementing the growing medium with 500 μM Spm and BD23 induced an enlargement of the apical region in some pollen tubes after 10 min but the swelling became a permanent feature after 15 min and was more evident after extended incubations (Fig. 6B).

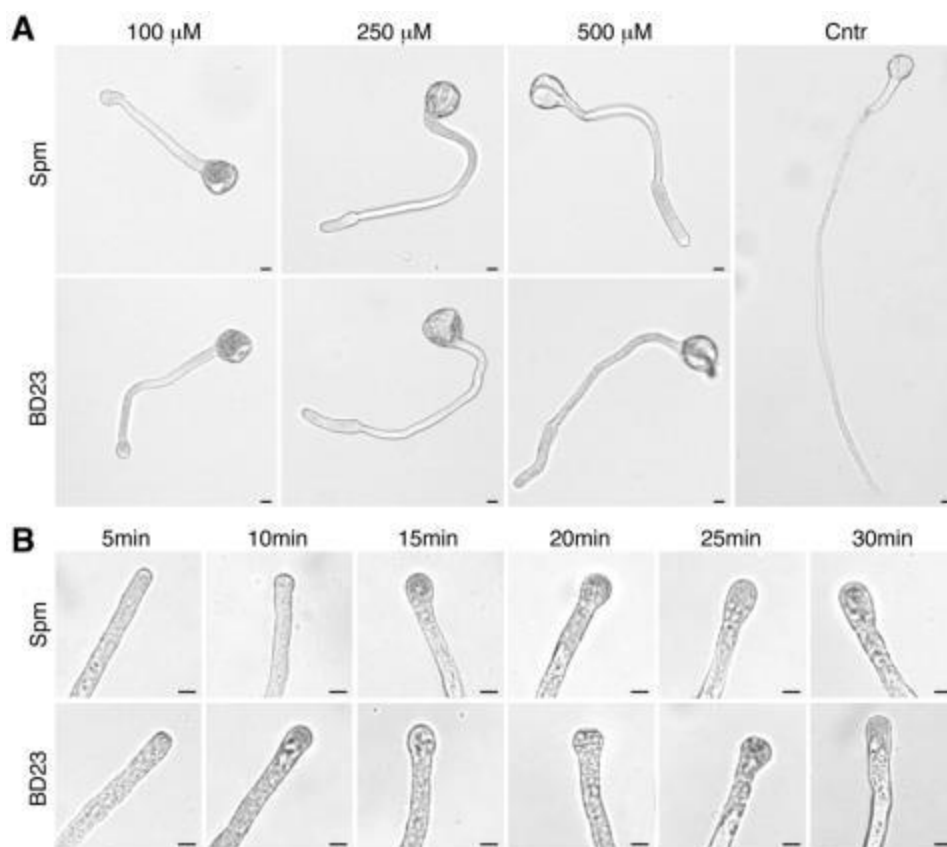


FIGURE 6. Morphological changes in pollen tubes treated with different concentration of Spm and BD23. (A) Dose-dependent swelling of the pollen tube tip after treatment with Spm and BD23 in comparison to a control pollen tube. **(B)** Time-lapse swelling of the pollen tube tip after addition of Spm and BD23 500 μM . Bars = 10 μm .

We performed a growth recovery assay to understand if the removal of PAs from the medium might allow pollen tubes to recover growth. The average recovery from Spm and BD23 effects was affected by both duration of treatment and concentration of PAs (as shown in Table 1). No complete recovery was detected

but a time-dependent trend was observed when pollen was treated with 100 μM of Spm and BD23. In fact, more than 32% recovery of growth rate occurred after 5 min of PAs treatment (36.17% for Spm and 32.92% for BD23); this rate gradually decreased to around 24% after 10 min (23.8% for Spm and 29.91% for BD23) and to 15% on average after 20 min treatment (18.97 for Spm and 12.03% for BD23). No recovery was observed for longer incubation with the two PAs. More drastic was the effect of treatment with 500 μM PAs that allowed a little recovery just after 5 min treatment with a recovery rate of 26.52% and 18.21% for Spm and BD23, respectively.

	100 μM				500 μM			
	5 min	10 min	20 min	45 min	5 min	10 min	20 min	45 min
Spm								
Recovery	36,17 \pm 7,91	23,8 \pm 6,14	18,97 \pm 6,85	-	26,52 \pm 5,9	-	-	-
BD23								
Recovery	32,92 \pm 7,8	29,91 \pm 8,01	12,03 \pm 8,27	-	18,21 \pm 6,4	-	-	-

TABLE 1. Recovery experiment after PAs supplementation. Recovery is expressed, in percentage, as mean of pollen tube length after Spm and BD23 treatment for different times, in comparison to control samples. Means derive from at least 60 measurements and the experiment was repeated three times. Means of treated samples were compared with control sample after 1 h germination by Dunnett's Multiple Comparison Test. All values reported are statistically significant ($p \leq 0.01$, $SD < 0.15$).

Spm and BD23 effect on $\text{O}_2^{\bullet-}$ and H_2O_2 concentration

The overall decrease of tip-localized ROS after PAs treatment was confirmed by using two compounds that are specific for two types of ROS: NBT and DAB. In fact, the capacity of NBT to be reduced by $\text{O}_2^{\bullet-}$ and to form intense purple formazan deposits was evaluated. After 10 min of incubation with NBT, one hour-germinated pollens showed formazan deposits (Fig. 7A). The staining was much more intense in the tip domain, but it also extended for several micrometres (40-60 μm in mean) backwards. Formazan deposits were detectable in the same zones after pollen treatment with 1 μM Spm and BD23. In contrast, NBT reduction in the apical zone was completely abolished in pollen tubes treated with 100 μM Spm and BD23. In addition, pollen treated with the NOX inhibitor diphenylene iodonium (DPI), which prevents the production of $\text{O}_2^{\bullet-}$, showed no formazan deposits. This result is

consistent with the possible activity of NOX as the source of ROS production, essential for pollen tube tip-growth (Figure 7A).

Detection of H₂O₂ by DAB staining showed dark brown precipitates diffusely present along the entire pollen tubes not treated with PAs. In contrast, formation of precipitates was completely abolished in the apical zone when treated with Spm or with BD23 at 100 μM, whereas at 500 μM Spm had a stronger and more diffused effect (Fig. 7B).

To measure the relative levels of endogenous ROS in both germinated control and PAs treated pollen, we performed a ROS quantification using NBT and, in particular, by measuring the absorbance of the purple formazan sediment (Fig. 7C). The NBT-reducing activity was enhanced by the addition of NADH thus suggesting that it was due to the generation of ROS by pollen NOX. Both Spm and BD23 at 100 μM nearly completely inhibit the formation of formazan sediments. A similar result was obtained when pollen was treated with 200 μM DPI, whereas 100 μM concentration had a significantly lower inhibiting effect (Fig. 7C).

To check the precise concentration of both Spm and BD23 that inhibits ROS formation, a dose dependent-experiment has been performed (Fig. 7D). 10 μM Spm very slightly decreased ROS-mediated NBT reduction, while its analogue BD23 was not effective at the same concentration. A drastic decrease of formazan production was clear for both PAs at 50 μM, in fact Spm and BD23 decreased NBT reduction by 51.2% and 70.5% respectively, whereas at 100 μM, the absorbance of the formazan fall down to background levels, with a final drop of NBT reduction by 78.5% and 90.1% respectively for Spm and BD23 (Fig. 7D).

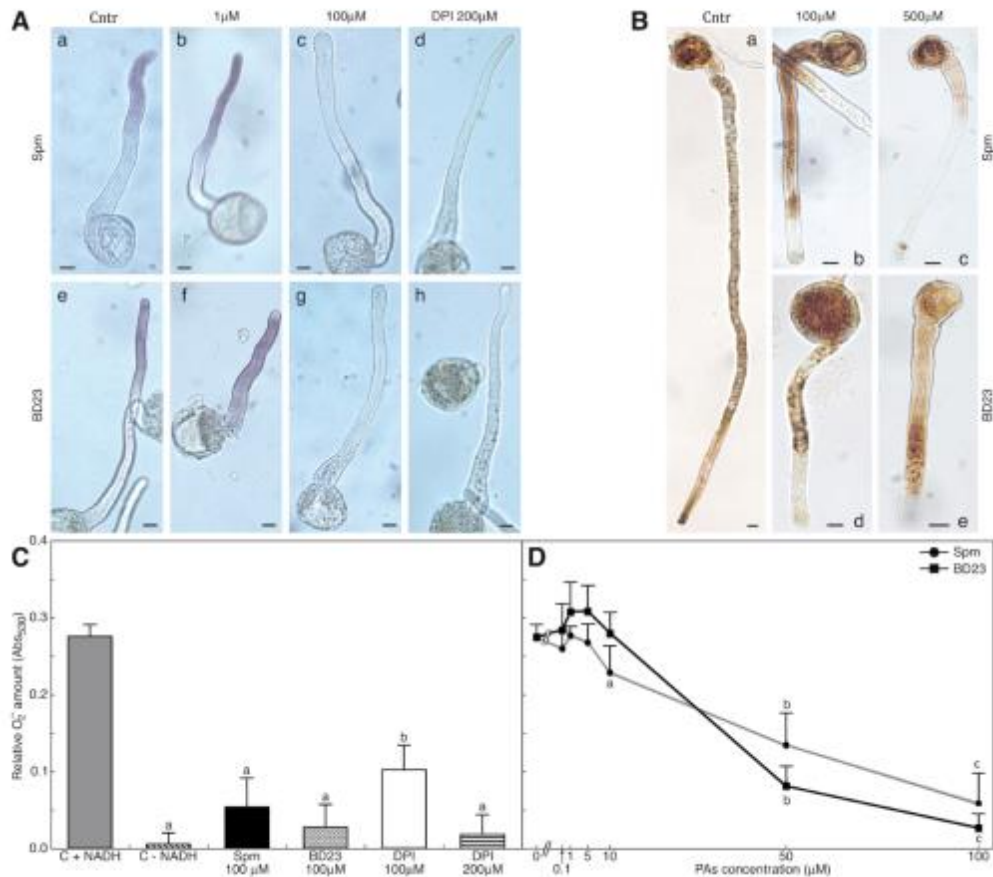


FIGURE 7. Spm and the Spm-analogue BD23 decrease ROS concentration in germinating pollen. (A) O₂⁻ distribution in control pollen and in pollen treated with Spm and BD23 1 and 100 μM. As negative control, pollen was treated with 200 μM of DPI, inhibitor of NOX. Bars = 10 μm. (B) H₂O₂ distribution in control pollen and in pollen treated with Spm and BD23 100 and 500 μM. Bars = 10 μm. (C) Relative amount of O₂⁻ in pollen samples treated with Spm and BD23 100 μM in comparison to control samples. As negative control DPI 100 and 200 μM was used. Background is defined by a control sample not supplemented with NADH. Means derive from at least 12 measurements and the experiment was repeated four times. Means of treated samples were compared with control sample by Dunnett's Multiple Comparison Test. (D) Dose-dependent O₂⁻ scavenging by Spm and BD23. Means derive from at least 12 measurements and the experiment was repeated four times. Means of treated samples were compared with control sample by Dunnett's Multiple Comparison Test.

Ca²⁺ gradient alteration and effect on NOX enzyme activity by Spm and BD23

It is well known that PAs play also a role in modulating Ca²⁺ signalling and that Ca²⁺ gradient and the tip-localized Ca²⁺ influx play a pivotal role in the apical growth of pollen tubes also in relation to ROS production (Pottosin and Shabala, 2014; Pottosin *et al.*, 2014). We decided to investigate if/how exogenous PAs supplementation could affect the tip-focused intracellular Ca²⁺ gradient, since the above-mentioned results showed that PAs affect pollen tube morphology. Figure 8A shows that the tip-focused Ca²⁺ gradient was drastically altered within 2-10

min after addition of PAs as Ca^{2+} distribution was less focused at the tip and more diffused in the sub-apical region of the pollen tube. The Ca^{2+} gradient was restored during the formation of the swollen apex, when it became tip-localized again.

Considering that PAs affect ROS and Ca^{2+} distribution and that NOX enzymes are sensitively affected by Ca^{2+} perturbations, the activity of the $\text{O}_2^{\cdot-}$ producing enzyme was investigated. The two PAs induced a sudden but short-lasting stimulation in the activity of the enzyme. In particular, both Spm and less significantly BD23 increased the activity of the enzyme by 130-150% within the first 2-5 min treatment but their effects were not detectable for times longer than 15 min (Fig. 8B).

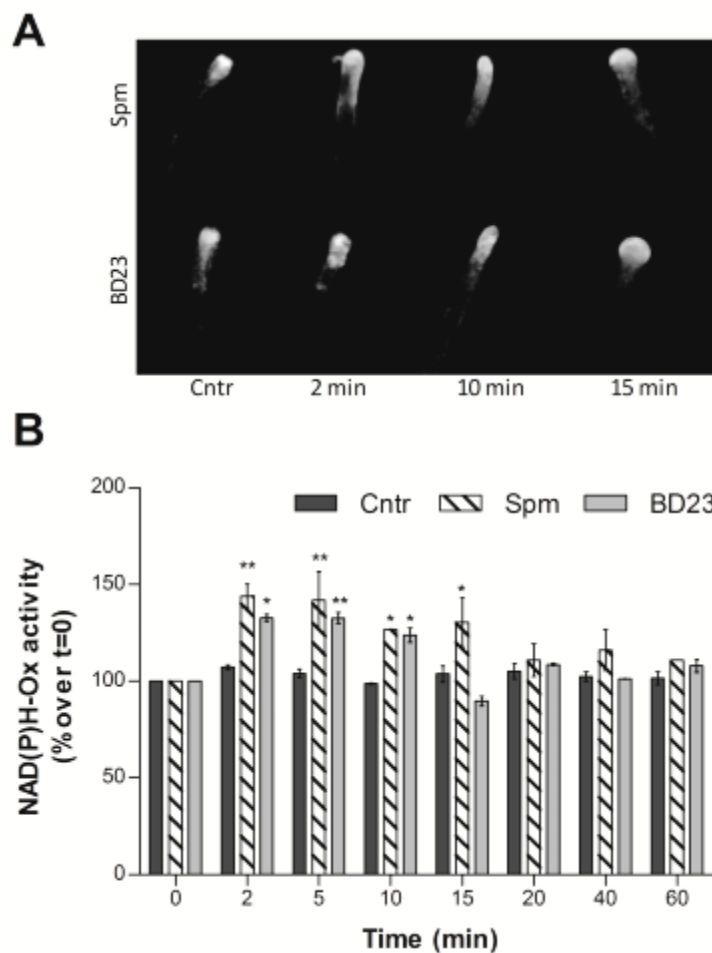


FIGURE 8. Calcium distribution and NOX activity are altered by PAs supplementation. (A) Tip-localized fluorescence due to the Ca^{2+} probe CTC is completely dissipated after 2 and 10 min PAs supplementation. The gradient is restored after 15 min, when the swollen apex has formed. **(B)** Effect of Spm and BD23 on the NOX enzyme over time. Control samples (t=0) were set as 100%. Means derive from at three independent experiments. Means of treated samples were compared with control by Dunnett's Multiple Comparison Test. * = $p \leq 0.05$; ** = $p \leq 0.01$.

Spm and BD23 effect on pollen antioxidant machinery

As the two PAs stimulate ROS production nearly instantly after supplementation, but ROS were generally decreased by both Spm and BD23, the next goal was to understand if pollen activates its antioxidant machinery in response to the exogenous PAs and NOX enzyme activation. Specific activities of the antioxidant enzymes SOD and CAT were measured. Gels for the SOD in-gel activity showed two major bands in the protein extracts of pear pollen, indicating the presence of two SOD isozymes (Fig. 9A). The two PAs induced changes in the activities of both SOD isozymes; in particular, Spm induced a drastic (by 250%) and long-lasting effect with enzyme-stimulation that persisted through the whole treatment. Conversely, BD23 affected the activity of the enzyme that was increased by 180% after 5 min treatment but the effect on both SOD isozymes was not notable for longer times (Fig. 9A).

CAT activity was also analyzed. CAT isozymes were not distinguished and only one large band was observed in all of the times assayed. CAT activity was also affected by the two PAs with a slight time-shift (10-15 min) in comparison to SOD activity. This enzyme was also differently affected by the two PAs, since Spm induced an almost steady increase for 30 min while CAT activity after BD23 treatment was rapidly decreased remaining lower than the controls at 40-60 min post-treatment (Fig. 9B).

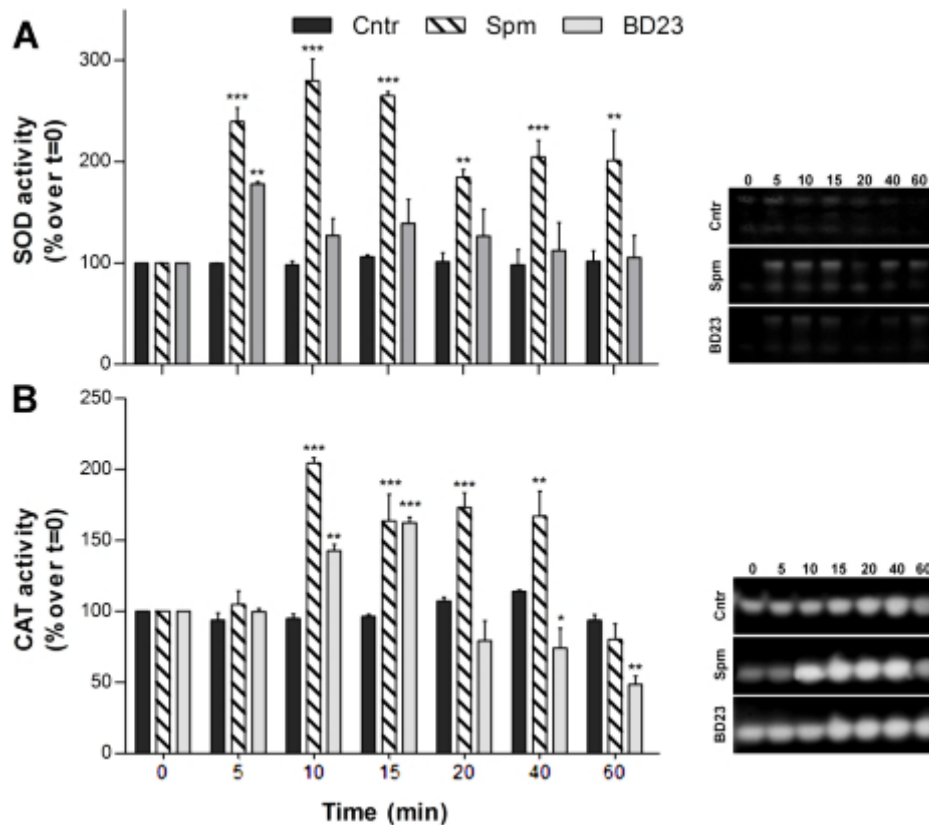


FIGURE 9. Spm and BD23 stimulate the antioxidant machinery. Effect of Spm and BD23 on SOD (A) and CAT (B) enzymes over time. Control samples (t=0) were set as 100%. Means derive from three independent experiments. Means of treated samples were compared with control by Dunnett's Multiple Comparison Test. *= p<0.05; **= p<0.01; ***=p<0.001. On the right of fig A and B, representative images of the in gel activity of both enzymes are shown.

Effect of Spm and BD23 on pollen viability, DNA and nuclei

To determine if the reduction of the apical pool of ROS might have detrimental effects, a time-course viability test was performed. The germination medium was supplemented with Spm or BD23 after the first hour of germination, and pollen viability was assessed using MTT (2,5-diphenyl tetrazolium bromide) staining. As comparison, DPI was also assayed. As shown in Figure 10A, the two PAs, when supplemented at 100 μ M, halved the viability of pollens after 50 min (110 min germination), while after 60 min incubation the viability drastically dropped by 21.1% and 24.5% for Spm and BD23, respectively (Fig. 10A). More effective was the treatment with 500 μ M PAs, which halved the viability of pollens after 30-40 min with no viable pollens detected after 60 min (120 min germination). More drastic was the treatment with 100 μ M DPI, whose supplementation in the germination medium halved the viability of pollens after only 10 min (Fig. 10A).

To test whether PAs-induced ROS-decrease could lead towards cell death, 60 min-germinated pollen was treated for additional time lapses with 500 μM Spm or BD23 and DNA fragmentation was assessed after different incubation times. Spm and BD23 stimulated DNA fragmentation after 30 min incubation, as demonstrated by DNA-laddering, while there were no evidences of DNA fragmentation in control pollen after 2 hours germination. Incubation with 100 μM DPI induced DNA laddering after 15 min and the extent of fragmentation was significantly higher when compared with PAs (Fig. 10B). The sizes of DNA bands were approximately multiples of 200 bp, which is consistent with fragmentation at inter-nucleosomal sites.

As the DNA degradation showed a large increase after PA treatment, the number and characteristics of nuclei in treated or untreated pollens was evaluated by the DNA fluorescent stain DAPI. Pollen tubes with two nuclei were regarded as normal, and the generative and vegetative nuclei were clearly distinguishable since the chromatin of generative cell nuclei was more highly condensed and more deeply stained with DAPI than that of vegetative nuclei. The complete absence of the two nuclei was observed as well as the presence of a single nucleus, suggesting that the vegetative nucleus had degraded. As shown in Figure 10C, treatment with 100 μM PAs decreased the percentage of bi-nucleated pollens and increased especially the number of pollens with one nucleus. Conversely, treatment with 500 μM PAs caused a drop in the number of bi- and mono-nucleated pollens, leading to a majority of pollens with no nucleus. In addition, the Ac-DEVD-CHO peptide (DEVD), an inhibitor of caspase-3, has been supplied to pollen to determine if it could reduce the process of DNA degradation. The degradation of nuclei was completely abolished when pollens were pre-treated with the DEVD peptide and then with PAs 100 μM , while pre-treatment with DEVD could not completely counteract the effects of PAs supplemented at 500 μM . In this case, only the number of mono-nucleated pollens increased, but not the number of bi-nucleated ones.

Treatment with 100 μM DPI drastically decreased the percentage of bi-nucleated pollens and increased especially the number of pollens with no nucleus in comparison to control pollens.

The pre-treatment with DEVD could counteract the effects of DPI and led to an increase in pollens showing only one nucleus.

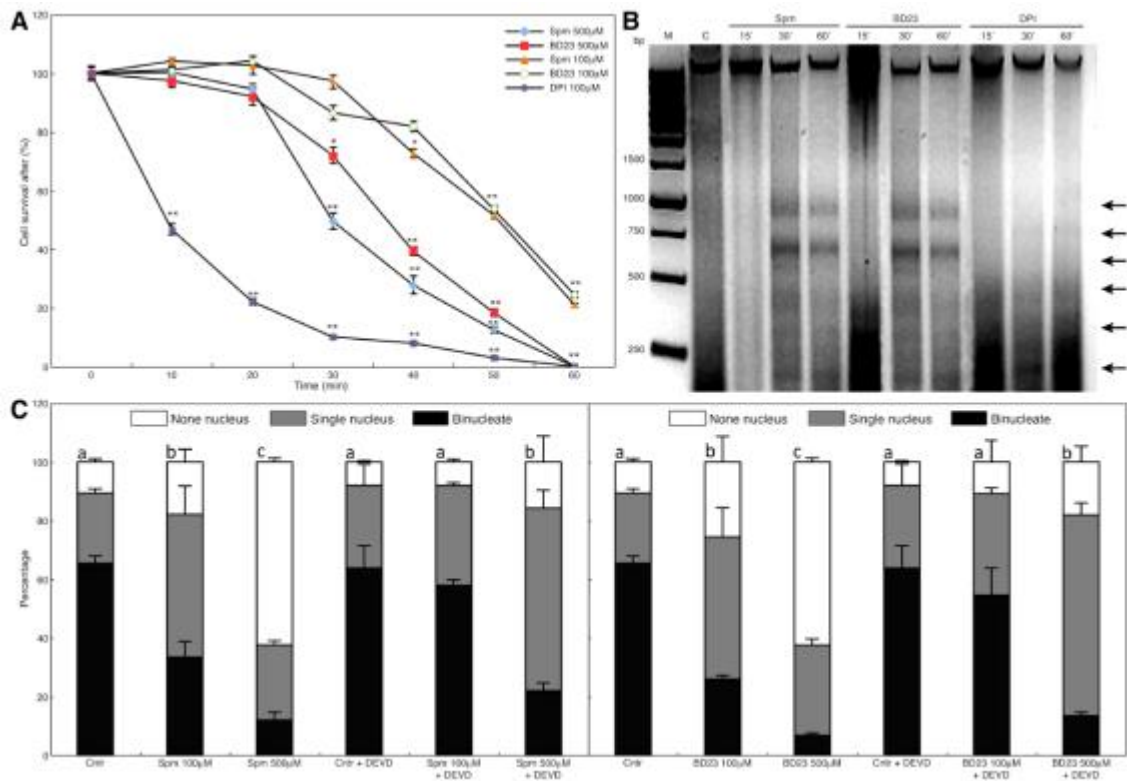


FIGURE 10. PAs induce DNA degradation and lead to cell death. (A) Time-dependent viability test after treatment with DPI 100 µM, Spm and BD23 100 and 500 µM. In each treatment, at least 200 pollens were counted and the experiment was repeated twice. Means of treated samples were compared with control by Dunnett's Multiple Comparison Test. *= $p \leq 0.05$; **= $p \leq 0.01$. Results are normalized on control samples. **(B)** DPI 100 µM, Spm and BD23 500 µM induce DNA-laddering. **(C)** Rate of degradation of nuclear DNA after treatment with DPI, Spm or BD23 and inhibition of this process by the DEVD peptide, an inhibitor of caspase-3. In each treatment, at least 100 pollen tubes were counted and the experiment was repeated twice. Bars labeled by the same letter are not significantly different. Analysis of variance was performed by two-way ANOVA test, with Bonferroni post-test.

Besides the preferentially degradation of the vegetative nucleus, treatment with 100 µM Spm and BD23 induced chromatin condensation in the generative nucleus, that resulted more intensely stained with DAPI (Fig. 11A and D) and smaller (Fig. 11B and D). Moreover, the two nuclei appeared more closed each other in respect to untreated control (Fig. 11C and D).

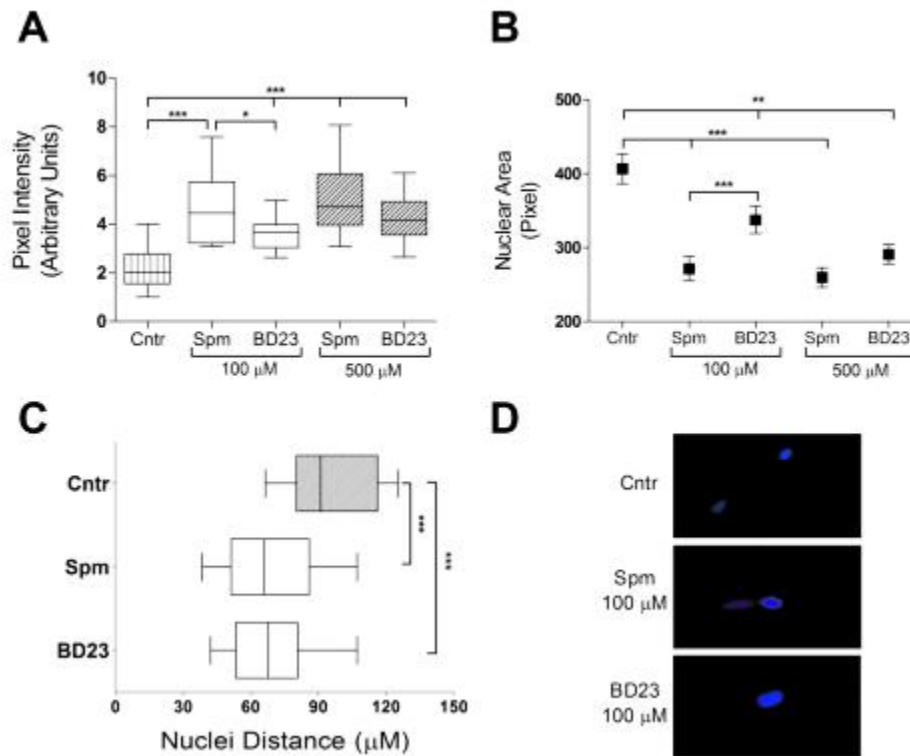


Figure 11. PAs induce nuclear alterations. (A) Dose-dependent nuclear intensity and (B) nuclear condensation after treatment with Spm and BD23 100 and 500 μM. In each treatment, at least 30 nuclei were counted and the experiment was repeated twice. (C) Distance between vegetative and generative nuclei in control pollens and after treatment with Spm and BD23 100. Means of treated samples were compared with control by Dunnett's Multiple Comparison Test. *= p≤0.05; **= p≤0.01; ***=p≤0.001. (D) Nuclei stained with DAPI of control pollen showing the less condensed vegetative nucleus and the highly condensed generative nucleus. Treatment with 100 μM Spm and BD23 induced the preferential degradation of the vegetative nucleus and caused chromatin condensation in the generative nucleus. Representative images were chosen.

Discussion

Exogenous application of natural and synthetic PAs to the germination medium of *Pyrus communis* pollen arrested the process of pollen tube elongation according to the concentration of PAs supplied. Spm was the most effective among the four natural PAs tested because it inhibited pollen growth from 10 μM onwards and modified the morphology of the apex, also leading towards cell death. The different natural PAs are effective according to the length of their backbone whereas the diamine Cad, demonstrated to enter the pollen tube (Iorio *et al.*, 2012), is without effect on pollen tube elongation according to the reported limited role of Cad in plants (Tomar *et al.*, 2013).

The effect of natural PAs has been also observed in other pollen from Rosaceae i.e. *Prunus dulcis*, in which the effect of Put, Spd and Spm has been shown to be dose-dependent thereby promoting pollen tube elongation at PAs concentrations up to 50 μM , whereas higher concentration resulted inhibitory for pollen tube elongation (Sorkheh *et al.*, 2011). Furthermore, in *Actinidia deliciosa* high levels of PAs correlate with male sterility thereby causing reduced pollen development and tube growth (Biasi *et al.*, 2001; Antognoni and Bagni, 2008). The exogenously supplied Spd might modify the cell wall, as it is generally accepted that most of the cellular Spd pool is localized to the cell wall compartment (Mariani *et al.*, 1989), including the pollen cell wall in the form of hydroxycinnamic acid amides (Grienenberger *et al.*, 2009).

Plants are known to produce a complex mixture of amide conjugates of the more common PAs with various phenolic acids, namely hydroxycinnamic acids, differing in numbers of hydroxyl and methoxyl groups. For example, presence of hydroxycinnamoyl-Spd was linked to pollen grain development in *Arabidopsis* (Grienenberger *et al.*, 2009). Although some of the PAs assayed in the present study contain hydroxy- and/or methoxy-substituted aromatic rings, the substitution performed on the terminal amine function preserves its basicity. Thus, all the molecules maintain the tetracationic form as Spm at physiological conditions and are not amide derivatives. Moreover, the focus here was just to determine the effects of Spm and its aromatic analogues on pollen tube growth.

Present data clarify that Spm also rapidly enters tube pollen tip and affects cytoplasmic and nuclear metabolism, thus not simply altering cell wall rebuilding. Spm then diffuses and localizes in the apical and sub-apical regions, according to a gradient profile with maximum concentration at the tip. Apical localization of PAs was also previously observed (Iorio *et al.*, 2012) and it was shown that these polycations are component of the pollen cell wall (Del Duca *et al.*, 2014). The swelling of the apex as well as its lollipop-shape clearly show that the cell wall is severely affected by the PA supplied. It was previously observed that PAs co-localized with TGase and are its substrates *in vivo* by conjugating one (mono-PA) or both (bis-PA) terminal aminic group/s of PAs to protein glutamyl residues. If a cross linkage is formed by bis-PA, proteins remain bound to each other forming a strong net that is no more degraded by proteases; if only mono-PA are formed, the

net cannot be built or it is less strong, thus allowing swelling (Serafini-Fracassini and Del Duca, 2008; Del Duca *et al.*, 2014; Cai *et al.*, 2015). It was also shown that PAs are covalently bound via the enzyme TGase, to actin and tubulin and that at relatively high concentration they block the cytoskeleton-based movement (Del Duca *et al.*, 1997; Del Duca *et al.*, 2013). These reports suggest that one of the possible mechanisms by which Spm and other aliphatic PAs arrested the germination of pollen tubes involves the cytoskeleton-based trafficking, which is essential for pollen tube growth and proper formation of the cell wall.

The reversibility of the growth inhibitory effect is only partial and decreased with time, thus the action of PAs is irreversible and increases in time. This evidence is in agreement with data that show that the linkage of PAs to the cytoskeleton proteins is irreversible, forming rigid actin bundle-like aggregates that cannot move further (Del Duca *et al.*, 2013).

However, the effect of Spm seems to be even more complex, as in addition to the events possibly related to TGase-mediated cell wall and cytoskeleton alteration, other events take place by involving ROS formation/scavenging and, finally, by affecting pollen viability. New data obtained with the present research highlight the co-localization of PAs with pollen tube ROS, as well as changes of different oxidative enzyme activities, showing that also the redox events are deeply and rapidly affected by PAs in the pollen tube. The same relationships between PAs and ROS have been suggested by literature data in other plant models (Swanson and Gilroy, 2010; Zepeda-Jazo *et al.*, 2011; Pottosin *et al.*, 2014). ROS act up/downstream of various signalling cascades (Olsen *et al.*, 2013) and are essential during cell development and pollen tube elongation (Schopfer, 2001; Speranza *et al.*, 2012).

Present results clearly show that a large amount of ROS formation derives rapidly from pollen NOX activity as the NOX inhibitor DPI caused the disappearance of ROS along the tube apical region and inhibited pollen tube growth. Moreover, Spm suddenly stimulated NOX activity and thus ROS formation, also probably altering Ca²⁺ influx. NOX activity stimulation was followed by SOD and CAT activity increase, probably as consequence of the increased ROS production. It was suggested that PAs, except for Cad, could be involved in the plant defence

mechanism by stimulating the antioxidant machinery and decreasing the oxidative stress intensity under water deficit conditions (Kubis, 2003; 2005).

In addition, the eight synthetic PAs included in this study were shown to be effective, inhibiting pollen tube elongation from 100 μM onwards with the exception of DL5 and BD23 that showed inhibitory effect at 10 μM . Within the Spm-derivative series with one aryl-substituted primary amine group, the pattern of activity seemed to be related to the steric hindrance of the aryl group and to the presence of electron-donating groups on it. As results, BD23 was the most effective PAs, followed by DL5, BD6 and finally BD26, the latter characterized by the most bulky naphthalene ring. In general, the presence of two aromatic groups at both ends of the PA backbone caused a reduction in activity. As shown by comparing DL6 to DL5, which bear two and one vanillyl groups, respectively, at least one primary amine function is essential. The longer polymethylene tetramines (Met 6-5-6, Met 6-10-6 and Met 5-10-5) characterized by two 2-methoxybenzyl groups were also effective, but they did not cause a swollen tube tip, pointing out a different mechanism in the inhibition of pollen tube elongation. In a previous study it was found that these polymethylene tetramines act at different cellular levels, as they bind to DNA with a higher affinity than Spm and lead to oxidative stress [40].

In summary, the structure-activity relationships found in the present study indicates that the general activity of PA derivatives is tuned by: I) the presence or absence of one primary amino group, II) the steric hindrance of the aromatic group, III) the length of the carbon backbone and IV) the presence of hydrophilic and/or electron-donating groups on the aryl ring. All these evidences suggest that those compounds probably enter the cell, in accordance with their solubility and ability to pass through the plasma membrane. Moreover, recently, the L-type amino acid transporter (LAT) family transmembrane proteins have been identified as transporters of both PAs and the herbicide paraquat (1,1'-Dimethyl-4,4'-bipyridinium dichloride) characterized by two quaternary ammonium cations. Arabidopsis LAT family proteins showed different subcellular localization properties (plasma membrane, Golgi and endoplasmic reticulum), which suggested that these transporters were involved in intracellular PA trafficking and PA uptake across the plasma membrane (Fujita and Shinozaki, 2014).

The pyridine Spm-derivative BD23 showed, even if at higher concentration, in many cases no significantly different effects from those of Spm, causing the arrest of tube elongation, changes in tip morphology, vitality, nuclei persistence, cell death, growth recovery, ROS gradient and H₂O₂ production. Further, SOD and CAT showed very similar activities but evidenced a more marked transient enhancement of activities elicited by Spm in respect to BD23. These data suggest that, although BD23 and Spm show an overall similar biological profile the additional pyridine group of BD23, slightly affects the physiological characteristics. Taken together, our data suggest a strict relationship between Spm and its derivative BD23 and ROS concentration, in which also the Ca²⁺-gradient is involved. ROS are known to play key roles in modulating cell wall extensibility, that must be loosen enough to allow expansion but also strong enough to prevent tip bursting (Muller *et al.*, 2009). Our results show that decreased ROS level promotes loss of polarity and induces tip swelling, probably altering the balance between ROS that promotes wall stiffening and relaxation (Pottosin and Shabala, 2014). This suggests that O^{2•-} and H₂O₂ may play a role in modulating cell wall strengthening.

Wu and co-workers (Wu *et al.*, 2010) reported that Spd might enter pollen tubes and induce an accumulation of H₂O₂ as result of oxidation mechanisms involving the activity of enzymes such as PAO. The increase of H₂O₂ might in turn stimulate the opening of hyperpolarization-activated Ca²⁺ channels in the plasma membrane leading to an increase of cytosolic Ca²⁺. Accumulation of Ca²⁺ may trigger a series of dramatic effects on the actin cytoskeleton such as depolymerisation. In the present work, Spm might cause comparable effects. Spm can be potentially subjected to oxidation processes thereby leading to accumulation of H₂O₂. Catabolism of Spm may also lead to production of Spd, which can in turn increase the content of H₂O₂ (Wu *et al.*, 2010). Therefore, the effects of Spm on cytosolic Ca²⁺ might be mediated by the levels of ROS, at least until the concentration of ROS is re-equilibrated by the ROS-scavenging system based on SOD and CAT. If an excess of Ca²⁺ enter the pollen tube, the mechanism supporting Ca²⁺ gradient is unbalanced with fast (about 1 min after the SI) and dramatic consequence on pollen tube growth as shown in *Papaver rhoeas* pollen tubes after self-incompatibility (SI) response (Wu *et al.*, 2011).

Therefore, Spm and BD23 could alter the pollen tube tip morphology either directly by being covalently linked to wall components through TGase or indirectly by altering ROS concentration and perturbing Ca^{2+} influx. The final event of Spm supplementation was DNA laddering and the degradation of the nuclei (especially the vegetative one usually located at the tip region) thus leading to cell death. This could be induced by the altered redox state or by Ca^{2+} -activated signalling; however, the possibility that PAs affect nuclear DNA stability, as suggested by well-established literature data, cannot be ruled out (Ha *et al.*, 1998; Das and Misra, 2004). Moreover, the shorter distance between DAPI- stained nuclei of treated pollen might depend on the male germ unit not efficiently transported by the cytoskeleton, as it occurs in untreated samples. In the attempt to provide a timeline of events occurring after supplementation of Spm, we have depicted a hypothetical sequence in Figure 12.

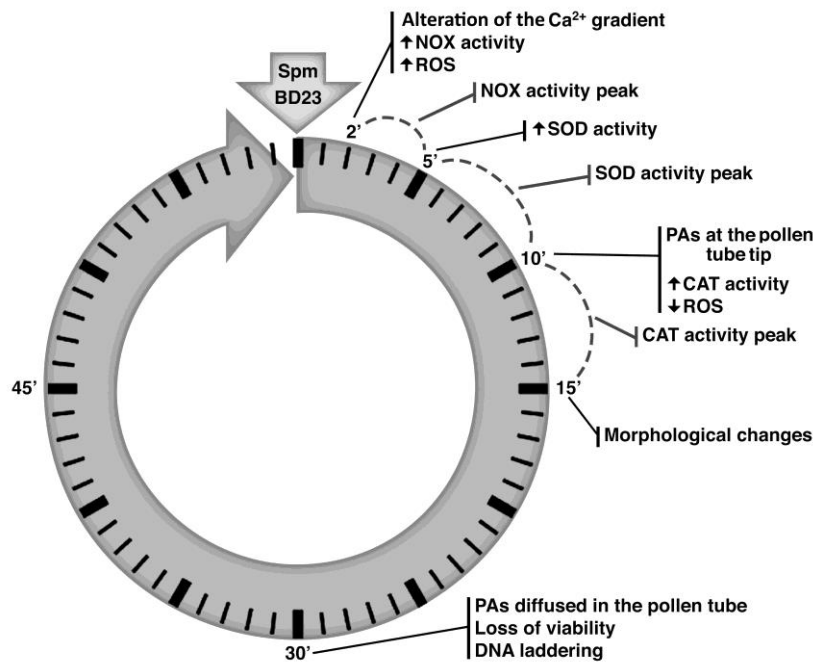


FIGURE 12. From exogenous PAs supply to cell death: an overview of the timing. After 10 min from Spm and BD23 supply, the Ca^{2+} apical gradient was altered and NOX activity increased, with a maximum peak within 2 and 5 min. At 5 min SOD activity was increased with a maximum peak within 5 and 10 min, depending on the PAs supplied. At 10 min PAs localized at the tip of the pollen tube then they diffuse along the subapical region. At 10 min, CAT activity was stimulated and ROS concentration decreased. At 15 min, signs of morphological changes start to be visible and at 30 min, DNA laddering occurred followed by cell death.

Altogether, these results show how fine-tuned must be the modulation of free and conjugated PAs, and show that the level of PAs is regulated by different processes such as catabolism, biosynthesis, conjugation, inter-conversion and transport. The PA homeostasis is essential for a proper pollen tube growth because it controls ROS titre, whose balance is controlled by production and scavenging. Furthermore, these findings may contribute to give a new spark in understanding the intricate networks involved in pollen tube germination, and how the major players involved in this process (PAs, ROS, cytoskeleton and Ca²⁺) could be interconnected.

References

- Andronis, E.A., Moschou, P.N., Touni, I., and Roubelakis-Angelakis, K.A. (2014). Peroxisomal polyamine oxidase and NADPH-oxidase cross-talk for ROS homeostasis which affects respiration rate in *Arabidopsis thaliana*. *Front Plant Sci* 5, 132.
- Antognoni, F., and Bagni, N. (2008). Bis(guanylhydrazones) negatively affect in vitro germination of kiwifruit pollen and alter the endogenous polyamine pool. *Plant Biol (Stuttg)* 10, 334-341.
- Bagni, N., Adamo, P., and Serafini-Fracassini, D. (1981). RNA, proteins and polyamines during tube growth in germinating apple pollen. *Plant Physiol* 68, 727-730.
- Belda-Palazon, B., Ruiz, L., Marti, E., Tarraga, S., Tiburcio, A.F., Culiarez, F., Farras, R., Carrasco, P., and Ferrando, A. (2012). Amino-propyl transferases involved in polyamine biosynthesis localize preferentially in the nucleus of plant cells. *PLoS One* 7, e46907.
- Biasi, R., Falasca, G., Speranza, A., De Stradis, A., Scozzianti, V., Franceschetti, M., Bagni, N., and Altamura, M.M. (2001). Biochemical and ultra-structural features related to male sterility in the dioecious species *Actinidia deliciosa*. *Plant Physiol. Biochem.* 39 395–406.
- Bonaiuto, E., Milelli, A., Cozza, G., Tumiatti, V., Marchetti, C., Agostinelli, E., Fimognari, C., Hrelia, P., Minarini, A., and Di Paolo, M.L. (2013). Novel polyamine analogues: from substrates towards potential inhibitors of monoamine oxidases. *Eur J Med Chem* 70, 88-101.
- Bonaiuto, E., Minarini, A., Tumiatti, V., Milelli, A., Lunelli, M., Pegoraro, M., Rizzoli, V., and Di Paolo, M.L. (2012). Synthetic polyamines as potential amine oxidase inhibitors: a preliminary study. *Amino Acids* 42, 913-928.
- Cai, G., and Cresti, M. (2009). Organelle motility in the pollen tube: a tale of 20 years. *J Exp Bot* 60, 495-508.
- Cai, G., Sobieszczuk-Nowicka, E., Aloisi, I., Fattorini, L., Serafini-Fracassini, D., and Del Duca, S. (2015). Polyamines are common players in different facets of plant programmed cell death. *Amino Acids* 47, 27-44.
- Das, K.C., and Misra, H.P. (2004). Hydroxyl radical scavenging and singlet oxygen quenching properties of polyamines. *Mol Cell Biochem* 262, 127-133.
- Daudi, A., Cheng, Z., O'brien, J.A., Mammarella, N., Khan, S., Ausubel, F.M., and Bolwell, G.P. (2012). The apoplastic oxidative burst peroxidase in *Arabidopsis* is a major component of pattern-triggered immunity. *Plant Cell* 24, 275-287.
- Del Duca, S., Bregoli, A.M., Bergaini, C., and Serafini-Fracassini, D. (1997). Transglutaminase-catalyzed modification of cytoskeletal proteins by polyamines during the germination of *Malus domestica* pollen. *Sexual Plant Reproduction* 10, 89-95.

- Del Duca, S., Faleri, C., Iorio, R.A., Cresti, M., Serafini-Fracassini, D., and Cai, G. (2013). Distribution of transglutaminase in pear pollen tubes in relation to cytoskeleton and membrane dynamics. *Plant Physiol* 161, 1706-1721.
- Del Duca, S., Serafini-Fracassini, D., Bonner, P., Cresti, M., and Cai, G. (2009). Effects of post-translational modifications catalysed by pollen transglutaminase on the functional properties of microtubules and actin filaments. *Biochem J* 418, 651-664.
- Del Duca, S., Serafini-Fracassini, D., and Cai, G. (2014). Senescence and programmed cell death in plants: polyamine action mediated by transglutaminase. *Front Plant Sci* 5, 120.
- Di Sandro, A., Del Duca, S., Verderio, E., Hargreaves, A.J., Scarpellini, A., Cai, G., Cresti, M., Faleri, C., Iorio, R.A., Hirose, S., Furutani, Y., Coutts, I.G., Griffin, M., Bonner, P.L., and Serafini-Fracassini, D. (2010). An extracellular transglutaminase is required for apple pollen tube growth. *Biochem J* 429, 261-271.
- Dutra, N.T., Silveira, V., De Azevedo, I.G., Gomes-Neto, L.R., Facanha, A.R., Steiner, N., Guerra, M.P., Floh, E.I., and Santa-Catarina, C. (2013). Polyamines affect the cellular growth and structure of pro-embryogenic masses in *Araucaria angustifolia* embryogenic cultures through the modulation of proton pump activities and endogenous levels of polyamines. *Physiol Plant* 148, 121-132.
- Forde, B.G., and Roberts, M.R. (2014). Glutamate receptor-like channels in plants: a role as amino acid sensors in plant defence? *Prime Rep* 6, 37.
- Foreman, J., Demidchik, V., Bothwell, J.H., Mylona, P., Miedema, H., Torres, M.A., Linstead, P., Costa, S., Brownlee, C., Jones, J.D., Davies, J.M., and Dolan, L. (2003). Reactive oxygen species produced by NADPH oxidase regulate plant cell growth. *Nature* 422, 442-446.
- Fujita, M., and Shinozaki, K. (2014). Identification of polyamine transporters in plants: paraquat transport provides crucial clues. *Plant Cell Physiol* 55, 855-861.
- Grienenberger, E., Besseau, S., Geoffroy, P., Debayle, D., Heintz, D., Lapierre, C., Pollet, B., Heitz, T., and Legrand, M. (2009). A BAH domain acyltransferase is expressed in the tapetum of Arabidopsis anthers and is involved in the synthesis of hydroxycinnamoyl spermidines. *Plant J* 58, 246-259.
- Ha, H.C., Sirisoma, N.S., Kuppusamy, P., Zweier, J.L., Woster, P.M., and Casero, R.A., Jr. (1998). The natural polyamine spermine functions directly as a free radical scavenger. *Proc Natl Acad Sci U S A* 95, 11140-11145.
- Iorio, R.A., Di Sandro, A., Paris, R., Pagliarani, G., Tartarini, S., Ricci, G., Serafini-Fracassini, D., Verderio, E., and Del Duca, S. (2012). Simulated environmental criticalities affect transglutaminase of *Malus* and *Corylus* pollens having different allergenic potential. *Amino Acids* 42, 1007-1024.
- Kubis, J. (2003). Polyamines and "scavenging system": influence of exogenous spermidine on catalase and guaiacol peroxidase activities, and free polyamine level in barley leaves under water deficit. *Acta Physiol Plant* 25 337-343.
- Kubis, J. (2005). The effect of exogenous spermidine on superoxide dismutase activity, H₂O₂ and superoxide radical level in barley leaves under water deficit conditions. *Acta Physiol Plant* 27, 289-295.
- Lade, B.D., Patil, A.S., and Paikrao, H.M. (2014). Efficient genomic DNA extraction protocol from medicinal rich *Passiflora foetida* containing high level of polysaccharide and polyphenol. *Springerplus* 3, 457.
- Mariani, P., D'orazi, D., and Bagni, N. (1989). Polyamines in primary wall of carrot cells: endogenous content and interactions. *J. Plant Physiol.* 135, 508-510.
- Melchiorre, C., Cassinelli, A., and Quaglia, W. (1987). Differential blockade of muscarinic receptor subtypes by polymethylene tetraamines. Novel class of selective antagonists of cardiac M-2 muscarinic receptors. *J Med Chem* 30, 201-204.
- Minarini, A., Budriesi, R., Chiarini, A., Melchiorre, C., and Tumiatti, V. (1991). Further investigation on methoctramine-related tetraamines: effects of terminal N-substitution and of chain

- length separating the four nitrogens on M2 muscarinic receptor blocking activity. *Farmaco* 46, 1167-1178.
- Minarini, A., Milelli, A., Tumiatti, V., Rosini, M., Bolognesi, M.L., and Melchiorre, C. (2010). Synthetic polyamines: an overview of their multiple biological activities. *Amino Acids* 38, 383-392.
- Minarini, A., Milelli, A., Tumiatti, V., Rosini, M., Lenzi, M., Ferruzzi, L., Turrini, E., Hrelia, P., Sestili, P., Calcabrini, C., and Fimognari, C. (2013). Exploiting RNA as a new biomolecular target for synthetic polyamines. *Gene* 524, 232-240.
- Minocha, R., Majumdar, R., and Minocha, S.C. (2014). Polyamines and abiotic stress in plants: a complex relationship. *Front Plant Sci* 5, 175.
- Moschou, P.N., and Roubelakis-Angelakis, K.A. (2014). Polyamines and programmed cell death. *J Exp Bot* 65, 1285-1296.
- Muller, K., Linkies, A., Vreeburg, R.A., Fry, S.C., Krieger-Liszkay, A., and Leubner-Metzger, G. (2009). In vivo cell wall loosening by hydroxyl radicals during cress seed germination and elongation growth. *Plant Physiol* 150, 1855-1865.
- Olsen, L.F., Issinger, O.G., and Guerra, B. (2013). The Yin and Yang of redox regulation. *Redox Rep* 18, 245-252.
- Pasqualini, S., Tedeschini, E., Frenguelli, G., Wopfner, N., Ferreira, F., D'amato, G., and Ederli, L. (2011). Ozone affects pollen viability and NAD(P)H oxidase release from *Ambrosia artemisiifolia* pollen. *Environ Pollut* 159, 2823-2830.
- Potocky, M., Jones, M.A., Bezdova, R., Smirnoff, N., and Zarsky, V. (2007). Reactive oxygen species produced by NADPH oxidase are involved in pollen tube growth. *New Phytol* 174, 742-751.
- Pottosin, I., and Shabala, S. (2014). Polyamines control of cation transport across plant membranes: implications for ion homeostasis and abiotic stress signaling. *Front Plant Sci* 5, 154.
- Pottosin, I., Velarde-Buendia, A.M., Bose, J., Zepeda-Jazo, I., Shabala, S., and Dobrovinskaya, O. (2014). Cross-talk between reactive oxygen species and polyamines in regulation of ion transport across the plasma membrane: implications for plant adaptive responses. *J Exp Bot* 65, 1271-1283.
- Pottosin, I., Velarde-Buendia, A.M., Zepeda-Jazo, I., Dobrovinskaya, O., and Shabala, S. (2012). Synergism between polyamines and ROS in the induction of Ca (2+) and K (+) fluxes in roots. *Plant Signal Behav* 7, 1084-1087.
- Sagi, M., and Fluhr, R. (2001). Superoxide production by plant homologues of the gp91 NADPH oxidase. Modulation of activity by calcium and by tobacco mosaic virus infection. *Plant Physiol* 126, 1281-1290.
- Saiki, R., Yoshizawa, Y., Minarini, A., Milelli, A., Marchetti, C., Tumiatti, V., Toida, T., Kashiwagi, K., and Igarashi, K. (2013). In vitro and in vivo evaluation of polymethylene tetraamine derivatives as NMDA receptor channel blockers. *Bioorg Med Chem Lett* 23, 3901-3904.
- Schopfer, P. (2001). Hydroxyl radical-induced cell-wall loosening in vitro and in vivo: implications for the control of elongation growth. *The Plant Journal* 28, 679-688.
- Serafini-Fracassini, D., and Del Duca, S. (2008). Transglutaminases: widespread cross-linking enzymes in plants. *Ann Bot* 102, 145-152.
- Sorkheh, K., Shiran, B., Rouhi, V., Khodambashi, M., Wolukau, J.N., and Ercisli, S. (2011). Response of *in vitro* pollen germination and pollen tube growth of almond (*Prunus dulcis* Mill.) to temperature, polyamines and polyamine synthesis inhibitor. *Biochemical Systematics and Ecology* 39, 749-757.
- Speranza, A., and Calzoni, G.L. (1980). Compounds released from incompatible apple pollen during in vitro germination. *Z. Pflanzenphysiol.* 97, 95-102.
- Speranza, A., Crinelli, R., Scoccianti, V., and Geitmann, A. (2012). Reactive oxygen species are involved in pollen tube initiation in kiwifruit. *Plant Biol (Stuttg)* 14, 64-76.
- Swanson, S., and Gilroy, S. (2010). ROS in plant development. *Physiol Plant* 138, 384-392.

- Takano, A., Kakehi, J., and Takahashi, T. (2012). Thermospermine is not a minor polyamine in the plant kingdom. *Plant Cell Physiol* 53, 606-616.
- Tiburcio, A.F., Altabella, T., Bitrian, M., and Alcazar, R. (2014). The roles of polyamines during the lifespan of plants: from development to stress. *Planta* 240, 1-18.
- Tomar, P.C., Lakra, N., and Mishra, S.N. (2013). Cadaverine: a lysine catabolite involved in plant growth and development. *Plant Signal Behav* 8, doi: 10.4161/psb.25850.
- Walden, R., Cordeiro, A., and Tiburcio, A.F. (1997). Polyamines: small molecules triggering pathways in plant growth and development. *Plant Physiol* 113, 1009-1013.
- Wang, X.L., Takai, T., Kamijo, S., Gunawan, H., Ogawa, H., and Okumura, K. (2009). NADPH oxidase activity in allergenic pollen grains of different plant species. *Biochem Biophys Res Commun* 387, 430-434.
- Weydert, C.J., and Cullen, J.J. (2010). Measurement of superoxide dismutase, catalase and glutathione peroxidase in cultured cells and tissue. *Nat Protoc* 5, 51-66.
- Wu, J., Shang, Z., Jiang, X., Moschou, P.N., Sun, W., Roubelakis-Angelakis, K.A., and Zhang, S. (2010). Spermidine oxidase-derived H₂O₂ regulates pollen plasma membrane hyperpolarization-activated Ca²⁺-permeable channels and pollen tube growth. *Plant J* 63, 1042-1053.
- Wu, J., Wang, S., Gu, Y., Zhang, S., Publicover, S.J., and Franklin-Tong, V.E. (2011). Self-incompatibility in *Papaver rhoeas* activates nonspecific cation conductance permeable to Ca²⁺ and K⁺. *Plant Physiol* 155, 963-973.
- Wudick, M.M., and Feijo, J.A. (2014). At the intersection: merging Ca²⁺ and ROS signaling pathways in pollen. *Mol Plant* 7, 1595-1597.
- Zepeda-Jazo, I., Velarde-Buendia, A.M., Enriquez-Figueroa, R., Bose, J., Shabala, S., Muniz-Murguía, J., and Pottosin, I. (2011). Polyamines interact with hydroxyl radicals in activating Ca²⁺ and K⁺ transport across the root epidermal plasma membranes. *Plant Physiol* 157, 2167-2180.

Chapter 3

Spermine affects pollen tube growth by perturbing calcium concentration, actin organization and cell wall structure

Abstract

Pollen is fundamental in the reproductive process of seed plants and the proper growth of the pollen tube depends on an elaborate mechanism that integrates several molecular and cytological sub-processes and ensures a cell shape adapted to the transport of gametes. The growth mechanism is also controlled by several signaling molecules such as polyamines (PAs), which control different aspects of pollen tube germination, e.g. by structuring pollen cell wall and by modulating protein (mainly cytoskeletal) assembly. Both cytoplasmic and apoplastic PAs take part in these complex processes. In this work, we analyzed the effects of spermine on the growth of pear pollen tubes. Spm is able to reshape pollen tubes by inducing the formation of apical swellings, which are triggered by severe modifications of the cytosolic calcium concentration and pH values. This consecutively causes a major reorganization of actin filaments and leads to alterations of cytoplasmic organelle movement. Regulation of the growth mechanism also takes place through modification of pectin, cellulose and callose deposition. In summary, Spm is able to deregulate pollen tube growth and therefore it could be an important molecule in the relationship between pollen tube and pistil in flowering plants.

Introduction

The pollen tube growth represents a remarkable example of polarized expansion, which consists in the deposition of new cell wall material only at the extending tip (Hepler et al., 2013). In fact, the pollen tube cell wall is not comparable to that of

other plant cells. The most striking difference is that deposition of new cell wall components occurs along the growth axis in an accurate temporal sequence. Methyl-esterified pectins are first secreted at the apex of pollen tubes (O' Neill et al., 1990). After deposition, they are chemically converted into acid pectins at the apex/subapex edge (Rockel et al., 2008), where they bind calcium, thereby contributing to strengthen the cell wall (Palin and Geitmann, 2012; Wolf and Greiner, 2012). This prevents additional deformation of the cell wall and contributes to maintain the cylindrical shape of pollen tubes. The balance between pectin secretion and activity of pectin methyl-esterase (PME) thus yields a gradient at the pollen tube apex with highly methyl-esterified pectins at the extreme apex and a less esterified mix of polymers progressively away from the apex. As a consequence, the extreme apical wall is 'softer' than the cell wall in the pollen tube shank and, during oscillatory growth, episodes of rapid growth are preceded by local softening of the apical cell wall (Wolf and Greiner, 2012). In addition to pectins, the pollen tube cell wall contains other components such as callose, cellulose and arabinogalactan proteins. Callose is usually absent from the apex while both arabinogalactan proteins and cellulose could also be detected in the hemispherical apical dome (Mollet et al., 2013). In support of this, the cellulose synthase complex has been found close to the pollen tube apex in *Nicotiana tabacum* (Cai et al., 2011) and *Arabidopsis thaliana* (Chebli et al., 2012).

Newly synthesized cell wall components are transported along the actin cytoskeleton, packed into vesicles, and reach the apical domain where they fuse and progressively replaces the previously deposited material, which is moved behind from the tip by cell expansion (Rojas et al., 2011). However, recent studies questioned this conclusion by providing evidence that vesicles may actually fuse and secrete their contents in an annulus in the immediate vicinity of the tube tip (Bove et al., 2008; Hepler et al., 2013). Apart from promoting organelle and vesicle streaming, the actin cytoskeleton also regulates the pollen tube morphology because actin depolymerization not only blocks pollen tube growth and inhibits cytoplasmic streaming but also promotes the formation of swollen tube tips (Cárdenas et al., 2005). The spatial organization of actin filaments in the pollen tube apex is thus a key factor during pollen tube elongation (Lovy-Wheeler et al., 2005) and has to be finely modulated by the activity of Rho proteins and actin

binding proteins (ABPs) (Qu et al., 2015). ROP1 (Rho-Of-Plant) proteins might regulate actin filaments by enhancing F-actin assembly or increasing Ca^{2+} concentration thereby leading to actin disassembly. ABPs include actin depolymerization factors, actin-fringe-localized actin interacting proteins, formins, profilins and others (Qu et al., 2015). All these ABPs are finely regulated to allow the correct polymerization and organization of actin filaments by several factors, such as the preference for ADP/ATP-loaded actin, monomeric or filamentous actin, a pH-gradient and a tip-focused Ca^{2+} gradient (Feijo et al., 2001;Hepler et al., 2001;Holdaway-Clarke and Hepler, 2003).

A gradient of free Ca^{2+} concentration in tube apical region is essential for pollen tube growth (Feijo et al., 2001;Steinhorst and Kudla, 2013;Himschoot et al., 2015). This tip-focused gradient is necessary both for vesicle fusion and for regulating the direction of pollen tube growth, presumably by controlling the site of secretion (Malho and Trewavas, 1996). An apical influx of Ca^{2+} ions from the extracellular milieu has been firmly established as the main source of this Ca^{2+} gradient. Extensive research has started to unravel the identity of the plasma membrane-located Ca^{2+} -permeable channels involved in the observed Ca^{2+} fluxes, such as stretch-activated Ca^{2+} channels (Dutta and Robinson, 2004), cyclic nucleotide-gated channels (Frietsch et al., 2007) and glutamate receptor-like channels (Michard et al., 2011). Among factors that could affect cytosolic free Ca^{2+} levels there are polyamines (PAs) (Wu et al., 2010;Aloisi et al., 2015), aliphatic polycations widespread in all living organisms.

Pollen contains high amounts PAs and high activities of their corresponding biosynthetic enzymes (Bagni et al., 1981;Falasca et al., 2010), whose inhibition strongly affected pollen germination (Antognoni and Bagni, 2008). Exogenous application of PAs also inhibited both pollen germination and tube growth (Antognoni and Bagni, 2008;Wu et al., 2010;Aloisi et al., 2015). The effect of exogenous PAs during pollen tube growth seems multifactorial and was shown to involve the organization and assembly of the cytoskeleton, by affecting actin and tubulin assembly and their interaction with motor proteins (Del Duca et al., 2009) as well as cell wall deposition (Di Sandro et al., 2010). The action of PAs is partially mediated by the Ca^{2+} - dependent conjugating enzyme transglutaminase (TGase) that is present in distinct cell compartments (e.g. cytosol, organelles, membranes

and cell walls). The conjugation of PAs to cytoskeleton proteins by TGase regulates membrane trafficking along actin filaments and microtubules in pear pollen tubes (Del Duca et al., 2009); moreover, the activity of an extracellular TGase is necessary for apple pollen tube growth (Di Sandro et al., 2010).

In plant cells, part of the cellular pool of PAs is localized in the cell wall compartment. These PAs are mostly in the form of conjugates to hydroxycinnamic acids (HCCAs). The PA-HCCA derivatives, which are able to cross-link different cell wall polymers, have been shown to modulate the rigidity of the cell wall (Tiburcio et al., 2014) thus contributing to the wall architecture. Nevertheless, PAs, by regulating PME enzymes, could control wall stiffening also indirectly (Charnay et al., 1992). What is worth of notice is that PAs can modulate cytosolic free Ca^{2+} levels (Wu et al., 2010; Aloisi et al., 2015) and thus control a huge variety of processes, from secretion of molecules to intracellular dynamics of organelles and cytoskeleton.

We recently demonstrated that the inhibitory effect of exogenous PAs on the *in vitro* growth of pear pollen tubes was related to a decrement of ROS level. Among the different PAs we tested, Spm showed the strongest inhibitory effect; it was also shown that Spm entered through the pollen tube tip, then diffused in the sub-apical region and led to an enlarged tip (Aloisi et al., 2015).

The purpose of the present work was to study the specific molecular mechanism by which Spm altered the deposition of cell wall at the swollen pollen tube tip. Because cell wall deposition depends on the proper organization of the cytoskeletal apparatus and on vesicular trafficking, emphasis was placed on issues related to both processes. Therefore, the dynamics of actin filaments the apical trafficking of vesicles, the delivery of newly-synthesized cell wall material and factors (such as pH and Ca^{2+} fluxes) that act as general controllers of the entire process were analyzed.

Materials and methods

Chemicals, plant material and spermine treatment

All chemicals (unless otherwise indicated) were obtained from Sigma–Aldrich (Milan, Italy). Mature pollen of pear (*Pyrus communis* cv. Williams) was collected

from plants grown in experimental plots at the University of Bologna (Department of Agricultural Sciences, University of Bologna). Handling, storage, pollen hydration and germination were performed as previously reported (Bagni et al., 1981; Del Duca et al., 1997). LaCl₃, GdCl₃ and EGTA were alternatively added to the growing medium 20 min (40 min of germination) prior Spm supplementation (60 min of germination). Pollen was visualized under a light microscope (Nikon Eclipse E600) equipped with a digital camera (Nikon DXM1200). 2,5-diphenyl tetrazoliumbromide (MTT) assay was performed as previously reported (Aloisi et al., 2015).

Kymograph analysis of pollen tubes

Pollen tubes of pear were observed using a Nikon inverted microscope Diaphot TMD equipped with a 40X objective. Video clips were captured using a CCD camera C2400-75i Hamamatsu (Hamamatsu Photonics) connected to Argus-20 (Hamamatsu) and converted into MPEG-2 files by a video capture system (PCTV Center) (Cai et al. 2000) working at a resolution of 720×576 pixels. MPEG-2 files were converted into AVI (MJPEG compression) by VirtualDub (<http://virtualdub.org/>). Video files were opened in ImageJ software (<http://rsbweb.nih.gov/ij/index.html>) and analyzed by the plug-in Kymograph to measure the speed of moving objects (organelles) in a series of images. The Kymograph plugin analyzes and measures the grey values in a region of interest (ROI) selected manually for each video frame. A kymograph (a space-time graph) was generated; the X-axis was the time axis (the unit is the frame interval) and the Y-axis indicated the movement rate of ROI (the unit of measurement is the distance covered by the object expressed in pixels). The speed of objects was measured directly by the plug-in. At least 30 pollen tubes for each sample were analyzed.

Imaging of pH and calcium levels

The BCECF-AM ester probe was used for visualizing the proton levels (namely, pH) in pear pollen tubes (Qu et al., 2012). A final concentration of 5 μM was obtained from a dimethyl sulfoxide (DMSO) stock solution of 1 mM; the required volume was directly added to the germination medium containing the re-suspended pollen grains. The cytosolic pH was immediately visualized after addition of the probe to

prevent uptake of the pH probe by organelles. In experiments with Spm, the pH probe was either added in concomitant with Spm or alternatively after progressive incubation of 5-min steps following its addition. In doing so, all significant growth stages of pear pollen tubes after Spm treatment were detected. Samples were observed with the Zeiss Apotome fluorescence microscope in the FITC filter.

Ca²⁺ fluorescence was measured after chlortetracycline (CTC) addition and incubation for 2 min. The optimal concentration of CTC which did not affect pear pollen growth but still provided good fluorescence signal was determined to be about 100 μM (Aloisi et al., 2015). Then samples were observed under a fluorescence microscope [Nikon Eclipse E600].

TAT-Aequorin-based Ca²⁺ measurements

Pollen (10 mg) was germinated in growth medium supplemented with 5 μM coelenterazine (Prolume) for 1 h in the dark, washed three times with 3 volumes of fresh medium, and then incubated with 30 μM TAT-Aequorin for 10 min in the dark. After extensive washing as above, 100 μl of germinated pollen were transferred in the luminometer chamber. Luminescence measurements were performed with a custom-built luminometer (Electron Tubes Ltd.) containing a 9893/350A photomultiplier (Thorn EMI), as previously described (Zonin et al., 2011). Ca²⁺ measurement assays were carried out in control conditions (injection of an equal volume of germination medium) or after addition of 100 μM Spm. Residual aequorin were discharged by injection of 0.33 M CaCl₂. The light signal was calibrated off-line into Ca²⁺ concentration values by using a computer algorithm based on the Ca²⁺ response curve of aequorin (Brini et al., 1995).

Actin labeling

For labeling actin filaments, pollen tubes of pear were fixed and permeabilized in 100 mM Pipes pH 6.9, 5 mM MgSO₄, 0.5 mM CaCl₂, 0.05% Triton X-100, 1.5% formaldehyde, 0.05% glutaraldehyde for 30 min according to Lovy-Wheeler et al. (2005). Samples were washed twice with the same buffer except that pH was 7 and the buffer contained 10 mM EGTA and 6.6 μM Alexa 543-phalloidin (Invitrogen). Samples were placed on slides and covered with a drop of Citifluor as anti-fading agent.

Monitoring the trafficking of organelles in pollen tubes

Growing pollen tubes were imaged for at least 60 s (or until the organelle was in focus), with frames acquired every 0.5 sec. Video clips were captured by the Apotome software (Axiovision) as ZVI files. Files were then converted into AVI files (MJPEG compression) and then opened in ImageJ software. Image stacks were calibrated with the scale command using the scale bar generated by the Apotome software. Image (stack) sequences were analyzed by ImageJ using the Manual Tracking plugin and the trajectories of selected organelles were superimposed onto the initial frame. For each organelle, the absolute velocities were calculated and averaged over the entire trajectory.

Staining of cell wall for pectin, callose and cellulose

Labelling of cell wall-secreted material was performed using propidium iodide (PI). Evidences that PI labels pectins have been previously described (Rounds et al., 2014; Parrotta et al., 2015). As reported, the PI fluorescence matched the fluorescent signal of GFP-labelled pectin methyl esterase; PI also competes with Ca^{2+} in binding to pectins suggesting that PI binds pectin and it can be used as a dye for pectins. Callose and cellulose were labelled as previously described by Cai *et al.* (2011). Measurement of PI, Calcofluor White and Aniline Blue fluorescence was performed along the cell edge using the Segmented Line tool of ImageJ. The selection width was about 2 μm (adequate to cover the fluorescence signal). Several pollen tubes of almost identical length were measured. The background was measured outside pollen tubes and it was subtracted from the average of measurements.

Immunocytochemical analysis of callose synthase

Indirect immunofluorescence microscopy was performed according to standard procedures (Cai et al., 2011). Briefly, samples were fixed with 3% paraformaldehyde in PM buffer (50 mM PIPES, pH 6.9, 1 mM EGTA, 0.5 mM MgCl_2) for 30 min, washed with PM for 10 min and then incubated with 1.5% cellulysin (Sigma) for 7 min in the dark. After two washes in PM buffer, samples were incubated with the primary antibodies to callose synthase (Cai et al., 2011) at a

dilution of 1:50. Antibodies were incubated at 4°C overnight. After two washes with PM buffer, samples were incubated in the dark with a goat anti-rabbit secondary antibody conjugated to Alexa Fluor 488 (Invitrogen) diluted 1:150 for 45 min. After two washes in PM buffer, samples were placed on slides and covered with a drop of Citifluor. Observations were made using a microscope Zeiss Axio Imager equipped with an Apotome module and a 63x objective; images were captured with an AxioCam MRm camera using the software AxioVision. In controls, primary antibodies were omitted.

Inhibitors used: taxol, oryzalin and Brefeldin A

The following inhibitors were used. Oryzalin at 1 μm was used in combination with Spm and treated samples were observed after 30-60 min; the concentration used is capable of depolymerizing most microtubules in pollen tubes (Åström et al., 1995;Gossot and Geitmann, 2007). Taxol (still in combination with Spm) was used for 30-60 min at 10 μm , a concentration that is known to stabilize microtubules in pollen tubes (Åström, 1992). Brefeldin A (BFA) was used for 30-60 min at 5 $\mu\text{g/ml}$, a concentration able of establishing a stable and dynamic system of membranes in pollen tubes (Rutten and Knuiman, 1993;Parton et al., 2003). All drugs were prepared at higher concentrated stock solution in DMSO. In controls, pollen tubes were analyzed in either standard medium or in medium supplemented with equivalent concentrations of DMSO. No differences were observed.

Data and Statistics

Pollen tube length has been measured using ImageJ software. Differences between sample sets were determined by analysis of variance (two-way ANOVA, with a threshold P-value of 0.05), performed using GraphPad Prism.

Results

The growth speed and shape of Spm-treated pollen tubes are altered

The untreated pollen develops a regular cylindrical tube (Figure 1A) whose growth velocity is constant at approximately $3.8 \mu\text{m}/\text{min}$, when analyzed by kymograph (Figure 1C). When pollen tubes were treated with Spm, few minutes thereafter their apex isotropically enlarged into the so-called balloon stage (Figure 1D). The pollen tubes were also characterized by a lower growth velocity (about $0.41 \mu\text{m}/\text{min}$). The apex then modified its shape and entered the so-called “snake stage” and thereafter it developed into an enlarged tubular form, described as “shovel stage”. The pollen tube diameter increased from $7\text{-}8 \mu\text{m}$ of the shank of treated tubes (Figure 1B, arrows), as well as of control tubes, to $10\text{-}11 \mu\text{m}$ (Figure 1B). In concomitance, the growth speed increased until $2 \mu\text{m}/\text{min}$ but never recovered the original growth rate. This process occurred $80\text{-}90$ min after supplementation of Spm (Figure 1D).

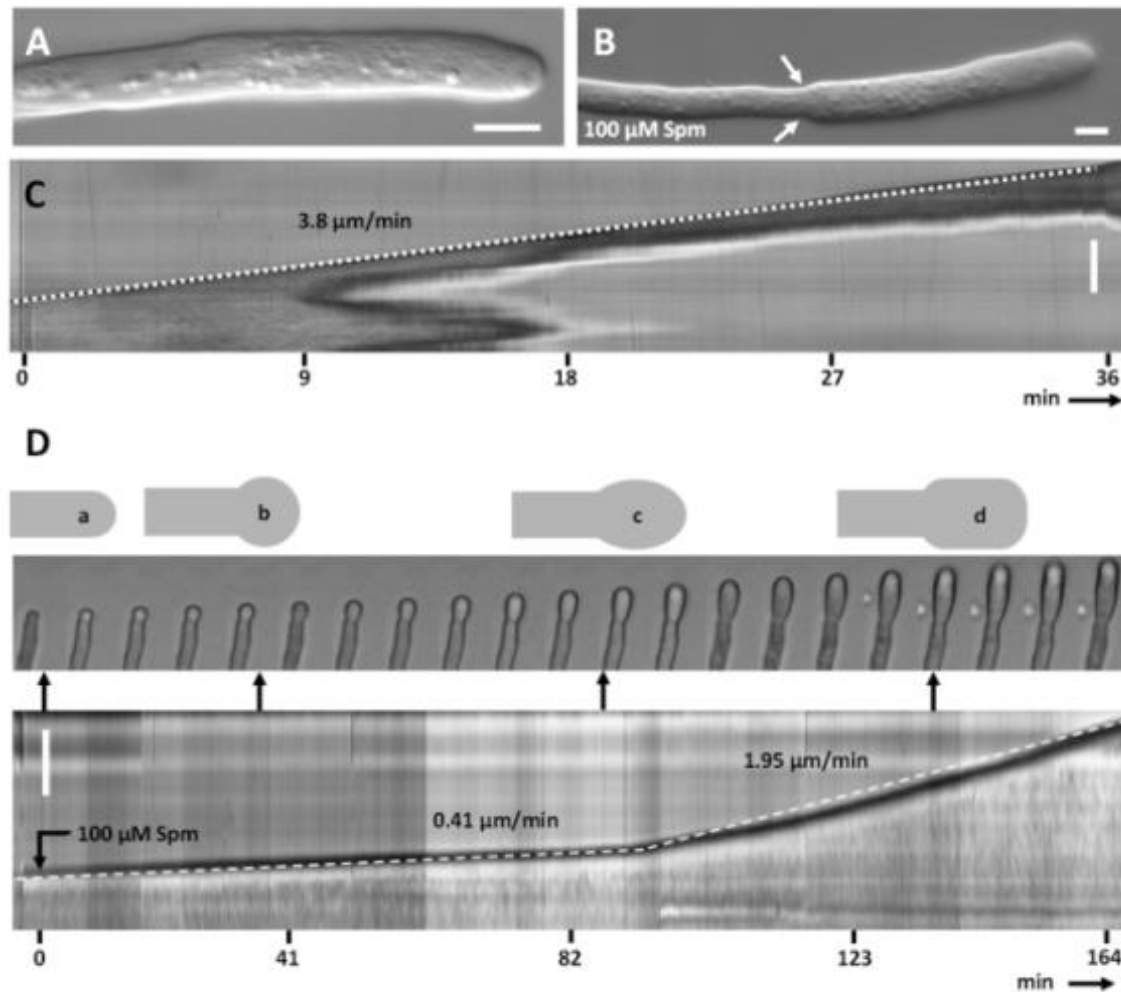


FIGURE 1. Kymograph analysis of pear pollen tubes after Spm treatment. (A) DIC view of a control pollen tube. (B) A typical enlarged pollen tube after Spm treatment. Bars: 20 μm . (C) Control pollen tube analyzed by kymograph. Dotted line indicates the linearity of growth. X-axis is the time in minutes, while Y-axis is the distance covered by the tube tip (scale bar for Y-axis is 50 μm). (D) (top part) Video frames showing the effects induced by Spm on pollen tube. Cartoons indicate the main morphological stages that characterize pollen tubes after Spm treatment; (a) no Spm; (b) balloon shape; (c) snake shape; (d) shovel shape. (bottom part) Kymograph analysis of a Spm-treated pollen tube. Spm was added at time zero. Scale bar for Y-axis is 100 μm . Small black arrows connecting the kymograph with video frames indicate approximately the time characterized by the four pollen tube shapes.

Spermine treatment alters the tip-focused Ca^{2+} gradient and pH gradient

Pollen tubes of pear exhibited a tip-focused cytosolic free Ca^{2+} gradient (Fig. 2A1-2). Upon addition of 100 μM Spm, the tip-localized Ca^{2+} gradient was drastically altered and the signal due to CTC fluorescence diffused several micrometers behind the pollen tube tip within the first 10 min, then the Ca^{2+} gradient started to reform again. The pollen tube tips began to swell and to form first the balloon (within the first 15 min) (Fig. 2B) then the shovel-shape (within 20 min). To

demonstrate that an influx of external Ca^{2+} was responsible for the apical cytosolic Ca^{2+} gradient, lanthanum (La^{3+}) and gadolinium (Gd^{3+}), which competitively block Ca^{2+} channels, were supplied 20 min before Spm, namely at 40 min germination, alternatively to the Ca^{2+} -chelating agent EGTA. Addition of La^{3+} , Gd^{3+} or EGTA arrested pollen tube growth in a dose-dependent manner and also dissipated the tip-focused cytosolic free Ca^{2+} gradient as expected (Fig. 2C). When Ca^{2+} uptake was inhibited, there were no morphological changes over 2 h, including no tip swelling or increase in the pollen tube diameter (Fig. 2D). By contrast, elongation was significantly inhibited by addition of 10, 50 or 100 μM La^{3+} or Gd^{3+} and 400, 1-5 mM EGTA in germination medium (containing 1.27 mM Ca^{2+}) after the first hour of germination (Table 1).

	Concentration (μM)	Tube length (μm)		N° of counted pollens
Cntr	0	413,9		106
LaCl3	1	395,5		115
LaCl3	10	337,0	<i>a</i>	120
LaCl3	50	259,0	<i>a</i>	108
LaCl3	100	269,7	<i>a</i>	111
GdCl3	1	385,8		106
GdCl3	10	314,8	<i>a</i>	107
GdCl3	50	236,3	<i>a</i>	108
GdCl3	100	233,1	<i>a</i>	100
EGTA	400	297,6	<i>a</i>	118
EGTA	1000	239,0	<i>a</i>	110
EGTA	5000	242,2	<i>a</i>	113

TABLE 1. The perturbation of Ca^{2+} dynamics by externally applied La^{3+} , Gd^{3+} or EGTA inhibits pollen tube elongation. Values marked with 'a' are significantly different from controls based on Tukey's multiple comparison test at $P < 0.05$.

Moreover, pretreatment with La^{3+} , Gd^{3+} and EGTA counteracted in a dose-dependent manner the extension of the shovel-shaped apical region and thus the effects of Spm, confirming the involvement of Ca^{2+} in the formation of the shovel-shaped tip (Fig. 2E).

To further analyze and precisely quantify the alteration in Ca^{2+} fluxes induced by Spm in germinating pollen, Ca^{2+} dynamics were monitored in pear pollen tubes by using the TAT-aequorin method (Zonin et al., 2011). The translocating properties of the cell-penetrating peptide TAT were used to internalize into germinating pollen the covalently-linked bioluminescent Ca^{2+} reporter aequorin. TAT-aequorin-based Ca^{2+} measurement assays demonstrated that the cytosolic free Ca^{2+} concentration ($[\text{Ca}^{2+}]_{\text{cyt}}$) in germinating pear pollen was maintained at about $0.50 \mu\text{M}$ (Fig. 2F). Upon stimulation with $100 \mu\text{M}$ Spm, pear pollen was found to respond with a rapid $[\text{Ca}^{2+}]_{\text{cyt}}$ increase, that reached a peak value of about $0.90 \mu\text{M}$ after 20 s and then gradually decreased almost to basal values within 10 min (Fig. 2F, black line). On the other hand, the mechanical perturbation caused by the injection of an equal volume of germination medium (touch control) induced only a modest $[\text{Ca}^{2+}]$ change characterized by a very limited amplitude (about $0.55 \mu\text{M}$, Fig. 2F, grey line).

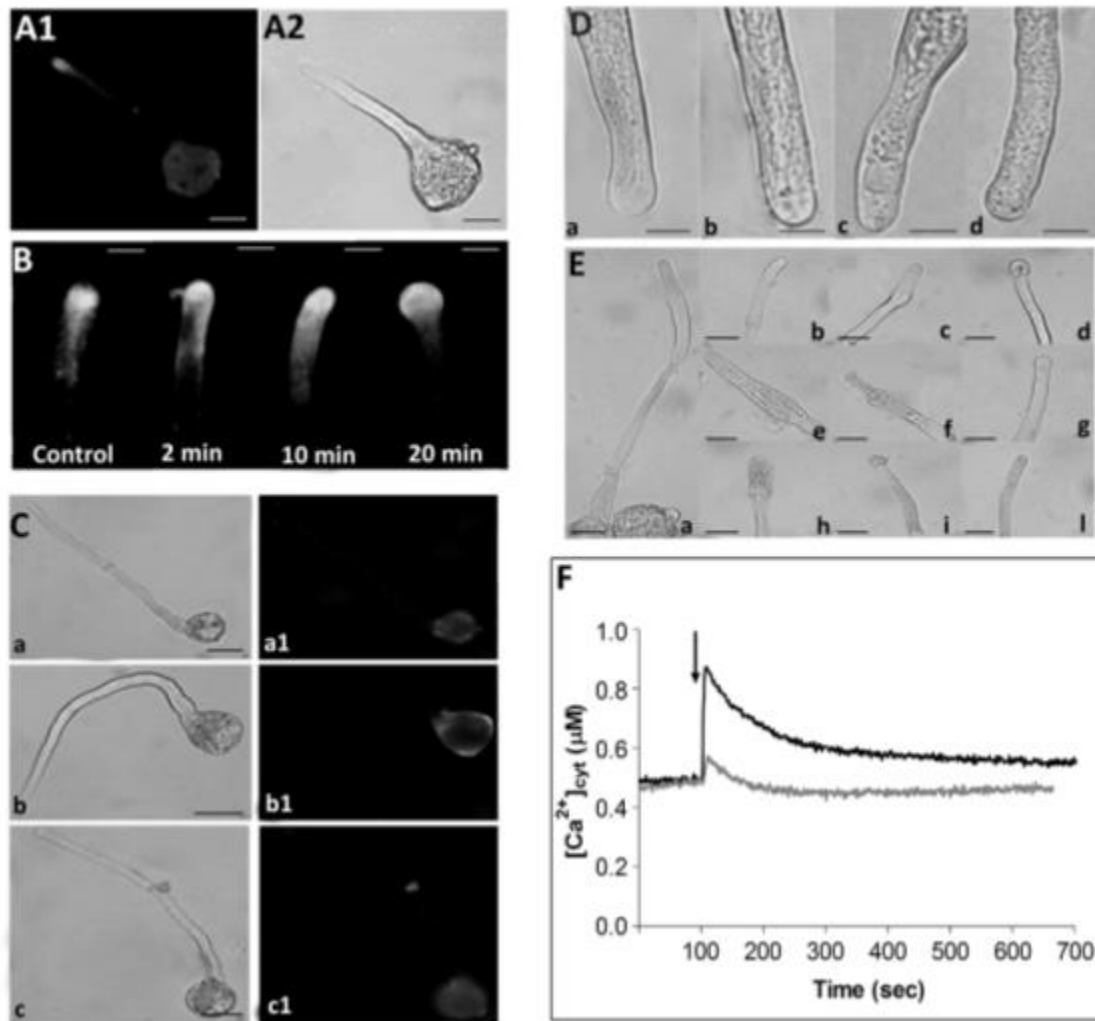


FIGURE 2. Spm disrupts the tip-focused Ca²⁺ gradient in germinating pollen and alters its morphology. (A1) Pear pollen tube under UV light exhibits an apical Ca²⁺ gradient; (A2) Same pollen tube in white light. Bars: 20 μm. (B) Spm (100 mM) drastically alters the tip-focused Ca²⁺ gradient, with Ca²⁺ ions diffusing several micrometers behind the pollen tube tip within the first 10 min, then the Ca²⁺ gradient started to reform again. Bars: 10 μm. (C) La³⁺ (a-a1), Gd³⁺ (b-b1) and EGTA (c-c1) dissipate the apical calcium gradient. Bars: 30 μm. (D) Apical region of control pollen tube (a) or pollen treated with La³⁺ 100 μM (b), Gd³⁺ 100 μM (c), or EGTA 1 mM (d) show no changes in external morphology. Bars: 10 μm. (E) The pretreatment with La³⁺, Gd³⁺ and EGTA counteracts in a dose-dependent manner the extension of the shovel-shaped apical region. (a) Pollen treated with 100 μM Spm only. (b, c, d) Pollen pretreated with 10, 25 and 50 μM La³⁺ and 100 μM Spm. (e, f, g) Pollen pretreated with 10, 25 and 50 μM Gd³⁺ and 100 μM Spm. (h, i, l) pollen pretreated with 200, 400 and 1000 μM EGTA and 100 μM Spm. Bars: 30 μm. (F) Monitoring of cytosolic Ca²⁺ dynamics in germinating pollen by using TAT-aequorin. Cytosolic free Ca²⁺ concentration ([Ca²⁺]_{cyt}) was measured after 10 min incubation of germinating pollen with TAT-aequorin and subsequent challenge (arrow, 100 s) with either the germination medium (grey trace) or 100 mM Spm (black trace). Ca²⁺ traces are representative of three independent experiments that gave very similar results.

After 2 h of pollen germination a two-fold increase in the basal [Ca²⁺]_{cyt} was observed, with a concomitant loss of responsiveness to Spm, in agreement with a

physiological and progressive decrease of viability during in vitro germination (Fig. 3).

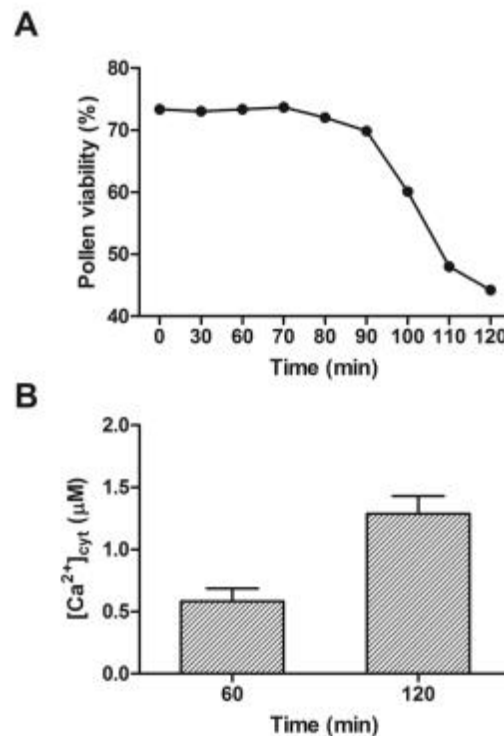


FIGURE 3. Physiological and progressive decrease of pollen viability during in vitro germination **(A)** and concomitant increase in the basal [Ca²⁺]_{cyt} **(B)**.

In addition to the Ca²⁺ gradient, the proton gradient is also a distinctive feature of growing pollen tubes and a low pH value at the tube tip is supposed to be necessary for optimal growth. Growing pollen tubes are also characterized by increase in pH value behind the tip domain (the so-called alkaline band). We therefore analyzed potential changes in pH values during Spm treatment at different times. In control pollen tubes, we constantly observed the lowest pH values in the extreme tube region (the tip). The peak of fluorescence, representing the lowest pH region, covered approximately the first 5-μm tip region and then the signal dropped rapidly and stabilized at background values (Fig. 4A-B). Few minutes after Spm treatment, pollen tubes changed their shape into the balloon stage. At this stage, the proton concentration transiently increases into the tip region but rapidly decreases and the fluorescence signal might be clearly observed as diffused in the subapex (Fig. 4C). At the balloon stage, the most frequent picture

of pollen tubes was characterized by a diffuse signal sometimes in the form of local fluorescence aggregates (Fig. 4D). Therefore, the balloon stage is characterized by the rapid loss of pH gradient. When pollen tubes resumed their growth and passed from the snake to the shovel stage, we did not observe the reforming of pH gradient. As shown in Figures 4E-F, the shovel stage is characterized by a diffuse fluorescence signal that sometimes appeared as fluorescence aggregates (Fig. 4E). As the pollen tubes continue to grow, fluorescence became typically uniform along the entire shovel domain with no specific localization pattern (Fig. 4F). This indicates that a specific pH gradient is not re-established after pollen tubes restart to grow.

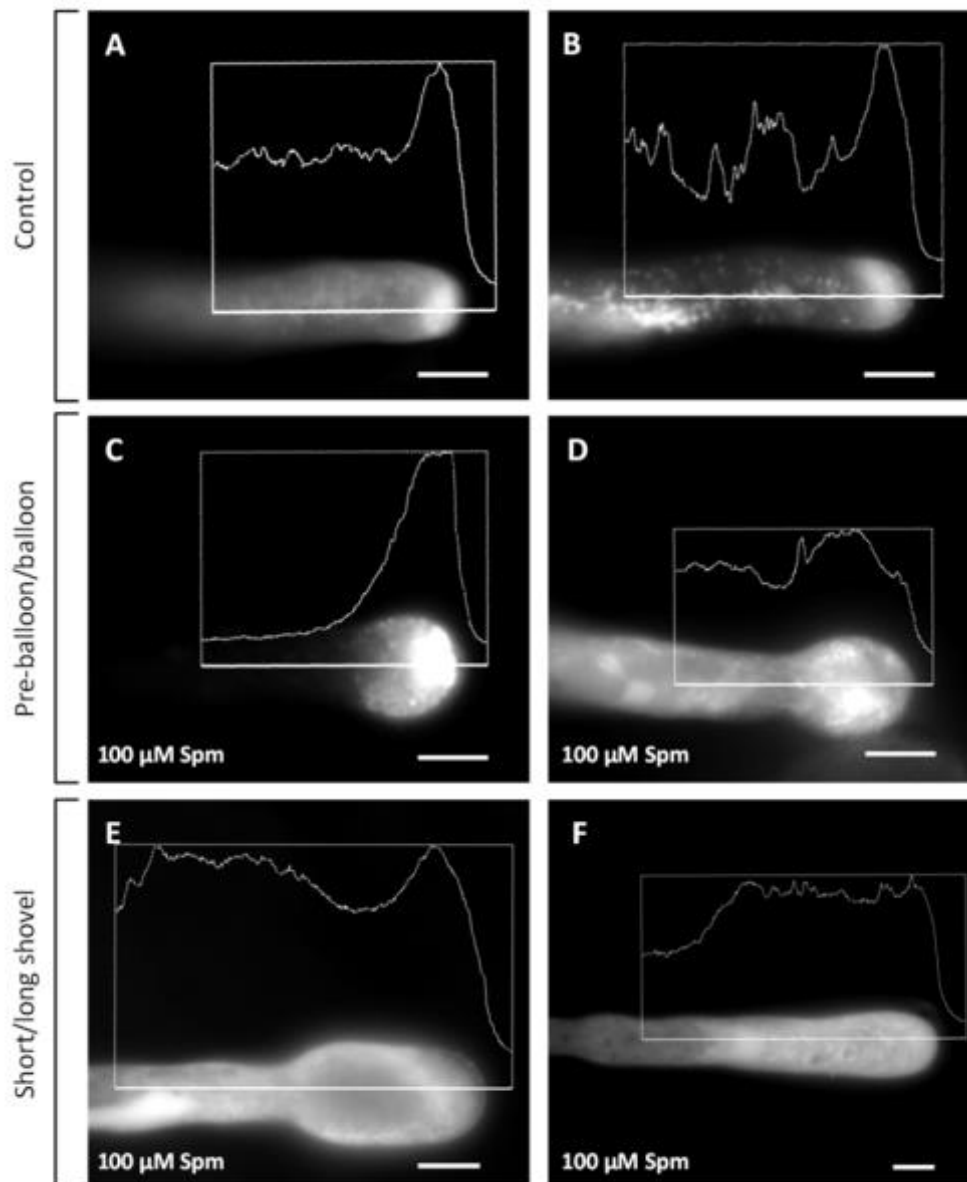


FIGURE 4. Spm treatment drastically alters the pH gradient at the pollen tube tip. (A, B) In controls, pear pollen tubes exhibit a tip-focused pH gradient with an acidic region strictly localized at the tube tip. The acidic pH region disappears just 5-10 μm from the tip and only a background level can be observed. **(C, D)** When Spm treatment starts to affect pollen tube morphology leading to the balloon-like stage, the pH gradient suddenly changes from a tip-focused into a more diffused pattern. **(E, F)** At the shovel stage, the concentration of protons is approximately homogenous along the entire shovel-like structure and no specific accumulation of protons could be detected in the new tip domain. Graphs superimposed to single images were generated by the AxioVision software. Bars in all pictures: 10 μm .

Spm induces changes in the actin cytoskeleton of growing pollen tubes

Perturbation of pollen tube growth might suggest that changes to the cytoskeleton also occurred. Moreover, because the Ca^{2+} gradient was likely to be involved in the formation of the swollen pollen tube tip and the Ca^{2+} gradient is a key regulator of the cytoskeleton dynamics, the first attempt was to analyze the actin cytoskeleton. Figure 5A1 and A2 illustrates typical images of actin in pear pollen tubes visualized by fluorescence microscopy. A delicate pattern of longitudinal actin filaments is present in the shank of pollen tubes. Actin filaments occasionally showed a helical arrangement (arrow in Fig.5 A1) and they extend until the tube tip; nevertheless, the intensity of fluorescence labeling at the very tip region is always lower as it was devoid of prominent actin labeling; in addition, actin in the tip appeared as less organized and did not show evidence of fringe-like structures (Figure 5A3).

When pollen tubes were treated with 100 μM Spm, changes to the actin cytoskeleton mirrored the morphological changes and growth rates described previously. After Spm addition, the actin configuration in the apex and sub-apex changed as the subapical mesh lost its organization and actin filaments appeared as short, disorganized and randomly distributed with several fluorescent dots suggesting actin aggregation and depolymerization (Figure 5B1). In the subapical region, the actin filaments appeared as partially damaged while actin filaments in the shanks appeared relatively normal. Therefore, when Spm-treated pollen tubes assumed the balloon shape, the actin array in the apical dome appeared as disordered, which likely correlates to the dissipation of the Ca^{2+} gradient and to the isotropy expansion of pollen tubes. An ordered pattern of actin filaments was partially restored as soon as pollen tubes resumed growth and the pollen tube apex changed from the balloon into the snake shape. In this new condition, a delicate fibrillar pattern might form in the expanded tip, with actin fibrils penetrating into the new apex (Figure 5B2). Moreover, actin filaments in the new

developing tube shank underwent configurational changes, as they started organizing into thicker cables. In the new enlarged tube shank, actin filaments appeared as arising from the unchanged distal region of pollen tubes and penetrating into the enlarged tube section where they opened assuming a fan shape (Figure 5B3). This new pattern of actin filaments was more evident when pollen tubes started assuming a shovel shape (Figure 5B4) and became progressively clear while the shovel-shaped pollen tube expanded (Figure 5B5). Actin filament bundles in the unchanged part of the pollen tube shank did not seem to be affected by Spm treatment.

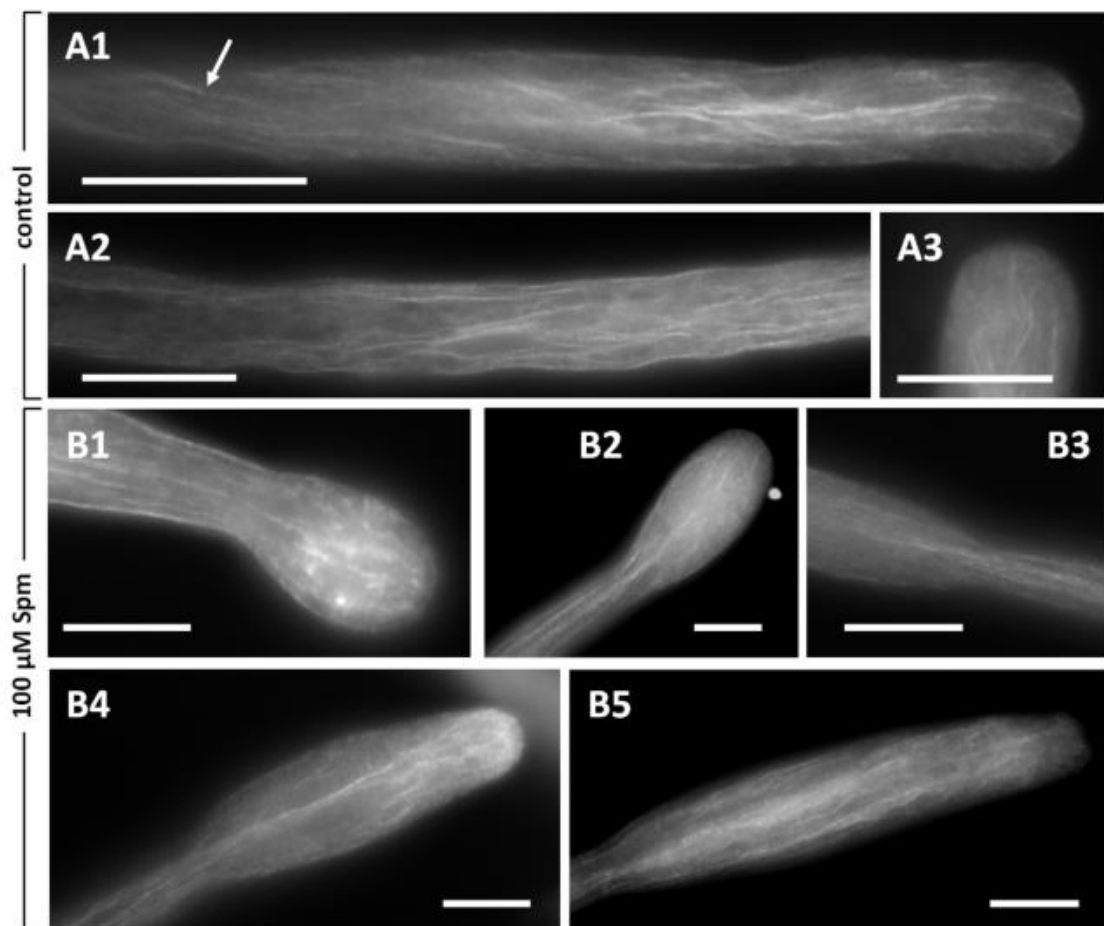


FIGURE 5. Distribution of actin filaments. (A1, A2) Control pollen tubes. The arrow indicates a longitudinal helicoidally-arranged like actin filament. **(A3)** Detail of a control pollen tube apex. **(B1-B5)** Pollen tubes treated with 100 mM Spm. **(B1)** A balloon-shaped pollen tube showing completely disorganized actin filaments in the apex. **(B2)** Reorganization of actin filaments at the snake-shaped stage. **(B3)** When the pollen tube starts newly to grow, actin filaments run in the cortical region of pollen tubes opening like a fan at the neck level. **(B4, B5)** Actin filaments can be observed as the new shovel-shaped pollen tube resumes its growth. Bars in all pictures: 10 μm .

Microtubules are not apparently involved in establishing the new growth pattern

Previous analysis indicated that actin filaments are critically involved in the reshaping process occurring after Spm treatment. Even if microtubules are reported not to be involved in promoting pollen tube growth, the involvement of the microtubular cytoskeleton was investigated in order to understand if it also might take part in the swelling process. Microtubules were investigated by applying two known inhibitors, namely oryzalin and taxol. Pollen tubes were treated simultaneously with Spm and one of the two inhibitors, and then the growth rate was monitored until growth stopped. In control pollen tubes, no effects due to oryzalin or taxol treatment were observed and growth of pollen tubes was comparable to untreated pollen tubes in terms of growth rate and tube morphology (data not shown). When the effects of Spm were evaluated, worth of notice was that neither taxol (Figure 6A-B) nor oryzalin (Figure 6C-D) could affect the morphological changes induced by Spm. Both timing of changes and shaping of Spm-treated pollen tubes in the presence of inhibitors were comparable to Spm-treated pollen tubes. Figure 6A is a large view of several pollen tubes treated with Spm and taxol while Figure 5B is a detailed view of a single treated pollen tube. No specific alterations due to taxol were observed. Similar results were obtained in the case of Spm- and oryzalin-treated pollen tubes (Figure 6C-D) for both 30 and 60 min. Current results suggest that microtubules are not involved in either the initial isotropy growth induced by Spm or the re-growth subsequently occurring, namely in the process of tip-growth and swelling.

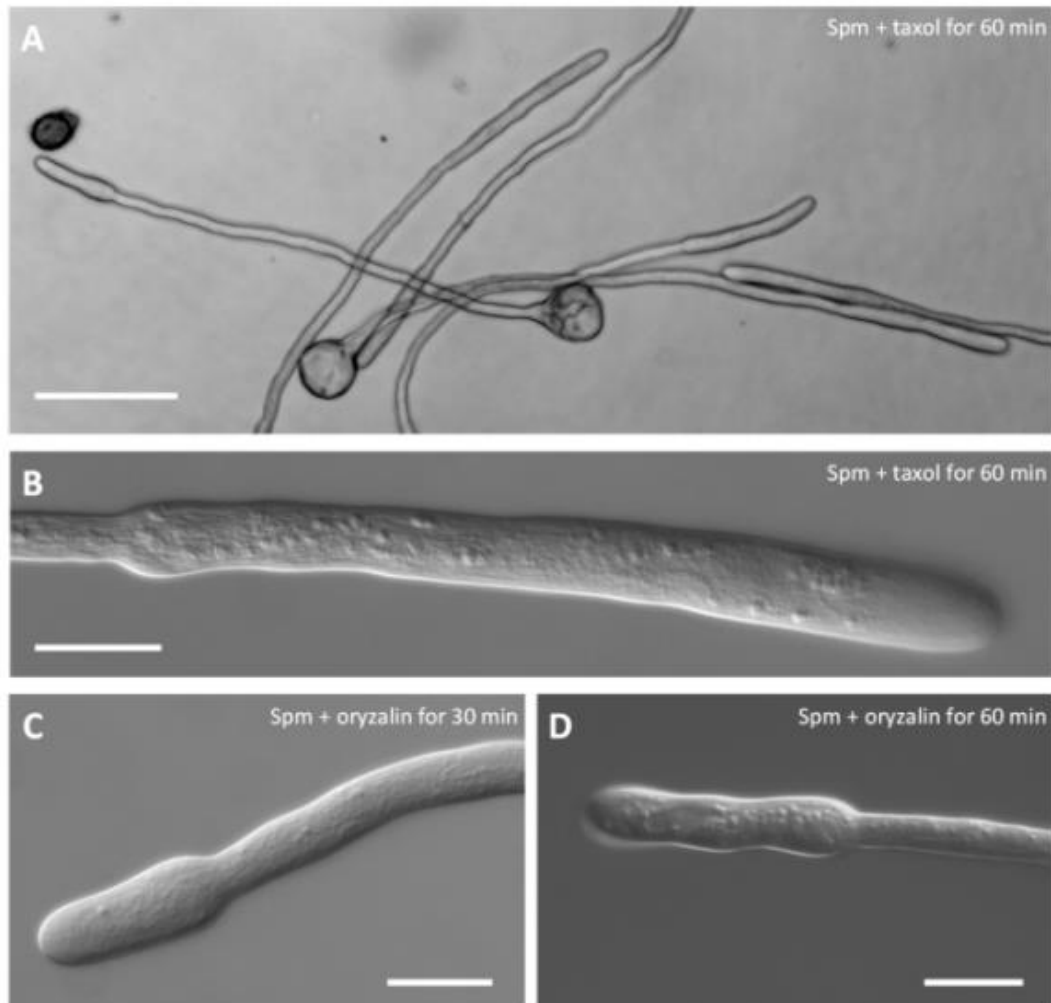


FIGURE 6. Co-treatment of pear pollen tubes with Spm and microtubule inhibitors. (A) DIC view of pollen tubes after treatment with Spm and taxol. **(B)** Detail of a single pollen tube after Spm-taxol treatment (DIC view). **(C-D)** DIC views of pollen tubes after co-treatment with Spm and oryzalin. Neither inhibitors have effects on the formation of the shovel shape. Images were captured after the incubation time with Spm/drug as indicated in each picture. Both analyses were performed at least until one hour after supplementation of Spm and drugs. Bar in A: 100 μm ; bars in B-C-D: 20 μm .

Organelles in shovel-shaped pollen tubes move differently

Given that Spm stimulated F-actin to undergo major changes that involved actin depolymerization followed by the formation of thick actin cables, alterations to organelle distribution and dynamics after Spm treatment were investigated, as F-actin is the major structural factor supporting long-distance organelle transport in pollen tubes. Observation of the shank region in normally-growing pollen tubes revealed rapid movement of organelles parallel to the longitudinal axis of the cell

(Figure 7A). Larger organelles were rapidly transported toward the growing apex with speeds that could be clustered in distinct range. In particular, most of the organelles exhibited a speed of 0.3-0.5 $\mu\text{m}/\text{sec}$ but some specific organelle showed speeds up to 0.7 $\mu\text{m}/\text{sec}$ (histograms in Figure 7C). In the apical area, larger organelles were then transported back in a basipetal direction resuming the same speed as before. Small vesicles supposedly crossed this area and accumulated in the apex where they could not be distinguished clearly due to their small size (Fig 7A and B). After supplementation of 100 μM Spm, cytoplasmic streaming was not arrested (Figure 7B) but organelles moved with noteworthy enhanced speeds, with most of the organelles showing speed of 0.8 $\mu\text{m}/\text{sec}$ (histograms in Figure 7C). Organelles followed the normal streaming direction seen in control pollens; however, in most cases organelles were marginalized in the cortical region of pollen tubes, thus avoiding crossing the central distended area. Therefore, this sometimes produced a central stationary area in which many organelles stopped or moved slowly. Organelles moving quickly along actin cables could enter the stationary area, pausing inside and then getting back on track.

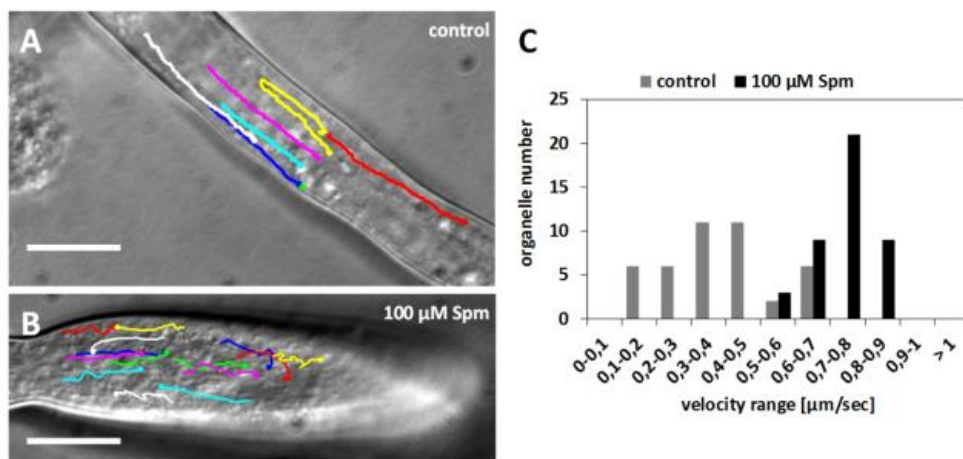


FIGURE 7. Velocity distribution of organelles in control and Spm-treated pollen tubes. (A) Control pollen tube with lines indicating the pathway of some monitored organelles. **(B)** Pathway of some organelles in a Spm-treated pollen tube. Bars: 10 μm . **(C)** Velocity distribution of representative organelles in control and Spm-treated pollen tubes. Y-axis indicates the number of organelles while X-axis indicates the range of velocity (in $\mu\text{m}/\text{sec}$).

Proper accumulation of vesicles is required for Spm to expand the pollen tube apex

Polarized pollen tube growth results from the constant fusion with the plasma membrane of secretory vesicles containing new plasma membrane and cell wall components. A balance between exocytosis of cell wall components and endocytosis of molecules is therefore essential for the proper growth of pollen tubes. Given that Spm drastically altered pollen tube morphology, the effects of the co-treatment with Spm and Brefeldin A (BFA) was investigated. The latter is known to affect the secretory and endocytotic pathways. As shown in Figure 8A, co-treatment with Spm and Brefeldin A gave not rise to the typical shovel-shaped apex even after 30 min of Spm supplementation. Results were essentially the same until 60 min of Spm/BFA treatment, suggesting an essential role of vesicles turnover in the process of apical swelling. As shown in the histogram of Figure 8B, co-treatment with Spm and BFA prevented the expansion of the apical dome but caused a strong reduction or even arrest of pollen tube growth. While control pollen tubes exhibited an increase in length of about 100-150 μm , pollen tubes treated with Spm/BFA grew very slowly (no more than 20-30 μm after one hour of co-treatment). Anyway, this also prevented the apex to deform. Statistical analysis using one-way ANOVA showed that pollen tubes grown for 60 min + 30 min with Spm/BFA resulted significantly different with respect both to pollen samples grown for 60 min and for 60 min + 30 min in standard conditions. On the contrary, the sample grown for 60 min + 60 min with Spm/BFA showed no significant difference when compared to the pollen sample treated for 30 min with Spm/BFA. This indicates that treatment with Spm/BFA affected growth during the first 30 min of incubation but more drastically (until stopping tube growth) during the following 30 min.

Co-treatment with Spm and BFA also affected the deposition of cell wall components, as demonstrated by propidium iodide (PI), which vitally stains plant cell walls by binding to carboxyl residues on pectins, allowing the analysis of the link between cell wall deposition and cell growth. PI-stained pectins appeared uniformly distributed in the pollen tube border and no specific accumulation could be observed in the tip (Figure 8C; see 9A below for control). Because pectins are secreted by secretory vesicles, this finding indicates that the accumulation and

fusion of secretory vesicles might be altered. On the other hand, the deposition of callose in the cell wall is not modified (Figure 8D) because callose appeared as a uniform surrounding sheet around the pollen tube except for the tip region.

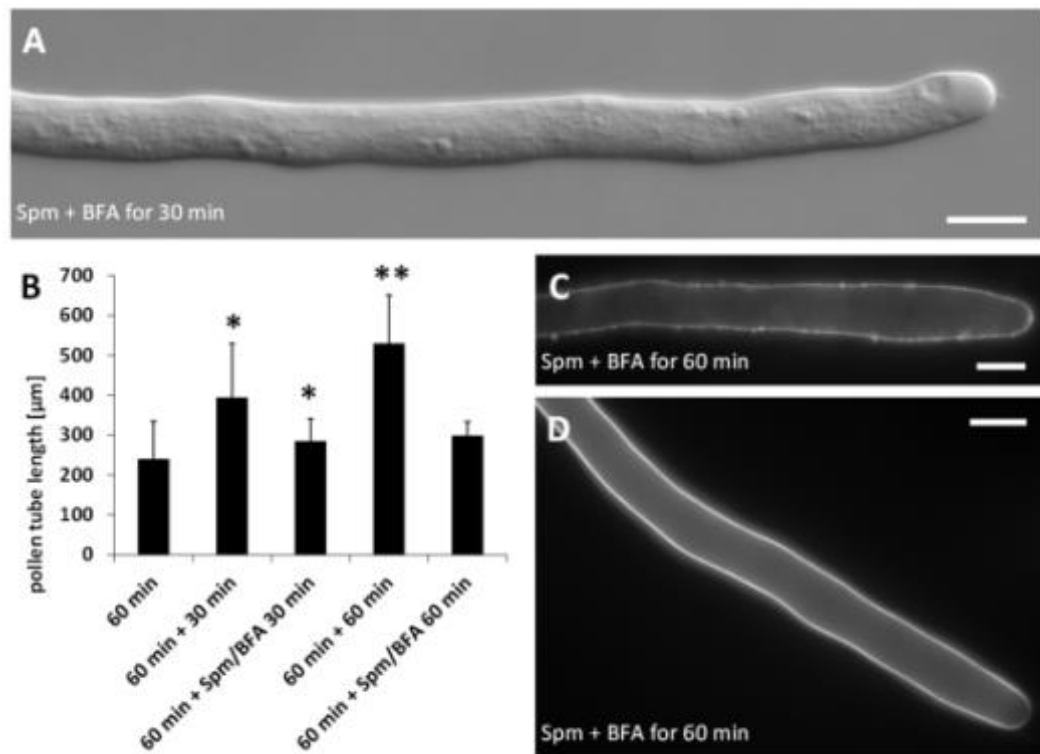


FIGURE 8. Treatment with Brefeldin A (BFA) and Spm on pear pollen tubes. (A) A DIC view of 30 min-treated pollen tube showing no defects in tube morphology. All bars 10 μm. **(B)** Growth rates of control pollen tubes and of Spm/BFA-treated pollen tubes. The 60 min stage (first bar on the left) represents pollen tube growth before addition of chemicals. Pollen tubes were either supplemented with Spm/BFA for extra 30-60 min or grown under control conditions. One asterisk indicates statistical significant difference of samples with respect to 60 min-grown pollen tubes. Two asterisks indicate that the sample is significantly different from all other samples. The last sample with no asterisks is not different from the 60 min-grown sample and from the 60 + 30 min Spm/BFA sample. **(C)** Labeling of pectins by PI. Pectins appear uniformly distributed. Bar: 10 μm. **(D)** Staining of callose by aniline blue (A, B). Callose is distributed like in control conditions and is absent in the very tip region. Bar: 10 μm.

Spm alters the distribution of cell wall components

As shown above, the distribution of pectins is altered by co-treatment with Spm and BFA; however, such distribution may simply reflect the absence of tube growth. Therefore, the deposition of pectins in Spm-treated pollen tubes was investigated in order to understand if Spm might affect the deposition pattern of

newly synthesized cell wall components. In untreated pollen tubes, PI fluorescence was localized along the pollen tube walls but mostly in a 5-10 μm -wide apical zone (Fig. 9A). After Spm application, at the balloon stage, newly deposited methoxylated pectins were no longer depleted from the subapical region and could be observed along a wider circumference (at least 20 μm) (Fig. 9B). In some cases, the staining with PI extended to the periphery of the entire tube portion involved in the formation of the swollen apex (Fig. 9C). This suggests that the apex surface involved in exocytosis of methoxylated pectins extended considerably in comparison with control pollen tubes. As pollen growth continued, distribution of PI fluorescence changed in Spm-treated pollen tubes; as soon as the balloon shape changed into the snake apex, the PI fluorescence was progressively refocused into a 5- μm -wide apical region (Figure 9D-E), which represents the new growth site. When the newly-growing pollen tube reached the shovel shape, PI accumulated again generating a novel tip-focused secretion area of about 5-10 μm (Fig. 9F-G). The differential distribution of PI-labelled pectins can be appreciated more after measuring the relative fluorescence intensity in Spm-treated pollen tubes representing the typical morphological stages (Figure 9H).

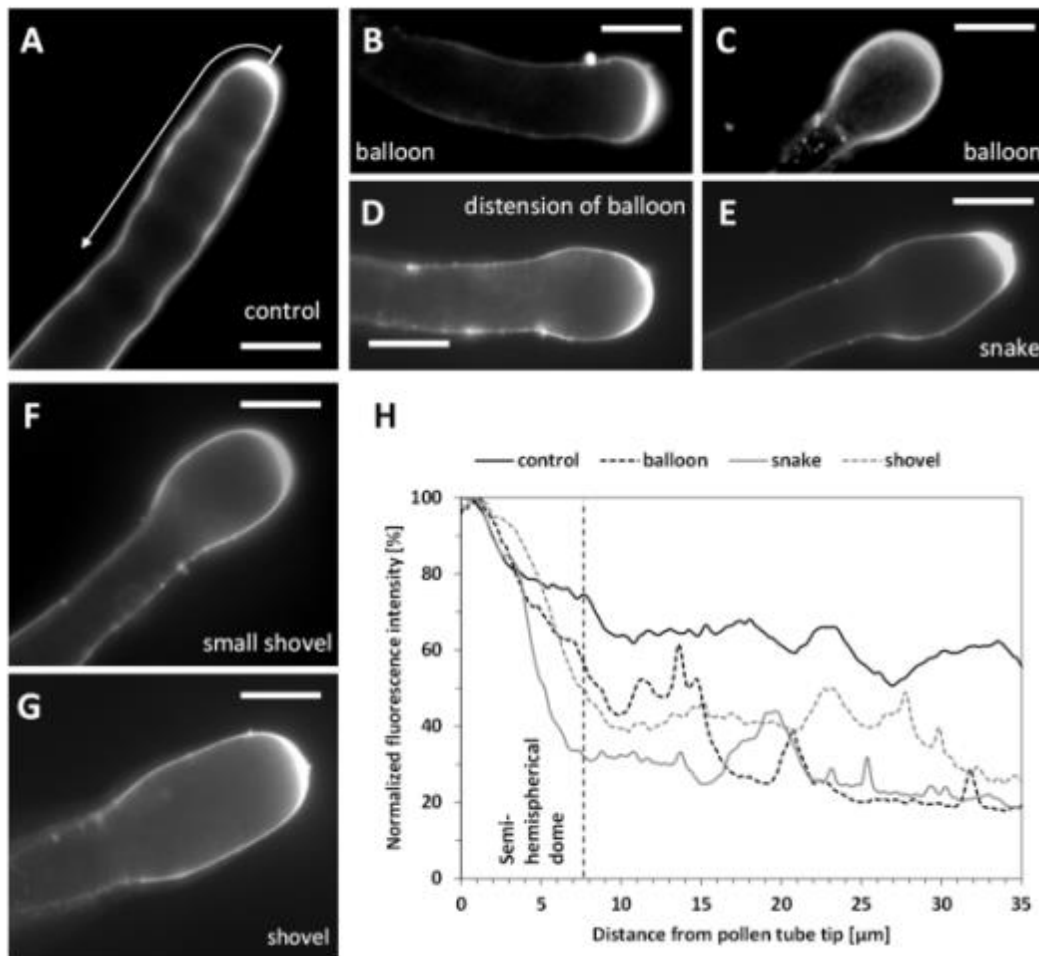


FIGURE 9. Pectin distribution in control and Spm-treated pollen tubes. (A) Distribution of PI-stained cell wall polysaccharides in control pollen tubes. Arrow indicates the surface analyzed for PI fluorescence intensity. (B-C) Balloon stage. (D) A pollen tube resuming growth and switching from the balloon to the snake stage. (E) A typical example of a snake-shaped pollen tube. (F-G) Initial stage of shovel formation and a mature shovel-shaped pollen tube, in which PI-labelled pectins accumulate again in the tip. Bars for all pictures: 10 μm . (H) Relative quantitation of PI fluorescence intensity in pollen tubes treated with 100 mM Spm. The intensity profile is reported as relative fluorescence intensity starting from the tip. The analyzed half curvature of the pollen tube apex was called as “semi-hemispherical dome”. Graphs are calculated for the main steps of Spm treatment as indicated by the graph legend.

In addition to pectins and callose, the cell wall of pollen tubes also contains cellulose. In control pollen tubes, cellulose (as stained by the Calcofluor white fluorescent dye) appeared to be distributed according to a standard pattern characterized by a relatively uniform distribution along the pollen tube cell wall (Figure 10A). Unlike the uniform deposition in control cells, cellulose deposition was altered in the swollen tip region of pollen tubes after Spm treatment. As soon as the tip became swollen, a stronger accumulation of cellulose was observed in the “neck” of the swollen tip (Figure 10B). Relative quantization of the

fluorescence signal clearly showed the accumulation of cellulose around 15-20 μm from the tip (Figure 10C). In some cases, cellulose extended completely into the apical region involved in the formation of the swollen apex (Fig. 10D). When the new enlarged pollen tube resumes to grow, cellulose deposition was observed along the border of the shovel-shaped tube (Figure 10E); however, measurement of relative fluorescence intensity revealed accumulation of cellulose in the subapical region. Higher levels of cellulose deposition extended for the entire length of the shovel until the neck region (Figure 10F).

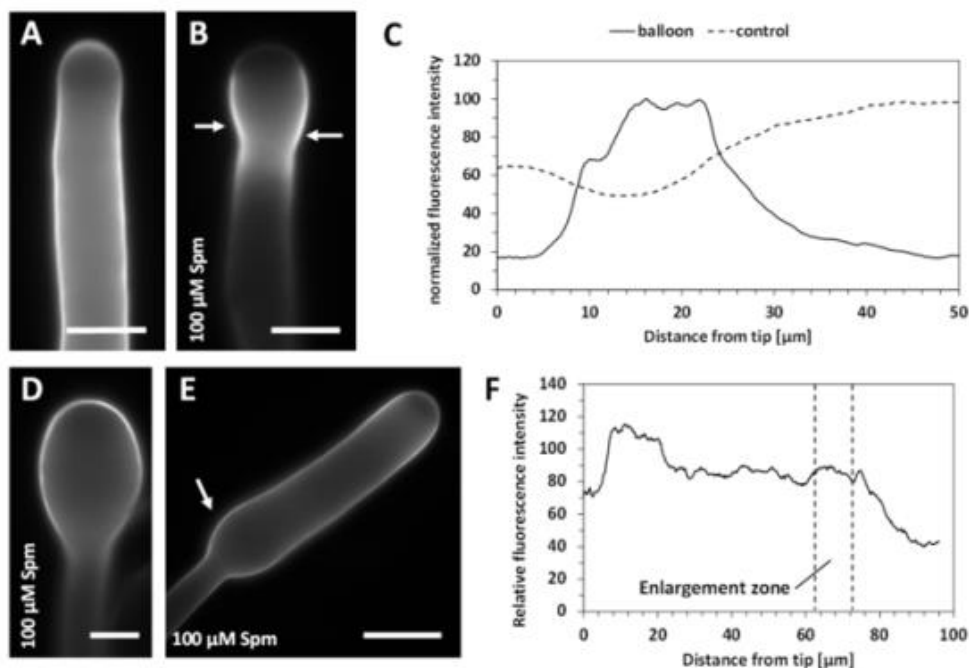


FIGURE 10. Distribution of cellulose in Spm-treated pollen tubes. (A) Pattern of cellulose in control pollen tubes. **(B)** Cellulose distribution at the onset of Spm treatment. Arrows indicate accumulation of cellulose in the neck. **(C)** Graph of relative fluorescence intensity at the balloon stage (compared to control) starting from the tip. **(D)** Image of a pollen tube switching from the balloon to the shovel-like shape showing accumulation of cellulose also in the tip region. **(E)** A mature shovel-shaped pollen tube in which cellulose accumulates consistently in the subapical region and, to a lesser extent, in the neck. The arrow indicates the enlargement zone. Bars in A, B, D: 10 μm . Bar in E: 20 μm . **(F)** Graph reporting the relative fluorescence intensity in pollen tubes at the shovel stage starting from the tip. The so-called “enlargement zone” represents the point where the diameter of that specific pollen tube increases.

Distribution of callose is comparable to the pattern of cellulose

While in control pollen tubes callose was detected as uniformly distributed except in the very tip region (Figure 11A), callose accumulated in the neck of Spm-treated pollen tubes at the onset of treatment (Figure 11B, arrows). Accumulation of

callose in the neck region was more prominent at the snake stage (Figure 11C) and callose level remained constantly higher in the neck during the switch from the snake stage to the shovel stage (Figure 11D, square bracket). This observation was confirmed by measuring the relative fluorescence intensity in typical pollen tubes at both control and shovel stages (graph in Figure 11E). While control pollen tubes exhibited no callose deposition in the tip and a progressive accumulation starting from 20-30 μm , shovel-shaped pollen tubes were characterized by a consistent accumulation of callose in the neck region, which corresponds approximately to 30 μm from the tip in the examples of Figure 11D-E.

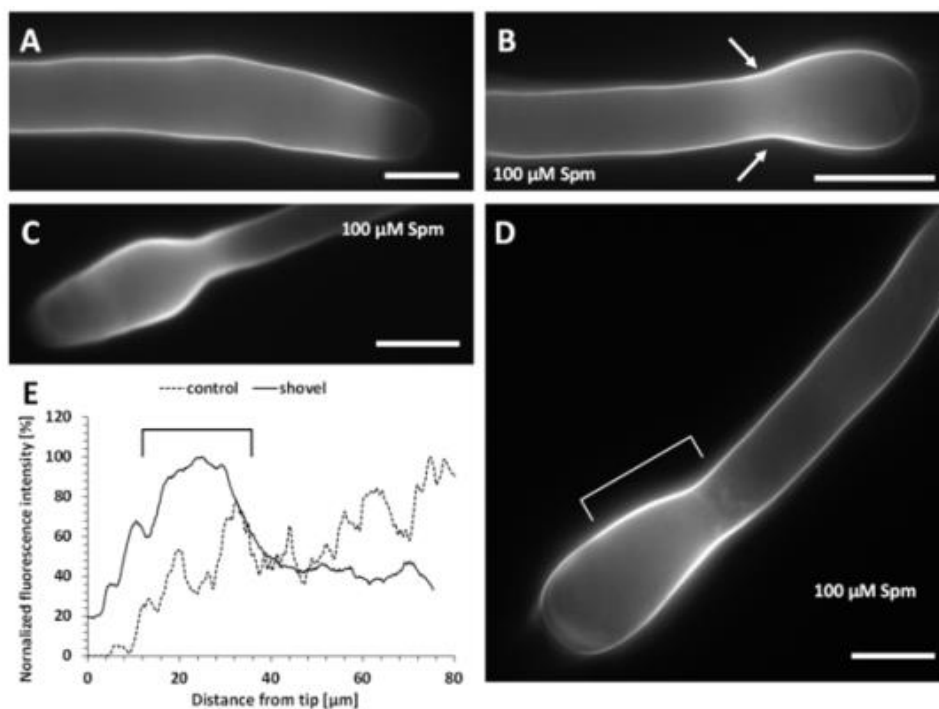


FIGURE 11. Distribution of callose in Spm-treated pollen tubes. (A) A control pollen tube showing absence of callose in the tip. (B) In balloon-shaped pollen tubes, callose accumulates in the neck region (arrows). (C) In snake-shaped pollen tubes, callose still accumulates in the neck region and it is still absent from the tip. (D) In shovel-shaped pollen tubes, callose showed a consistent accumulation around 20-30 μm , as also shown by the relative fluorescence intensity (E). The square bracket in panel D corresponds to the region indicated by the square bracket in the graph of panel E. Bars: 10 μm .

Changes to the callose pattern is accompanied by changes to callose synthase distribution

As the distribution of callose was affected in Spm-treated pollen tubes (probably as consequence of adaptation of cells to the new conditions), in order to assess if the altered distribution of callose might depend on irregular localization of callose synthase, immunofluorescence microscopy was used to localize the callose synthase enzyme. As shown in Figure 12A, in control pollen tubes, the enzyme was detected along the entire periphery of pollen tubes, most likely in the plasma membrane. Distribution of callose synthase was not uniform but it can be described as organized in patches, more abundant in the apical zone (the hypothetical insertion site). After Spm treatment, at the balloon step, callose synthase accumulated in the plasma membrane of the swollen apex (Fig 12B) again with a patch-like appearance. Labeling was not limited to the swollen apex but also extended to distal segments of pollen tubes (Figure 12C1-C2). Accumulation of callose synthase in the balloon-like region may reflect an irregular but consistent deposition of the enzyme following Spm treatment. When pollen tubes resumed growth (snake stage), callose synthase started to accumulate consistently in the neck region (Figure 12D1-D3) thus mirroring the neck-localized deposition of callose. Accumulation of callose synthase in the neck was a consistent feature at the snake and shovel stages suggesting that callose synthase may take part in stabilizing the new growth pattern. In some cases, deposition of callose synthase took the form of annulus-like structures surrounding the neck region (arrows in Figure 12E-F).

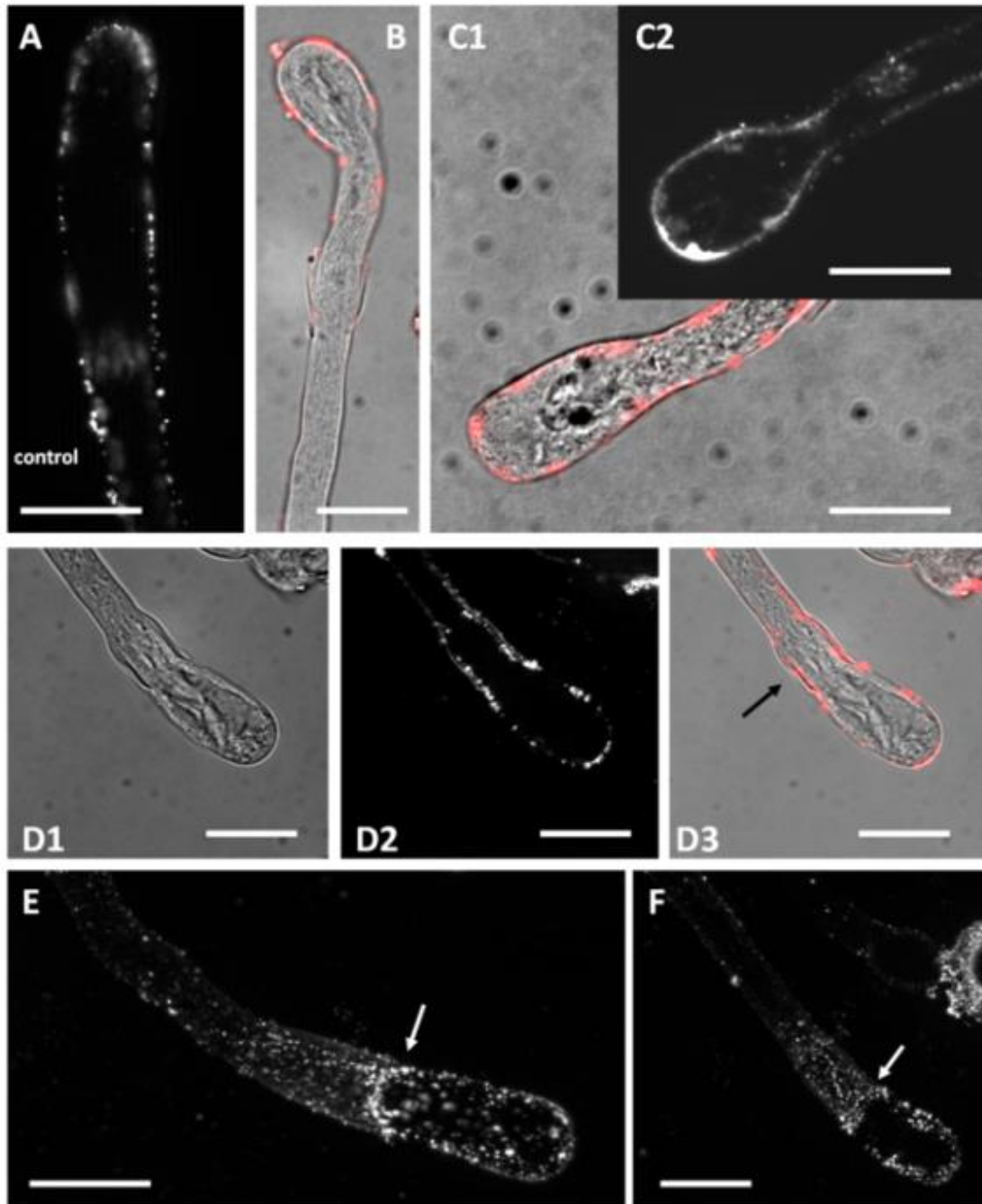


FIGURE 12. Distribution of callose synthase in control and Spm-treated pollen tubes. (A) Callose synthase is present as dots or patches along the entire border of control pollen tubes. **(B)** At the balloon-like step, callose synthase accumulates in the spherical domain. This image is a merge of phase contrast and immunofluorescence (red) pictures of the same pollen tube. **(C1, C2)** Accumulation of callose synthase in the apical domain is more evident at the transition between the balloon-like and the shovel-like step. Image in C1 is a merge of immunolocalized callose synthase (red) with phase contrast view of the same pollen tube. Image in C2 is an immunofluorescence view of another pollen tube. **(D1, D2, D3)** Accumulation of callose synthase in the neck (arrow) becomes evident when pollen tubes develop into the snake shape and start assuming the shovel shape. **(E-F)** Two additional views of Spm-treated pollen tubes showing a consistent accumulation of callose synthase in the neck region (arrows), with an annulus-like configuration. Bars 10 μ m.

Discussion

This work provides experimental evidence that Spm can function as a regulator of growth and shape of pollen tubes. Although there is a known natural variability in the germination of pollen and in the growth of pollen tubes in response to external factors, the data indicate a new panorama of either response or partial recovery of pollen tubes after Spm treatment. The two events (response and re-growth) are characterized by a series of modifications at the molecular and structural level, discussed below and summarized in Fig. 13.

Noticeable is the fact that 100 μM Spm, whose entrance is very rapid (Aloisi et al, 2015) and probably allowed by PA channels present in the plant cell membranes (Colombo et al., 1992; Pottosin and Shabala, 2014) caused in few minutes an irreversible enlargement of the pollen tube tip and a transient ten folds decrease of growth velocity. Then, after 15-20 min, the structural growth program was resumed and the enlarged diameter of the apex in the balloon stage was maintained in the growing snake and shovel tubes (Fig. 13 B, C). In addition, the growth rate recovered but only at half of its original value. These data suggest that the inhibition has been only partially counteracted or that some of the changes irreversibly affected the pollen tube.

Present data confirm the relevant role of actin in the complex changes induced by Spm. Changes of actin longitudinal filaments (Fig. 13 A) into unorganized short ones observed in the balloon tube apex (Fig. 13 B) resembled those described when the actin cytoskeleton is altered by the actin stabilizer jasplakinolide (Cárdenas et al., 2005). The possibility that Spm exerted a direct effect on actin is supported by the fact that, in pollen, actin was found covalently linked with PAs by a Ca^{2+} -dependent cytoplasmic TGase (Del Duca et al., 1997; Del Duca et al., 2013). In planta, this enzyme is present in the growing region of pear pollen tubes (Del Duca et al., 2013). Thus, in the Spm-treated pollen the activity of TGase may be enhanced by the concomitant increased concentrations of Spm and $[\text{Ca}^{2+}]_{\text{cyt}}$ affecting as consequence the proper polymerization of actin (Del Duca et al., 2009). In addition, it can be hypothesized that an irregular modulation of ROP GTPases might tentatively be involved because, when excessively activated, ROP lead to the extension of the secretion zone causing the swelling of the apical dome (Qin and

Yang, 2011). Therefore, the overall picture is further complicated by the possible inter-connection between Ca^{2+} levels, F-actin organization and ROP activation (Yan et al., 2009). In our system, we observed changes in $[\text{Ca}^{2+}]_{\text{cyt}}$, which may hypothetically unbalance the regulation of ROP activity, thereby leading to extensive secretion and to the balloon shape.

In the balloon stage, the movement of organelles was subjected to a more enhanced but disordered transport. Assuming that the myosin activity is not altered, the new disorganized actin configuration could be responsible for the modified organelle transport. There are currently very few information on the relationships between actin filament arrays and organelle speed. What is well known is that organelles move straightforwardly in the presence of longitudinal actin filaments and more disorderly at the level of the actin fringe (Lovy-Wheeler et al., 2007). The local organization of actin filaments is therefore responsible for the specific movement of organelles and vesicles (Kroeger et al., 2009). It can be assumed that a different density of actin filaments in Spm-treated pollen tubes could increase the speed of organelles by providing more contact points for myosin motors. An alternative explanation is that the increase in tube diameter results in a less crowded cytoplasm with a new organization of actin filaments and this new structure may lead to an unusual streaming of organelles.

The actin-based vesicle accumulation and fusion is strictly required for the appearance of the balloon shape in Spm-treated pollen tubes. In fact, the simultaneous addition of Spm and Brefeldin A (Fig. 13 B), an inhibitor of protein transport from the endoplasmic reticulum to the Golgi apparatus (Parton et al., 2003), prevented the swelling of pollen tube apex. Here, in pear pollen, the elongation rate was rapidly reduced in the presence of both molecules but pollen tubes never developed the characteristic balloon shape, indicating the importance of the secretory vesicles delivery to the apex for the remodeling of pollen tubes.

It is remarkable that microtubules are not apparently involved in the new growth and shape patterns exhibited by Spm-treated pollen tubes. On one hand, this is consistent with the evidence that microtubules are not generally involved in the tip-growth of pollen tubes (Cai et al., 2015). On the other hand, these data also suggest that Spm does not interfere with cellular processes mediated by microtubules. The precise role of microtubules in pollen tubes is not known but

hypothetically they could be involved in the regulation of exo/endocytosis (Idilli et al., 2013) as well as in the deposition of certain polymers of the cell wall; therefore, Spm may not interfere with these particular processes.

Regrowth of pollen tubes after Spm treatment (that is, shifting from the balloon to the snake phase) was characterized by appearance of fine elongated actin filaments in the middle of the snake pollen apex, partial recovery of growth and re-focusing of the secretion zone as shown by PI labeling. It is difficult to predict if this implies either the assembly of additional/supernumerary actin filaments or simply the organization of more radial actin arrays. Nevertheless, the new actin pattern supports an active streaming of organelles and vesicles and the growth recover, although with different features.

It can be hypothesized that the re-growth may be related either to the inactivation of Spm (e.g. by sequestration in the apoplast or by its linking to various cell components) or by its catabolism, e.g. by peroxisomal PAO found in pollen (Tavladoraki et al., 2016).

Many of the above described events may be related or dependent on local changes of Ca^{2+} concentration and pH. In the pollen treated with different PAs, we found that the gradient of Ca^{2+} was rapidly dissipated and reconstituted (Aloisi et al., 2015). In the current work, by using the bioluminescent Ca^{2+} reporter aequorin fused to the cell-penetrating peptide TAT, the Spm-induced Ca^{2+} change was measured. This sensitive and accurate technique has been previously successfully applied in suspension-cultured plant cells (Zonin et al., 2011) and in mycorrhizal fungi (Moscatiello et al., 2014; Salvioli et al., 2016). In control pollen tubes, a basal $[\text{Ca}^{2+}]_{\text{cyt}}$ of about $0.5 \mu\text{M}$ was measured, which represents an average concentration in the tip-focused Ca^{2+} gradient along the pollen tube axis during growth. The $[\text{Ca}^{2+}]_{\text{cyt}}$ measured well matches an average value between a maximal $[\text{Ca}^{2+}]$ of $1\text{-}10 \mu\text{M}$ at the tip apex depending on both pollen type and detection method (Holdaway-Clarke and Hepler, 2003) and a minimal $[\text{Ca}^{2+}]_{\text{cyt}}$ of $0.1\text{-}0.2 \mu\text{M}$ throughout the shank of the tube, measured with fluorescent Ca^{2+} probes (Steinhorst and Kudla 2013; Hepler and Winship 2015). Treatment with $100 \mu\text{M}$ Spm triggered a rapid and remarkable increase of $[\text{Ca}^{2+}]_{\text{cyt}}$, almost completely dissipated within 10 min. A two-fold increase in $[\text{Ca}^{2+}]_{\text{cyt}}$ was also induced by 1 mM spermidine in Arabidopsis pollen tubes as shown by the (FRET)-based Ca^{2+}

indicator cameleon (Wu et al., 2010). Present results are thus in agreement with data in the literature indicating that PAs might affect intracellular Ca^{2+} levels likely as a consequence of the activation of plasma membrane Ca^{2+} channels and may lead to membrane depolarization (Pottosin and Shabala, 2014).

Previously, sudden but transient stimulation of several activities of oxidative enzymes and an imbalance of ROS were observed in pear pollen tubes by supplying different PAs (Aloisi et al. 2015). Intracellular optimal ROS levels, necessary for pollen tube growth, are controlled by different mechanisms and are strictly interconnected with Ca^{2+} concentration, with a positive feedback regulation as observed in pollen (Potocky et al., 2007;Kaya et al., 2014;Lassig et al., 2014) which may enhance the responsiveness of pollen tubes to extracellular cues (Wudick and Feijo, 2014).

Despite the only transitory change of Ca^{2+} levels, this cation might affect different metabolisms or structures. It is known that Ca^{2+} regulates the dynamics of actin filaments through Ca^{2+} binding proteins (Zhang et al., 2010) as well as the PA binding to microfilaments that occur via TGase.

An interconnection between Ca^{2+} and pH has to be taken into consideration, as changes of pH values might be caused by modulation of plasma membrane H^{+} -ATPase because Spm, by causing a Ca^{2+} influx across the plasma membrane, can determine a Ca^{2+} uptake-synchronized imbalance between influx and efflux of H^{+} (Pottosin and Shabala, 2014;Pottosin et al., 2014a). Moreover, concomitant changes of ROS levels after Spm addition are also important because Ca^{2+} and ROS can mutually regulate their own levels (Wu et al., 2010;Kaya et al., 2014;Pottosin et al., 2014b;Wudick and Feijo, 2014).

New information arising from the present data is that Spm also induces a profound redistribution of new secreted cell wall components, like pectins, callose and cellulose. Pectins were deposited in a larger area leading to the balloon shape. Newly secreted methyl-esterified pectins refocused in narrow regions at the apex when pollen tubes transited from the balloon into the snake shape. Refocusing of pectin secretion occurred simultaneously to the re-growth, indicating that this feature is necessary for growth. Additional secretion of methyl-esterified pectins likely increased the softening of pollen tube cell wall thereby leading to apical swelling under the internal turgor pressure. In fact, assuming that the turgor

pressure does not change (Winship et al., 2011), the formation of swollen pollen tubes might depend on changes to the cell wall architecture. Ca^{2+} plays an essential role in the pectin net formation and stabilizing. As PAs can directly bind to pectic substances by ionic linkages, they may compete with Ca^{2+} for the formation of intermolecular bridges, affecting the net mesh, its charge and the packing of polygalacturonic chains (D'Orazi and Bagni, 1987; Berta et al., 1997; Lenucci et al., 2005).

As soon as a new growing tip started to reform, rearrangement of actin filaments may refocus the vesicle secretion. However, we cannot exclude a more complex scenario, in which the temporary deregulation of actin dynamics by Spm may inhibit secretion and/or activation of PME, which in turn changes the rigidity and pectin composition of the pollen tube cell wall (Wang et al., 2013).

The deposition pattern of two main glucose-based polysaccharides, cellulose and callose was also investigated. Both polymers have been reported to regulate the pollen tube shape by counteracting the internal turgor pressure. Callose content is usually more prominent than cellulose and it likely favors the fast growth rate of angiosperm pollen tubes (Abercrombie et al., 2011). Cellulose is found at lower levels but it may also be critical for regulating tube shape and diameter. Both digestion of cellulose by specific enzymes and inhibition of cellulose crystallization determine the formation of pollen tubes with increased diameter in *Solanum chacoense* and *Lilium orientalis* (Aouar et al., 2010). The inhibition of cellulose assembly results in a more consistent deposition of pectins, which likely counterbalance the lower mechanical resistance. It has been shown that cellulose levels in Spm-treated pollen tubes changed by increasing the deposition pattern in the neck region and subsequently in the enlarged pollen tube. This finding could be interpreted as a response of pollen tubes to the swelling process caused by the extension of the pectin deposition area, which weakens the cell wall structure. Therefore, the increase of cellulose deposition might counteract the altered deposition of pectins. It is still unknown whether the new deposition pattern of cellulose is either the result of a pure mechanical response or of the process by which pollen tubes resume growing.

Comparable results were also found for callose. While callose in control pollen tubes was deposited according to a common feature with absence of callose in the

tube tip (Chebli et al., 2012), Spm-treated pollen tubes were characterized by changes in callose distribution. The most evident alteration was a consistent deposition of callose in the neck region, which was prominent just when pollen tubes swelled and it was maintained during the transition from snake- to shovel-shaped pollen tubes. The most likely interpretation of this finding is that pollen tubes respond to the swelling process by depositing an excess of callose in the neck region in order to protect the pollen tube. Given its high tensile strength, callose is a good candidate for the regulation of pollen tube diameter. Digestion of callose by lyticase results in enhanced tube diameter and the relative stiffness of the growth medium might affect the content of callose in the cell wall (Parre and Geitmann, 2005). In Spm-treated pollen, callose was apparently deposited more consistently in the neck region as to protect the pollen tube in response to an excess of cell wall deformation. The absence of callose in the tip region was consistent with the evidence that pollen tube still grows, differently from what happens during the self-incompatibility response, when a callose plug is formed to arrest pollen tube growth.

The differential deposition of callose in Spm-treated pollen tubes was mirrored by changes in the distribution pattern of callose synthase. While in control pollen tubes the enzyme was present along the pollen tube edge with a relative concentration at the apex, Spm-treated pollen tubes were characterized by a prominent accumulation of callose synthase in the swelled apex and subsequently in the neck region, sometimes with an annulus-like distribution at the base of the enlarged pollen tube. This finding is consistent with the excess deposition of callose in the neck and suggests that the enlargement of the tube apex might induce the specific accumulation and activation of callose synthase in the neck, whereas it possibly remains inactive in the apex as no callose was found there. Unfortunately, how deposition and activation of callose synthase are regulated is poorly known. Callose synthase is likely transported through Golgi-derived secretory vesicles along actin filaments (Brownfield et al., 2008; Cai et al., 2011), while activation of its enzymatic features requires a lipid domain and possibly a proteolytic cleavage (Brownfield et al., 2008). Evidence linking the activation of callose synthase to cell wall deformation is missing in pollen tubes. More information is available on the regulation of callose plugs deposition. Microtubules

are reported to control the number of callose plugs in tobacco pollen tubes (Laitiainen et al., 2002) and microtubules are also possibly involved in the proper distribution of callose synthase in distal regions and around nascent callose plugs (Cai et al., 2011). In addition, formation of callose plugs is likely under the control of H⁺-ATPase activity and consequently of H⁺ flux into/out of pollen tubes (Ceral et al., 2008).

A direct involvement of PAs in the reorganization of the cell wall cannot be excluded, as it is known that PAs are linked to cell wall molecules, e.g. emicelluloses, lignin, pectins and HCCAs etc. (Aloisi et al., 2016). Moreover in Rosaceae pollen, PAs are conjugated to cell wall proteins via an extracellular TGase forming protein polymers (Della Mea et al. 2007). Finally, PA are known to be metabolized in the cell wall, i.e. by PAO which are involved in the cross-linking of extensin and polysaccharide-bound phenols and in ROS production (Yoda et al., 2006; Angelini et al., 2010), involved in wall loosening or stiffening (Swanson and Gilroy, 2010; Speranza et al., 2012).

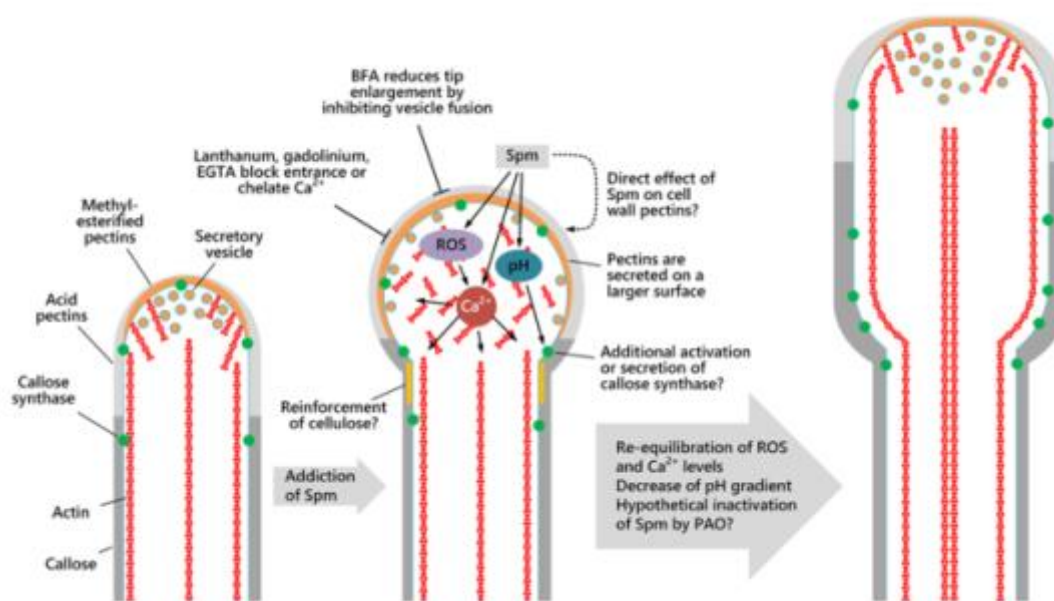


FIGURE 13. Schematic drawing showing the morphology of the apical region and the spatial distribution of actin filaments, secretory vesicles and cell wall components in pollen tubes and how Spm perturbs either their distribution or the morphology of the apical region . The pollen tube sub-apex is characterized by the actin fringe while in the shank region actin filaments form regular and longitudinal cables, which are essential for organelles and vesicles movement. Supplementation of Spm deeply alters Ca²⁺, H⁺ and ROS concentration and distribution, thereby affecting not only microfilament organization but also vesicle delivery. As final result, assembly of the cell wall and shaping of the growing pollen tube tip is altered. (a) Pollen tube after 1 h of germination; (b) Pollen tube after 1 h of germination in standard medium, then supplied with Spm for 1 additional hour; (c)

Pollen tube grown for 1 hour in standard medium and then supplemented with Spm for 2 additional hours. Still unknown mechanisms re-equilibrate ion distribution and concentration and allow pollen tube to grow again although the tube diameter is larger and growth speed is lower. Inactivation of Spm by oxidative enzymes is not to be excluded.

Final remarks

Our findings show that relatively low concentrations of Spm have remarkable effects on the growth rate of pollen tubes by affecting pollen tube morphology. Changes of pollen tube shape might be dependent on alteration of intracellular Ca^{2+} and pH, which reflects on both organization of actin filaments and cell wall structure (see the model in Figure 13). At the cyto-morphological level, Spm induces two main effects. First, actin filaments are disorganized and fragmented; it is plausible that fragmentation of actin filaments is caused by rapid increase of Ca^{2+} levels (Qu et al., 2015). Second, the zone of pectin deposition expands because of enlargement in the secretion area. This effect, which might be triggered by disorganization of actin filaments, consequently decreases anisotropy of pollen tube apex and determines the formation of apical swelling. As a result, pollen tube growth stops. Because pollen tubes can resume growth after a short time period, they must necessarily have a "detoxification" mechanism that restores optimal levels of intracellular Spm. Enzymes such as polyamine oxidase (PAO) might have a role also in pollen (Tavladoraki et al., 2016). Although actin filaments resume a control-like appearance, the new growth pattern is different from the pre-Spm stage because the pollen tube diameter is greater and the growth speed is reduced. In the new growth phase, secretion of pectins is again focused in the apex but the lateral cell wall of pollen tubes at the "neck" level is reinforced, possibly stabilized, by abnormal deposition of callose and cellulose. What is worth of notice is that the re-growth of pollen tube growth during Spm treatment is characterized by an increase in tube diameter and this process might interestingly underlie the mechanism used by pollen tubes to control exactly their diameter, an essential feature for the penetration of the style. Ultimately, these data indicate that Spm has the ability to control the growth of pollen tubes, which in turn have mechanisms for modulating (within limits) the intracellular concentration of Spm.

References

- Abercrombie, J.M., O'meara, B.C., Moffatt, A.R., and Williams, J.H. (2011). Developmental evolution of flowering plant pollen tube cell walls: callose synthase (CalS) gene expression patterns. *Evodevo* 2, 14.
- Aloisi, I., Cai, G., Serafini-Fracassini, D., and Del Duca, S. (2016). Polyamines in Pollen: From Microsporogenesis to Fertilization. *Front Plant Sci* 7, 155.
- Aloisi, I., Cai, G., Tumiatti, V., Minarini, A., and Del Duca, S. (2015). Natural polyamines and synthetic analogs modify the growth and the morphology of *Pyrus communis* pollen tubes affecting ROS levels and causing cell death. *Plant Sci* 239, 92-105.
- Angelini, R., Cona, A., Federico, R., Fincato, P., Tavloraki, P., and Tisi, A. (2010). Plant amine oxidases "on the move": an update. *Plant Physiol Biochem* 48, 560-564.
- Antognoni, F., and Bagni, N. (2008). Bis(guanylhydrazones) negatively affect in vitro germination of kiwifruit pollen and alter the endogenous polyamine pool. *Plant Biol (Stuttg)* 10, 334-341.
- Aouar, L., Chebli, Y., and Geitmann, A. (2010). Morphogenesis of complex plant cell shapes: the mechanical role of crystalline cellulose in growing pollen tubes. *Sex Plant Reprod* 23, 15-27.
- Åström, H. (1992). Acetylated alpha-tubulin in the pollen tube microtubules. *Cell Biol Int Rep* 16, 871-881.
- Åström, H., Sorri, O., and Raudaskoski, M. (1995). Role of microtubules in the movement of the vegetative nucleus and generative cell in tobacco pollen tubes. *Sex Plant Reprod* 8, 61-69.
- Bagni, N., Adamo, P., and Serafini-Fracassini, D. (1981). RNA, proteins and polyamines during tube growth in germinating apple pollen. *Plant Physiol* 68, 727-730.
- Berta, G., Altamura, M.M., Fusconi, A., Cerruti, F., Capitani, F., and Bagni, N. (1997). The plant cell wall is altered by inhibition of polyamine biosynthesis. *New Phytologist* 137, 569-577.
- Bove, J., Vaillancourt, B., Kroeger, J., Hepler, P.K., Wiseman, P.W., and Geitmann, A. (2008). Magnitude and direction of vesicle dynamics in growing pollen tubes using spatiotemporal image correlation spectroscopy and fluorescence recovery after photobleaching. *Plant Physiol* 147, 1646-1658.
- Brini, M., Marsault, R., Bastianutto, C., Alvarez, J., Pozzan, T., and Rizzuto, R. (1995). Transfected aequorin in the measurement of cytosolic Ca²⁺ concentration ([Ca²⁺]_c). A critical evaluation. *J Biol Chem* 270, 9896-9903.
- Brownfield, L., Wilson, S., Newbiggin, E., Bacic, A., and Read, S. (2008). Molecular control of the glucan synthase-like protein NaGSL1 and callose synthesis during growth of *Nicotiana glauca* pollen tubes. *Biochem J* 414, 43-52.
- Cai, G., Faleri, C., Del Casino, C., Emons, A.M., and Cresti, M. (2011). Distribution of callose synthase, cellulose synthase, and sucrose synthase in tobacco pollen tube is controlled in dissimilar ways by actin filaments and microtubules. *Plant Physiol* 155, 1169-1190.
- Cai, G., Parrotta, L., and Cresti, M. (2015). Organelle trafficking, the cytoskeleton, and pollen tube growth. *J Integr Plant Biol* 57, 63-78.
- Cárdenas, L., Lovy-Wheeler, A., Wilsen, K.L., and Hepler, P.K. (2005). Actin polymerization promotes the reversal of streaming in the apex of pollen tubes. *Cell Motil Cytoskeleton* 61, 112-127.
- Certal, A.C., Almeida, R.B., Carvalho, L.M., Wong, E., Moreno, N., Michard, E., Carneiro, J., Rodriguez-Leon, J., Wu, H.M., Cheung, A.Y., and Feijo, J.A. (2008). Exclusion of a proton ATPase from the apical membrane is associated with cell polarity and tip growth in *Nicotiana tabacum* pollen tubes. *Plant Cell* 20, 614-634.
- Charnay, D., Nari, J., and Noat, G. (1992). Regulation of plant cell-wall pectin methyl esterase by polyamines-interactions with the effects of metal ions. *Eur J Biochem* 205, 711-714.

- Chebli, Y., Kaneda, M., Zerzour, R., and Geitmann, A. (2012). The cell wall of the Arabidopsis pollen tube-spatial distribution, recycling, and network formation of polysaccharides. *Plant Physiol* 160, 1940-1955.
- Colombo, R., Cerana, R., and Bagni, N. (1992). Evidence for polyamine channels in protoplasts and vacuoles of Arabidopsis thaliana cells. *Biochem Biophys Res Commun* 182, 1187-1192.
- D'orazi, D., and Bagni, N. (1987). In vitro interactions between polyamines and pectic substances. *Biochemical and Biophysical Research Communications* 148 1259-1263.
- Del Duca, S., Bregoli, A.M., Bergaini, C., and Serafini-Fracassini, D. (1997). Transglutaminase-catalyzed modification of cytoskeletal proteins by polyamines during the germination of Malus domestica pollen. *Sexual Plant Reproduction* 10, 89-95.
- Del Duca, S., Faleri, C., Iorio, R.A., Cresti, M., Serafini-Fracassini, D., and Cai, G. (2013). Distribution of transglutaminase in pear pollen tubes in relation to cytoskeleton and membrane dynamics. *Plant Physiol* 161, 1706-1721.
- Del Duca, S., Serafini-Fracassini, D., Bonner, P., Cresti, M., and Cai, G. (2009). Effects of post-translational modifications catalysed by pollen transglutaminase on the functional properties of microtubules and actin filaments. *Biochem J* 418, 651-664.
- Di Sandro, A., Del Duca, S., Verderio, E., Hargreaves, A.J., Scarpellini, A., Cai, G., Cresti, M., Faleri, C., Iorio, R.A., Hirose, S., Furutani, Y., Coutts, I.G., Griffin, M., Bonner, P.L., and Serafini-Fracassini, D. (2010). An extracellular transglutaminase is required for apple pollen tube growth. *Biochem J* 429, 261-271.
- Dutta, R., and Robinson, K.R. (2004). Identification and characterization of stretch-activated ion channels in pollen protoplasts. *Plant Physiol* 135, 1398-1406.
- Falasca, G., Franceschetti, M., Bagni, N., Altamura, M.M., and Biasi, R. (2010). Polyamine biosynthesis and control of the development of functional pollen in kiwifruit. *Plant Physiol Biochem* 48, 565-573.
- Feijo, J.A., Sainhas, J., Holdaway-Clarke, T., Cordeiro, M.S., Kunkel, J.G., and Hepler, P.K. (2001). Cellular oscillations and the regulation of growth: the pollen tube paradigm. *Bioessays* 23, 86-94.
- Frietsch, S., Wang, Y.F., Sladek, C., Poulsen, L.R., Romanowsky, S.M., Schroeder, J.I., and Harper, J.F. (2007). A cyclic nucleotide-gated channel is essential for polarized tip growth of pollen. *Proc Natl Acad Sci U S A* 104, 14531-14536.
- Gossot, O., and Geitmann, A. (2007). Pollen tube growth: coping with mechanical obstacles involves the cytoskeleton. *Planta* 226, 405-416.
- Hepler, P.K., Rounds, C.M., and Winship, L.J. (2013). Control of cell wall extensibility during pollen tube growth. *Mol Plant* 6, 998-1017.
- Hepler, P.K., Vidali, L., and Cheung, A.Y. (2001). Polarized cell growth in higher plants. *Annu Rev Cell Dev Biol* 17, 159-187.
- Himschoot, E., Beeckman, T., Friml, J., and Vanneste, S. (2015). Calcium is an organizer of cell polarity in plants. *Biochim Biophys Acta* 1853, 2168-2172.
- Holdaway-Clarke, T.L., and Hepler, P.K. (2003). Control of pollen tube growth: role of ion gradients and fluxes. *New Phytol* 159, 539-563.
- Idilli, A.I., Morandini, P., Onelli, E., Rodighiero, S., Caccianiga, M., and Moscatelli, A. (2013). Microtubule depolymerization affects endocytosis and exocytosis in the tip and influences endosome movement in tobacco pollen tubes. *Mol Plant* 6, 1109-1130.
- Kaya, H., Nakajima, R., Iwano, M., Kanaoka, M.M., Kimura, S., Takeda, S., Kawarazaki, T., Senzaki, E., Hamamura, Y., Higashiyama, T., Takayama, S., Abe, M., and Kuchitsu, K. (2014). Ca²⁺-activated reactive oxygen species production by Arabidopsis RbohH and RbohJ is essential for proper pollen tube tip growth. *Plant Cell* 26, 1069-1080.
- Kroeger, J.H., Daher, F.B., Grant, M., and Geitmann, A. (2009). Microfilament orientation constrains vesicle flow and spatial distribution in growing pollen tubes. *Biophys J* 97, 1822-1831.

- Laitinen, E., Nieminen, K.M., Vihinen, H., and Raudaskoski, M. (2002). Movement of generative cell and vegetative nucleus in tobacco pollen tubes is dependent on microtubule cytoskeleton but independent of the synthesis of callose plugs. *Sex Plant Reprod* 15, 195-204.
- Lassig, R., Gutermuth, T., Bey, T.D., Konrad, K.R., and Romeis, T. (2014). Pollen tube NAD(P)H oxidases act as a speed control to dampen growth rate oscillations during polarized cell growth. *Plant J* 78, 94-106.
- Lenucci, M., Piro, G., Miller, J.G., Dalessandro, G., and Fry, S.C. (2005). Do polyamines contribute to plant cell wall assembly by forming amide bonds with pectins? *Phytochemistry* 66, 2581-2594.
- Lovy-Wheeler, A., Cardenas, L., Kunkel, J.G., and Hepler, P.K. (2007). Differential organelle movement on the actin cytoskeleton in lily pollen tubes. *Cell Motil Cytoskeleton* 64, 217-232.
- Lovy-Wheeler, A., Wilsen, K.L., Baskin, T.I., and Hepler, P.K. (2005). Enhanced fixation reveals the apical cortical fringe of actin filaments as a consistent feature of the pollen tube. *Planta* 221, 95-104.
- Malho, R., and Trewavas, A.J. (1996). Localized apical increases of cytosolic free calcium control pollen tube orientation. *Plant Cell* 8, 1935-1949.
- Michard, E., Lima, P.T., Borges, F., Silva, A.C., Portes, M.T., Carvalho, J.E., Gilliam, M., Liu, L.H., Obermeyer, G., and Feijo, J.A. (2011). Glutamate receptor-like genes form Ca²⁺ channels in pollen tubes and are regulated by pistil D-serine. *Science* 332, 434-437.
- Mollet, J.C., Leroux, C., Dardelle, F., and Lehner, A. (2013). Cell wall composition, biosynthesis and remodelling during pollen tube growth. *Plants (Basel)* 2, 107-147.
- Moscatiello, R., Sello, S., Novero, M., Negro, A., Bonfante, P., and Navazio, L. (2014). The intracellular delivery of TAT-aequorin reveals calcium-mediated sensing of environmental and symbiotic signals by the arbuscular mycorrhizal fungus *Gigaspora margarita*. *New Phytol* 203, 1012-1020.
- O' Neill, M.A., Albersheim, P., and Darvill, A. (1990). The pectic polysaccharides of primary cell walls. . *Methods in Plant Biochemistry, Carbohydrates*, Dey P.M., Harborne J.B, editors. , Eds London: Academic Press; pp. 415-441.
- Palin, R., and Geitmann, A. (2012). The role of pectin in plant morphogenesis. *Biosystems* 109, 397-402.
- Parre, E., and Geitmann, A. (2005). More than a leak sealant. The mechanical properties of callose in pollen tubes. *Plant Physiol* 137, 274-286.
- Parrotta, L., Guerriero, G., Sergeant, K., Cai, G., and Hausman, J.F. (2015). Target or barrier? The cell wall of early- and later-diverging plants vs cadmium toxicity: differences in the response mechanisms. *Front Plant Sci* 6, 133.
- Parton, R.M., Fischer-Parton, S., Trewavas, A.J., and Watahiki, M.K. (2003). Pollen tubes exhibit regular periodic membrane trafficking events in the absence of apical extension. *J Cell Sci* 116, 2707-2719.
- Potocky, M., Jones, M.A., Bezvoda, R., Smirnov, N., and Zarsky, V. (2007). Reactive oxygen species produced by NADPH oxidase are involved in pollen tube growth. *New Phytol* 174, 742-751.
- Pottosin, I., and Shabala, S. (2014). Polyamines control of cation transport across plant membranes: implications for ion homeostasis and abiotic stress signaling. *Front Plant Sci* 5, 154.
- Pottosin, I., Velarde-Buendia, A.M., Bose, J., Fuglsang, A.T., and Shabala, S. (2014a). Polyamines cause plasma membrane depolarization, activate Ca²⁺, and modulate H⁺-ATPase pump activity in pea roots. *J Exp Bot* 65, 2463-2472.
- Pottosin, I., Velarde-Buendia, A.M., Bose, J., Zepeda-Jazo, I., Shabala, S., and Dobrovinskaya, O. (2014b). Cross-talk between reactive oxygen species and polyamines in regulation of ion transport across the plasma membrane: implications for plant adaptive responses. *J Exp Bot* 65, 1271-1283.

- Qin, Y., and Yang, Z. (2011). Rapid tip growth: insights from pollen tubes. *Semin Cell Dev Biol* 22, 816-824.
- Qu, H., Jiang, X., Shi, Z., Liu, L., and Zhang, S. (2012). Fast loading ester fluorescent Ca²⁺ and pH indicators into pollen of *Pyrus pyrifolia*. *J Plant Res* 125, 185-195.
- Qu, X., Jiang, Y., Chang, M., Liu, X., Zhang, R., and Huang, S. (2015). Organization and regulation of the actin cytoskeleton in the pollen tube. *Front Plant Sci* 5, 786.
- Rockel, N., Wolf, S., Kost, B., Rausch, T., and Greiner, S. (2008). Elaborate spatial patterning of cell-wall PME and PME1 at the pollen tube tip involves PME1 endocytosis, and reflects the distribution of esterified and de-esterified pectins. *Plant J* 53, 133-143.
- Rojas, E.R., Hotton, S., and Dumais, J. (2011). Chemically mediated mechanical expansion of the pollen tube cell wall. *Biophys J* 101, 1844-1853.
- Rounds, C.M., Hepler, P.K., and Winship, L.J. (2014). The apical actin fringe contributes to localized cell wall deposition and polarized growth in the lily pollen tube. *Plant Physiol* 166, 139-151.
- Rutten, T.L., and Knuiman, B. (1993). Brefeldin A effects on tobacco pollen tubes. *Eur J Cell Biol* 61, 247-255.
- Salvioli, A., Ghignone, S., Novero, M., Navazio, L., Venice, F., Bagnaresi, P., and Bonfante, P. (2016). Symbiosis with an endobacterium increases the fitness of a mycorrhizal fungus, raising its bioenergetic potential. *ISME J* 10, 130-144.
- Speranza, A., Crinelli, R., Scoccianti, V., and Geitmann, A. (2012). Reactive oxygen species are involved in pollen tube initiation in kiwifruit. *Plant Biol (Stuttg)* 14, 64-76.
- Steinhorst, L., and Kudla, J. (2013). Calcium - a central regulator of pollen germination and tube growth. *Biochim Biophys Acta* 1833, 1573-1581.
- Swanson, S., and Gilroy, S. (2010). ROS in plant development. *Physiol Plant* 138, 384-392.
- Tavladoraki, P., Cona, A., and Angelini, R. (2016). Copper-Containing Amine Oxidases and FAD-Dependent Polyamine Oxidases Are Key Players in Plant Tissue Differentiation and Organ Development. *Front Plant Sci* 7, 824.
- Tiburcio, A.F., Altabella, T., Bitrian, M., and Alcazar, R. (2014). The roles of polyamines during the lifespan of plants: from development to stress. *Planta* 240, 1-18.
- Wang, H., Zhuang, X., Cai, Y., Cheung, A.Y., and Jiang, L. (2013). Apical F-actin-regulated exocytic targeting of NtPPME1 is essential for construction and rigidity of the pollen tube cell wall. *Plant J* 76, 367-379.
- Winship, L.J., Obermeyer, G., Geitmann, A., and Hepler, P.K. (2011). Pollen tubes and the physical world. *Trends Plant Sci* 16, 353-355.
- Wolf, S., and Greiner, S. (2012). Growth control by cell wall pectins. *Protoplasma* 249 Suppl 2, S169-175.
- Wu, J., Shang, Z., Jiang, X., Moschou, P.N., Sun, W., Roubelakis-Angelakis, K.A., and Zhang, S. (2010). Spermidine oxidase-derived H₂O₂ regulates pollen plasma membrane hyperpolarization-activated Ca(2+) - permeable channels and pollen tube growth. *Plant J* 63, 1042-1053.
- Wudick, M.M., and Feijo, J.A. (2014). At the intersection: merging Ca²⁺ and ROS signaling pathways in pollen. *Mol Plant* 7, 1595-1597.
- Yan, A., Xu, G., and Yang, Z.B. (2009). Calcium participates in feedback regulation of the oscillating ROP1 Rho GTPase in pollen tubes. *Proc Natl Acad Sci U S A* 106, 22002-22007.
- Yoda, H., Hiroi, Y., and Sano, H. (2006). Polyamine oxidase is one of the key elements for oxidative burst to induce programmed cell death in tobacco cultured cells. *Plant Physiol* 142, 193-206.
- Zhang, H., Qu, X., Bao, C., Khurana, P., Wang, Q., Xie, Y., Zheng, Y., Chen, N., Blanchoin, L., Staiger, C.J., and Huang, S. (2010). Arabidopsis VILLIN5, an actin filament bundling and severing protein, is necessary for normal pollen tube growth. *Plant Cell* 22, 2749-2767.

Zonin, E., Moscatiello, R., Miuzzo, M., Cavallarin, N., Di Paolo, M.L., Sandona, D., Marin, O., Brini, M., Negro, A., and Navazio, L. (2011). TAT-mediated aequorin transduction: an alternative approach for effective calcium measurements in plant cells. *Plant Cell Physiol* 52, 2225-2235.

PART II

Pollen as a source of allergens: Air monitoring and *in vitro* studies

Chapter 4

Behavior of profilins in atmosphere and *in vitro*, and their relationship with the performance of airborne pollen

Abstract

Pollen, as well as smaller plant particles, contributes to the allergenicity of the air. The situation is made more complicated by meteorological factors that drastically affect the occurrence of pollen grains and allergen release in the atmosphere. In order to shed light on this phenomenon, the dynamics of pollen and the pollen panallergen profilin in the air of two Mediterranean cities, having different weather conditions, were analyzed. Sampling was performed using a Hirst volumetric trap and a Cyclone sampler from March to June 2015 in León (Spain) and in Bologna (Italy). Pollen concentrations were compared to the amounts of airborne profilin. In-vitro pollen tests were also performed in order to mimic pollen rehydration, occurring in natural conditions. In both cities, pollen and profilin concentrations followed a similar trend; however, peaks were often misaligned, with the profilin peaks following those of total airborne pollen. Several meteorological parameters, such as relative humidity, deeply influenced pollen and allergen dispersion. In-vitro tests revealed massive protein release from allergenic pollens during the early stages of pollen rehydration; profilin was also extruded from the grains. Thus, the different timing and amount of proteins released from different pollens during hydration could explain the non-synchronous pollen and profilin peaks in the atmosphere.

Introduction

Due to the steadily increasing cases of allergy to pollen (Bousquet et al., 2007; Eder et al., 2006), it is of great interest to monitor the allergenic potential of the air. To do this, the assessment of airborne pollen concentration is a traditional tool (D'Amato et al., 2007). In recent years, however, airborne pollen allergens were also found in non-pollen fractions (De Linares et al., 2010; Fernández-González et al., 2011), thus the question arises as to whether the methods currently available for measuring atmospheric allergenicity are adequate (Brito et al., 2011; Buters et al., 2012; D'Amato et al., 1998).

Knowledge regarding the influence of weather conditions on allergen release is still poor and debated (D'Amato and Cecchi, 2008). It is nevertheless well-known that meteorological factors deeply affect both pollen and allergen fluctuations. They can either directly affect the amount of airborne pollen or, indirectly, cause its rupture resulting in allergen release.

Allergens can be pollen-specific or, as in the case of panallergens, share sequence and structural conformation thereby leading to cross-reactions between unrelated pollens and often also between pollen and foods. Examples of panallergens are profilins, non-specific lipid transfer proteins, polcalcins, and Bet v 1-related proteins (Hauser et al., 2010). Profilins are small, ubiquitous, and multifunctional actin binding proteins (ABPs) involved in actin cytoskeleton dynamics.

Plant profilins have been shown to be highly cross-reactive allergens due to high conservation of their primary structure, reaching homologies of 86% and 73% in the case of olive (Ole e 2) with birch and pollen grass profilins, respectively (Ledesma et al., 1998; Martinez et al., 2002; Morales et al., 2008). Moreover, the 3-dimensional structure of these proteins is highly conserved from microorganisms to humans (Santos and Van Ree, 2011). Profilins have a high allergenic relevance as they can elicit both nasal and bronchial responses in sensitive patients (Ruiz-García et al., 2011).

Given that profilins are strongly allergenic and widespread proteins and that their airborne concentration may be influenced not only by pollen concentration but also by climatic factors, we determined the daily fluctuations of

airborne pollen and aero-profilin concentrations, and, in parallel, examined which meteorological factors most markedly influenced them. For this purpose, two Mediterranean cities with different weather conditions were chosen: León (Spain), which is characterized by a dry and windy climate, and Bologna (Italy) characterized by a low-rainfall but still humid climate.

Rapid release of allergenic proteins into aqueous media during pollen rehydration is a common event (de Dios Alche et al., 2004; Grote et al., 1993; Vega-Maray et al., 2006; Vrtala et al., 1993) and this condition mimics the interaction between pollen and human mucosa (Morales et al., 2008). Profilins are very abundant in pollen (Staiger and Blanchoin, 2006) and, due to their high solubility, are released in large amounts into the culture medium during in-vitro pollen hydration and germination (Morales et al., 2008; Vrtala et al., 1993). Thus, the effect of in-vitro pollen rehydration on the release of proteins, amongst which profilin, was investigated in pollen samples from the two cities.

Material and methods

Air sampling

Pollen sampling was performed continuously throughout from March to June 2015 using two Hirst-type seven-day recording volumetric trap (VPPS 2000 sampler, Lanzoni, Bologna, Italy) with a suction flow rate of 10 l/min. placed on a terrace 15 m above ground level at León University Campus (Spain), and installed 25 m above ground level on the roof of the ISAC-CNR building in Bologna (Italy). Pollen counts were expressed as daily mean pollen grains/m³ of air.

Particles for aeroallergen quantification were sampled with a Burkard Cyclone sampler (Burkard Manufacturing Co Ltd. Hertfordshire, UK), a continuous, wind-oriented volumetric sampler using a single reverse-flow miniature cyclone with an air throughput of 16.5 l/min. Particles were collected directly into a 1.5 ml Eppendorf vial every 24 hours of sampling, during the same period of pollen. Samples collected each day were stored at -20 °C. Both samplers were located in the same sampling pollen station.

Details of the monitoring stations

The city of León (830 m a.s.l.), is placed in the north-western Iberian Peninsula. Biogeographically, the city belongs to the Mediterranean region and has a continental climate; mean annual temperature is 11 °C, annual average rainfall is 522 mm, mainly in autumn and spring (with low rainfall and the storms type during the summer months) and the annual mean wind intensity exceeds 5 m/s. Bologna (54 m a.s.l.), is located at the foot of the Apennine Mountains (South) in the Po Plain, a vast flat area in the north of Italy and biogeographically belongs to the Eurosiberian Region. The area is characterized by a sub-continental climate (Köppen-Geiger Cfa) with cold winters and hot summers (typical monthly mean temperatures ranging from 1 to 26 °C), high humidity levels (typical monthly mean relative humidity ranging from 60% to 84%) and low wind intensities (typical annual mean wind intensities of about 2 m/s). The annual mean precipitation is between 760-800 mm with a xerothermic period in July and August

Protein extraction from Cyclone samples and immunochemical aero-profilin quantification

The dry Cyclone samples were centrifuged at 18000 x g, 1 min and extracted at room temperature for 2 h with 120 µL of phosphate buffer (50 mM pH 7.0) supplemented with 150 mM NaCl, 3 mM EDTA, 0.005% Tween 20, and 125 mM ammonium bicarbonate. The extract was separated by centrifugation at 2000 x g for 10 min and stored at -20 °C.

The profilin content in extracted samples was quantified using a double antibody sandwich ELISA method. The ELISA plates (Greiner, Frickenhausen, Germany) were previously coated overnight with 0.25 µg/well of monoclonal antibodies anti-profilin (3H8 and 5F2) (Bial Industrial Farmacéutica, Zamudio, Spain) at room temperature in a moist chamber and then blocked with 200 µL/well of PBS-BSA-T (PBS with 1% bovine serum albumin with 0.05% Tween 20). Afterwards, plates were incubated with 100 µL per well of extracted airborne samples, purified Ole e 2, starting from a stock of 1000 ng/ml, followed by 8 serial dilutions of 1/2 in PBS-BSA-T. Plates were incubated with 100 µL/well of biotinylated rabbit anti-Ole e 2 polyclonal antibody at 1 µg/ml (Bial Industrial Farmacéutica, Spain) and then, with

100 μL /well of streptavidin-conjugated peroxidase (0.25 $\mu\text{g}/\text{ml}$ in PBS-BSA-T). All the incubations were performed at 37°C for 1 hour, with 3 washes of 200 μL per well of PBS-B-T between successive steps. Finally, the enzyme activity was determined by adding 200 μL /well of o-phenylenediamine (Sigma-Fast™ tablet sets) and incubated for 30 min at room temperature in the dark. The standard curve was constructed from nine data points using a four parameter logistic curve fit and the concentration of crude extracts, assayed as dilution series, were interpolated from the linear portion of the standard curve and expressed in pg/ml . Subsequently, the data were converted to picograms per cubic meter according to the volume sampled by the apparatus.

Ole e 2, used as reference material, was purified from *Olea europaea* pollen extract by poly-L-proline (PLP)-Sepharose 4B (Pharmacia,Uppsala,Sweden).

In-vitro pollen hydration, protein quantification and Western blotting

For the in-vitro pollen hydration and protein release, the protocol described by Pasquini and coworkers (2011) was used, with minor modification. Briefly, pollen grains (100 mg) were hydrated in 1 mL hydration medium (1.6 mM boric acid, 27 μM calcium chloride in 12% sucrose) for 5 min at room temperature, with gentle shaking. The pollen suspensions were then centrifuged at 10000 $\times g$ for 10 min and the supernatants were recovered (5 min hydration). The pollen pellets were resuspended with 1 mL hydration medium, shaken for more 5 min and then centrifuged again to obtain the second supernatants (10 min hydration). This procedure was repeated twice again to obtain the supernatants after 25 and 50 min. The pellets were then resuspended sonicated to have a complete rupture of the pollen grains, centrifuged at 14000 $\times g$ for 10 min, and the supernatants were recovered (grain). The protein content in the supernatants was measured using the dye-binding method of Bradford, with bovine serum albumin as the standard. Pollen supernatants (20 μg total protein) were separated by denaturing sodium dodecyl sulphate–polyacrylamide gel electrophoresis (SDS-PAGE) thus proteins were electroblotted onto nitrocellulose membranes and incubated with mouse polyclonal profilin antibody for 2 h. After washing, the membranes were incubated with alkaline-phosphatase-conjugated anti-mouse IgG (1:10000; Sigma–Aldrich),

for 1 h at room temperature. Labelling was detected using the colorimetric substrate CTAB (Sigma–Aldrich). For quantification, membranes were scanned and band intensities were determined with the image analysis software ImageJ (<http://rsb.info.nih.gov/ij>).

Meteorological data

Weather data were supplied by the Spanish Meteorology Agency (AEMET) and IdroMeteoClima Service (ARPA Emilia-Romagna, Italia). Temperatures ($^{\circ}\text{C}$), rainfall (mm), relative humidity (%) and wind speed (m/s) were recorded continuously and aggregated for the aeroallergen sampling period and also for the periods immediately before and after the sampling period.

Statistical analysis

Spearman's Rank Correlation Coefficient was used for nonparametric data in order to analyze the correlations between meteorological parameters and pollen/allergens concentration. The level of significance was assessed between $P < 0.01$ and $P < 0.05$. SPSS statistical software, version 21.0 (SPSS Inc, Chicago, IL) was used for all statistical analyses.

Even if Principal Components Analysis (PCA) is a not factor analysis, some methodologists have argued that PCA is a reasonably suitable for analyses of common factors (Velicer and Jackson, 1990). In this case PCA was performed using the SPSS program to reduce data set to a lower dimension and reveal some hidden and simplified structure that often underlie it (Worden & Farrar, 2007). It was used a VARIMAX rotation that is a change of coordinates used in principal component analysis (PCA) that maximizes the sum of the variances of the squared loadings. Thus, all the coefficients (squared correlation with factors) will be either large or near zero, with few intermediate values. The goal is to associate each variable to at most one factor.

Differences between sample sets were determined by analysis of variance (one-way ANOVA, with a threshold P-value of 0.05) and Tukey's post-test, performed using GraphPad Prism.

In order to calculate the origin of certain episodes of high concentrations of allergens, the HYSPLIT Model developed by the National Oceanic and Atmospheric Administration (NOAA) was applied. This methodology allows obtaining hourly back trajectories in 3D (latitude, longitude and elevation) from meteorological data. Following this model (Rolph, 2016) the isentropic backtrajectories of air masses arriving in León at 12:00 UTC were calculated. The backward trajectories were calculated for different heights from the surface of the earth (250, 500 and 750 m). Besides, the modelling of the trajectories was designed in 24 and 48 h back in time.

Results

Concentration of pollen grains and its dependence on meteorological parameters

During the period of observation, several taxa were determined in the atmosphere of Bologna and León, but the most important in both cities were Corylaceae/Betula, Cupressaceae, Oleaceae, Pinaceae, Plantago, Poaceae, Populus, Quercus, Rumex and Urticaceae. In this period the sum of daily pollen concentration (pollen index: Σ pollen grains/m³) varied between 18478 in Bologna and 27013 in León.

Tree pollen was dominant in both cities atmosphere forming 69,1 and 78,4%, of the total amount of pollen collected over the period in Bologna and León respectively, while grasses formed 16,4 and 10,9 % and the allergenic herbaceous (Plantago, Rumex and Urticaceae) 14 and 10,1% in Bologna and León respectively. Several peaks in pollen concentration were recognized. Concerning Bologna, the first and highest occurred in March and was mainly caused by Cupressaceae pollen, while Oleaceae and Corylaceae pollen were present but in lower amount. While the pollination of these plants was decreasing they were joined by Quercus and Platanus, which caused a second peak during the second half of April. The period from the end of April to the first half of May was characterized by huge amounts of pollens belonging to Poaceae, Urticaceae, Oleaceae and Pinaceae.

There was a noticeable delay in Cupressaceae pollen concentrations between Bologna and León. In fact, while Cupressaceae pollens were abundant from the end of February until the end of March in Bologna, they were present in León only starting from the 20th of March. Similarly, also Quercus pollens showed one-month delay between Bologna (max peak 15th March) and León (max peak 11th May). Moreover, León was not characterized by the presence of airborne pollen belonging to Corylaceae, while Bologna was not characterized by the presence of airborne pollen belonging to Betulaceae.

The nonparametric Spearman's rank correlation provided coefficients for total pollen concentrations in the atmosphere of Bologna and León as opposed to pollens belonging to the identified taxa and several meteorological parameters, in particular temperature, rainfall, relative humidity, wind. All the identified taxa, except of Pinaceae and Rumex for Bologna and Populus for León, significantly contributed to the total concentration of airborne pollen (Table 1). The four meteorological variables analyzed significantly affected the occurrence of pollen grains in the atmosphere in a different way in the two examined cities. In fact, the correlation coefficients showed significant correlations between total airborne pollen and temperatures (T max and T med) for the city of León, while these meteorological variables did not significantly affect pollen dispersion in Bologna, where only the T min affected pollen dispersion with a negative correlation. In both cities, relative humidity negatively affected the amount of airborne pollen; likewise precipitations did only in the city of Bologna (Table 1). Wind seemed to not correlate significantly with the occurrence of pollen grains in both cities, while there was a negative correlation with the minimum temperature. In general, higher relative humidity and more rain corresponded with a lower concentration of pollen grains in the atmosphere.

Table 1. correlation coefficients (rs) between airborne pollen grains, Ole e 2 panallergen and meteorological parameters calculated with the nonparametric Spearman's test				
	BOLOGNA		LÉON	
	Total pollen	Ole e 2	Total pollen	Ole e 2
Total pollen	1,000	,357**	1,000	,590**
Ole e 2	,357**	1,000	,590**	1,000
T max (°C)	-,132	,025	,436**	,413**
T min (°C)	-,270**	-,070	,155	,178
T med (°C)	-,177	,003	,384**	,388**
P (mm)	-,397**	-,120	-,148	-,154
HR (%)	-,265**	-,188*	-,389**	-,322**
Vel. V (m/s)	,044	,161	,009	-,021
<i>Quercus</i>	,599**	,440**	,546**	,592**
<i>Oleaceae</i>	,682**	,171	,211*	,106
<i>Cupressaceae</i>	,736**	,144	,228*	-,047
<i>Platanaceae</i>	,352**	,282**	,529**	,162
<i>Pinaceae</i>	,096	-,075	,704**	,600**
<i>Populus</i>	,515**	,200*	,019	-,240**
<i>Poaceae</i>	,292**	,131	,412**	,529**
<i>Urticaceae</i>	,254**	,160	,297**	,349**
<i>Plantaginaceae</i>	-,291**	-,170	,451**	,597**
<i>Rumex</i>	,140	,048	,473**	,616**
<i>Corylaceae</i>	,788**	,323**	-	-
<i>Betulaceae</i>	-	-	,255**	-,130

Atmospheric profilin concentration and its dependence on the amount of airborne pollen and meteorological parameters

The panallergen profilin was identified by quantitative ELISA in extracts of filters from a high-volume sampler. The sum of daily profilin concentration (allergenic index: Σ pg Ole e 2/m³) varied between 2776.41 in Bologna and 10400.39 in León. When ELISA data were compared with the corresponding pollen concentration, there was a direct correlation between the amount of profilin and the daily incidence of pollen and the Spearman's rank correlation, provided correlation coefficient (rs) of 0.357, $p < 0.0001$ for Bologna and $r_s = 0.590$, $p < 0.0001$ for León for total profilin concentrations as opposed to the pollen concentration.

The rates pollen/allergen between the two sampled sites varied with 3 times higher for Bologna but the allergenic potency is highest in León city (0.38 vs 0.15). There were however some misaligned peaks of profilin and total pollen, e.g., the profilin peaks in Bologna during the 27th-28th March, 15th -16th April, 28th April and 9th June did not correlate with high pollen concentrations. The same scenario was seen for León, where none of the profilin peaks occurred during the days with highest pollen concentration (Fig. 1A-B). The concentration of pollens that mostly correlated with the concentration of profilin (Table 1) was thus plotted and compared to profilin peaks and what was notable was a more underlined misalignment between single taxa pollen and profilin concentration, both in Bologna (Fig. 1C) and in León (Fig. 1D). Only the concentration of Rumex pollen in León showed high alignment with profilin peaks, however, as the contribution of Rumex pollen to the total amount of airborne pollen was lower than the contribution of other taxa (e.g. Quercus, Pinaceae e Plantaginaceae), this could not totally explain the peaks of profilin.

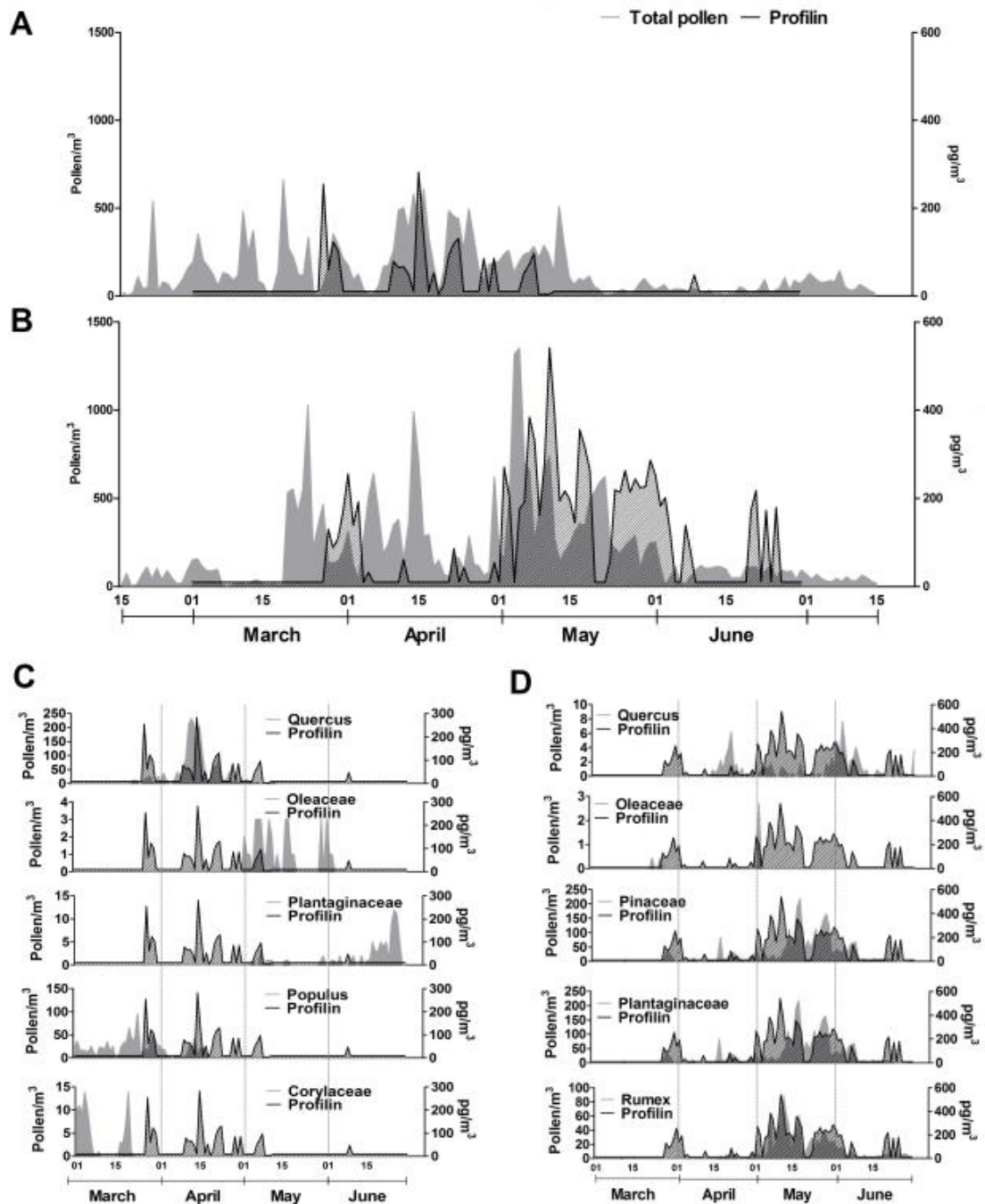


FIGURE 1. Comparison between daily fluctuations in total airborne pollen concentration (pollen/m³) and airborne profilin (pg/m³) in Bologna **(A)** and León **(B)** from March to June 2015. Pollen concentration of different taxa (pollen/m³) and profilin concentration (pg/m³) during the studied period in Bologna **(C)** and León **(D)**.

What was worth of notice was the highest peak of profilin occurring during the 11th-12th May in León, days that were not characterized by the presence of Oleaceae pollen (0 pollen/m³) nor by the highest total pollen peaks (742.05

pollen/m³ 11th and 276.30 pollen/m³ 12th May). Variations in weather conditions or long distance transport processes could explain the discordance between the daily pollen and profilin concentrations. Back trajectory analysis showed that the most important contributions of Ole e 2 in atmosphere of Léon were coincident with air masses passing through important olive groves areas located in the South of Spain the 11th May (Fig. 2 A-B) and North-eastern of Portugal the 12th May (Fig. 2 C-D).

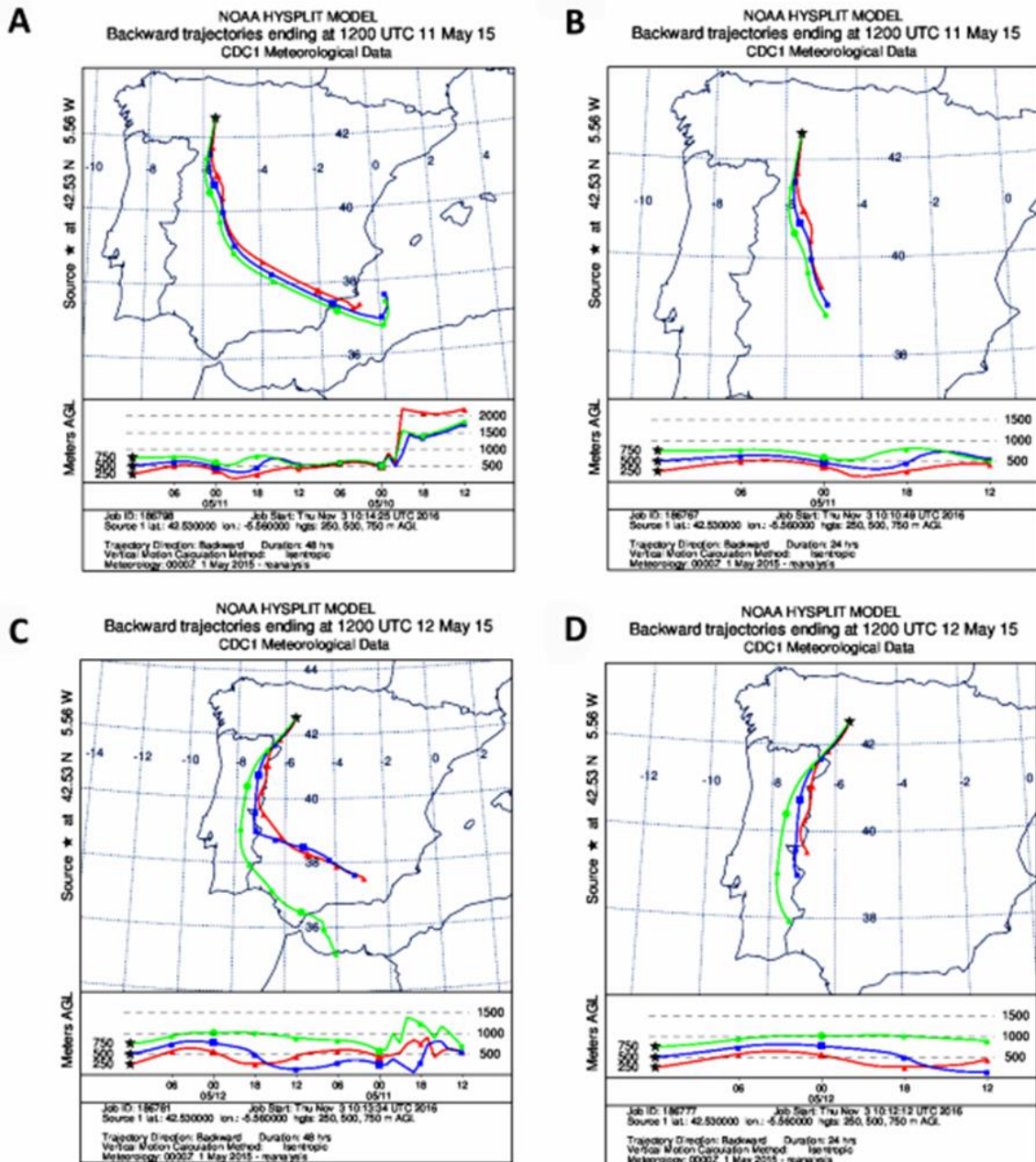


FIGURE 2. Maps showing 48-h and 24-h HYSPLIT backward trajectories at a final height of 250, 500 and 750 m agl in León during the 11th and 12th May. 48-h 11th May 2015 **(A)**, 24-h 11th May 2015 **(B)**, 48-h 12th May 2015 **(C)**, 24-h 12th May 2015 **(D)**.

A principal components (PC) analysis was performed as a classificatory method of the more influencing variables on profilin presence in the atmosphere, in order to investigate the influence of meteorological factors on the concentration of airborne profilin (Table 2). The purpose of the analysis was to obtain a small number of linear combinations of the different variables which account for most of the variability in the data. In the case of meteorological factors in Bologna, three main components explaining 94.1% of variance have been extracted, highlighting Component 1 (temperatures) and Component 2 (relative humidity and rainfall) and Component 3 (wind speed). For the city of León two main components for meteorological factors have been extracted, explaining 76.9% and corresponding to temperature (Component 1) and relative humidity, precipitation and wind speed (Component 2).

In relation to various pollen types (Table 3, ordered according pollen seasonal appearance), four are the PCs extracted explaining 75% of variance in Bologna. Four PCs among the highest correlations corresponded to the components 1 and 2, with the pollen types *Corylus*, *Quercus*, *Platanus*, *Oleaceae*, *Pinaceae* and *Rumex*. In León, in relation to pollen types tree main components have been extracted explaining 69.7% of the variance, Component 1 being due to the pollen types with the highest percentage correlation: *Oleaceae*, *Pinaceae*, *Quercus*, *Plantago*, *Poaceae* and *Rumex*.

Tab. 2. PC analysis of meteorological factors affecting airborne profilin concentration					
Component	BOLOGNA			LEÓN	
	1	2	3	1	2
Eigenvalue	3.128	1.491	1.028	2.627	1.987
Percent of variance %	52.137	24.849	17.131	43.778	33.778
Cumulative percentage %	52.137	76.985	94.116	43.115	76.893
Maximum temperature	.953	-.259	.029	.821	-.517
Minimum temperature	.982	.047	.012	.918	.228
Average temperature	.985	-.156	.034	.971	-.220
Rainfall	-.080	.924	.149	.214	.740
Relative humidity	-.173	.829	-.384	-.318	.814
Wind speed	.016	-.052	.979	-.141	.640

Table 3. PC analysis of pollen types affecting airborne profilin concentration								
BOLOGNA					LEÓN			
Component	1	2	3	4	Component	1	2	3
Eigenvalue	2.730	2.054	1.828	1.655	Eigenvalue	4.044	1.901	1.728
Percent of variance %	24.814	18.669	16.622	15.049	Percent of variance %	36.761	17.281	15.709
Cumulative percentage %	24.814	43.483	60.105	75.155	Cumulative percentage %	36.761	54.043	69.752
<i>Corylaceae</i>	.900	-.029	.091	.031	<i>Betulaceae</i>	-.132	.188	-.694
<i>Quercus</i>	.914	.011	.048	.088	<i>Cupressac</i>	-.094	.814	-.049
<i>Oleaceae</i>	-.028	.886	.208	.156	<i>Oleaceae</i>	.601	.589	-.143
<i>Cupressac eae</i>	-.081	.061	.735	-.285	<i>Pinus</i>	.603	-.167	.216
<i>Platanacea e</i>	.967	-.035	.014	-.067	<i>Platanus</i>	-.033	-.276	-.687
<i>Pinaceae</i>	-.099	.847	-.039	.121	<i>Populus</i>	-.158	.823	-.056
<i>Populus</i>	.301	-.008	.716	-.331	<i>Quercus</i>	.973	.017	.020
<i>Poaceae</i>	-.021	.403	-.169	.741	<i>Plantago</i>	.919	-.089	.156
<i>Urticaceae</i>	.053	.020	-.040	.867	<i>Poaceae</i>	.741	-.092	.472
<i>Plantago</i>	-.104	.025	-.663	-.331	<i>Rumex</i>	.944	-.062	.101
<i>Rumex</i>	.167	.618	-.501	-.042	<i>Urticaceae</i>	.188	-.232	.666

Protein release by hydrated pollen grains

We further investigate the relationship between profilin release from the pollen grain and relative humidity; we investigated the effects of in-vitro hydration and protein release. Pollen of *Parietaria judaica*, *Betula pendula*, *Olea europaea*, *Phleum pratense*, *Ambrosia artemisiifolia*, *Corylus avellana*, *Populus deltoides* and *Citrus clementine* was used for this purpose because of their allergenic potential. Moreover there are common allergenic pollens in either one or both cities of study during their flowering seasons.

In general, there was a large release of soluble proteins within the first 10 min of pollen hydration in all pollen analyzed, excepted for *Betula* and *Ambrosia*. While *Betula* did not show a massive release of proteins in the germination medium within the analyzed time, *Ambrosia* pollen showed a time dependent protein release during the first 25 min of hydration. In general, the most of the proteins

were however present in the pollen grains even after hydration and *Populus* and *Citrus* pollen were the only two exceptions (Fig. 2).

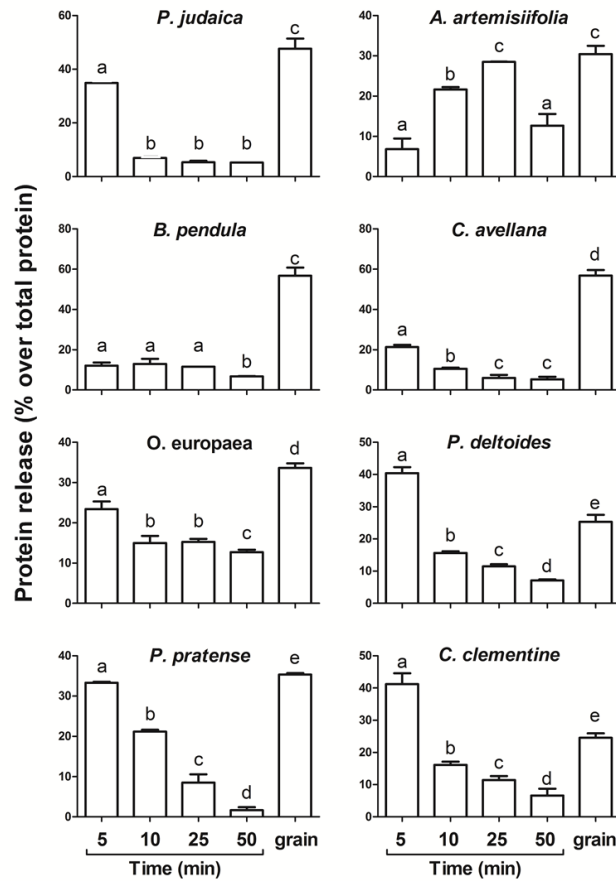


FIGURE 3. Protein release during *in-vitro* pollen hydration. Short times (5 and 10 min) and long times (25-50) were analyzed and compared to the total protein present in the pollen grains after 50 min hydration (“grain”). Protein release is expressed as percentage over total protein. Each data point represents the mean of two independent experiments undertaken in triplicate. The data were analyzed by one-way ANOVA and Tukey’s post-test. Bars marked with the same letter are not significantly different.

The crude protein released during hydration of the different pollen studied was analyzed by immunoblotting and probed with a polyclonal antibody against profilin (Fig. 3). The panallergen was detectable in all pollens with the polyclonal antibody and it showed a small molecular weight band (12 to 15 kDa) only, indicating a very high specificity of the antibody against the protein of interest. There were several quantitative differences among the different pollen grains tested. Moreover, the release of profilin not always mirrored the release of total protein showed in Fig. 2. In particular, only the release of profilin in *Parietaria*, *Ambrosia*, *Populus* and *Olea* mirrored the release of total proteins from these

grains. *Betula*, *Corylus*, *Phleum* and *Citrus* showed instead a time-dependent release of profilin during hydration. Altogether, these data indicate that hydration causes a significant released of protein from pollen grains, and that also cytoplasmic protein, as the panallergen profilin, can be released.

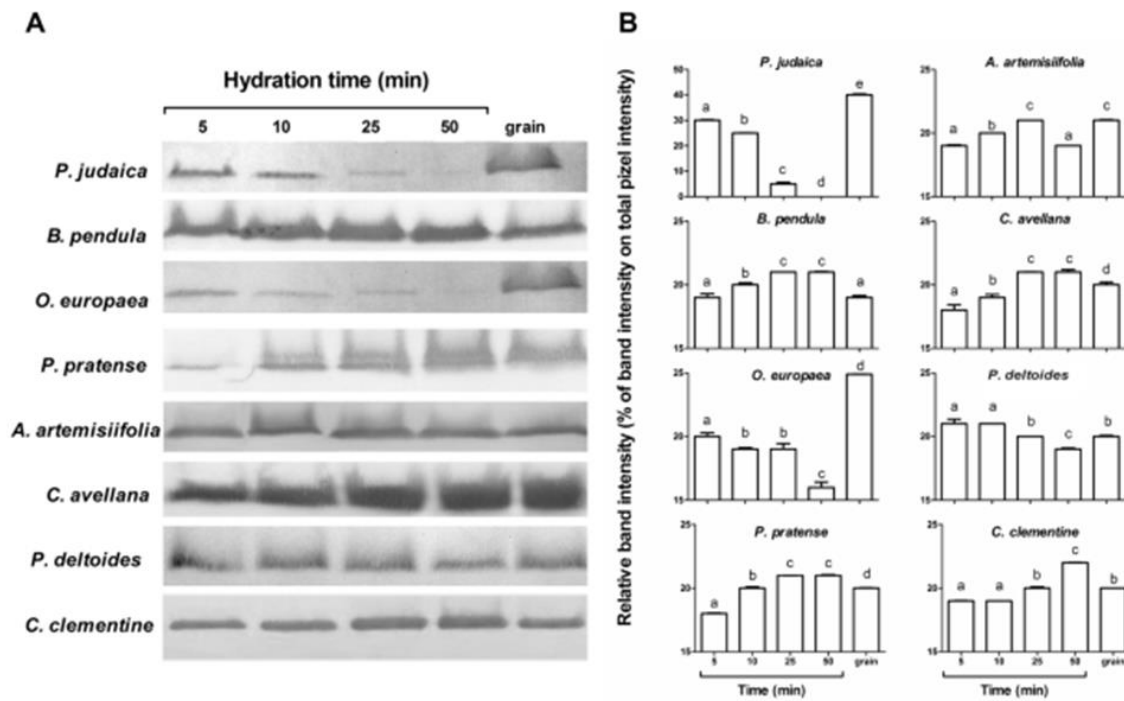


Figure 4. Profilin release during *in-vitro* pollen hydration. Short times (5 and 10 min) and long times (25-50) were analyzed and compared to the total protein present in the pollen grains after 50 min hydration (“grain”). Western blots (A) and band quantification (B) are shown. Each data point represents the mean of two independent experiments undertaken in triplicate. The data were analyzed by one-way ANOVA and Tukey’s post-test. Bars marked with the same letter are not significantly different.

Discussion

Total pollen and the pollen panallergen profilin were sampled during the spring season in León (Spain) and Bologna (Italy), in order to evaluate their concentrations in the air and correlate their abundance with meteorological factors. A Hirst-volumetric trap, considered a standard method since more than 30 years, was used to sample the atmosphere in both cities during the high-pollen season, from March to June. Results revealed differences in the occurrence of pollen and of profilin, depending on the different pollination seasons. In particular,

tree pollens displayed the major seasonal differences in the two cities, with the maximum concentrations of Cupressaceae and Quercus pollens being delayed in León by 15 and 30 days respectively, relative to Bologna presumably due to delayed pollen seasons in the former as compared with the latter city. The duration of certain seasons (e.g. Oleaceae) and the dates of some pollen peaks (e.g. Pinaceae) were, instead, comparable between León and Bologna. Different from trees, grass and other herbaceous pollens exhibited similar behaviors, both in terms of pollen season duration and maximum concentrations.

Temperature and RH strongly correlated with the concentration of airborne pollen; in general, the highest R and the lowest temperatures corresponded to the lowest concentration of pollen grains. This is in agreement with the notion that means temperature and photoperiod significantly affect pollen amounts (Kizilpinar et al., 2011). Moreover, meteorological factors, such as temperature, affect flowering time, thus also the release of pollen (Kizilpinar et al., 2011; Thuzar et al., 2010). In our study, we showed a positive correlation between daily temperature and total concentration of pollen from tree, grass and other herbaceous species, confirming data from earlier studies (Alwadie, 2008; Gioulekas et al., 2004; Riberio et al., 2003; Rodríguez-Rajo et al., 2005).

We also observed a negative correlation between R and daily tree, grass, and herbaceous pollen concentration. This negative correlation has been reported in a number of studies and is known as the “rain washing” phenomenon (Kizilpinar et al., 2011; Rodríguez-Rajo et al., 2005; Sahney and Chaurasia, 2008). Wind is another key factor as it causes the release of pollen grains from plants. It also causes pollen dispersal in the atmosphere and may carry pollen far from the site of origin, giving rise to long-range transport of entire pollen grains, as well as pollen particles and even allergens (Galan et al., 2013; Hernández-Ceballos et al., 2011; Moreno-Grau et al., 2016; Sikoparija et al., 2013). Present results do not point to a significant correlation between WS and total airborne pollen counts, but high concentrations of profilin detected on May 11th and 12th in the city of León corresponded largely to Oleaceae and Quercus pollen. The HYSPLIT models obtained in our study suggest that air masses coming from extensive olive groves located elsewhere (southern Spain and Portugal) caused the major peaks of olive pollen and, consequently, profilin (Ole e 2) in the atmosphere, since in León no

olive trees nor other taxa of the Oleaceae family were in bloom at this time. Taken together, our data show that meteorological parameters significantly affect the occurrence and the distribution of airborne pollen grains belonging to several taxa. There was a high correlation between airborne pollen concentrations and the presence of the panallergen profilin, as already shown for several other allergenic proteins (Moreno-Grau et al., 2006). However, our results also show that the pollen calendar and the association with meteorological factors should be taken into account when monitoring the real allergenic risk. In fact, temperature, R and RH were shown to deeply affect not only the concentration of pollen, but also the amount of airborne profilin. In general, as for pollen, a higher RH, low T min, and high R corresponded to a lower concentration of profilin in the atmosphere.

Studies conducted with red oak (Fernandez-Caldas et al., 1989), birch (Rantio-Lehtimäki et al., 1994), *Cryptomeria* (Takahashi et al., 2001), *Plantago* (González-Parrado et al., 2015), plane tree, and grass pollens (Fernández-González et al., 2011; González-Parrado et al., 2015) have shown low or medium correlations between airborne allergen and pollen concentrations. Other reports highlighted the fact that atmospheric plane tree and olive pollen concentrations are not representative of the exposure to their main allergens, Pla a 1, and Ole e 1 (Fernández-González et al., 2010; Galan et al., 2013; Vara et al., 2016a; Vara et al., 2016b). Similarly, our study showed that peaks in profilin concentration did not always overlap with total pollen peaks.

It is well known during in-vitro germination of pollen a huge number of proteins mainly involved in carbohydrate and energy metabolism, transport and wall remodeling are overexpressed and released into the germination medium (Sheoran et al., 2009). This is consistent with evidences about the amounts of proteins that are rapidly released when pollen grains come into contact with fluids (Grote et al., 2003; Grote et al., 1993) and is coherent with their role in the cross-talk between pollen and pistil (Vega-Maray et al., 2006). These findings are in agreement with data reported in our study, in which we demonstrated a sudden and consistent protein release upon in-vitro pollen rehydration. Amongst the released proteins, it was reported that allergens of *Cryptomeria japonica* (Miki-Hirosige et al., 1994), Poaceae (Márquez et al., 1997a; Márquez et al., 1997b; Taylor et al., 1994), *Lolium perenne* (Grote et al., 2000), *Zygophyllum fabago*

(Castells et al., 2002), *Cupressus arizonica* and *C. sempervirens* (Suárez-Cervera et al., 2003) were also released into the external medium.

In our system, the release of a large amount of pollen proteins was a common feature, but the timing was species-specific, probably due to the different pollen wall architecture, i.e. exine and intine structures. A European study on the release of allergens (The HIALINE Project) showed that grass pollen released 2.0 to 2.5 pg per pollen grain of group 5 allergens, the major grass pollen allergens. However, plant species, phenology, pollen concentration in air, and climatic conditions deeply altered this value (Buters et al., 2012).

Present results confirm that profilin, a cytoplasmic protein was also released upon pollen rehydration. As profilins are involved in the modulation of the actin cytoskeleton in germinating pollen (Kandasamy et al., 2007), it is unclear why profilin should be detected outside the pollen grain upon pollen hydration, unless one assumes a function in the pollen-stigma interaction. The timing of this release could explain the misalignment of airborne pollen and airborne profilin peaks. The different time required to extrude the protein into the external medium may depend upon its subcellular localization. In fact, in rehydrated birch pollen grains, the localization of profilin was different from that observed in the dry grain already a few minutes after rehydration; in the latter, aggregates of these cytoplasmic proteins were found both inside and outside the grain (Grote et al., 1993). The timing of allergen release is an important parameter as it correlates with allergenicity. In fact, in birch pollen, glutathione-S-transferase (GST), an abundant allergen, is considered a minor allergen because its release is limited when compared to other allergens (e.g., Bet v 1), showing that allergenicity might also depend on the release kinetics of proteins from the pollen grains (Deifl et al., 2014).

Finally, profilin and other allergenic proteins could derive not only from entire pollen grains, but also from smaller particles, which are dispersed even faster (Moreno-Grau et al., 2016). To complete this scenario, high humidity was found to favor allergen release detected in smaller particles that might penetrate deeper into respiratory tracts (Buters et al., 2015).

Conclusions

In conclusion, our findings point to the need to consider molecular aerobiology in addition to pollen counts in order to monitor the health risk associated with exposure to airborne allergens (Buters et al., 2015). A more relevant parameter may be the actual concentration of airborne allergenic particles rather than pollen grains. For this purpose, a device for monitoring such particles is highly recommended. Moreover, several parameters should be considered when attempting to explain the misalignments between pollen and allergen concentrations (Rodríguez-Rajo et al., 2011), such as variations in weather conditions and long-distance transport (Moreno-Grau et al., 2016). Finally, it may be useful to complement the forecasting of allergenic pollen proteins in the atmosphere with in-vitro studies on the percentage of hydration that each pollen type needs for its metabolic activation.

References

- Alwadie HM. Pollen concentration in the atmosphere of Abha City, Saudi Arabia and its relationship with meteorological parameters. *J Appl Sci* 2008; 8: 842–847. doi:10.3923/jas.2008.842.847
- Bousquet PJ, Chinn S, Janson C, Kogevinas M, Burney P, Jarvis D. Geographical variation in the prevalence of positive skin tests to environmental aeroallergens in the European Community Respiratory Health Survey I. *Allergy* 2007; 62: 301-9. doi:10.1111/j.1398-9995.2006.01293.x
- Brito FF, Gimeno PM, Carnes J, Martin R, Fernandez-Caldas E, Lara P, et al. *Olea europaea* pollen counts and aeroallergen levels predict clinical symptoms in patients allergic to olive pollen. *Ann Allergy Asthma Immunol* 2011; 106: 146-52. doi:10.1016/j.anai.2010.11.003
- Buters J, Prank M, Sofiev M, Pusch G, Albertini R, Annesi-Maesano I, et al. Variation of the group 5 grass pollen allergen content of airborne pollen in relation to geographic location and time in season. *J Allergy Clin Immunol* 2015; 136: 87-95 e6. doi:10.1016/j.jaci.2015.01.049
- Buters JTM, M. T, M. S, R. K, A. R-L, R. A, et al. Release of Bet v 1 from birch pollen from 5 European countries. Results from the HIALINE Study. *Atmos Environ* 2012; 55: 496–505. doi:10.1016/j.atmosenv.2012.01.054

- Castells T, Arcalis E, Moreno-Grau S, Bayo J, Elvira-Rendueles B, Belchi J, et al. Immunocytochemical localization of allergenic proteins from mature to activated *Zygophyllum fabago* L. (Zygophyllaceae) pollen grains. *Eur J Cell Biol* 2002; 81: 107-15. doi:10.1078/0171-9335-00223
- Castro A, Alonso-Blanco E, González-Colino M, Calvo AI, Fernández-Raga M, Fraile R. Aerosol size distribution in precipitation events in León, Spain. *Atmos. Res.* 2010; 96: 421-435. doi:10.1016/j.atmosres.2010.01.014
- D'Amato G, Cecchi L. Effects of climate change on environmental factors in respiratory allergic diseases. *Clin Exp Allergy* 2008; 38: 1264-74. doi:10.1111/j.1365-2222.2008.03033.x
- D'Amato G, Cecchi L, Bonini S, Nunes C, Annesi-Maesano I, Behrendt H, et al. Allergenic pollen and pollen allergy in Europe. *Allergy* 2007; 62: 976-90. doi:10.1111/j.1398-9995.2007.01393.x
- D'Amato G, Spieksma FT, Liccardi G, Jager S, Russo M, Kontou-Fili K, et al. Pollen-related allergy in Europe. *Allergy* 1998; 53: 567-78. doi:10.1111/j.1398-9995.1998.tb03932.x
- de Dios Alche J, M'Rani-Alaoui M, Castro AJ, Rodriguez-Garcia MI. Ole e 1, the major allergen from olive (*Olea europaea* L.) pollen, increases its expression and is released to the culture medium during in vitro germination. *Plant Cell Physiol* 2004; 45: 1149-57. doi:10.1093/pcp/pch127
- De Linares C, Diaz de la Guardia C, Nieto Lugilde D, Alba F. Airborne study of grass allergen (Lol p 1) in different-sized particles. *Int Arch Allergy Immunol* 2010; 152: 49-57. doi:10.1159/000260083
- Deifl S, Zwicker C, Vejvar E, Kitzmuller C, Gadermaier G, Nagl B, et al. Glutathione-S-transferase: a minor allergen in birch pollen due to limited release from hydrated pollen. *PLoS One* 2014; 9: e109075. doi:10.1371/journal.pone.0109075
- Eder W, Ege MJ, von Mutius E. The asthma epidemic. *N Engl J Med* 2006; 355: 2226-35. doi:10.1056/NEJMra054308
- Fernandez-Caldas E, Swanson MC, Pavda J, Welsh P, Yunginger W, Redd CE. Immunochemical demonstration of Red Oak pollen aeroallergens outside the pollen season. *Grana* 1989; 28: 205-209. doi:10.1080/00173138909427432
- Fernández-González D, González-Parrado Z, Vega-Maray AM, Valencia-Barrera RM, Camazón-Izquierdo B, De Nuntiis P, et al. Platanus pollen allergen, Pla a 1: quantification in the atmosphere and influence on a sensitizing population. *Clin Exp Allergy* 2010; 40: 1701-8. doi:10.1111/j.1365-2222.2010.03595.x
- Fernández-González D, Rodríguez Rajo JF, González Parrado Z, Valencia Barrera RM, Jato V, Grau Moreno S. Differences in atmospheric emissions of Poaceae pollen and Lol p 1 allergen. *Aerobiologia* 2011; 27: 301-309. doi:10.1007/s10453-011-9199-x
- Galan C, Antunes C, Brandao R, Torres C, Garcia-Mozo H, Caeiro E, et al. Airborne olive pollen counts are not representative of exposure to the major olive allergen Ole e 1. *Allergy* 2013; 68: 809-12. doi:10.1111/all.12144

- Gilles S, Fekete A, Zhang X, Beck I, Blume C, Ring J, et al. Pollen metabolome analysis reveals adenosine as a major regulator of dendritic cell-primed T(H) cell responses. *J Allergy Clin Immunol* 2011; 127: 454-461 e1-9. doi:10.1016/j.jaci.2010.12.1082
- Gilles S, Mariani V, Bryce M, Mueller MJ, Ring J, Behrendt H, et al. Pollen allergens do not come alone: pollen associated lipid mediators (PALMS) shift the human immune systems towards a T(H)2-dominated response. *Allergy Asthma Clin Immunol* 2009; 5: 3. doi:10.1186/1710-1492-5-3
- Gioulekas D, Balafoutis C, Damialis A, Papakosta D, Gioulekas G, Patakas D. Fifteen years' record of airborne allergenic pollen and meteorological parameters in Thessaloniki, Greece. *Int J Biometeorol* 2004; 48: 128-36. doi:10.1007/s00484-003-0190-2
- González-Parrado Z, Fernández-González D, Vega-Maray A, Valencia-Barrera R. Relationship between flowering phenology, pollen production and atmospheric pollen concentration of *Plantago lanceolata* (L.). *Aerobiologia* 2015; 31: 481-498. doi:10.1007/s10453-015-9377-3
- Grote M, Valenta R, Reichelt R. Abortive pollen germination: a mechanism of allergen release in birch, alder, and hazel revealed by immunogold electron microscopy. *J Allergy Clin Immunol* 2003; 111: 1017-23. doi:10.1067/mai.2003.1452
- Grote M, Vrtala S, Niederberger V, Valenta R, Reichelt R. Expulsion of allergen-containing materials from hydrated rye grass (*Lolium perenne*) pollen revealed by using immunogold field emission scanning and transmission electron microscopy. *J Allergy Clin Immunol* 2000; 105: 1140-5. doi:10.1067/mai.2000.107044
- Grote M, Vrtala S, Niederberger V, Wiermann R, Valenta R, Reichelt R. Release of allergen-bearing cytoplasm from hydrated pollen: a mechanism common to a variety of grass (Poaceae) species revealed by electron microscopy. *J Allergy Clin Immunol* 2001; 108: 109-15. doi:10.1067/mai.2001.116431
- Grote M, Vrtala S, Valenta R. Monitoring of two allergens, Bet v I and profilin, in dry and rehydrated birch pollen by immunogold electron microscopy and immunoblotting. *J Histochem Cytochem* 1993; 41: 745-50
- Hauser M, Roulias A, Ferreira F, Egger M. Panallergens and their impact on the allergic patient. *Allergy Asthma Clin Immunol* 2010; 6: 1. doi:10.1186/1710-1492-6-1
- Henricks PA, Nijkamp FP. Reactive oxygen species as mediators in asthma. *Pulm Pharmacol Ther* 2001; 14: 409-20. doi:10.1006/pupt.2001.0319
- Hernández-Ceballos MA, García-Mozo H, Adame JA, Domínguez-Vilches E, De la Morena BA, Bolívar JP, et al. Determination of potential sources of Quercus airborne pollen in Córdoba city (southern Spain) using back-trajectory analysis. *Aerobiologia* 2011; 27: 261-276. doi: 10.1007/s10453-011-9195-1
- Kandasamy MK, Burgos-Rivera B, McKinney EC, Ruzicka DR, Meagher RB. Class-specific interaction of profilin and ADF isoforms with actin in the regulation of plant development. *Plant Cell* 2007; 19: 3111-26. doi:10.1105/tpc.107.052621

- Kizilpınar I, Civelek E, Tuncer A, Dogan C, Karabulut E, Sahiner UM, et al. Pollen counts and their relationship to meteorological factors in Ankara, Turkey during 2005–2008. *Int J Biometeorol* 2011; 55: 623–631. doi:10.1007/s00484-010-0363-8
- Ledesma A, Rodriguez R, Villalba M. Olive-pollen profilin. Molecular and immunologic properties. *Allergy* 1998; 53: 520-6. doi:10.1111/j.1398-9995.1998.tb04090.x
- Márquez J, Seoane-Camba JA, Suárez-Cervera M. Allergenic and antigenic proteins released in the apertural sporoderm during the activation process in grass pollen grains. *Sex Plant Reprod* 1997a; 10: 269–278. doi:10.1007/s004970050097
- Márquez J, Seoane-Camba JA, Suárez-Cervera M. The role of the intine and cytoplasm in the activation and germination processes of Poaceae pollen grains. *Grana* 1997b; 36: 328–342. doi:10.1080/00173139709362626
- Martinez A, Asturias JA, Monteseirin J, Moreno V, Garcia-Cubillana A, Hernandez M, et al. The allergenic relevance of profilin (Ole e 2) from *Olea europaea* pollen. *Allergy* 2002; 57 Suppl 71: 17-23. doi:10.1034/j.1398-9995.2002.057s71017.x
- Miki-Hirosige H, Nakamura S, Yasueda H, Shida T, Takahashi Y. Immunocytochemical localization of the allergenic proteins in the pollen of *Cryptomeria japonica*. *Sex Plant Reprod* 1994; 7: 95–100. doi:10.1007/BF00230577
- Morales S, Jimenez-Lopez JC, Castro AJ, Rodriguez-Garcia MI, Alche JD. Olive pollen profilin (Ole e 2 allergen) co-localizes with highly active areas of the actin cytoskeleton and is released to the culture medium during in vitro pollen germination. *J Microsc* 2008; 231: 332-41. doi:10.1111/j.1365-2818.2008.02044.x
- Moreno-Grau S, Aira MJ, Elvira-Rendueles B, Fernández-González M, Fernández-González D, García-Sánchez A, et al. Assessment of the *Olea* pollen and its major allergen Ole e 1 concentrations in the bioaerosol of two biogeographical areas. *Atmos. Environ.* 2016; 145: 264-271. doi:10.1016/j.atmosenv.2016.09.040
- Moreno-Grau S, Elvira-Rendueles B, Moreno J, Garcia-Sanchez A, Vergara N, Asturias JA, et al. Correlation between *Olea europaea* and *Parietaria judaica* pollen counts and quantification of their major allergens Ole e 1 and Par j 1-Par j 2. *Ann Allergy Asthma Immunol* 2006; 96: 858-64. doi:10.1016/S1081-1206(10)61350-6
- Pasqualini S, Tedeschini E, Frenguelli G, Wopfner N, Ferreira F, D'Amato G, et al. Ozone affects pollen viability and NAD(P)H oxidase release from *Ambrosia artemisiifolia* pollen. *Environ Pollut* 2011; 159: 2823-30. doi:10.1016/j.envpol.2011.05.003
- Plötz SG, Traidl-Hoffmann C, Feussner I, Kasche A, Feser A, Ring J, et al. Chemotaxis and activation of human peripheral blood eosinophils induced by pollen-associated lipid mediators. *J Allergy Clin Immunol* 2004; 113: 1152-60. doi:10.1016/j.jaci.2004.03.011
- Rantio-Lehtimäki A, Viander M, Koivikko A. Airborne birch pollen antigens in different particle sizes. *Clin Exp Allergy* 1994; 24: 23-8
- Riberio H, Cunha M, Abreu I. Airborne pollen concentration in the region of Braga, Portugal, and its relationship with meteorological parameters. *Aerobiologia* 2003; 19: 21–27. doi:10.1023/A:1022620431167

- Rodríguez-Rajo FJ, Jato V, González-Parrado Z, Elvira-Rendueles B, Moreno-Grau S, Vega-Maray A, et al. The combination of airborne pollen and allergen quantification to reliably assess the real pollinosis risk in different bioclimatic areas. *Aerobiologia* 2011; 27: 1-12. doi:10.1007/s10453-010-9170-2
- Rodríguez-Rajo FJ, Méndez J, Jato V. Airborne Ericaceae pollen grains in the atmosphere of Vigo (Northwest Spain) and its relationship with meteorological factors. *J Integr Plant Biol* 2005; 47: 792–800. doi:10.1111/j.1744-7909.2005.00092.x
- Rolph GD. Real-time Environmental Applications and Display System (READY). Website NOAA Air Resources Laboratory, College Park, MD. <http://www.ready.noaa.gov> 2016.
- Ruiz-García M, Garcia del Potre M, Fernández Nieto M, Barber D, Jimeno-Nogales L, Sastre J. Profilin: a relevant aeroallergen. *J Allergy Clin Immunol* 2011; 128: 416-418. doi:10.1016/j.jaci.2011.06.011
- Sahney M, Chaurasia S. Seasonal variations of airborne pollen in Allahabad, India. *Ann Agric Environ Med* 2008; 15: 287-93
- Santos A, Van Ree R. Profilins: mimickers of allergy or relevant allergens? *Int Arch Allergy Immunol* 2011; 155: 191-204. doi:10.1159/000321178
- Sheoran IS, Pedersen EJ, Ross AR, Sawhney VK. Dynamics of protein expression during pollen germination in canola (*Brassica napus*). *Planta* 2009; 230: 779-93. doi:10.1007/s00425-009-0983-6
- Sikoparija B, Skjøth CA, Alm Kübler K, Dahl A, Sommer J, Grewling L, et al. A mechanism for long distance transport of *Ambrosia* pollen from the Pannonian Plain. *Agric. For. Meteorol.* 2013; 180: 112-117. doi:10.1016/j.agrformet.2013.05.014
- Staiger CJ, Blanchoin L. Actin dynamics: old friends with new stories. *Curr Opin Plant Biol* 2006; 9: 554-62. doi:10.1016/j.pbi.2006.09.013
- Suárez-Cervera M, Takahashi Y, Vega-Maray AM, Seoane-Camba JA. Immunocytochemical localization of Cry j 1, the major allergen of *Cryptomeria japonica* (Taxodiaceae) in *Cupressus arizonica* and *Cupressus sempervirens* (Cupressaceae) pollen grains. *Sex Plant Reprod* 2003; 16: 9–15. doi: 10.1007/s00497-003-0164-x
- Takahashi Y, Ohashi T, Nagoya T, Sakaguchi M, Yasueda H, Nitta H. Possibility of real-time measurement of an airborne *Cryptomeria japonica* pollen allergen based on the principle of surface plasmon resonance. *Aerobiologia* 2001; 17: 313-318. doi:10.1023/A:1013002001583
- Taylor PE, Staff IA, Singh MB, Knox RB. Localization of the two major allergens in rye-grass pollen using specific monoclonal antibodies and quantitative analysis of immunogold labelling. *Histochem J* 1994; 26: 392-401. doi:10.1007/BF00160051
- Thuzar M, Puteh AB, Abdullah NAP, Lassim Mohd. MB, Jusoff K. The effects of temperature stress on the quality and yield of soya bean [*Glycine max* L.] Merrill.]. *J Agric Sci* 2010; 2: 172–179. doi:10.5539/jas.v2n1p172

- Valenta R, Duchene M, Pettenburger K, Sillaber C, Valent P, Bettelheim P, et al. Identification of profilin as a novel pollen allergen; IgE autoreactivity in sensitized individuals. *Science* 1991; 253: 557-60. doi:10.1126/science.1857985
- Vara A, Fernandez-Gonzalez M, Aira MJ, Rodriguez-Rajo FJ. Fraxinus pollen and allergen concentrations in Ourense (South-western Europe). *Environ Res* 2016a; 147: 241-8. doi:10.1016/j.envres.2016.02.014
- Vara A, Fernandez-Gonzalez M, Aira MJ, Rodriguez-Rajo FJ. Oleaceae cross-reactions as potential pollinosis cause in urban areas. *Sci Total Environ* 2016b; 542: 435-40. doi:10.1016/j.scitotenv.2015.10.107
- Vega-Maray AM, Fernandez-Gonzalez D, Valencia-Barrera R, Suarez-Cervera M. Detection and release of allergenic proteins in *Parietaria judaica* pollen grains. *Protoplasma* 2006; 228: 115-20. doi:10.1007/s00709-006-0172-4
- Vrtala S, Grote M, Duchene M, van Ree R, Kraft D, Scheiner O, et al. Properties of tree and grass pollen allergens: reinvestigation of the linkage between solubility and allergenicity. *Int Arch Allergy Immunol* 1993; 102: 160-9
- Zaidi MA, O'Leary S, Wu S, Gleddie S, Eudes F, Laroche A, et al. A molecular and proteomic investigation of proteins rapidly released from triticale pollen upon hydration. *Plant Mol Biol* 2012; 79: 101-21. doi:10.1007/s11103-012-9897-y

Chapter 5

Differences in atmospheric concentration of airborne *Poaceae* pollen and allergens

Abstract

The *Poaceae* family is considered one of the main causes of pollen allergy and the incidence of allergenic cross-reactivity among allergens of different grass species that share similar physicochemical and immunological features complicate the risk exposure of allergic patients. The exposure to these allergens mostly relies on the available information about the concentration of airborne pollen grains their temporal distribution; however, discordance between pollen concentrations and allergic symptoms has been often detected. In this scenario, the purpose of this research was to evaluate the relationship between grass pollen counts and the aeroallergens concentrations in two Mediterranean cities having different weather conditions, i.e. León (Spain) and in Bologna (Italy). In particular, the concentration of Lol p 1 and Lol p 5 allergens from *Poaceae* pollen was studied in relation to meteorological factors. Our results show that Lol p 1 and Lol p 5 concentrations strong relate to pollen counts, but the release of the allergens also depend on relative humidity. This could explain the appearance of protein peaks at times when little or no grass pollen is present.

Introduction

Poaceae pollen is one of the major outdoor seasonal source of airborne allergens and the allergenic role and importance of grass pollen in triggering hay fever and allergic asthma is well known and extensively (Weber, 2007a). Between 8 and 35% of adult patients in various European countries showed specific antibodies to

Poaceae pollen allergens, and these rates were higher in children and adolescents (Fernández-González et al., 2011). The allergenicity of grass pollen is attributed to a small number of proteins that are rapidly released from pollen grains after hydration in the air and following contact with human mucosa. These allergens share similar physicochemical and immunological features, that cause a high incidence of allergenic cross-reactivity on one hand, and on the other, allowed their classification into 14 groups (Weber, 2007a). Up to 95% of patients allergic to grass pollen possess IgE specific for group 1 allergens (glycoproteins with a molecular mass of 32–35 kDa) and 80% for group 5 allergens (28–32 kDa), these two groups forming the major allergens of grass pollen (Schäppi et al., 1999). Group 1 proteins are recognized by 90% of patients allergic to grass pollen and play an important role in IgE binding to pollen extract, while the prevalence of sensitization to Group 5 allergens is between 65 and 85% (Andersson and Lidholm, 2003; Mari, 2003; Weber, 2007a). Group 1 allergens comprise Lol p 1, the first major allergen described in *Lolium perenne* and the most widely studied (Radauer and Breiteneder, 2006; Fernández-González et al., 2011). Lol p 1 corresponds to an acidic glycoprotein with 60–70% sequence identity with the β -expansins, proteins involved in breaking hydrogen bonds between cellulose of the plant cell walls, thereby facilitating cell growth. Like many other group 1 allergens, Lol p 1 shows high cross-allergenicity based on a marked homology (Weber, 2007b; Weber, 2007a; Fernández-González et al., 2011). It has multiple isoforms which appear to be immunologically indistinguishable, and its prevalence in people that are sensitive to *Poaceae* can reach up to 95% (Johnson and Marsh, 1965; Kahn and Marsh, 1986; De Linares et al., 2010). Besides Lol p 1, Lol p 5 is another major allergen of *Lolium perenne*. It shows ribonuclease activity and was shown to be present in inhalable starch granules, usually released into the atmosphere upon rainfall by bursting of pollen grains (Suphioglu et al., 1992; Schäppi et al., 1999). In fact, even if there is a strong correlation with the grass pollen counts and asthma or hay fever among individuals sensitive (Fernandez-Caldas et al., 1989; Schäppi et al., 1999; Grote et al., 2000; Grote et al., 2001; Vega-Maray et al., 2006; D'Amato and Cecchi, 2008; De Linares et al., 2010), grass pollen has a low probability of entering the lower airways to trigger asthma because of its aerodynamic diameter (Schäppi et al., 1999). Grass pollen allergens

have been recorded in atmospheric particles smaller than pollen grains (Spieksma et al., 1990;Schäppi et al., 1996;Schäppi et al., 1997;Schäppi et al., 1999). Unlike grass pollen grains, these micronic particles are small enough to enter the human airways and cause allergic reactions in the distal parts of the lungs (Wilson et al., 1973;Schäppi et al., 1999;Grote et al., 2001;D'Amato and Cecchi, 2008). For this reason, not only the number of pollen grains, but also the real concentration of airborne allergens must be determined for a more effective assessment of the risk factors for asthma and hay fever in individuals sensitive to grass pollen (Fernández-González et al., 2011;Rodríguez-Rajo et al., 2011). In this scenario, this study monitored airborne pollen concentrations of grasses and Lol p 1 and Lol p 5 aeroallergens to gain more information on the correlation between *Poaceae* airborne pollen and allergen concentration and hence makes a reliable assessment of true pollen exposure. The study was performed in León (Spain) and in Bologna (Italy), two Mediterranean cities having different weather conditions.

Material and methods

Air sampling

Pollen sampling was performed continuously throughout from March to June 2015 using two Hirst-type seven-day recording volumetric trap (VPPS 2000 sampler, Lanzoni, Bologna, Italy) with a suction flow rate of 10 l/min. placed on a terrace 15 m above ground level at León University Campus (Spain), and installed 25 m above ground level on the roof of the ISAC-CNR building in Bologna (Italy). Pollen counts were expressed as daily mean pollen grains/m³ of air.

Particles for aeroallergen quantification were sampled with a Burkard Cyclone sampler (Burkard Manufacturing Co Ltd. Hertfordshire, UK), a continuous, wind-oriented volumetric sampler using a single reverse-flow miniature cyclone with an air throughput of 16.5 l/min. Particles were collected directly into a 1.5 ml Eppendorf vial every 24 hours of sampling, during the same period of pollen. Samples collected each day were stored at -20 °C. Both samplers were located in the same sampling pollen station.

Details of the monitoring stations

The city of León (830 m a.s.l.), is placed in the north-western Iberian Peninsula. Biogeographically, the city belongs to the Mediterranean region and has a continental climate; mean annual temperature is 11 °C, annual average rainfall is 522 mm, mainly in autumn and spring (with low rainfall and the storms type during the summer months) and the annual mean wind intensity exceeds 5 m/s. Bologna (54 m a.s.l.), is located at the foot of the Apennine Mountains (South) in the Po Plain, a vast flat area in the north of Italy and biogeographically belongs to the Eurosiberian Region. The area is characterized by a sub-continental climate (Köppen-Geiger Cfa) with cold winters and hot summers (typical monthly mean temperatures ranging from 1 to 26 °C), high humidity levels (typical monthly mean relative humidity ranging from 60% to 84%) and low wind intensities (typical annual mean wind intensities of about 2 m/s). The annual mean precipitation is between 760-800 mm with a xerothermic period in July and August

Protein extraction from Cyclone samples and immunochemical aero-allergen quantification

The dry Cyclone samples were centrifuged at 18000 x g, 1 min and extracted at room temperature for 2 h with 120 µL of phosphate buffer (50 mM pH 7.0) supplemented with 150 mM NaCl, 3 mM EDTA, 0.005% Tween 20, and 125 mM ammonium bicarbonate. The extract was separated by centrifugation at 2000 x g for 10 min and stored at -20 °C.

The allergen content in extracted samples was quantified using a double antibody sandwich ELISA method. The ELISA plates (Greiner, Frickenhausen, Germany) were previously coated overnight with 0.25 µg/well of monoclonal antibodies anti-Lol p 1 (7A8 and 9F6) or anti-Phl p 5 (10B1 and 10C12) (Bial Industrial Farmacéutica, Zamudio, Spain) at room temperature in a moist chamber and then blocked with 200 µL/well of PBS-BSA-T (PBS with 1% bovine serum albumin with 0.05% Tween 20). Afterwards, plates were incubated with 100 µL per well of extracted airborne samples. Plates were incubated with 100 µL/well of biotinylated anti-Lol p 1 or Phl p 5 polyclonal antibody at 1 µg/ml (Bial Industrial Farmacéutica, Spain) and then, with 100 µL/well of streptavidin-conjugated peroxidase (0.25 µg/ml in PBS-BSA-T). All the incubations were performed at 37°C

for 1 hour, with 3 washes of 200 μ L per well of PBS-B-T between successive steps. Finally, the enzyme activity was determined by adding 200 μ L/well of o-phenylenediamine (Sigma-Fast™ tablet sets) and incubated for 30 min at room temperature in the dark. The standard curve was constructed from nine data points using a four parameter logistic curve fit and the concentration of crude extracts, assayed as dilution series, were interpolated from the linear portion of the standard curve and expressed in pg/ml. Subsequently, the data were converted to picograms per cubic meter according to the volume sampled by the apparatus. Purified Lol p 1 and Lol p 5 were used as reference standards.

Meteorological data

Weather data were supplied by the Spanish Meteorology Agency (AEMET) and IdroMeteoClima Service (ARPA Emilia-Romagna, Italia). Temperatures ($^{\circ}$ C), rainfall (mm), relative humidity (%) and wind speed (m/s) were recorded continuously and aggregated for the aeroallergen sampling period and also for the periods immediately before and after the sampling period.

Statistical analysis

Spearman's Rank Correlation Coefficient was used for nonparametric data in order to analyze the correlations between meteorological parameters and pollen/allergens concentration. The level of significance was assessed between $P < 0.01$ and $P < 0.05$ by using GraphPad Prism.

Results

The features of grass pollen emission in Bologna and León were very similar even if León showed a delayed blossom season. Grass pollen was recorded in the atmosphere of Bologna from mid-April to June. The pollination period of greatest intensity occurred from April 23 to May 23 with the highest peak on April 25 (223 grains/ m^3) (Fig. 1 A). In León, a delayed but intense *Poaceae* blossom was recorded and grass pollens were recorded from May 8 to the end of the sampling. The period of highest pollen intensity was recorded between May 10 and June 20 with a peak of 179 grains/ m^3 on May 11 (Fig. 1 B). The delay was due to the different meteorological conditions of the two cities. In fact, both precipitation and

temperature drastically affected the concentration of airborne *Poaceae* pollen grains (Tab. 1). Temperatures, in particular the maximum temperature (Tmax), deeply and positively influenced grass pollen concentration. This was evident for both cities, however, more underlined for León, as characterized by deep daily temperature fluctuations. In contrast, precipitations, and as consequence relative humidity decreased airborne pollen amount.

Tab 1. Spearman's correlation coefficients *Poaceae* pollen concentration and main meteorological parameters for Bologna and León

	Bologna	León
Tmax(°C)	0,5674	0,7254
Tmin(°C)	0,5611	0,3967
Tmed(°C)	0,5960	0,6585
P (mm)	-0,2006	-0,1183
HR (%)	-0,1716	-0,4594
Vel. V (m/s)	0,1248	-0,3276

Plotting pollen concentration versus maximum temperature and precipitation, it became evident how the maximum concentrations of airborne *Poaceae* pollen grains were present when the maximum temperature was above 15°C and precipitations were absent (Fig 1).

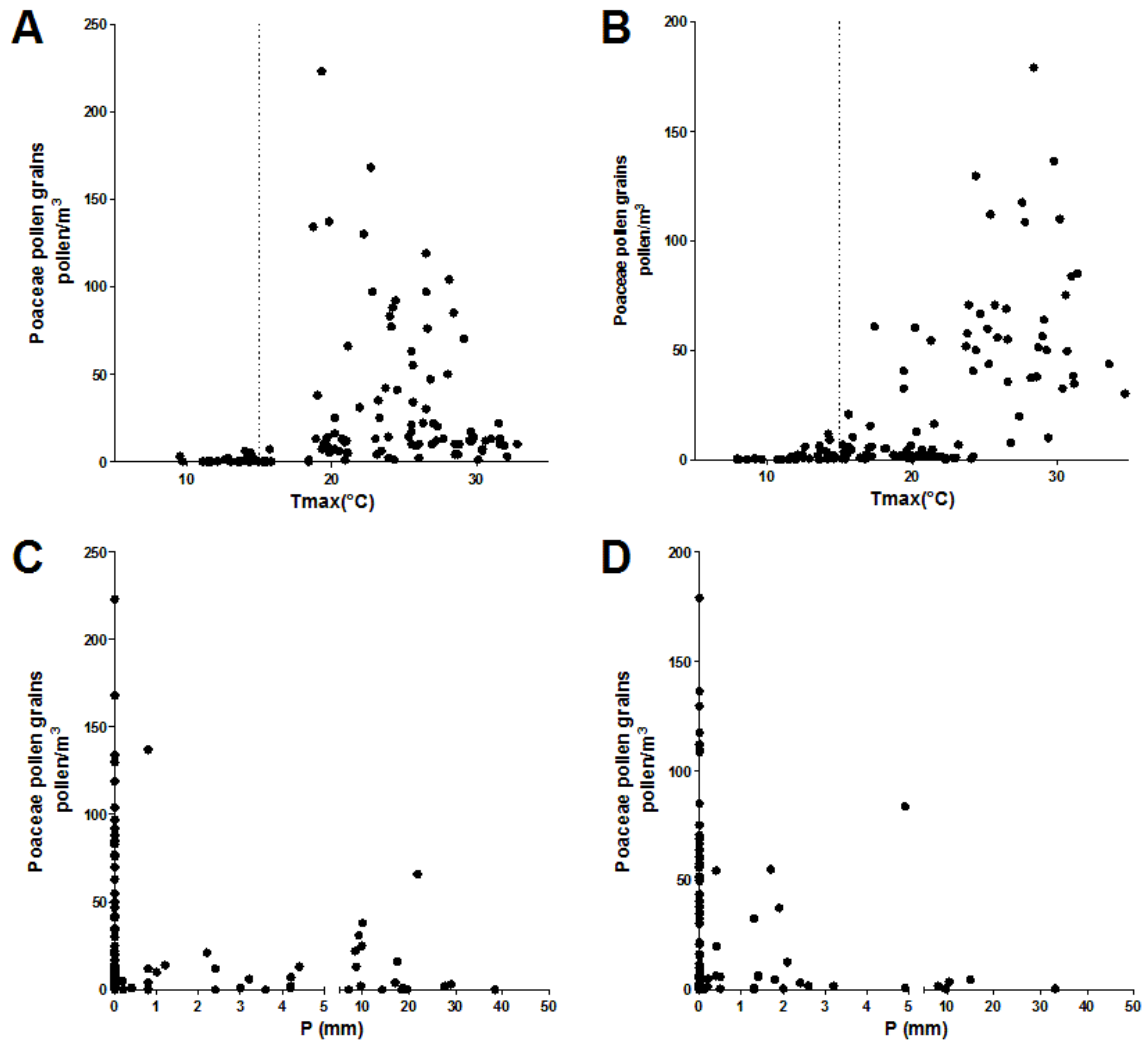


FIGURE 1. Correlation between daily fluctuations in *Poaceae* airborne pollen concentration (pollen/m³) and maximum daily temperature, Tmax(°C) in Bologna **(A)** and León **(B)** and precipitations, P(mm) in Bologna **(C)** and León **(D)**.

Even if León and Bologna were characterized by a similar amount of *Poaceae* pollen grains in the monitored period, a huge discrepancy in total amount of allergens was evident, and León showed Lol p 1 and Lol p 5 concentrations that were three-fold higher compared to Bologna. In both areas, the concentrations of Lol p 1 and Lol p 5 showed relatively high values between the beginning of May and the end of June. The concentrations of Lol p 1 and of Lol p 5 followed a similar trend of pollen concentration. However, the main peaks of allergens concentration usually followed the peaks of pollen concentration. In fact, high allergen concentrations were often recorded during periods characterized by relatively low

pollen concentrations. This was evident in both cities, even if it was more highlighted in Bologna (Fig. 2, asterisks).

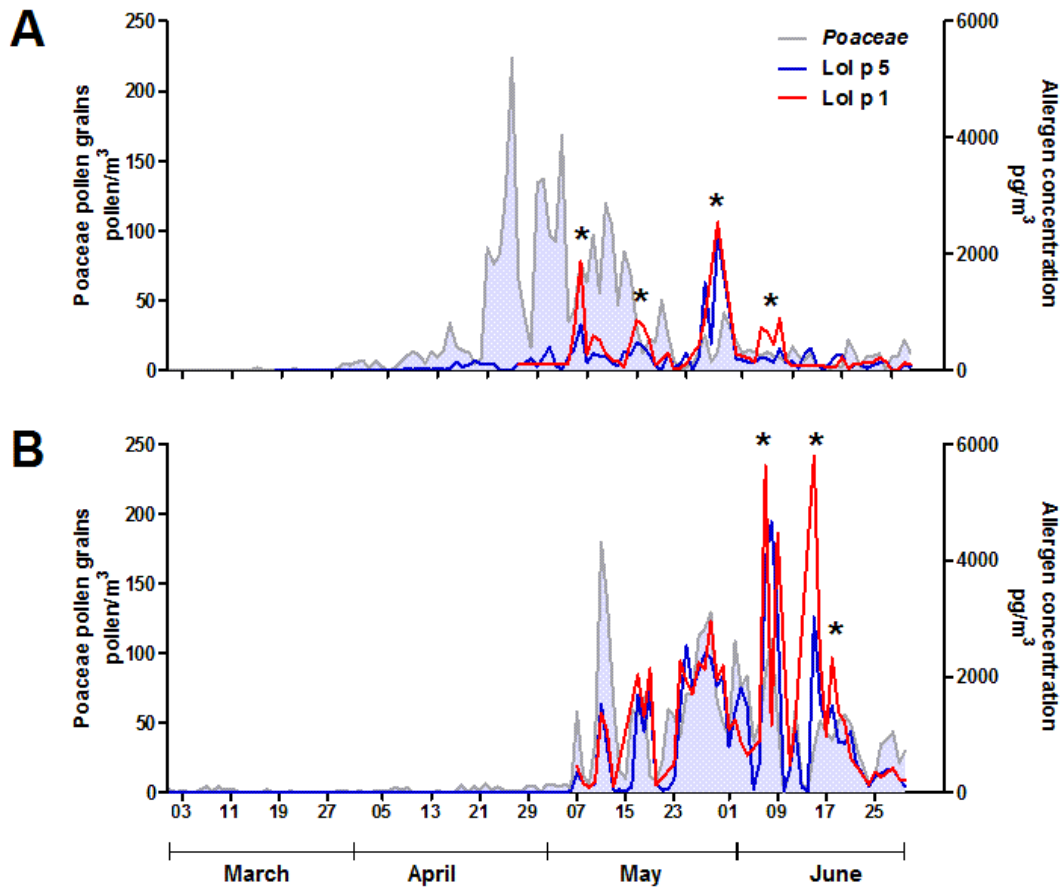


FIGURE 2. Comparison between daily fluctuations in Poaceae airborne pollen concentration (pollen/m³) and airborne Lol p 1 and Lol p 5 (pg/m³) in Bologna (A) and León (B) from March to June 2015.

Therefore, statistical analysis applying Spearman's correlation coefficient between atmospheric concentrations of allergens, *Poaceae* pollen concentration, and the main meteorological was performed. The analyzed parameters showed a significant correlation as reported in Table 2. The highest level of association was obtained with grass pollen and temperature in Bologna, and with *Poaceae* concentration, relative humidity, temperature and precipitation in León. The degree of association with the maximum temperature was significant ($P < 0.05$) in both sites. In León, sufficiently significant and negative correlations were observed with precipitation and relative humidity.

Tab 2. Spearman's correlation coefficients between allergens' Lol p 1 and Lol p 5, *Poaceae* pollen concentration, and main meteorological parameters for Bologna and León

	Bologna		León	
	Lol p 5	Lol p 1	Lol p 5	Lol p 1
<i>Poaceae</i> (pollen/m ³)	0,6207	0,4209	0,8918	0,8037
Tmax(°C)	0,6020	0,5543	0,6391	0,6742
Tmin(°C)	0,6575	0,5994	0,4902	0,3969
Tmed(°C)	0,6379	0,5904	0,6635	0,6439
P (mm)	0,07176	0,0289	-0,0769	-0,1777
HR (%)	0,0129	0,0509	-0,3082	-0,4365
Vel. V (m/s)	0,05452	-0,0495	-0,2424	-0,2896

To further investigate the correlation between allergen concentration and meteorological factors, data about Lol p 1/ Lol p 5 concentration and the main atmospheric parameters were analyzed, but only within the peaks in allergen concentration. In this case data of Bologna and León were analyzed together. The Spearman's rank correlations, provided significant and positive coefficients only for Lol p 5 and Lol p 1 concentrations as opposed to relative humidity ($r_s = 0.295$, $p < 0.005$ for Lol p 5 vs RH; $r_s = 0.268$, $p < 0.005$ for Lol p 1 vs RH). Plotting the analyzed date, it became evident how a relative humidity between 40% and 70% was the condition that mostly enhanced the concentration of airborne allergens (Fig. 3).

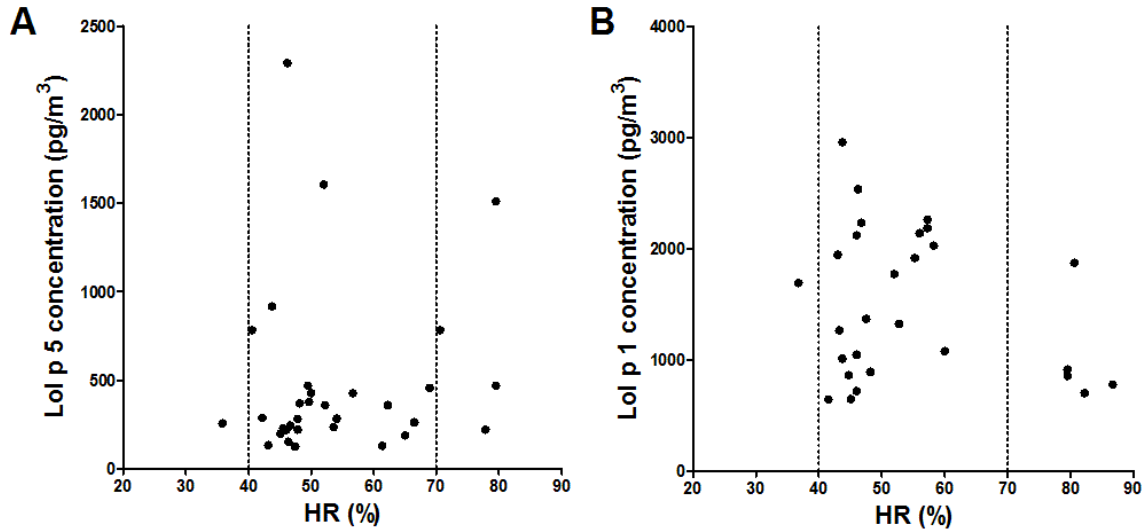


FIGURE 3. Correlation between peaks of airborne allergen concentration (pollen/m³) and relative humidity (%) for Lol p 5 (**A**) and Lol p 1 (**B**). Values of Bologna and León are plotted together.

Discussion

The major *Poaceae* allergens Lol p 1 and Lol p 5 in the atmosphere of two cities with different climatic conditions even if both Mediterranean; i.e. Bologna (Italy) and León (Spain), were monitored and correlated to meteorological parameters. *Poaceae* pollen comprises a wide variety of species and is linked to multiple ecosystems, ranging from natural plant communities to eminently anthropic rural environments. Given the broad range of sources of *Poaceae* pollen emission, the pollen season is very long and days with values posing an allergy risk (over 25 pollen grains/m³) (Rojo et al., 2016) were recorded in May and June.

Data presented in this work show how meteorological factors affected both grass pollen and allergen concentrations. Grass pollen season was notably delayed in León compared with Bologna and this phenomenon was likely due to the great daily fluctuations in temperature that characterize the Spanish city. In fact, temperature was the parameter that mostly influenced airborne pollen concentration and in particular the maximum temperature. This was evident for both cities, however, more underlined for León, as characterized by deep daily temperature fluctuations. A number of phenological features including pollen season start and peaks in pollen counts are known to be governed by local weather

conditions and, especially, by temperature (Aguilera et al., 2014). This positive correlation between temperature and mean daily pollen concentration has been studied for both woody species and herbaceous species and was found to be higher in the latest (Rojo et al., 2016). In contrast, precipitations, and as consequence relative humidity decreased airborne pollen amount. A negative correlation between rainfall and pollen concentration has been found in a wide number of studies and is known as “rain washing” phenomenon (Rodríguez-Rajo et al., 2005; Sahney and Chaurasia, 2008; Kizilpınar et al., 2011). Wind is another key factor, playing an important role in bio-particle distribution, also pollen, as it causes pollen grains to be released from plants and be spread in the atmosphere. Moreover, the wind lifts non-vital pollen grains that are dehydrated and partially damaged from the ground and distributes these to different layers of the atmosphere (Ballero and Maxia, 2003). In our study however we found a significant correlation with total airborne pollen counts and wind only for the city of León and this phenomenon could be related to large-range transport of particles (Hernández-Ceballos et al., 2011; Galan et al., 2013; Sikoparija et al., 2013; Moreno-Grau et al., 2016).

The concentration of airborne Lol p 1 and Lol p 5 differed between areas depending on variables like biological sources and meteorological factors. Also in this case, León showed a significant delay compared to Bologna. Moreover, what was worth of notice was that the airborne pollen spectrum for the analyzed cities was not similar in magnitude and León showed a three-fold concentration compared to Bologna, even if the amount of airborne pollen grains was comparable. The concentration trends of both investigated allergens was similar to the pollen concentration as demonstrated by the good correlation between the two parameters in both cities and this confirms recent data about Lol p 1 concentration (Fernández-González et al., 2011). In fact, in both areas the correlation with total airborne grass pollen was high; confirming that in the analysis period the majority of pollen dispersed into the atmosphere was grass pollen. The correlation between Lol p 5/Lol p 1 and total grass pollen was lower in Bologna than in León, indicating that other parameters are involved in the spread of the allergens, e.g. temperature and relative humidity. These parameters could be deeply involved in the misalignment of peaks of allergens and *Poaceae* pollen. In fact, while we found a

significant negative and low correlation between Lol p 5/ Lol p 1 and, respectively, rainfall and mean relative humidity, it was notably that allergen concentrations were increased on the days after rainfall. For this reason, plotting only relative humidity vs allergen concentrations in the timespan of the allergen peaks, gave significant correlation values between relative humidity and airborne allergen concentrations. Increased concentrations of grass allergens after a period of precipitation are already reported and it was shown that only a small amount of Group 1 grass allergens is found in dry pollen of *Lolium perenne*. However, after hydration of the pollen grain with rainwater, some cytoplasmic material, mainly starch granules and polysaccharide proteins corresponding to Groups 1 and 5 grass allergens, is discharged outside the pollen (Grote et al., 2000; Grote et al., 2001). This could explain the appearance of protein peaks at times when little or no grass pollen is present.

Taken together, our results thus show that pollen calendar and the association with meteorological factors may be a useful, but not thorough tool in helping to diagnose allergic patients and advise precautions. In fact, meteorological factors were shown to deeply affect the amount of the airborne grass pollen allergens.

References

- Aguilera, F., Ruiz, L., Fornaciari, M., Romano, B., Galan, C., Oteros, J., Ben Dhiab, A., Msallem, M., and Orlandi, F. (2014). Heat accumulation period in the Mediterranean region: phenological response of the olive in different climate areas (Spain, Italy and Tunisia). *Int J Biometeorol* 58, 867-876.
- Andersson, K., and Lidholm, J. (2003). Characteristics and immunobiology of grass pollen allergens. *Int Arch Allergy Immunol* 130, 87-107.
- Ballero, M., and Maxia, A. (2003). Pollen spectrum variations in the atmosphere of Cagliari, Italy. *Aerobiologia* 19, 251-259.
- D'amato, G., and Cecchi, L. (2008). Effects of climate change on environmental factors in respiratory allergic diseases. *Clin Exp Allergy* 38, 1264-1274.
- De Linares, C., Diaz De La Guardia, C., Nieto Lugilde, D., and Alba, F. (2010). Airborne study of grass allergen (Lol p 1) in different-sized particles. *Int Arch Allergy Immunol* 152, 49-57.
- Fernandez-Caldas, E., Swanson, M.C., Pavda, J., Welsh, P., Yunginger, W., and Redd, C.E. (1989). Immunochemical demonstration of Red Oak pollen aeroallergens outside the pollen season. *Grana* 28, 205-209.
- Fernández-González, D., Rodríguez Rajo, F., González Parrado, Z., Valencia Barrera, R.M., Jato, V., and Grau Moreno, S. (2011). Differences in atmospheric emissions of Poaceae pollen and Lol p 1 allergen. *Aerobiologia* 27, 301-309.

- Galan, C., Antunes, C., Brandao, R., Torres, C., Garcia-Mozo, H., Caeiro, E., Ferro, R., Prank, M., Sofiev, M., Albertini, R., Berger, U., Cecchi, L., Celenk, S., Grewling, L., Jackowiak, B., Jager, S., Kennedy, R., Rantio-Lehtimäki, A., Reese, G., Sauliene, I., Smith, M., Thibaudon, M., Weber, B., Weichenmeier, I., Pusch, G., and Buters, J.T. (2013). Airborne olive pollen counts are not representative of exposure to the major olive allergen Ole e 1. *Allergy* 68, 809-812.
- Grote, M., Vrtala, S., Niederberger, V., Valenta, R., and Reichelt, R. (2000). Expulsion of allergen-containing materials from hydrated rye grass (*Lolium perenne*) pollen revealed by using immunogold field emission scanning and transmission electron microscopy. *J Allergy Clin Immunol* 105, 1140-1145.
- Grote, M., Vrtala, S., Niederberger, V., Wiermann, R., Valenta, R., and Reichelt, R. (2001). Release of allergen-bearing cytoplasm from hydrated pollen: a mechanism common to a variety of grass (Poaceae) species revealed by electron microscopy. *J Allergy Clin Immunol* 108, 109-115.
- Hernández-Ceballos, M.A., García-Mozo, H., Adame, J.A., Domínguez-Vilches, E., De La Morena, B.A., Bolívar, J.P., Pérez-Badía, R., and Galán, C. (2011). Determination of potential sources of *Quercus* airborne pollen in Córdoba city (southern Spain) using back-trajectory analysis. *Aerobiologia* 27, 261-276.
- Johnson, P., and Marsh, D.G. (1965). Allergens from common ryegrass pollen (*Lolium perenne*). The allergenic determinants and carbohydrate moiety. *Immunochemistry* 3, 101-110.
- Kahn, C.R., and Marsh, D.G. (1986). Monoclonal antibodies to the major *Lolium perenne* (ryegrass) pollen allergen Lol p I (Rye I). *Mol Immunol* 23, 1281-1288.
- Kizilpinar, I., Civelek, E., Tuncer, A., Dogan, C., Karabulut, E., Sahiner, U.M., Yavuz, S.T., and Sackesen, C. (2011). Pollen counts and their relationship to meteorological factors in Ankara, Turkey during 2005-2008. *Int J Biometeorol* 55, 623-631.
- Mari, A. (2003). Skin test with a timothy grass (*Phleum pratense*) pollen extract vs. IgE to a timothy extract vs. IgE to rPhl p 1, rPhl p 2, nPhl p 4, rPhl p 5, rPhl p 6, rPhl p 7, rPhl p 11, and rPhl p 12: epidemiological and diagnostic data. *Clin Exp Allergy* 33, 43-51.
- Moreno-Grau, S., Aira, M.J., Elvira-Rendueles, B., Fernández-González, M., Fernández-González, D., García-Sánchez, A., Martínez-García, M.J., Moreno, J.M., Negral, L., Vara, A., and Rodríguez-Rajo, F.J. (2016). Assessment of the *Olea* pollen and its major allergen Ole e 1 concentrations in the bioaerosol of two biogeographical areas. *Atmos. Environ.* 145, 264-271.
- Radauer, C., and Breiteneder, H. (2006). Pollen allergens are restricted to few protein families and show distinct patterns of species distribution. *J Allergy Clin Immunol* 117, 141-147.
- Rodríguez-Rajo, F.J., Jato, V., González-Parrado, Z., Elvira-Rendueles, B., Moreno-Grau, S., Vega-Maray, A., Fernández-González, D., and Suárez, M. (2011). The combination of airborne pollen and allergen quantification to reliably assess the real pollinosis risk in different bioclimatic areas. *Aerobiologia* 27, 1-12.
- Rodríguez-Rajo, F.J., Méndez, J., and Jato, V. (2005). Airborne Ericaceae pollen grains in the atmosphere of Vigo (Northwest Spain) and its relationship with meteorological factors. *J Integr Plant Biol* 47, 792-800.
- Rojó, J., Rapp, A., Lara, B., Sabariego, S., Fernández-González, F., and Pérez-Badía, R. (2016). Characterisation of the airborne pollen spectrum in Guadalajara (central Spain) and estimation of the potential allergy risk. *Environ Monit Assess* 188, 130.
- Sahney, M., and Chaurasia, S. (2008). Seasonal variations of airborne pollen in Allahabad, India. *Ann Agric Environ Med* 15, 287-293.
- Schäppi, G.F., Monn, C., Wuthrich, B., and Wanner, H.U. (1996). Direct determination of allergens in ambient aerosols: methodological aspects. *Int Arch Allergy Immunol* 110, 364-370.
- Schäppi, G.F., Suphioglu, C., Taylor, P.E., and Knox, R.B. (1997). Concentrations of the major birch tree allergen Bet v 1 in pollen and respirable fine particles in the atmosphere. *J Allergy Clin Immunol* 100, 656-661.

- Schäppi, G.F., Taylor, P.E., Pain, M.C., Cameron, P.A., Dent, A.W., Staff, I.A., and Suphioglu, C. (1999). Concentrations of major grass group 5 allergens in pollen grains and atmospheric particles: implications for hay fever and allergic asthma sufferers sensitized to grass pollen allergens. *Clin Exp Allergy* 29, 633-641.
- Sikoparija, B., Skjøth, C.A., Alm Kübler, K., Dahl, A., Sommer, J., Grewling, L., Radisic, P., and Smith, M. (2013). A mechanism for long distance transport of Ambrosia pollen from the Pannonian Plain. *Agric. For. Meteorol.* 180, 112-117.
- Spieksma, F.T., Kramps, J.A., Van Der Linden, A.C., Nikkels, B.H., Plomp, A., Koerten, H.K., and Dijkman, J.H. (1990). Evidence of grass-pollen allergenic activity in the smaller micronic atmospheric aerosol fraction. *Clin Exp Allergy* 20, 273-280.
- Suphioglu, C., Singh, M.B., Taylor, P., Bellomo, R., Holmes, P., Puy, R., and Knox, R.B. (1992). Mechanism of grass-pollen-induced asthma. *Lancet* 339, 569-572.
- Vega-Maray, A.M., Fernandez-Gonzalez, D., Valencia-Barrera, R., and Suarez-Cervera, M. (2006). Detection and release of allergenic proteins in *Parietaria judaica* pollen grains. *Protoplasma* 228, 115-120.
- Weber, R.W. (2007a). Cross-reactivity of pollen allergens: impact on allergen immunotherapy. *Ann Allergy Asthma Immunol* 99, 203-211; quiz 212-203, 231.
- Weber, R.W. (2007b). Patterns of pollen cross-reactivity of pollen allergens: impact on allergen immunotherapy. *Ann Allergy Asthma Immunol* 99, 203-211.
- Wilson, A.F., Novey, H.S., Berke, R.A., and Surprenant, E.L. (1973). Deposition of inhaled pollen and pollen extract in human airways. *N Engl J Med* 288, 1056-1058.

Chapter 6

Purification and characterization of Amb a 1 and Art v 6, two pectate lyase enzymes from weed pollen

Abstract

Weed pollen is one of the main causes of allergic pollinosis all over the world. A major allergen family with high incidence of cross-reactivity is pectate lyase enzymes, involved in pollen tube emergence and fertilization. In the present study, Amb a 1 and Art v6, two pectate lyases of *Ambrosia artemisiifolia* and *Artemisia vulgaris* respectively, were purified and proteins were characterized using an array of physicochemical methods, tested for antibody-binding using human sera, and evaluated for their activity. Analyses of ragweed pollen extracts confirmed the presence of five different isoforms of the major allergen Amb a 1 that showed different immunological properties and reactivity. Also Art v 6 showed several isoforms, leading to the need to update the available database with its sequence. Finally, for the first time, both allergenic proteins were shown to be active after purification.

Introduction

Pollen wall protects male sperms from harsh conditions, facilitates the interaction among the pollen grains and the stigma, and discriminates self or other pollen grains to avoid inadequate fertilization. Pollen walls may vary in surface morphology but its general structure is generally composed of two main layers, i. e. the external exine and the inner intine. While exine consists of a robust material called sporopollenin, made of aliphatic derivatives such as fatty acids and phenolic

compounds covalently coupled by ether and ester linkages (Blackmore et al., 2007; Ariizumi and Toriyama, 2011), intine mostly consists of pectic polymers, celluloses, and hemicelluloses (Hasegawa et al., 2000; Jiang et al., 2014). Pectin, cellulose, and callose metabolism have been identified to be associated with intine formation. However, the mechanism underlying pollen wall development is far from clear (Jiang et al., 2014).

The germination and rapid growth requires a considerable amount of cell wall synthesis (Turcich et al., 1993) and possibly breakdown of stylar components (Lyu et al., 2015) and these processes are allowed by enzymes present in the mature pollen grain and developing tube (Allen and Lonsdale, 1993; Robert et al., 1993; Zhang et al., 2008; Zaidi et al., 2012). It is not surprising that many of the pollen-specific genes reported to date appear to have homology to cell wall degradation enzymes such as polygalacturonase (Allen and Lonsdale, 1993), pectin esterase (Bosch and Hepler, 2005), and pectate lyase (Rogers et al., 1992) (Wu et al., 1996). Based on the intrusive nature of the growth exhibited during germination and pollen tube elongation, one might expect that genes of this type would be highly expressed in pollen. Pectin are high molecular weight acid polysaccharides primarily made up of α -(1 \rightarrow 4) linked D-galacturonic acid residues (Caffall and Mohnen, 2009) and pectinases target methyl-esterified galacturonic acid, yielding substrates for polygalacturonases and pectate lyases to cleave the galacturonic acid backbones. Pectate lyases act by depolymerizing cell-wall polygalacturonides in the presence of calcium ions, thus destroying the integrity of the plant tissues. In particular, pectate lyases cleave the α -(1 \rightarrow 4) glycosidic linkages in galacturonic acid to produce unsaturated oligosaccharides (Charnay et al., 1992; Jiang et al., 2014). Pectate lyases have been extensively studied in several plant pathogenic microorganisms like *Erwinia chrysanthemi* as extracellular causal agents in soft root disease that affects a wide range of plant species (Shevchik et al., 1997; Kazemi-Pour et al., 2004). In plants, pectate lyases genes are highly expressed in pollen and anthers during the late stages of development (Rogers et al., 1992; Turcich et al., 1993; Wu et al., 1996; Jiang et al., 2014).

Besides the role of those enzymes during microsporogenesis, they are of great interest because of their role in triggering pollen sensitization and allergy. So far

allergenic pectate lyases have been identified and acknowledged in the pollen of 11 plant species and (www.allergome.org) (Pichler et al., 2015).

Among these, the major Cupressaceae allergens Cup s 1 from *Cupressus sempervirens* (Charpin et al., 2005), Cup a 1 from *Cupressus arizonica* (Aceituno et al., 2000), Cry j 1 from *Cryptomeria japonica* (Miki-Hirosige et al., 1994; Taniguchi et al., 1995; Suárez-Cervera et al., 2003), and Jun a 1 from *Juniperus ashei* (Midoro-Horiuti et al., 1999), but also weed allergens like Amb a 1 from *Ambrosia artemisiifolia* (Griffith et al., 1991; Rafnar et al., 1991) and Art v 6 from *Artemisia vulgaris* (Wopfner et al., 2005) also belong to this allergen family (Pichler et al., 2015). Whereas pectate lyases represent major allergens in almost all allergenic pollen where they have been identified, sensitization rates of only 26% have been reported for Art v 6 in mugwort allergic patients (Gadermaier et al., 2014), which might be a consequence of the very low expression levels of Art v 6 in the pollen (Himly et al., 2003).

Clinically relevant are weed pollen pectate lyases as they represent a threat to human health as their pollen is an important source of seasonal allergens. The scenario is even more exacerbated by the invasive nature and high ability to adapt in adverse environments of weeds (Gadermaier et al., 2014). Moreover, high prevalence of concomitant sensitization to *Ambrosia artemisiifolia* and *Artemisia vulgaris* pollens is often observed and these observations have prompted the consideration of potential cross-reactivity between ragweed and mugwort pollen. It was shown how Amb a 1 and Art v 6 cross-react, even if the homology of the two proteins is < 60% (Jahn-Schmid et al., 2012; Asero et al., 2014; Pichler et al., 2015). Although both allergens have been widely studied and IgE epitopes have been mapped, the characterization and the enzyme activity of these allergens as well as their allergenic potential have not fully been elucidated so far. From here the aim to purify natural Amb a 1 and Art v 6 in order to further characterize the two allergenic pectate lyases and to test their enzymatic activity, that has never been studied.

Material and Methods

Protein purification

Natural Amb a 1 was purified from 6 g of *Ambrosia artemisiifolia* pollen (Allergon AB, Ängelholm, Sweden), extracted with 180 ml of 5mM NaP buffer pH 6.8 for 16h at 4°C. Crude pollen extract was clarified by centrifugation at 4000 x g for 20 min. The supernatant was treated twice with polyvinylpyrrolidone (Sigma-Aldrich, St. Louis, USA) soaked in extraction buffer, followed by centrifugation at 1000 x g to remove aromatic pollen colors. After filtering through a 0.45 µm filter, the pollen extract was loaded onto a 15ml column, CHT Type I resin (BioRad Laboratories Ges.m.b.H., Vienna, Austria) and eluted in a 4-segment linear gradient (0-15% in 45 ml; 15-40% in 20 ml; 40-65% in 130 ml; 65-100% in 20 ml) with 500 mM NaP buffer pH 6.8. Fractions containing pure Amb a 1.02 were pooled and dialyzed against 10 mM NaP pH 8.5. The flow-through as well as early fractions containing a mix of Amb a 1.02 and Amb 1.03 were adjusted to pH 9.5 with 1M Tris-HCl buffer and loaded on a QHP Sepharose column (GE Healthcare) equilibrated with 50 mM Tris-HCl pH 9.5 and eluted in a 3-segment linear gradient (0-20% in 200 ml; 20-50% in 100 ml; 50-100% in 50 ml) with 50 mM Tris-HCl pH 9.5 supplemented with 1M NaCl. Fractions containing either Amb a 1.01 or Amb a 1.03 were pooled and dialyzed against 10 mM NaP pH 8.5.

Natural Art v 6 was extracted from 10 g of *Artemisia vulgaris* pollen (Allergon AB, Ängelholm, Sweden) in 70 ml of PBS buffer pH 7.5 by shaking 2h at room temperature. Crude pollen extract was clarified by centrifugation at 4000 x g for 20 min and the supernatant was concentrated through a 30 kDa filter. 20 mM Tris-HCl pH 9.5 was added till volume reached 100 ml. Pollen extract was loaded on a 5 ml QHP Sepharose column (GE Healthcare) equilibrated with 20 mM Tris pH 9.5 and eluted in 120 ml linear pH gradient with 20 mM NaAc pH 4.0, 0.5 M Urea. Fractions containing Art v 6 were pooled and dialyzed against 10 mM TrisHCl pH 8.5.

Natural Amb a 1 and natural Art v 6 were further purified size exclusion chromatography.

Peptide Analysis by nano-LC-MS/MS

Tryptic digests of purified natural allergens were performed with a ProteoExtract Trypsin Digestion kit (Calbiochem, Gibbstown, NJ, USA). Peptides were separated by reversed phase-capillary HPLC and analyzed with an ESI-QTOF mass spectrometer (Waters, Milford, Massachusetts). For more detail see (Erler et al., 2011).

Amino acid analysis

Amino acid composition of the protein preparations was analyzed by amino acid analyses according to the PicoTag™ method (Waters, Milford, MA, USA) using a HP1100 HPLC system (Hewlett-Packard, San Jose, CA, USA) equipped with a 3.9 x 150mm Novapak C₁₈ column (Waters).

Peptide Analysis by nano-LC-MS/MS

1 µg protein of pollen extracts and purified preparations were digested with the ProteoExtract All-in-One Trypsin Digestion Kit (EMD Millipore, Billerica, MA, USA). Resulting peptides were separated by reverse-phase nano-HPLC (Dionex Ultimate 3000, Thermo Fisher Scientific, Bremen, Germany, column: PepSwift Monolithic Nano Column, 100 µm x 25 cm, Dionex). After the digest, samples were desalted using C₁₈ ZipTips (EMD Millipore, Billerica, MA, USA). The column was developed with an acetonitrile gradient (Solvent A: 0.1% (v/v) FA/0.01% (v/v) TFA/5% (v/v) ACN; solvent B: 0.1% (v/v) FA/0.01% (v/v) TFA/90% (v/v) ACN; 5–45% B in 60 min) at a flow rate of 1 µl/min at 55°C). The HPLC was directly coupled via nano electrospray to a Q Exactive Orbitrap mass spectrometer (Thermo Fisher Scientific). Capillary voltage was 2 kV. For peptide identification, the top 12 method was used with the normalized fragmentation energy at 27%. Survey and fragment spectra were analyzed with Proteome Discoverer version 1.4 (Thermo Fisher Scientific) or Peaks Studio 7 (Bioinformatics Solutions, Waterloo, Canada), respectively. For a semi-quantitative determination of the purity and isoform content of samples, the precursor ion intensity of diagnostic peptides as determined by Proteome Discoverer was used.

Immunoblots and Cross-inhibition ELISA

Proteins were separated by 1 or 2D SDS-PAGE using 15% polyacrylamide gels. 2D gels were performed with a pH gradient from 4-7 using the ReadyStrip™ IPG Strip system from Biorad (Biorad, Hercules, CA, USA). Thereafter, proteins were either detected by Coomassie Brilliant Blue G-250 (Biorad, Hercules, CA, USA) or blotted onto a nitrocellulose membrane (Whatman, Maidstone, UK). Blots were incubated with a 1:10 diluted serum pool of 10 ragweed allergic patients and bound IgE was detected using an AP-conjugated anti-human IgE antibody (1:10000) (BD Biosciences, Franklin Lakes, USA). For ELISA experiments, Maxisorp plates (Nunc, Thermo Fisher, Waltham, MA, USA) were coated with 100 ng/well protein in 50µl PBS overnight at 4°C. After washing and blocking, plates were incubated overnight at 4°C with diluted human sera 1:50 pre-incubated for 16 h with the inhibitory protein at different concentrations (buffer: TBS, pH 7.4, 0.05% (v/v) Tween, 1% (w/v) BSA). Bound human IgE was detected using an AP-conjugated mouse anti-human IgE antibody (Clone G7-26) (BD Biosciences, Franklin Lakes, USA), After incubation for 1h at 37°C and 1h at 4°C, colorimetric detection with 10 mM 4-nitrophenyl phosphate (Sigma-Aldrich, St. Louis, MO, USA) was performed. All measurements were done in duplicates.

Activity assay

Solutions of pectin and polygalacturonic acid substrates (Sigma-Aldrich, St. Louis) were prepared by heating to 60°C and stirring for 10 min, followed by centrifugation for 10 min to remove any insoluble material. Pectate lyase assays were conducted as already described by (Guo et al., 1996), with minor modifications. Briefly, assay was performed in a multiwell-plate (Nunclon 96 Flat Bottom Black Polystyrol LumiNunc FluoroNunc) with 100 mM Tris-HCl pH 8.5, 1 mM CaCl₂, and 5 µg of purified protein. The final volume of the reaction was 200 µl. The change in absorbance at 230 nm was monitored over 16 h at 25°C with a multiwell-plate spectrophotometer (Tecan-infinite 200Pro). Specific activity was defined as the amount of enzyme that forms 1 µmol of 4, 5-unsaturated product in 1 min under the conditions of assay. The molar extinction coefficient for the unsaturated product at 235 nm is 4,600 M⁻¹cm⁻¹ (Collmer et al., 1988).

Results and Discussion

Purification and characterization of Amb a 1

Mass spectrometry analyses extracts showed that Amb a 1 comprises 78% of the allergen content in total ragweed pollen extracts (data not shown). In addition, our analyses revealed that natural Amb a 1 is composed to 36% of Amb a 1.01, 11% of Amb a 1.02, 16% of Amb a 1.03, 5% of Amb a 1.04, and 32% of Amb a 1.05, respectively. These findings are in agreement with the hypothesis of a lower expression of Amb a 1.02 and Amb a 1.04 compared with Amb a 1.01 in mature ragweed pollen (Asero et al., 2014). As isoforms 01, 02, and 03 were shown to display higher IgE-binding activity than isoforms 04 and 05 (Augustin et al., 2013), they were purified and selected for further characterization.

Isoforms 01, 02, and 03 were purified from ragweed pollen extracts by standard chromatography. Amb a 1.02 and a mixture of Amb a 1.01 and Amb a 1.03 were purified in the first step by cation exchange chromatography (Fig 1A and 1B). The mixture of Amb a 1.01 and Amb a 1.03 was further purified in order to obtain the separation of the isoforms. For this purpose an anion exchange chromatography was performed (Fig 1C and 1D). After purification, the identity, purity, and isoform composition of all preparations were analyzed by mass spectrometry and amino acid analysis.

Isoform 03 was also produced as a recombinant protein in *P. pastoris*. The bacterial-derived pectate lyase C (DC-pelC) was produced as soluble recombinant protein in *E. coli*. Using sera from ragweed-allergic patients in ELISA and mediator release assays, no significant differences in the IgE-binding properties of recombinant and natural isoform 03 could be detected (under publication). Thus, the recombinant isoform 03 was selected for further experiments.

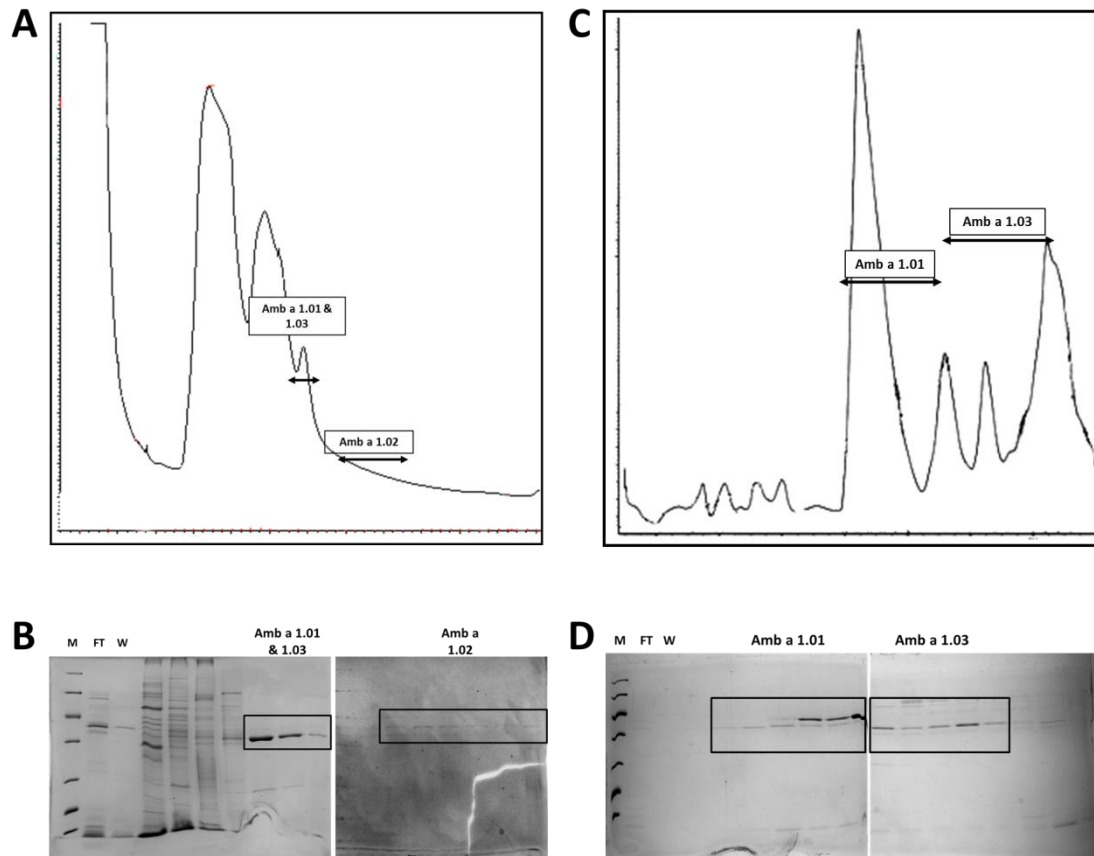


FIGURE 1. Purification of Amb a 1 isoforms (01-03). Cation exchange chromatography on CHT Type I column **(A)** and relative SDS-PAGE **(B)**. M molecular marker standard; FT flow through; W wash. All fractions were checked. Anion exchange chromatography on QHP sepharose column **(C)** and relative SDS-PAGE **(D)**. M molecular marker standard; FT flow through; W wash. All fractions were checked.

A pool of Amb a 1 isoforms was tested for antibody-binding of ragweed-allergic patients by immunoblot. In immunoblots, the majority (87%) of the ragweed-allergic patients reacted with Amb a 1 and gave positive signal for the purified protein at the expected molecular weight of 38 kDa and at lower molecular weights, as Amb a 1 is well known to undergo proteolytical cleavage (Wopfner et al., 2009) (Fig 2A). It is in fact well known that the natural protein easily undergoes proteolysis during purification resulting in two chains, designated α - and β -chain (King et al., 1974). The 26 kDa α -chain has been reported to associate non-covalently with the 12 kDa β -chain (King et al., 1974; King et al., 1981). What was worth of notice was that, while in ELISA, no significant differences in the binding of IgE, IgG1, or IgG4 to the tested Amb a 1 isoforms could be detected (data not shown), in cross-inhibition ELISA experiments with human sera, isoform 01 had

the greatest inhibitory capacity towards the other isoforms, meaning that it was the most efficient isoform in binding sera antibodies against Amb a 1. In fact 0.0022 μg , 0.0052 μg 0.031 μg of Amb a 1.01 were needed to obtain 50% of IgE inhibition towards Amb a 1.01, 1.02 and 1.03 respectively. Isoform 03 was the less cross-inhibiting with 50% inhibition values reaching 0.83 μg , 0.58 μg 0.0035 μg of towards Amb a 1.01, 1.02 and 1.03 respectively. Amb 1.02 showed intermediate values (Fig 2B). These evidences are in agreement with recent data that show that all these ragweed-sensitized patients usually react to all the main Amb a 1 isoforms expressed in ragweed pollen, but usually have an highest reaction against Amb a 1.01 (Asero et al., 2014).

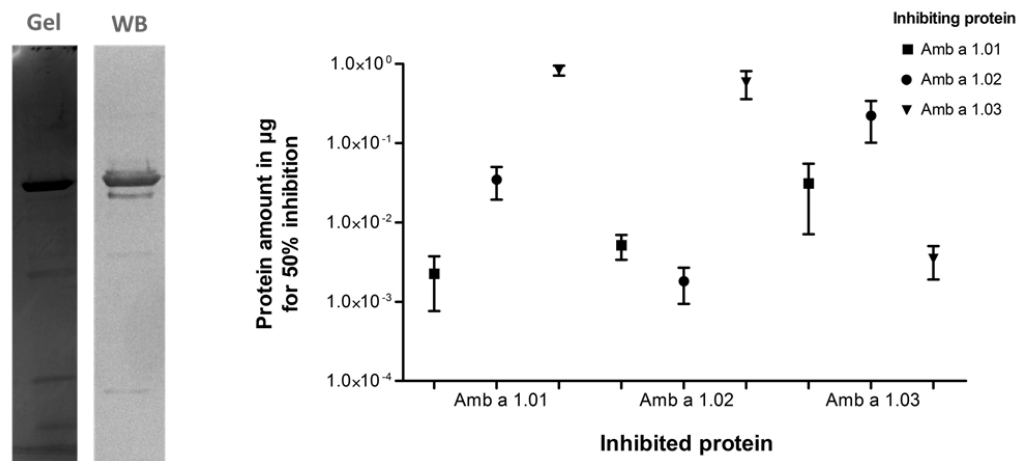


FIGURE 2. IgE reactivity of purified Amb a 1 and its isoforms. SDS-PAGE and relative western-blotting performed with a pool of allergic sera (A) cross inhibition ELISA experiment performed with the single isoforms (B).

To biochemically test Amb a 1 pectate lyase, the change in absorbance is determined both with pectin and polygalacturonic acid as a substrate. Release of unsaturated galacturonide product will result in a net increase in the absorbance at 232 (Guo et al., 1996). Using this assay, the enzymatic activity of natural Amb a 1 was then characterized under various conditions.

Like other pectate lyases, Amb a 1 activity required the presence of Ca^{2+} (Shevchik et al., 1997; Doyle and Lambert, 2002) as demonstrated by the fact that the addition of EDTA to a final concentration of 1 mM almost completely abolishes

activity. Amb a 1 showed high and substrate concentration-dependent specific activity (10 mU/mg) on pectin and no activity with polygalacturonic acid as a substrate (Fig 3).

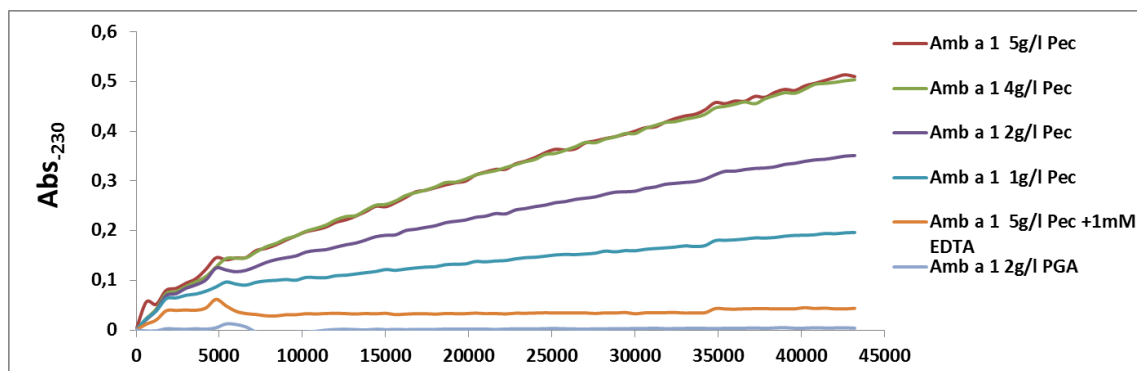


FIGURE 3. Characterization of the Ca^{2+} dependence and substrate specificity (polygalacturonic acid, PGA or pectin) of Amb a 1.

Purification and characterization of Art v6

Art v 6 was purified from mugwort pollen extracts by standard anion exchange chromatography. After purification, the identity and the purity were analyzed by mass spectrometry and amino acid analysis. Art v 6 purity was also checked by SDS-PAGE (Fig 4A) and its immunoreactivity was checked by immunoblotting with a pool of sera of mugwort-sensitized patients (data not shown) and a pool of sera derived from ragweed allergic patients (Fig 4B). What was worth of notice was a cross-recognition between the two pectate lyase enzymes, as already previously suggested (Asero et al., 2006;Asero et al., 2014). In fact, cross-inhibition experiments indicate that Amb a 1-specific IgE antibodies largely cross-react with Art v 6 and also show. Moreover Amb a 1 shows a broader epitope range or, alternatively, a higher affinity to IgE antibodies to Art v 6; classifying Amb a 1 as the stronger sensitizing molecule (Jahn-Schmid et al., 2012).

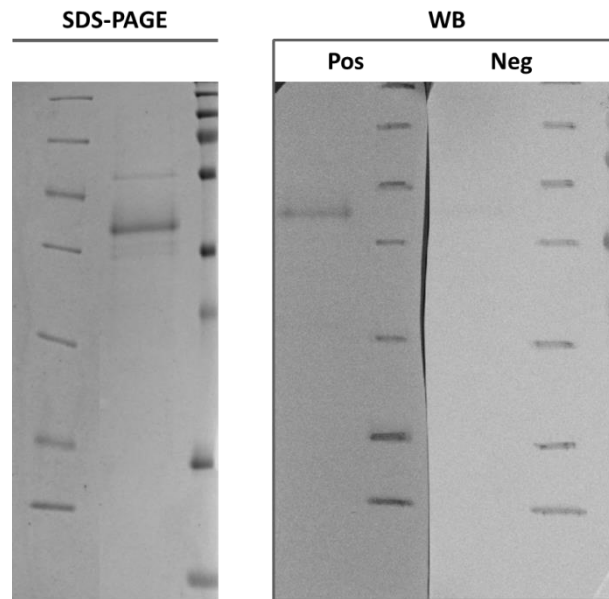


FIGURE 4. SDS-PAGE and immunoblotting of Art v 6. Purified allergen was separated on 15% polyacrylamide gel and stained with Coomassie Brilliant Blue R250 or electroblotted onto a nitrocellulose membrane, and the allergen on the membrane was immunostained with a pool of allergic sera.

As no isoforms of Art v 6 are reported in bibliography as they were never investigated, the purified Art v 6 was analyzed by 2-DE followed by electro-blotting and immuno-recognition with pool of sera derived from ragweed and mugwort allergic patients. Figure 5 shows the 2-DE immunoblotting of natural Art v 6. Eight of the most significant spots recognized by the pool of sera and analyzed by LC-MS/MS. were referable to Art v 6, although sequence differences between spots were detected and none of the analyzed spots had a high similarity with the only sequence present in the databases. In fact, as shown in the table below, all the analyzed spots covered the sequence of Art v 6 present in the database with a percentage between 41 and 58%. Moreover, by in solution digestion and a quantitative analysis, it was demonstrated that the sequence present in the database represents only 1% of the total amount of Art v 6 present in the crude extract. All these evidences highlight thus the possible existence of several isoforms of the pectate lyase of *Artemisia vulgaris*.

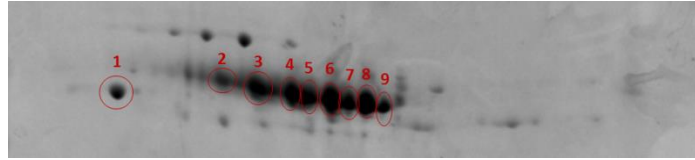


FIGURE 5. Two-dimensional electrophoresis of the purified allergen. The purified allergen was subjected to two-dimensional electrophoresis on three polyacrylamide gels and electroblotted onto a nitrocellulose membrane and immunostained with the patients' sera. Spot 2 to spot 9 correspond Art v 6 allergen.

	Description	Score	Coverage	# Peptides	Area
In-solution digestion	Pectate lyase new2 - [AOPJ1x_ARTVU]	1077,24	62,63	25	2,523E10
Spot 2	Pectate lyase new2 - [AOPJ1x_ARTVU]	109,92	41,41	12	1,138E9
Spot 3	Pectate lyase new2 - [AOPJ1x_ARTVU]	156,44	41,16	13	2,019E9
Spot 4	Pectate lyase new2 - [AOPJ1x_ARTVU]	152,11	44,19	16	1,850E9
Spot 5	Pectate lyase new2 - [AOPJ1x_ARTVU]	209,47	48,99	21	2,217E9
Spot 6	Pectate lyase new2 - [AOPJ1x_ARTVU]	230,92	51,77	19	3,710E9
Spot 7	Pectate lyase new2 - [AOPJ1x_ARTVU]	121,58	35,86	12	1,615E9
Spot 8	Pectate lyase new2 - [AOPJ1x_ARTVU]	211,60	48,99	21	4,955E9
Spot 9	Pectate lyase new2 - [AOPJ1x_ARTVU]	131,30	39,39	13	1,516E9

Like Amb a 1, Art v6 activity required the presence of Ca²⁺ as demonstrated by the fact that the addition of EDTA to a final concentration of 1 mM abolishes activity. Like in the case of Amb a 1, Art v 6 showed high and substrate concentration-dependent specific activity. The specific activity of Art v 6 was slightly higher compared to the one of Amb a 1 (20mU/mg) on pectin and had a significant activity (2 mU/mg) also on polygalacturonic acid (Fig 6).

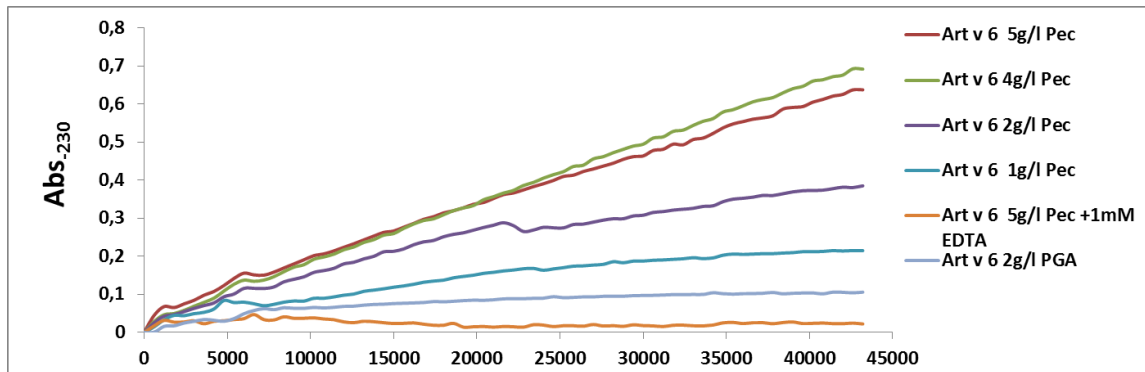


FIGURE 6. Characterization of the Ca^{2+} dependence and substrate specificity (polygalacturonic acid, PGA or pectin) of Art v 6.

Conclusions and future perspectives

In the present study, Amb a 1 and Art v6, two pectate lyases of *Ambrosia artemisiifolia* and *Artemisia vulgaris* respectively, were purified and proteins were characterized. Analyses of ragweed pollen extracts confirmed the presence of five different isoforms of the major allergen Amb a 1 that showed different immunological properties. A similar scenario was suggested also for the homologue protein Art v 6.

The possible existence of several isoforms of the pectate lyase of *Artemisia vulgaris* should be further investigated in order to spread light on the recognition of the human immune system against those possible isoforms, similarly for the homologue Amb a 1. Moreover, these findings lead to the need to update the available database with Art v 6 sequence and to possibly confirm LC-MS/MS data by the production and sequencing of recombinant proteins.

Finally, the exact reason for the presence of multiple isoforms of Amb a 1 and Art v 6 remains unclear and a promising field for research.

Besides the different isoforms, also post-transcriptional modifications of Amb a 1 and Art v 6 should be studied in depth. In fact, from LC-MS/MS analysis, both proteins are predicted to have *N*-glycosylation sites, creating more complexity to the study of the different roles of both pectate lyases during pollen development and germination as it remains to be elucidated if glycosylation is needed for protein activity. Nevertheless, the role of these sugar moieties during antibody-

allergen recognition also should be further investigated and also the substrate-specificity of the two enzymes.

Taken together, our results raise the question whether a single Amb a 1/ Art v 6 isoform would be sufficient for a molecule-based approach in weed immunotherapy and prompt new research topics for a deeper investigation of pectate lyase in pollen germination and human sensitization.

References

- Aceituno, E., Del Pozo, V., Minguez, A., Arrieta, I., Cortegano, I., Cardaba, B., Gallardo, S., Rojo, M., Palomino, P., and Lahoz, C. (2000). Molecular cloning of major allergen from *Cupressus arizonica* pollen: Cup a 1. *Clin Exp Allergy* 30, 1750-1758.
- Allen, R.L., and Lonsdale, D.M. (1993). Molecular characterization of one of the maize polygalacturonase gene family members which are expressed during late pollen development. *Plant J* 3, 261-271.
- Ariizumi, T., and Toriyama, K. (2011). Genetic regulation of sporopollenin synthesis and pollen exine development. *Annu Rev Plant Biol* 62, 437-460.
- Asero, R., Bellotto, E., Ghiani, A., Aina, R., Villalta, D., and Citterio, S. (2014). Concomitant sensitization to ragweed and mugwort pollen: who is who in clinical allergy? *Ann Allergy Asthma Immunol* 113, 307-313.
- Asero, R., Wopfner, N., Gruber, P., Gadermaier, G., and Ferreira, F. (2006). Artemisia and Ambrosia hypersensitivity: co-sensitization or co-recognition? *Clin Exp Allergy* 36, 658-665.
- Augustin, S., Waldi, M., Asero, R., Reese, G., Klysner, S., and Nandy, A. (2013). Assessment of Amb a 1 isoallergens as basis for development of a recombinant ragweed immunotherapeutic vaccine. *Allergy* 68, 111.
- Blackmore, S., Wortley, A.H., Skvarla, J.J., and Rowley, J.R. (2007). Pollen wall development in flowering plants. *New Phytol* 174, 483-498.
- Bosch, M., and Hepler, P.K. (2005). Pectin methylesterases and pectin dynamics in pollen tubes. *Plant Cell* 17, 3219-3226.
- Caffall, K.H., and Mohnen, D. (2009). The structure, function, and biosynthesis of plant cell wall pectic polysaccharides. *Carbohydr Res* 344, 1879-1900.
- Charnay, D., Nari, J., and Noat, G. (1992). Regulation of plant cell-wall pectin methyl esterase by polyamines-interactions with the effects of metal ions. *Eur J Biochem* 205, 711-714.
- Charpin, D., Calleja, M., Lahoz, C., Pichot, C., and Waisel, Y. (2005). Allergy to cypress pollen. *Allergy* 60, 293-301.
- Collmer, A., Ried, J.L., and Mount, M.S. (1988). Assay methods for pectic enzymes. *Methods Enzymol* 161, 329-335.

- Doyle, E.A., and Lambert, K.N. (2002). Cloning and characterization of an esophageal-gland-specific pectate lyase from the root-knot nematode *Meloidogyne javanica*. *Mol Plant Microbe Interact* 15, 549-556.
- Erler, A., Hawranek, T., Kruckemeier, L., Asam, C., Egger, M., Ferreira, F., and Briza, P. (2011). Proteomic profiling of birch (*Betula verrucosa*) pollen extracts from different origins. *Proteomics* 11, 1486-1498.
- Gadermaier, G., Hauser, M., and Ferreira, F. (2014). Allergens of weed pollen: an overview on recombinant and natural molecules. *Methods* 66, 55-66.
- Griffith, I.J., Pollock, J., Klapper, D.G., Rogers, B.L., and Nault, A.K. (1991). Sequence polymorphism of Amb a I and Amb a II, the major allergens in *Ambrosia artemisiifolia* (short ragweed). *Int Arch Allergy Appl Immunol* 96, 296-304.
- Guo, W., Gonzalez-Candelas, L., and Kolattukudy, P.E. (1996). Identification of a novel pelD gene expressed uniquely in planta by *Fusarium solani* f. sp. pisi (*Nectria haematococca*, mating type VI) and characterization of its protein product as an endo-pectate lyase. *Arch Biochem Biophys* 332, 305-312.
- Hasegawa, Y., Nakamura, S., Uheda, E., and Nakamura, N. (2000). Immunolocalization and possible roles of pectins during pollen growth and callose plug formation in angiosperms. *Grana* 39, 46-55.
- Himly, M., Jahn-Schmid, B., Dedic, A., Kelemen, P., Wopfner, N., Altmann, F., Van Ree, R., Briza, P., Richter, K., Ebner, C., and Ferreira, F. (2003). Art v 1, the major allergen of mugwort pollen, is a modular glycoprotein with a defensin-like and a hydroxyproline-rich domain. *FASEB J* 17, 106-108.
- Jahn-Schmid, B., Hauser, M., Wopfner, N., Briza, P., Berger, U.E., Asero, R., Ebner, C., Ferreira, F., and Bohle, B. (2012). Humoral and cellular cross-reactivity between Amb a 1, the major ragweed pollen allergen, and its mugwort homolog Art v 6. *J Immunol* 188, 1559-1567.
- Jiang, J., Yao, L., Yu, Y., Lv, M., Miao, Y., and Cao, J. (2014). PECTATE LYASE-LIKE10 is associated with pollen wall development in *Brassica campestris*. *J Integr Plant Biol* 56, 1095-1105.
- Kazemi-Pour, N., Condemine, G., and Hugouvieux-Cotte-Pattat, N. (2004). The secretome of the plant pathogenic bacterium *Erwinia chrysanthemi*. *Proteomics* 4, 3177-3186.
- King, T.P., Alagon, A., Kochoumian, L., Kuan, J., Sobotka, A., and Lichtenstein, L.M. (1981). Limited proteolysis of antigens E and K from ragweed pollen. *Arch Biochem Biophys* 212, 127-135.
- King, T.P., Norman, P.S., and Tao, N. (1974). Chemical modifications of the major allergen of ragweed pollen, antigen E. *Immunochemistry* 11, 83-92.
- Lyu, M., Liang, Y., Yu, Y., Ma, Z., Song, L., Yue, X., and Cao, J. (2015). Identification and expression analysis of BoMF25, a novel polygalacturonase gene involved in pollen development of *Brassica oleracea*. *Plant Reprod* 28, 121-132.
- Midoro-Horiuti, T., Goldblum, R.M., Kurosky, A., Goetz, D.W., and Brooks, E.G. (1999). Isolation and characterization of the mountain cedar (*Juniperus ashei*) pollen major allergen, Jun a 1. *J Allergy Clin Immunol* 104, 608-612.
- Miki-Hirosige, H., Nakamura, S., Yasueda, H., Shida, T., and Takahashi, Y. (1994). Immunocytochemical localization of the allergenic proteins in the pollen of *Cryptomeria japonica*. *Sex Plant Reprod* 7, 95-100.

- Pichler, U., Hauser, M., Wolf, M., Bernardi, M.L., Gadermaier, G., Weiss, R., Ebner, C., Yokoi, H., Takai, T., Didierlaurent, A., Rafaiiani, C., Briza, P., Mari, A., Behrendt, H., Wallner, M., and Ferreira, F. (2015). Pectate lyase pollen allergens: sensitization profiles and cross-reactivity pattern. *PLoS One* 10, e0120038.
- Rafnar, T., Griffith, I.J., Kuo, M.C., Bond, J.F., Rogers, B.L., and Klapper, D.G. (1991). Cloning of Amb a I (antigen E), the major allergen family of short ragweed pollen. *J Biol Chem* 266, 1229-1236.
- Robert, L.S., Allard, S., Gerster, J.L., Cass, L., and Simmonds, J. (1993). Isolation and characterization of a polygalacturonase gene highly expressed in Brassica napus pollen. *Plant Mol Biol* 23, 1273-1278.
- Rogers, H.J., Harvey, A., and Lonsdale, D.M. (1992). Isolation and characterization of a tobacco gene with homology to pectate lyase which is specifically expressed during microsporogenesis. *Plant Mol Biol* 20, 493-502.
- Shevchik, V.E., Robert-Baudouy, J., and Hugouvieux-Cotte-Pattat, N. (1997). Pectate lyase Pell of *Erwinia chrysanthemi* 3937 belongs to a new family. *J Bacteriol* 179, 7321-7330.
- Suárez-Cervera, M., Takahashi, Y., Vega-Maray, A.M., and Seoane-Camba, J.A. (2003). Immunocytochemical localization of Cry j 1, the major allergen of *Cryptomeria japonica* (Taxodiaceae) in *Cupressus arizonica* and *Cupressus sempervirens* (Cupressaceae) pollen grains. *Sex Plant Reprod* 16, 9–15.
- Taniguchi, Y., Ono, A., Sawatani, M., Nanba, M., Kohno, K., Usui, M., Kurimoto, M., and Matuhasi, T. (1995). Cry j I, a major allergen of Japanese cedar pollen, has pectate lyase enzyme activity. *Allergy* 50, 90-93.
- Turcich, M.P., Hamilton, D.A., and Mascarenhas, J.P. (1993). Isolation and characterization of pollen-specific maize genes with sequence homology to ragweed allergens and pectate lyases. *Plant Mol Biol* 23, 1061-1065.
- Wopfner, N., Gadermaier, G., Egger, M., Asero, R., Ebner, C., Jahn-Schmid, B., and Ferreira, F. (2005). The spectrum of allergens in ragweed and mugwort pollen. *Int Arch Allergy Immunol* 138, 337-346.
- Wopfner, N., Jahn-Schmid, B., Schmidt, G., Christ, T., Hubinger, G., Briza, P., Radauer, C., Bohle, B., Vogel, L., Ebner, C., Asero, R., Ferreira, F., and Schwarzenbacher, R. (2009). The alpha and beta subchain of Amb a 1, the major ragweed-pollen allergen show divergent reactivity at the IgE and T-cell level. *Mol Immunol* 46, 2090-2097.
- Wu, Y., Qiu, X., Du, S., and Erickson, L. (1996). PO149, a new member of pollen pectate lyase-like gene family from alfalfa. *Plant Mol Biol* 32, 1037-1042.
- Zaidi, M.A., O'leary, S., Wu, S., Gleddie, S., Eudes, F., Laroche, A., and Robert, L.S. (2012). A molecular and proteomic investigation of proteins rapidly released from triticale pollen upon hydration. *Plant Mol Biol* 79, 101-121.
- Zhang, Q., Huang, L., Liu, T., Yu, X., and Cao, J. (2008). Functional analysis of a pollen-expressed polygalacturonase gene BcMF6 in Chinese cabbage (*Brassica campestris* L. ssp. *chinensis* Makino). *Plant Cell Rep* 27, 1207-1215.

Final remarks

“Nature loves to hide” said Heraclitus more than 2000 years ago and despite science and research have made huge steps forward, many secrets are still kept and many ideas are still to be conceived. For this reason many things are still unknown and they reside in the mystery of nature. This is one of the reasons why we continue searching for answers and this is also the reason why the aim of a researcher should be exploring the unknown and staying curious and open to a world full of new possibilities. My PhD study gave me the possibility to deeply investigate phenomena and biological processes concerning different aspects of pollen: from the astonishing process of pollen tube growth to the release of proteins during its rehydration, from the complex structure of the pollen cell wall to the immune recognition of allergens. While many things have been discovered and light has been spread, my research also prompted new questions not only for more thirst for knowledge about the investigated topics but also for new research topics aiming to a deeper investigation of the multifaceted nature of pollen.

List of publications

Iorio R.A., Serafini-Fracassini D., Aloisi I., Del Duca S., De Franceschi P., Dondini L., Sansavini S., Cai G., Faleri C. Post-translational modification by transglutaminase of proteins involved in pear self-incompatibility. *Acta Horticulturae*, 2012, 967, pp. 141–148

Cai G., Sobieszczuk-Nowicka E., Aloisi I., Fattorini L., Serafini-Fracassini D., Del Duca S. Polyamines are common players in different facets of plant programmed cell death, *Amino Acids*, 2015, 47, pp. 27-44.

Aloisi I., Cai C., Tumiatti V., Minarini A., Del Duca S., Natural polyamines and synthetic analogs modify the growth and the morphology of *Pyrus communis* pollen tubes affecting ROS levels and causing cell death, *Plant Science*, 2015, 239, pp. 92–105

Cai C., Della Mea M., Faleri C., Fattorini L., Aloisi I., Serafini-Fracassini D., Del Duca S., Spermine can oppositely delay or promote cell death in *Nicotiana tabacum* L. corolla according to the floral developmental stage and affects the distribution of transglutaminase, *Plant Science*, 2015, 241, pp. 11-22

Marinello J., Bertocchini S., Aloisi I., Cristini A., Malagoli Tagliazucchi G., Forcato M., Sordet O., Capranico G., Dynamic Effects of Topoisomerase I Inhibition on R-Loops and Short Transcripts at Active Promoters, *PlosONE*, 2016, DOI:10.1371/journal.pone.0147053

Ruiz K.B, Aloisi I., Del Duca S., Canelo V., Torrigiani P., Silva H., Biondi S., Salares versus coastal ecotypes of quinoa: Salinity responses in Chilean landraces from contrasting habitats, *Plant Physiology and Biochemistry*, 2016 101:1-13, DOI:10.1016/j.plaphy.2016.01.010

Aloisi I., Cai G., Serafini-Fracassini D., Del Duca S., Polyamines in pollen: from microsporogenesis to fertilization, *Frontiers in Plant Science*, 2016, 7:155. DOI: 10.3389/fpls.2016.00155

Aloisi I., Cai G., Serafini-Fracassini D., Del Duca S., Transglutaminase as polyamine mediator in plant growth and differentiation, *Amino Acids*, 2016, DOI 10.1007/s00726-016-2235-y

Aloisi I., Parrotta L., Ruiz K.B, Landi C., Bini L., Cai G., Biondi S., Del Duca S., New insight into quinoa seed quality under salinity: changes in proteomic and amino acid profiles, phenolic content, and antioxidant activity of protein extracts, *Frontiers in Plant Science*, 2016, DOI: 10.3389/fpls.2016.00656

Scarnato L., Aloisi I., Montanari C., Serrazanetti D.I., Balestra F., Lanciotti R., Del Duca S., Combination of transglutaminase and sourdough on gluten-free flours to improve dough structure, *Amino Acids*, 2016, DOI 10.1007/s00726-016-2258-4

Scarnato L., Montanari C., Serrazanetti D.I., Aloisi I., Balestra F., Del Duca S., Lanciotti R., New bread formulation with improved rheological properties and longer shelf-life by the combined use of transglutaminase and sourdough, *LWT - Food Science and Technology*, 2017, DOI 10.1016/j.lwt.2017.03.042

